National Technical University of Athens
School of Civil Engineering
Department of Water Resources & Environmental Engineering

Hydrodynamic habitat modelling based on freshwater macroinvertebrates

Christos Theodoropoulos
PhD Thesis

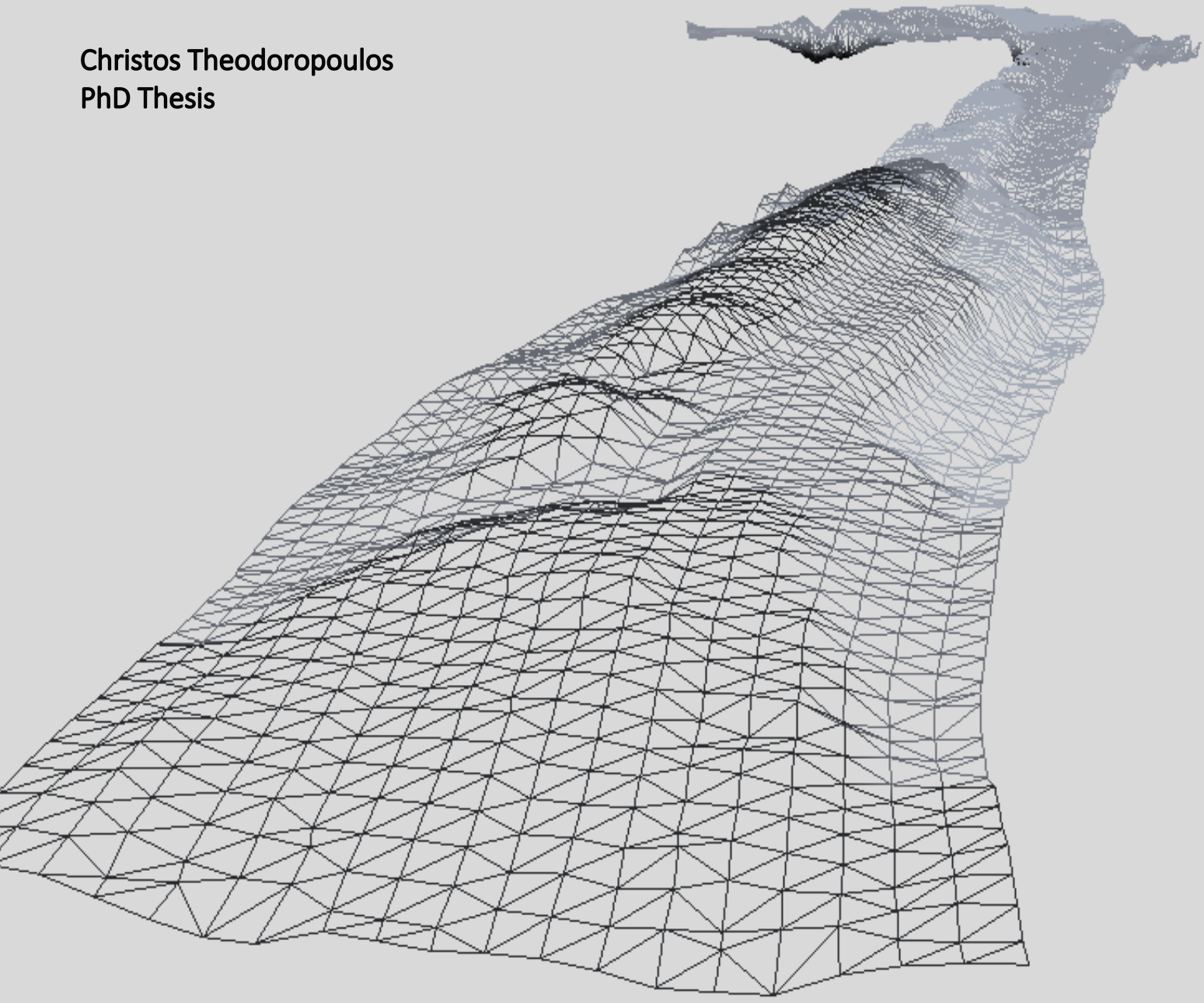

Athens 2020

National Technical University of Athens
School of Civil Engineering
Department of Water Resources and Environmental Engineering

Hydrodynamic habitat modelling based on freshwater macroinvertebrates

Ph.D. Thesis

Christos A. Theodoropoulos

Graduate of the Department of Biology - University of Patras, Greece

Supervisor

Prof. Anastasios I. Stamou
-National Technical University of Athens-

Advisory committee

Prof. Peter Rutschmann
-Technical University of Munich-

Dr. Nikolaos Skoulikidis
-Hellenic Centre for Marine Research-

Athens 2020

THESIS COMMITTEE

Supervisor
Prof. Anastasios I. Stamou, NTUA

Advisory committee
Prof. Anastasios I. Stamou, NTUA
Prof. Peter Rutschmann, TUM
Dr. Nikolaos Skoulikidis, IMBRIW, HCMR

Evaluation committee
Prof. Anastasios I. Stamou, NTUA
Prof. Peter Rutschmann, TUM
Dr. Nikolaos Skoulikidis, IMBRIW, HCMR
Prof. Vassilios Tsihrintzis, NTUA
Prof. Evangelos Baltas, NTUA
Assoc. Prof. Constantinos Noutsopoulos, NTUA
Dr. Elias Dimitriou, IMBRIW, HCMR

Η συγκεκριμένη διατριβή εκπονήθηκε με χρηματοδότηση από τον Ειδικό Λογαριασμό Κονδυλίων Έρευνας ΕΜΠ

Funded by the Special Account for Research Funds of the National Technical University of Athens, Greece

To my parents
to my wife Demetra
to my children Athanasios and Antonia

‘We make a living by what we get, but we make a life by what we give’
Winston Churchill

Acknowledgements

At first, I would like to thank my supervisor, Dr. Anastasios I. Stamou, Professor at the National Technical University of Athens, School of Civil Engineering, for his continuous support of my PhD study and related research, for his patience, motivation, and immense knowledge. His guidance helped me in all the time of research and writing of this thesis. When I first met him in 2015 as an environmental biologist, my knowledge on hydraulics-hydrodynamics was just 'elementary' and now, in 2020, thanks to the continuous scientific guidance and management of Prof. Stamou, I can apply hydrodynamic simulations, acquire topographic representations of river reaches and carry out accurate, model-based environmental flow assessments in rivers. There was no possibility of implementing this work without the relevant scientific knowledge-expertise of Prof. Stamou, which was gradually and successfully communicated to me during these years.

My sincere thanks also goes to Dr. Nikolaos Th. Skoulikidis, Research Director at the Hellenic Centre for Marine Research, Institute of Marine Biological Resources and Inland Waters, with whom I had an excellent collaboration during specific projects on the ecological monitoring of surface waters. His scientific guidance on the ecological-habitat component of hydrodynamic habitat modelling was crucial for the successful implementation of my study. In addition, his management capabilities were also valuable, guiding me appropriately towards my personal advancing from a post-M.Sc. student to a skilled researcher.

I am also thankful to Dr. Peter Rutschmann, Professor at the Technical University of Munich, Department of Civil, Geo and Environmental Engineering for his valuable contribution to various parts of the implementation and writing of this thesis. His insightful comments, within our constructive scientific conversations during my visits at TUM resulted in a much upgraded PhD thesis.

My many thanks also goes to Theocharis Vavalidis, Eleni Bintoudi and Aikaterini Vourka, three colleagues and friends that helped me during the many sampling campaigns for the collection of the reference micro-habitat dataset. Thank you for travelling more than 3,000 km around Greece for my PhD study, for crossing mountains and for spending hours inside the river during spring, summer and autumn, despite the rain and against the wind!

I would also like to thank my wife Demetra for her patience during these years, in which I had to work during afternoons or even nights in order to 'be on time' with my PhD, instead of being with my family. Finally, I would like to thank my parents who believed in my skills when I was a high-school student and continue to support me every day.

Thank you all!

Preface

This thesis is the outcome of interdisciplinary research between environmental biology-ecology and environmental engineering-hydraulics. Often integrated under the terms 'ecohydrology', 'hydroecology', or more recently, 'ecohydraulics', these very diverse scientific disciplines explore and attempt to interpret the natural phenomena and ecological processes using two conceptually different approaches. Hydraulics/hydrodynamics, a scientific field of Physics, accepts that as the natural (physical) phenomena obey the laws of nature, they can be numerically interpreted and fully comprehended and described by using simple or complex, deterministic mathematical equations. The three-dimensional movement of water in a river, for example, can thus be fully determined and accurately simulated/predicted. On the contrary, due to the complex and variable, stochastic nature of biological-ecological phenomena, biology/ecology focuses on intensively observing them in nature, and afterwards attempts to draw wider conclusions based on repeating observations, which seem to constitute evidence of generic 'ecological norms' or 'ecological laws'. This, results in lower accuracy (from the physicist's, engineer's or mathematician's perspective), but in equally detailed descriptions and predictions of, for example, how aquatic organisms are distributed across a river reach, based on the local climatological, hydrological and hydraulic conditions.

Based on the aforementioned, environmental engineers initially assume that habitat models are equally accurate to the hydrodynamic/hydraulic models, often disregarding the complex, interactive nature of hydro-ecological processes. Consequently, they may often get disappointed when they conclude that this accuracy cannot be achieved. On the other hand, ecologists acknowledge this inherent complexity but usually lack the proper mathematical background to go any further than just descriptively interpreting their field observations, and rarely engage in a process of numerical description and modelling.

For the scientist-ecologist however, a detailed and accurate observation, description and prediction of the response of ecological communities to hydrological and habitat changes, is of paramount importance for the protection of ecosystems from possible degradation caused by the human presence and activity. And when it comes to studying and modelling hydroecological relationships and interactions, increased predictive accuracy cannot be achieved without the use of hydraulic/hydrodynamic habitat models, and consequently, without the cooperation and knowledge-exchange between hydraulic engineers and biologists-ecologists.

The current PhD Thesis has been conducted by an environmental biologist and includes two interacting parts; a numerical-hydraulic part and an ecological part, which are often integrated throughout the text to derive common results and conclusions. The ecology-oriented reader may find it difficult to 'follow' the numerical-mathematical focus of the first part, as well as the engineering-oriented reader may find it difficult to 'follow' the ecological focus and terminology used in the second part, despite the effort of the writer to fully describe all terms and processes of the study. I consider this absolutely normal and should not discourage the reader from further reading. Ecologists, for example, may see lots of equations describing the movement of water along a river reach; still there is no need to learn them in detail in order to understand what has been applied. Understanding the fundamental principles of water movement is more than enough to proceed with hydrodynamic modelling for ecologists.

This is one of the few in-depth attempts in Greece to integrate different scientific disciplines, with the purpose of predicting and modelling the response of aquatic organisms (in this case the benthic macroinvertebrates) to multiple gradients of hydraulic variability. The ultimate aim has been to develop model-based environmental flow scenarios in hydrologically-

altered river reaches, in order to keep dams operating without compromising the long-term integrity and functionality of the downstream aquatic ecosystems.

I wish you a happy reading,
Christos Theodoropoulos

Table of Contents

List of Figures

List of Tables

Abstract

Hydrodynamic habitat models (HHMs) have long been used in environmental flow assessments (EFAs); currently, they are considered as the most robust EFA option, applicable in situations where a high degree of certainty is required to provide water managers and stakeholders with defensible environmental flow recommendations. Despite the wide recognition of the effectiveness of HHMs to provide accurate environmental flow predictions, their practical application remains disproportionately limited compared to their hydrology-based alternatives and is primarily focused on fish. Model-based frameworks focusing on other components of the aquatic ecosystem -benthic macroinvertebrates, macrophytes and riparian vegetation- are currently missing. Yet, within a holistic perspective, the habitat requirements of all aquatic-ecosystem components should be considered in model-based EFAs. Moreover, the habitats that are suitable for fish may not be equally suitable for other organisms in the aquatic ecosystem. In this study, we developed an HHM-based EFA framework focused on benthic macroinvertebrates (BMs). Their habitat preferences were evaluated based on a reference dataset collected from nine sites, over three seasons, in Greece. A BM-based habitat suitability (K) index, integrating four primary BM-community metrics, was developed and included in an optimal-flow-scenario index to facilitate the development of model-based environmental flow predictions. Based on these indices, the predictive accuracy of various habitat modelling algorithms was evaluated and a fuzzy rule-based Bayesian algorithm (FRB) was selected as the most suitable option. A habitat modelling software (HABFUZZ) was developed to implement this algorithm and a two-dimensional hydrodynamic model (TELEMAC 2D) was used to simulate flow velocities (V) and water depths (D) in various discharges in two river reaches in Greece. The results showed that BMs do respond to hydrological variation-alteration; the distribution, abundance and diversity of BMs before and after a rainfall-induced high flow event were significantly different, and this flow variation explained up to 42.9% of the overall BM community variation. The habitat preferences of BMs followed a Gaussian distribution with specific optimal values for V, D, substrate (S) and temperature (T). Not all habitat modelling algorithms can be used to simulate their habitat preferences; the predictive accuracy of the regression-based, machine-learning and fuzzy rule-based algorithms tested, ranged from 49.74% to 67.92%, with the FRB model reaching 61.2% accuracy. Using this algorithm, the habitat suitability of two river reaches was mapped in various discharges; the results showed that the model-based environmental flows were higher than those calculated using hydrological methods and thus, the delivery of environmental flows should be upwards-adjusted to ensure the long-term integrity of the aquatic communities. Apart from the developed BM-based, HHM methodology, this study showed that (i) complex -interactive- hydroecological relationships can be successfully described-modelled using fuzzy rule-based algorithms and (ii) multimetric indices can be effectively incorporated to describe the status of the benthic community in various discharges. The collection of robust hydro-ecological datasets, their spatiotemporal variation and the field-validation of HHMs should be future research targets towards the development of robust HHMs-based EFAs.

Chapter 1

Introduction

1.1. Historical background

1.1.1. Hydrodynamics

When *Claude-Louis Navier*, in France, and *George Gabriel Stokes*, in England, independently formulated the equations that describe the motion of viscous fluid substances in 1822, they would probably not have imagined the numerous applications that these equations would have during the next centuries. Although during the late 1800s - early 1900s engineers were actually simplifying these equations to the point they could be solved by hand, the increasing power of computing technology after the 1950s gave birth to a new era; the era of Computational Fluid Dynamics (CFD), that branch of fluid mechanics, which uses numerical analysis and data structures to solve and analyze problems that involve fluid flows. After the first CFD model solving the Navier-Stokes equations was implemented in 1957 by the T3 group at the Los Alamos Scientific Lab (Harlow, 2004), continuously upgraded CFD models have been routinely used to predict and simulate the weather, the movement of air in the atmosphere, ocean currents, the water flow in a pipe or an open channel and other numerous fluid-flow related phenomena. During the 1960s, the use of CFD models was also introduced in open channel hydraulics. In 1991, the initially simplified one-dimensional (1D) transect-based applications evolved to 2D- and 3D-based software of enhanced predictive accuracy and hence, the use of hydraulic-hydrodynamic models enabled scientists and engineers to quickly and accurately solve the complex fundamental Navier-Stokes equations to simulate/predict water depths and flow velocities in river reaches of interest. This, as a result, offered the opportunity for interdisciplinary hydroecological studies and introduced the first part of what we nowadays call 'hydrodynamic habitat modelling'.

1.1.2. Ecological niche - habitat - microhabitat

For ecologists, it all started in 1910 when *Roswell Hill Johnson* first used the word 'niche' to suggest that different species in a region occupy different environmental spaces (Johnson, 1910). But it was *Joseph Grinnell* and *Tracy Irwin Storer* in 1924 who theoretically defined the niche as 'the ultimate distributional unit, within which each species is held by its structural and instinctive limitations' (Grinnell and Storer, 1924). Soon afterwards, *Charles Sutherland Elton* (1927) enhanced this concept to include between-species interactions and competition, but it was *George Evelyn Hutchinson* (1957) who attempted to quantify the niche, describing it as a multi-dimensional hypervolume, where the different dimensions represent environmental conditions and resources, which define the requirements of an individual or a species to live and of its populations to persist and thrive.

As the processing power and data storage capacity of modern computers increased over the last decades, the aforementioned fundamental framework has been the springboard for operational applications aiming to explore, interpret and predict the distribution of biota to gradients of environmental-physical conditions, in search of the optimal physical location - called habitat- where a species or a group of species may select to live. Termed as habitat suitability models, ecological niche models, species distribution models or bioclimatic envelope models (Bradley et al., 2012), these applications have been widely used worldwide to define the habitat preferences of terrestrial and aquatic organisms. After the first aquatic habitat suitability methodology was introduced in 1978 (the Instream Flow Incremental Methodology - Bovee and Milhous, 1978) these applications advanced after 1999 to include complicated habitat modelling algorithms (e.g. machine learning, fuzzy logic, Bayesian inference) and were recently integrated into the terms *ecohydrology*, *hydroecology* and *ecohydraulics*, to highlight the interdisciplinary nature of the particular scientific field (Fig. 1.1).

1.2. Hydrodynamic modelling

Hydrodynamic models are computer software applications that aim to simulate surface flow dynamics using numerical formulas. These formulas are based on three fundamental laws of physics-mechanics (Anderson, 2009; Prichard, 2011):

1. Conservation of mass - the mass of an object or collection of objects never changes, no matter how the constituent parts rearrange themselves.
2. Newton's second law - the acceleration of an object (a) depends directly on the net force acting upon the object (F) and inversely on the mass (m) of the object (a=F/m).
3. Conservation of energy - in a closed system, a system isolated from its surroundings, the total energy of the system is conserved.

The purpose of hydrodynamic models is to calculate the water depths and the relevant flow velocities over a range of discharges at multiple points (nodes) in a one-, two- or three-dimensional geometric representation of the area under investigation, by solving various alternatives (transformations) of the following equations:

(Conservation of mass)[1]
$$\frac{\partial \rho}{\partial t} + \frac{\partial (\rho u)}{\partial x} + \frac{\partial (\rho v)}{\partial y} + \frac{\partial (\rho w)}{\partial z} = 0 \quad (1.1)$$

(X momentum)[2]
$$\frac{\partial u}{\partial t} + \frac{\partial u^2}{\partial x} + \frac{\partial uv}{\partial y} + \frac{\partial uw}{\partial z} + \frac{1}{\rho}\frac{\partial P}{\partial x} - g_x - \frac{\mu}{\rho}\left(\frac{\partial^2 u}{\partial x^2} + \frac{\partial^2 u}{\partial y^2} + \frac{\partial^2 u}{\partial z^2}\right) = 0 \quad (1.2)$$

(Y momentum)[2]
$$\frac{\partial v}{\partial t} + \frac{\partial uv}{\partial x} + \frac{\partial v^2}{\partial y} + \frac{\partial vw}{\partial z} + \frac{1}{\rho}\frac{\partial P}{\partial y} - g_y - \frac{\mu}{\rho}\left(\frac{\partial^2 v}{\partial x^2} + \frac{\partial^2 v}{\partial y^2} + \frac{\partial^2 v}{\partial z^2}\right) = 0 \quad (1.3)$$

(Z momentum)[2]
$$\frac{\partial w}{\partial t} + \frac{\partial wu}{\partial x} + \frac{\partial wv}{\partial y} + \frac{\partial w^2}{\partial z} + \frac{1}{\rho}\frac{\partial P}{\partial z} - g_z - \frac{\mu}{\rho}\left(\frac{\partial^2 w}{\partial x^2} + \frac{\partial^2 w}{\partial y^2} + \frac{\partial^2 w}{\partial z^2}\right) = 0 \quad (1.4)$$

(Conservation of energy)
$$\rho\frac{De}{Dt} = \rho q + \frac{\partial}{\partial x}\left(k\frac{\partial T}{\partial x}\right) + \frac{\partial}{\partial y}\left(k\frac{\partial T}{\partial y}\right) + \frac{\partial}{\partial z}\left(k\frac{\partial T}{\partial z}\right) - \rho\left(\frac{\partial u}{\partial x} + \frac{\partial v}{\partial y} + \frac{\partial w}{\partial z}\right) + \lambda\left(\frac{\partial u}{\partial x} + \frac{\partial v}{\partial y} + \frac{\partial w}{\partial z}\right)^2 + \mu\left[2\left(\frac{\partial u}{\partial x}\right)^2 + \left(\frac{\partial v}{\partial y}\right)^2 + \left(\frac{\partial w}{\partial z}\right)^2 + \left(\frac{\partial u}{\partial y} + \frac{\partial v}{\partial x}\right)^2 + \left(\frac{\partial u}{\partial z} + \frac{\partial w}{\partial x}\right)^2 + \left(\frac{\partial v}{\partial z} + \frac{\partial w}{\partial y}\right)^2\right] \quad (1.5)$$

where,
ρ (kg/m^3) density of water
u, v, w (m/s) velocity components along the x, y and z directions, respectively
μ (Pa s) fluid's dynamic viscosity
λ (Pa s) fluid's bulk viscosity
g (m/s^2) gravity acceleration
x, y, z (m) space coordinates
P (Pa) pressure
t (s) time
T (^{o}K) temperature
q rate of volumetric heat addition per unit mass
$\partial\ /\ \partial t$ time rate of change at a given point in space
$D/Dt = (\partial/\partial t + u\,\partial/\partial x + v\,\partial/\partial y + w\,\partial/\partial z)$ instantaneous time-rate of change between two points in space (substantial derivative)

[1] For incompressible flow (ρ constant; $\partial\rho/\partial t$ = 0) ρ can be omitted
[2] These are the Navier-Stokes equations for Newtonian, incompressible fluids (ρ and μ constant)

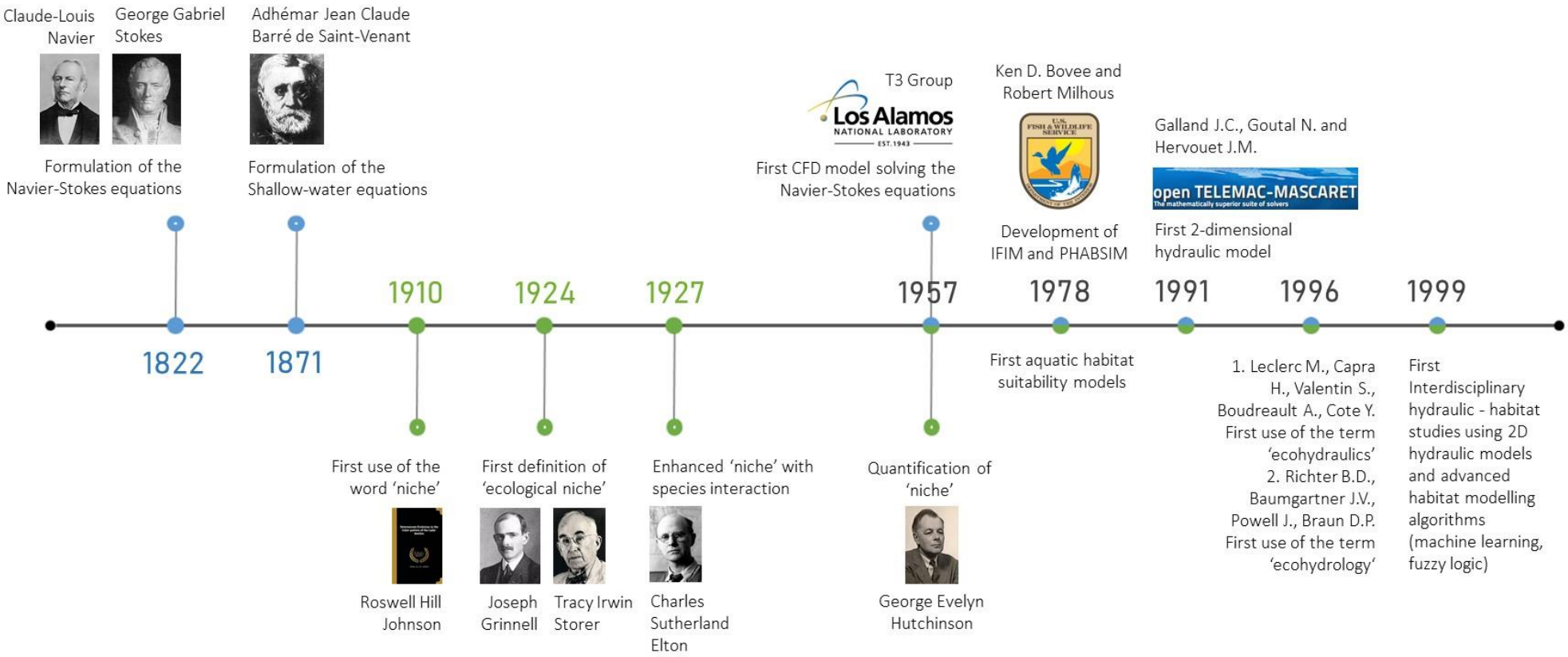

Fig. 1.1. Historical findings and developments leading to the current interdisciplinary hydroecological studies

Hydrodynamic models are categorized in three groups, based on the number of dimensions they use to simulate flow dynamics, and consequently, on the number and the form of the equations they include in the calculations; (i) one-dimensional (1D), (ii) two-dimensional (2D) and (iii) three-dimensional (3D). A different geometric representation of the reach to be simulated is required for each group.

1.2.1. One-dimensional hydrodynamic models

One-dimensional models are transect-based applications. The geometry of the study reach (channel geometry) is described using cross sections (transects) where the water depth, the water surface elevation (Z), the average flow velocity, the type of substrate and often shading, canopy cover and temperature are measured at specific user-defined intervals across each transect (Fig. 1.2), with the total number of cross sections depending on the detail required.

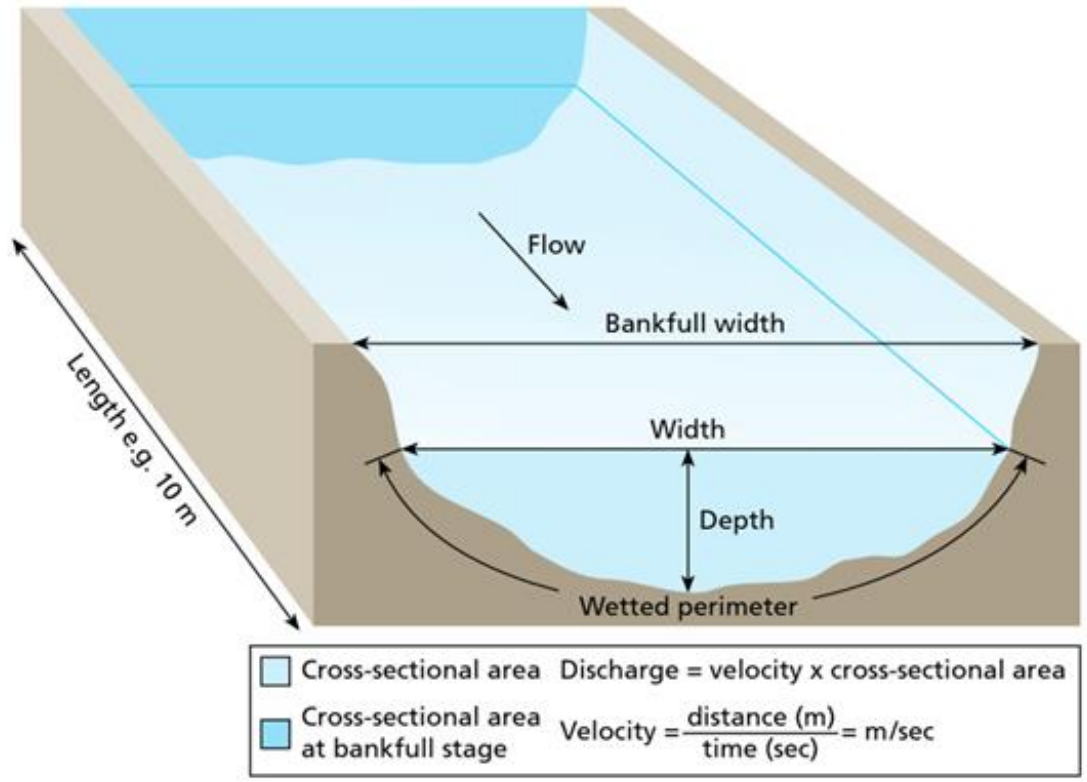

Fig. 1.2. A typical cross section. Image from http://www.geo41.com/discharge/

Based on the transect-based description of the area, there are two basic processes followed in the 1D hydrodynamic models:

1. For unsteady flows (when all conditions at any point in the reach, including the flow velocity, change over time) the model solves the continuity equation (conservation of mass) and the Reynold's averaged Navier-Stokes equations (RANS) to calculate the cross-sectional averaged water surface elevation (Z') and the cross-sectional averaged horizontal flow velocity vector (u) at each cross section of the study reach. Local depths (D) are then calculated as the difference between Z' and the local bed elevation, while the local u values are determined using the D values and uniform flow equations (Bovee, 1982; Benjankar, 2014). The RANS one-dimensional momentum equation (along the x axis) is the following:

$$\frac{\partial u}{\partial t}+\frac{\partial u^2}{\partial x}+\frac{\partial uv}{\partial y}+\frac{\partial uw}{\partial z}+\frac{1}{\rho}\frac{\partial P}{\partial x}-g_x-\frac{\mu}{\rho}\left(\frac{\partial^2 u}{\partial x^2}+\frac{\partial^2 u}{\partial y^2}+\frac{\partial^2 u}{\partial z^2}\right) + \frac{\partial \overline{u'u'}}{\partial x}+\frac{\partial \overline{u'v'}}{\partial y}+\frac{\partial \overline{u'w'}}{\partial z}=0 \quad (1.6)$$

where,
$\overline{u'}, \overline{v'}, \overline{w'}$ (m/s) are the time-averaged velocity components along the x, y and z directions, respectively

2. For steady flows (when all conditions including the flow velocity do not change over time) the model solves the continuity equation and an equation for the friction loss to compute the x velocity vector (u) and the water surface elevation. Based on an empirical friction coefficient (e.g. Manning's n) which depends on various factors including the channel's substrate, the following Manning's formula is often implemented:

$$u=\frac{1}{n}R_h^{2/3}S^{1/2} \quad (1.7)$$

where,
u (m/s) the velocity component along the x direction
n the Manning's friction coefficient
$R_h = A/P$ (m) hydraulic radius
A (m^2) the cross-sectional area of the channel
P (m) the channel's wetted perimeter
S the slope of the hydraulic grade line, which is the same as the channel bed slope in constant water depth

The fundamental assumptions of 1D models are that flow velocity is a function of local depth and energy slope, and that flow vectors have only the longitudinal direction (u). The most commonly used 1D hydrodynamic models are the PHABSIM (Milhous et al., 1989; Waddle, 2001), CASiMiR (Schneider et al., 2001), HEC RAS (USACE, 2016) and MIKE11 (DHI, 2017).

1.2.2. Two-dimensional hydrodynamic models

Two-dimensional hydrodynamic models require a detailed geometric representation of the study reach (channel topography). Using advanced spatial surveying and mapping equipment, such as Real-Time Kinematic GPS or LiDAR, the study reach is represented as a dense network of geographical coordinates (X, Y) and bed elevation data (H). Geospatial processing software applications, either as independent programs or incorporated into the hydrodynamic models, are then used to construct a computational mesh based on the set of X, Y, H point dataset (Fig. 1.3).

Using the aforementioned input, in combination with user-defined initial and boundary conditions, 2D hydrodynamic models solve the Navier-Stokes-derived shallow water equations developed by *Adhémar Jean Claude Barré de Saint-Venant* in 1871 to determine the water depth and depth-averaged flow velocity at each node of the computational mesh. The St. Venant equations for incompressible flow (ρ constant; $\partial\rho/\partial t = 0$) are the following:

(Conservation of mass) $$\frac{\partial h}{\partial t}+\frac{\partial (uh)}{\partial x}+\frac{\partial (vh)}{\partial y}=0 \quad (1.8)$$

(X momentum) $$\frac{\partial uh}{\partial t}+\frac{\partial}{\partial x}\left(u^2h+\frac{1}{2}gh^2\right)+\frac{\partial uvh}{\partial y}-gh(S_{0x}-S_{fx})=0 \quad (1.9)$$

(Y momentum) $$\frac{\partial vh}{\partial t}+\frac{\partial}{\partial y}(v^2h+\frac{1}{2}gh^2)+\frac{\partial uvh}{\partial x}-gh(S_{0y}-S_{fy})=0 \quad (1.10)$$

where,
h (m) depth of the water
u, v (m/s) velocity components along the x and y directions, respectively
g (m/s^2) gravity acceleration
x, y, z (m) space coordinates
t (s) time
$S_{0(x,y)}$ channel bottom slope in the (x, y) directions
$S_{f(x,y)}$ friction slopes in the (x, y) directions based on the Manning's equation

$$S_{fx}=\frac{n^2u\sqrt{u^2+v^2}}{C_0^2h^{1.33}};\ S_{fy}=\frac{n^2v\sqrt{u^2+v^2}}{C_0^2h^{1.33}}$$

n Manning's friction coefficient
C_0 correction factor (C_0 = 1 in SI units)

To solve these partial differential equations (PDEs) all 2D hydrodynamic models apply various alternatives of the same conceptual framework called 'discretization'; the numerical process that transforms the integral or the differential form of a partial differential equation into an equivalent but different set of algebraic equations, which provide results at a finite number of points within the numerical domain (Tonina and Jorde, 2013). The most popular discretization methods are the finite difference method, the finite element and the finite volume method.

1.2.2.1. The Finite Difference Method (FDM)

As with all the discretization methods, in the FDM, the continuous domain (the river reach to be simulated) is partitioned in space (a computational grid is constructed) and time (the same computational grid at multiple time steps) and the partial differential terms (equations 1.8, 1.9 and 1.10) are approximated at each node and for each time step using algebraic differences (Fig. 1.3). In the FDM, these differences are based on the Taylor's expansion theorem, devised in 1712, which states that if $n \geq 0$ is an integer and f is a function which is n times continuously differentiable on the closed interval $[a, x]$ and $n+1$ times differentiable on the open interval (a, x), then

$$f(x_0+\Delta x)=f(x_0)+\frac{f'(x_0)}{1!}\Delta x+\frac{f''(x_0)}{2!}\Delta x^2+\cdots+\frac{f^{(n)}(x_0)}{n!}\Delta x^n+R_{n+1}(x) \quad (1.11)$$

where,
$f^{(n)}(x_n)$ the n^{th} derivative of f evaluated at x_n
$R_{n+1}(x)=\frac{f^{n+1}(c)}{n+1!}(x-\Delta x)^{n+1}$ for some c between x and Δx

The Taylor series converges to f if and only if $\lim_{n\to\infty} R_n(x)=0$.
Applying the Taylor's expansion for the first derivative, we get

$$f(x_0+\Delta x)=f(x_0)+\frac{f'(x_0)}{1!}\Delta x+\frac{f''(c)}{2!}\Delta x^2 \Leftrightarrow \frac{f(x_0+\Delta x)-f(x_0)}{\Delta x} = f'(x_0)+\frac{f''(c)}{2!}\Delta x \quad (1.12)$$

The term $(f''(c)/2!)\Delta x$ is called the local truncation error, which denotes the error between the numerical approximation $(f(x_0 + \Delta x) - f(x_0))/\Delta x$ and the exact value $f'(x_0)$ and is usually symbolized with $O(\Delta x)$, so that the previous equation becomes

$$\frac{f(x_0 + \Delta x) - f(x_0)}{\Delta x} = f'(x_0) + O(\Delta x) \qquad (1.13)$$

Similarly $f(x_0 - \Delta x)$ may be expanded as

$$\frac{f(x_0) - f(x_0 - \Delta x)}{\Delta x} = f'(x_0) + O(\Delta x) \qquad (1.14)$$

Subtracting eq. 1.14 from eq. 1.13, rearranging and dividing by Δx, we get

$$\frac{f(x_0 + \Delta x) - f(x_0 - \Delta x)}{2\Delta x} = f'(x_0) + O(\Delta x)^2 \qquad (1.15)$$

The same process can be applied for higher order derivatives.
Equations 1.13, 1.14 and 1.15 comprise the three finite difference schemes (approximations) used in numerical modelling; the forward finite-difference, the backward finite-difference and the central finite-difference scheme (Stamou and Rutschmann, 2011).

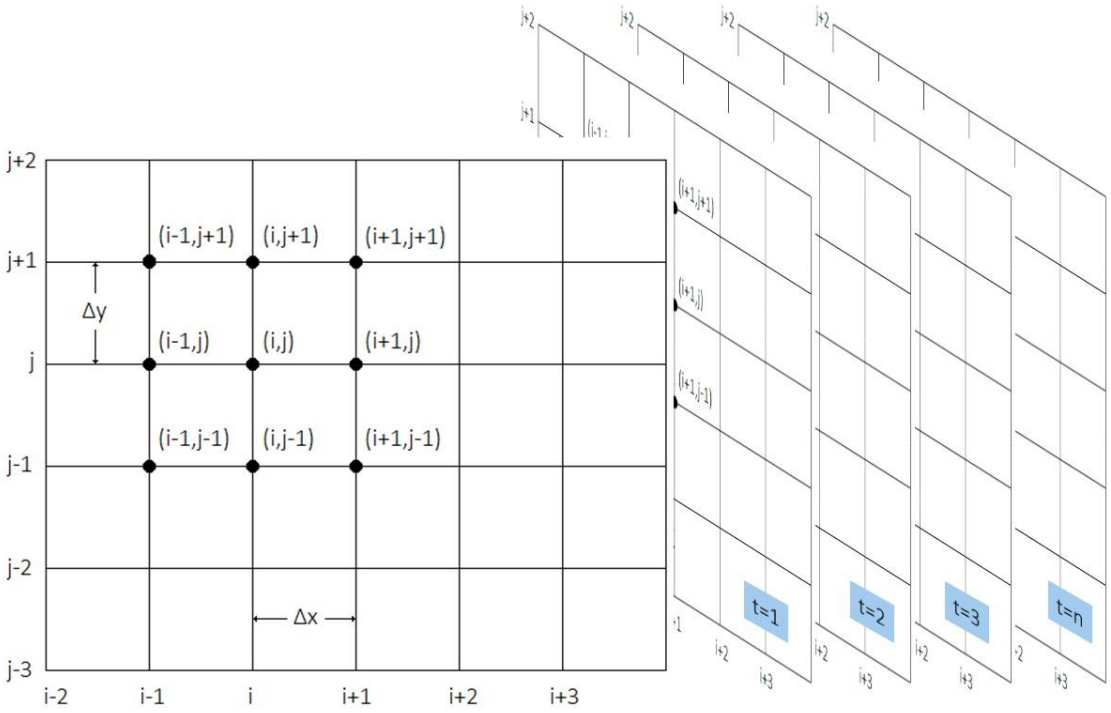

Fig. 1.3. A two-dimensional grid where the finite difference method is applied at each time step (t). Each simulated variable X in 2D-FDM models is described as X (i,j,t) denoting the two spatial and the one temporal indexes-coordinates. Consequently, the model creates a number of grids equal to the number of the time steps of the computation.

Based on the aforementioned, numerous algorithms have been developed to apply an FDM-oriented 2D hydrodynamic simulation where each modelled (dependent) variable is described by three grid coordinates, two spatial, i, j, denoting the fluid flow in the two-dimensional space, and one temporal, t, denoting the water flow in time. Prior to the initiation of the

computations, all algorithms require the user to provide specific conditions for the dependent variables in the boundaries of the domain (boundary conditions) and initial values of the dependent variables (t = 0) to start the FDM approximations (initial conditions). As an example, the MacCormack algorithm/scheme is described below (MacCormack, 1969).

To ease the equation manipulation, the St. Venant equations 1.8, 1.9 and 1.10 can be re-written using matrices in the following form:

$$U_t + E_x + F_y + S = 0 \qquad (1.16)$$

where,

$$U = \begin{bmatrix} h \\ uh \\ vh \end{bmatrix}; \quad E = \begin{bmatrix} uh \\ u^2h + \frac{1}{2}gh^2 \\ uvh \end{bmatrix}; \quad F = \begin{bmatrix} uh \\ uvh \\ u^2h + \frac{1}{2}gh^2 \end{bmatrix}; \quad S = \begin{bmatrix} 0 \\ -gh(S_{0x} - S_{fx}) \\ -gh(S_{0y} - S_{fy}) \end{bmatrix}$$

Replacing the partial differential terms with the forward, backward or central FDM schemes and after some appropriate rearrangement and transformation, equation 1.16 can be written as follows:

(Predictor) $$U^*_{i,j} = U^t_{i,j} - \frac{\Delta t}{\Delta x}\,\nabla_x E^t_{i,j} - \frac{\Delta t}{\Delta y}\,\nabla_y F^t_{i,j} - \Delta t S^t_{i,j} \qquad (1.17)$$

(Corrector) $$U^{**}_{i,j} = U^t_{i,j} - \frac{\Delta t}{\Delta x}\,\Delta_x E^*_{i,j} - \frac{\Delta t}{\Delta y}\,\Delta_y F^*_{i,j} - \Delta t S^*_{i,j} \qquad (1.18)$$

where,

$\Delta_x E^t_{i,j} = E^t_{i+1,j} - E^t_{i,j}$; $\nabla_x E^t_{i,j} = E^t_{i,j} - E^t_{i-1,j}$

$\Delta_y E^t_{i,j} = E^t_{i,j+1} - E^t_{i,j}$; $\nabla_x E^t_{i,j} = E^t_{i,j} - E^t_{i,j-1}$

$U^*_{i,j}$ and $U^{**}_{i,j}$ are intermediate values for U. The new U values at time t + 1 are

$$U^{t+1}_{i,j} = \frac{1}{2}\,(U^*_{i,j} + U^{**}_{i,j}) \qquad (1.19)$$

1.2.2.2. The Finite Element Method (FEM)

While the FDM uses the differential form of the equations 1.8, 1.9 and 1.10, the finite element and finite volume methods (FEM and FVM, respectively) use their integral form, with the advantage of handling complex mesh geometries, as the integral forms do not require a specific structure of the computational mesh. To ease understanding of the complex FEM method, the continuity and momentum equations (1.8, 1.9 and 1.10) can be abbreviated as

$C(h,u,v) = 0$ (1.20); $M_x(h,u,v) = 0$ (1.21); $M_y(h,u,v) = 0$ (1.22)

The concept in FEM is that 'trial functions', which are based on 'base functions' are introduced to approximate the aforementioned PDEs and the objective is to minimize the resulting residuals by using relevant weighting functions. Consequently, the replacement of the aforementioned equations by trial functions would result in

$C(\hat{h},\hat{u},\hat{v}) = R_C$ (1.23); $M_x(\hat{h},\hat{u},\hat{v}) = R_{Mx}$ (1.24); $M_y(\hat{h},\hat{u},\hat{v}) = R_{My}$ (1.25)

where

$\hat{h} = \sum_i h_i N_i;\ \hat{u} = \sum_i u_i P_i;\ \hat{v} = \sum_i v_i L_i$ trial functions of h, u, v

R_C, R_{Mx} and R_{My} the relevant residuals (errors of approximation)

N_i, P_i and L_i base functions of h, u, v

h_i, u_i and v_i the coefficients of the base functions approximating h, u and v with $\hat{h}, \hat{u}$ and $\hat{v}$

By using a weighting function W_i and integrating over the area A of the cells surrounding a node, equations 1.20, 1.21 and 1.22 become

$$\int W_i(A) C(\hat{h}, \hat{u}, \hat{v}) dA = 0 \quad (1.26); \qquad \int W_i(A) M_x(\hat{h}, \hat{u}, \hat{v}) dA = 0 \quad (1.27)$$

$$\int W_i(A) M_y(\hat{h}, \hat{u}, \hat{v}) dA = 0 \quad (1.28)$$

A one-dimensional approximation of a variable using the FEM is shown in Fig. 1.4.

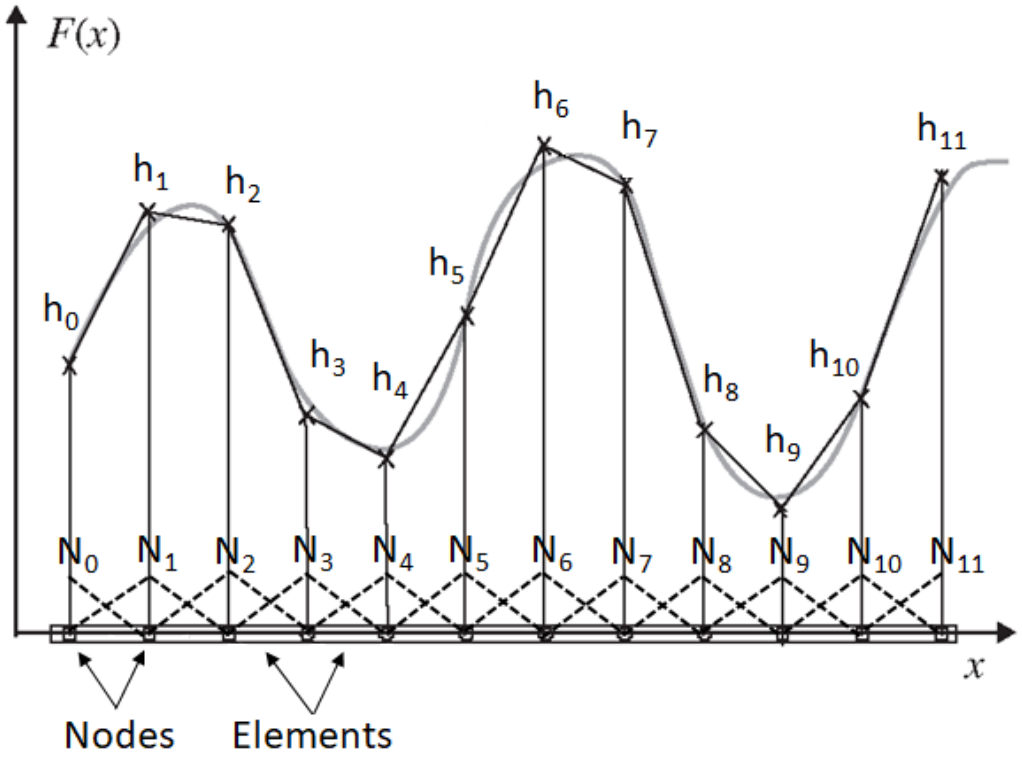

Fig. 1.4. One-dimensional river depth (h) approximation using the FEM concept. The h values at each node (the continuous h function - grey line)) along a theoretical x axis are approximated by $\hat{h}$ (straight black line), which is a linear combination of the linear base function N_i with coefficients h_i. Image adapted from http://what-when-how.com/the-finite-element-method/computational-modelling-finite-element-method/

1.2.2.3. The Finite Volume Method (FVM)

In the FVM (similarly to FEM), the study reach is divided into a set of cells, which can have irregular shape, in contrast to the FDM. Each cell is identified by its centre point (Fig. 1.5). Volume integrals represent the integral of the time evolution of the function of the cell area. Surface integrals represent the total normal flux through the cell boundaries. Equation 1.16 can be rewritten in its integral form as follows:

$$\int_{\forall} \frac{\partial U}{\partial t} du + \oint_{S} (Hn) ds = Sdu \qquad (1.29)$$

where,
H is the flux term at the control surface
$Hn = En_x + Gn_y$ where n_x and n_y are the x and y components of the unit vector n

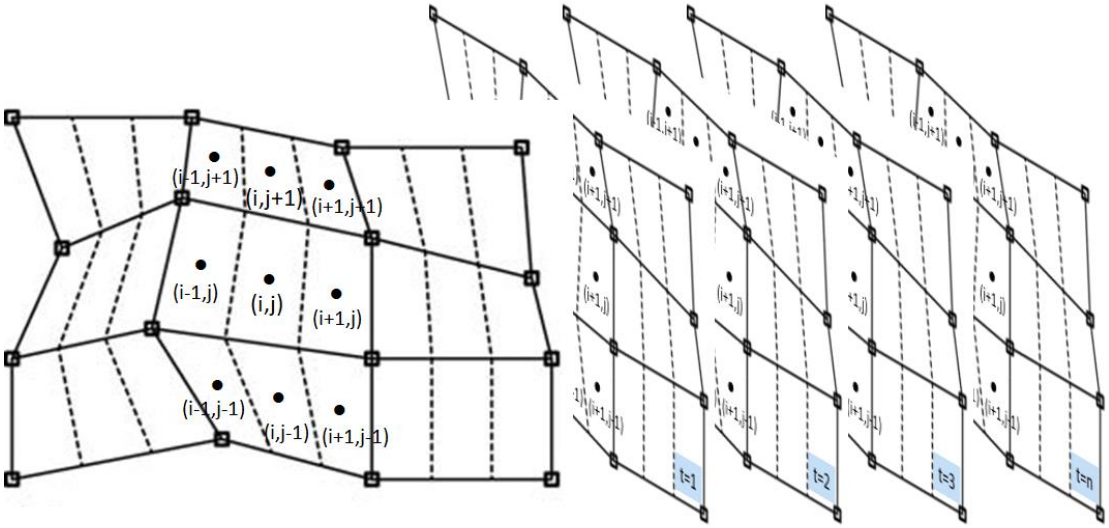

Fig. 1.5. A two-dimensional grid where the finite volume method is applied. The values of each simulated variable X in 2D-FVM models are integrated over the cell area, described by its centre point (i,j,t), which denotes the two spatial and the one temporal indexes-coordinates.

Assuming the vector U to be uniform over each cell and by approximating the surface integral by a sum over the four walls of the finite volume cell, the aforementioned equation 1.29 can be rewritten as

$$\frac{\partial U}{\partial t} \Delta A + \sum_{r=1}^{4} (H_r n_r) dS_r = S \Delta A \qquad (1.30)$$

where,
ΔA is the area of the finite volume cell
dS_r lengths of the four walls which surround the cell (i,j)
H_r the numerical flux through the cell faces r which contour the cell (i,j)

For example, the numerical flux for the cell face (e.g. 3) between the nodes i,j and i+1,j is

$$(H_3 n_3) dS_3 = (Hn)_{i+1/2,j} = \frac{1}{2}[H_R + H_L - a(U_R - U_L)] n_{i+1/2,j} \qquad (1.31)$$

where,
a is a positive coefficient
$H_R = f(U_R)$ the flux computed using the information from the right side of the cell face
$H_L = f(U_L)$ the flux computed using the information from the left side of the cell face

$$(U_L)_{i+1/2,j} = U_{i,j} + \frac{1}{2}\delta U_{i,j}$$
$$(U_R)_{i+1/2,j} = U_{i+1,j} - \frac{1}{2}\delta U_{i+1,j}$$

The time integration is applied by using a predictor-corrector approach as follows:

(Predictor)
$$U_{i,j}^{t+\Delta t} = U_{i,j}^{t} - \frac{\Delta t}{\Delta A_{i,j}} [H_{i+\frac{1}{2},j}^{t} dS_{i+\frac{1}{2},j} + H_{i,j+\frac{1}{2}}^{t} dS_{i,j+\frac{1}{2}} + H_{i-\frac{1}{2},j}^{t} dS_{i-\frac{1}{2},j} + H_{i,j-\frac{1}{2}}^{t} dS_{i,j-\frac{1}{2}} + \Delta t S_{i,j}^{t}] \quad (1.32)$$

(Corrector)
$$U_{i,j}^{t+\Delta t} = \frac{1}{2}[U_{i,j}^{t} + U_{i,j}^{t+\Delta t} - \frac{\Delta t}{\Delta A_{i,j}} (H_{i+\frac{1}{2},j}^{t+\Delta t} dS_{i+\frac{1}{2},j} + H_{i,j+\frac{1}{2}}^{t+\Delta t} dS_{i,j+\frac{1}{2}} + H_{i-\frac{1}{2},j}^{t+\Delta t} dS_{i-\frac{1}{2},j} + H_{i,j-\frac{1}{2}}^{t+\Delta t} dS_{i,j-\frac{1}{2}}) + \Delta t S_{i,j}^{t+\Delta t}] \quad (1.33)$$

1.3. Habitat and habitat modelling

1.3.1. A working definition of habitat and habitat suitability

The concept of habitat modelling is based on the ecological niche theory and assumes that a species or group of species prefers specific areas/places within its surrounding environment, where it can survive, grow and reproduce. Such areas are defined by specific environmental parameters/variables/factors; they are called habitats and, in accordance to Kearny (2006), the habitat should be distinguished from the ecological niche; the latter is that part of the habitat where a specific species selects as its 'home'. A habitat is a wider unit, it has a number of niches and supports a number of different species, which form a community. In rivers, for example, different species of aquatic insects may occupy the same habitat (forming a community) but different ecological niches within this habitat. Moreover, a species may occupy different niches within the same habitat throughout its life cycle.

Based on the aforementioned, and since the current thesis is focused on the aquatic environment, the following 'working definition' of aquatic habitat (hereafter called habitat) is proposed:

Aquatic habitat is the place in the river, characterized by specific environmental and hydraulic parameters, which supports the survival, growth and reproduction of one or more aquatic communities-populations

This definition implies that some areas in the river may be completely unsuitable to provide 'home' for the aquatic communities and other areas may be totally suitable, with places of varying suitability occurring among them. This gradient of habitat suitability is numerically expressed using habitat models in a scale between 0 (unsuitable) and 1 (totally suitable).

1.3.2. Habitat models

Habitat models are numerical processes and formulas (algorithms), which are based on the aforementioned concept and aim to explore and quantify the relationships between the environmental-hydraulic habitat parameters (hereafter called abiotic variables) and the distribution-response of the (aquatic) organisms (hereafter called biotic variables) to the environmental-hydraulic gradients. This process of exploring the relationship between habitat variability and biotic-ecological response (environmental-hydraulic parameters and aquatic communities) requires the following:

i. A reference hydroecological dataset - multiple observations (samples), which relate the variability of specific environmental factors with the distribution of (aquatic) organisms of interest. This hydroecological dataset is sampled in unpolluted areas with no or minor anthropogenic influence to account only for the natural ecological variation. Usually, the habitat variables studied are the flow velocity (V), the water depth (D), the type of substrate (S) and the water temperature (T), but additional or fewer parameters can be also included (see chapters 2 and 4 for details).
ii. A method to calculate the habitat suitability based on the distribution of organisms at each sample. Usually, the habitat suitability is directly related to the abundance of the organisms (Li et al., 2009; Muñoz-Mas et al., 2016) but other options, such as the use of community-based metrics have also been developed (Waddle and Holmquist, 2011; Theodoropoulos et al., 2018) (see chapter 3 for details).
iii. A method-algorithm, which will identify the correlations between habitat variability and ecological response.

What is often termed as a 'habitat model', is the third part of the aforementioned process. The first habitat model was the one described by Bovee (1986), which requires the development of three types of univariate habitat suitability curves (HSCs) based either on expert knowledge (category I - professional judgment curves), or on actual field data (categories II and III - habitat utilization and habitat preference curves) to quantify the relationship between the abiotic variables (V, D, S and/or T) and the biotic response variables (the abundance of organisms). During the last decades, complex mathematical methods evolved, including three basic types:

i. Multivariate statistical models, usually regression-oriented, which attempt to fit a curve between the abiotic predictors (environmental and hydraulic data) and the biotic response variables, based on specific assumptions about the distribution of data. Over time, these models have been enhanced to include various alternatives of the fundamental curve-fitting concept to avoid the assumptions of linearity between the predictor and response variables (Generalized Linear Models (GLMs) - McCullagh and Nelder, 1989) or to account for the cumulative influence of the predictors on the response variables (Generalized Additive Models (GAMs) - Hastie and Tibshirani, 1990).
ii. Machine learning models; a series of non-parametric algorithms, which combine regression or classification functions based on the characteristics of available data. These algorithms are able to deal with complex relationships and interactions between the environmental variables; they can handle large amounts of data with possible non-linear relationships between the predictors and are able to process complex and noisy data (Recknagel, 2001). The most widely used examples include Classification and Regression Trees (Breiman et al., 1984; Dakou et al., 2007), Artificial Neural Networks (Broomhead and Lowe, 1988; Tirelli and Pessani, 2009), Random Forests (Breiman 2001; Vezza et al. 2015; Booker, 2016) and Boosted Regression Trees (Elith et al., 2008; Theodoropoulos et al., 2017).
iii. Fuzzy-rule based models (Zadeh, 1965), often enhanced by Bayesian Belief Networks (BBNs - Pearl, 1988); based on sets of IF-THEN rules, fuzzy models convert the actual values of the predictor and response variables to membership functions ranging from 0 to 1 and calculate the habitat suitability by applying logical operators (AND/OR). These methods can handle the inherent vagueness of the input and output data, as well as the possible interaction between the predictor variables (Ahmadi-Nedushan et al., 2006) and have been applied in habitat modelling, in combination with BBNs to enhance predictive accuracy (Van Broekhoven et al. 2006; Liu et al. 2013; Lange et al. 2015).

1.3.2.1. Habitat suitability curves

In this model, the abiotic variables (usually V, D and S) are related to the habitat suitability (K)

with an index ranging from 0 (unsuitable) to 1 (totally suitable). According to the discrimination between habitat use and habitat preference applied in Bovee (1986), habitat suitability may be based on (i) the number of individuals observed in a particular microhabitat sample (N_i - habitat use) or (ii) on the quotient of N_i and the microhabitat availability (the number of the microhabitats having the same value of abiotic variable) (habitat preference). The HSCs developed using the habitat-use option are called category-II HSCs and those developed using the habitat-preference option are called category-III HSCs, both being different from the category-I HSCs, which are developed only based on expert judgment.

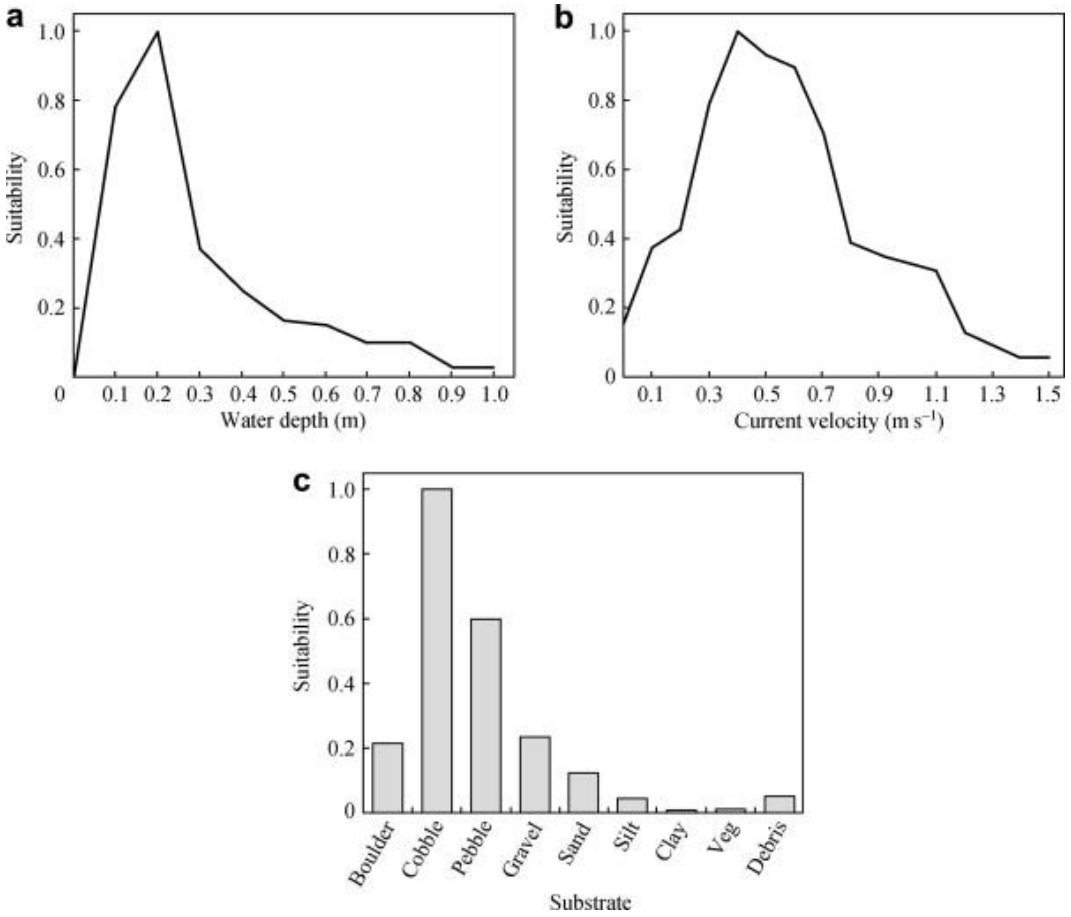

Fig. 1.6. Habitat suitability curves for water depth (a), flow velocity (b) and type of substrate (S) developed following the approach of Bovee (1986). Image from Li et al. (2009).

To develop category-III HSCs, each variable (V, D and S) is divided in bins, and the frequency of each bin (the number of individuals observed at each bin) is estimated and visualized using frequency histograms. The microhabitat availability is also visualized using histograms and the habitat preference is derived for each bin by dividing the habitat use value by the relevant availability value (Fig. 1.6). The values are normalized in a 0-1 scale. The individual habitat suitability indices (the three different HSCs, one for each abiotic variable) are then combined to form a composite index using the following equation:

$$K = \sqrt[3]{K_V \; x \; K_D x \; K_S} \qquad (1.34)$$

where,

K is the habitat suitability

K_V, K_D *and* K_S denote the individual habitat suitability values of V, D and S, respectively

1.3.2.2. Regression-based models

Instead of following a histogram-based approach, a more recent statistical process known as regression analysis is used to describe the dependence of one or more 'response' variables (in this case K) to one or more 'predictor' variables (in this case, the abiotic variables V, D and S). The general concept of curve fitting in regression analysis can be formulated as

$$Y = f(x) + e \qquad (1.35)$$

where,
Y are the actual values of the response variable for the predictor x
$f(x)$ are the modelled values of the response variable
e is the variability of the actual values around the modelled values (called 'regression residual')

The complexity of the model can be shifted from linear

$$f(x) = b_0 + b_1 x \qquad (1.36)$$

to a nth grade polynomial curve (usually 3rd or 4th grade) (Fig. 1.7)

$$f(x) = b_0 + b_1 x + b_2 x^2 + b_3 x^3 + \cdots + b_n x^n \qquad (1.37)$$

where b_0, b_1 … b_n are called 'regression coefficients'.

When multiple predictors $(x_1, x_2, \ldots, x_n)$ contribute to the determination of the response variable, the simplest form of the equation 1.35 (in which the predictors are linearly combined and the response variable has a normal distribution) becomes

$$Y = b_0 + b_1 x_1 + b_2 x_2 + b_3 x_3 + \cdots + b_n x_n + e \qquad (1.38)$$

or $$E(Y) = b_0 + b_1 x_1 + b_2 x_2 + b_3 x_3 + \cdots + b_n x_n = \mu \qquad (1.39)$$

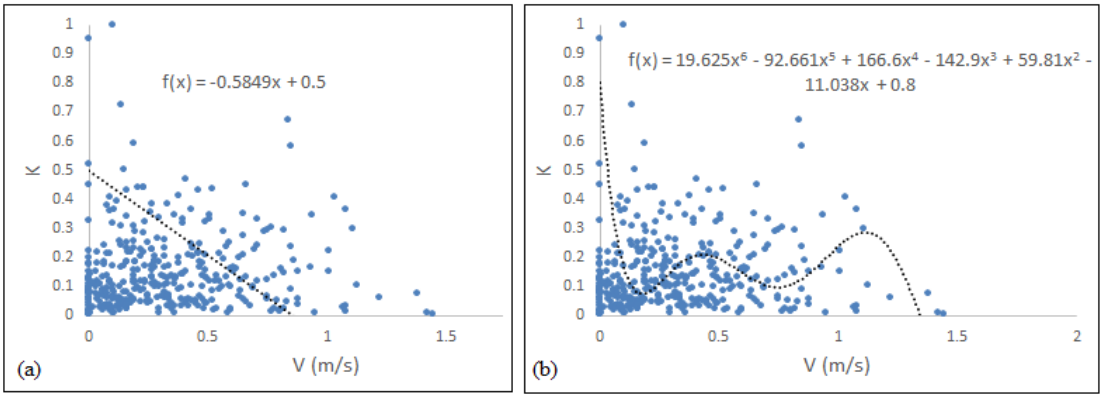

Fig. 1.7. Linear regression (a) and 6th grade polynomial regression models (b) to find the best fitting curve between the abiotic variable flow velocity (V) and the response variable habitat suitability (K)

The aforementioned linear regression model is termed as General Linear Model (GM). This model makes specific assumptions about the predictor and response variables and their relationships; the most important for habitat modelling are (i) the assumption that the response variable has a normal distribution and (ii) the assumption that the normal distribution of the response variable is based on a linear combination of the predictor variables. Moreover, it does not account for possible interactions between the predictor variables to determine the

distribution of the response variable; in habitat modelling however, K is the result of a specific V, combined with a specific D and in a specific S. Based on the aforementioned, enhanced algorithms have been developed to overcome these obstacles. Among them, the Generalized Linear Models (GLMs - McCullagh & Nelder, 1989) and the Generalized Additive Models (GAMs - Hastie & Tibshirani, 1990) have been widely used in habitat modelling.

In the GLMs, $E(Y)$ may not necessarily be equal to a linear combination of the predictor variables. This is achieved by the use of a 'link function', which is actually a transformation of $E(Y)$ to $g(E(Y))$ so that although $E(Y)$ may not be a linear combination of the predictors, $g(E(Y))$ may. Consequently, non-normal distributions of the response variable (e.g. Poisson, binomial, inverse Gaussian) are not a problem in the analysis, as long as $g(E(Y))$ is a linear combination of the predictor variables. Equation 1.38 within a GLM becomes

$$Y = f(b_0 + b_1x_1 + b_2x_2 + b_3x_3 + \cdots + b_nx_n) + e \qquad (1.40)$$

From equation 1.39, the inverse function of $E(Y)$, which is

$$g\big(E(Y)\big) = g(\mu) = b_0 + b_1x_1 + b_2x_2 + b_3x_3 + \cdots + b_nx_n \qquad (1.41)$$

is the link function; depending on the type of non-normal distribution of the response variable, different link functions are used in GLMs. Typical link functions include

(i) the logit function $g(\mu) = \log\left(\frac{\mu}{1-\mu}\right)$ (1.42)

(ii) identity $g(\mu) = \mu$ (1.43)

(iii) negative binomial $g(\mu) = \log\left(\frac{\mu}{\mu+k^{-1}}\right)$ (1.44)

where k is the ancillary parameter of the negative binomial distribution.

Still, $g(E(Y))$ must be a linear combination of the predictor variables, and in habitat modelling, predictors are not often linearly combined to predict the response variable. This can be overcome by applying the GAM models. In addition to the link functions applied in GLMs to account for a non-normal distribution of the response variable, GAMs use 'smooth functions' to additionally account for possible non-linear combinations of the predictors to determine the response variable. Thus, the equation 1.39 can be written as

$$E(Y) = b_0 + f_1(x_1) + f_2(x_2) + f_3(x_3) + \cdots + f_n(x_n) \qquad (1.45)$$

where $f_1, f_2, f_3 \ldots f_n$ the smooth functions, estimated from the data.

1.3.2.3. Boosted Regression Trees

Boosted Regression Trees (BRT) is a recent and very powerful machine-learning algorithm, which has been often used for curve-fitting. BRTs is an 'ensemble learning' algorithm; instead of searching for the most accurate model/curve (like HSC, GM and GAM), it develops multiple, internal models-predictors, and combines them to increase the accuracy of the final prediction. These models are actually decision trees, that is, schematic representations of the combined influence of the predictor variables on the determination of the response variable. In the case of BRT, this is done by applying 'gradient boosting', an optimization technique for minimizing the loss function (e in equation 1.35) by adding, at each step, a new tree that best reduces (steps down the gradient of) the loss function (Elith et al., 2008). The algorithm goes as follows (Fig. 1.8):

1. A single decision tree is initially developed, which maximally reduces e.
2. A second tree is fitted on the residuals of the previous tree. This tree may be developed using different predictor variables, which may be split at different points.
3. The algorithm is then updated to contain the two trees and the residuals of the two-tree model are calculated.

4. Another tree is fitted using the same process, the model is updated and new residuals are again calculated, in a stagewise process (existing trees are not changed as the process continues).
5. The final BRT model is a linear combination of all trees (usually hundreds to thousands) that can be thought of as a regression model where each term is a tree (Elith et al., 2008).

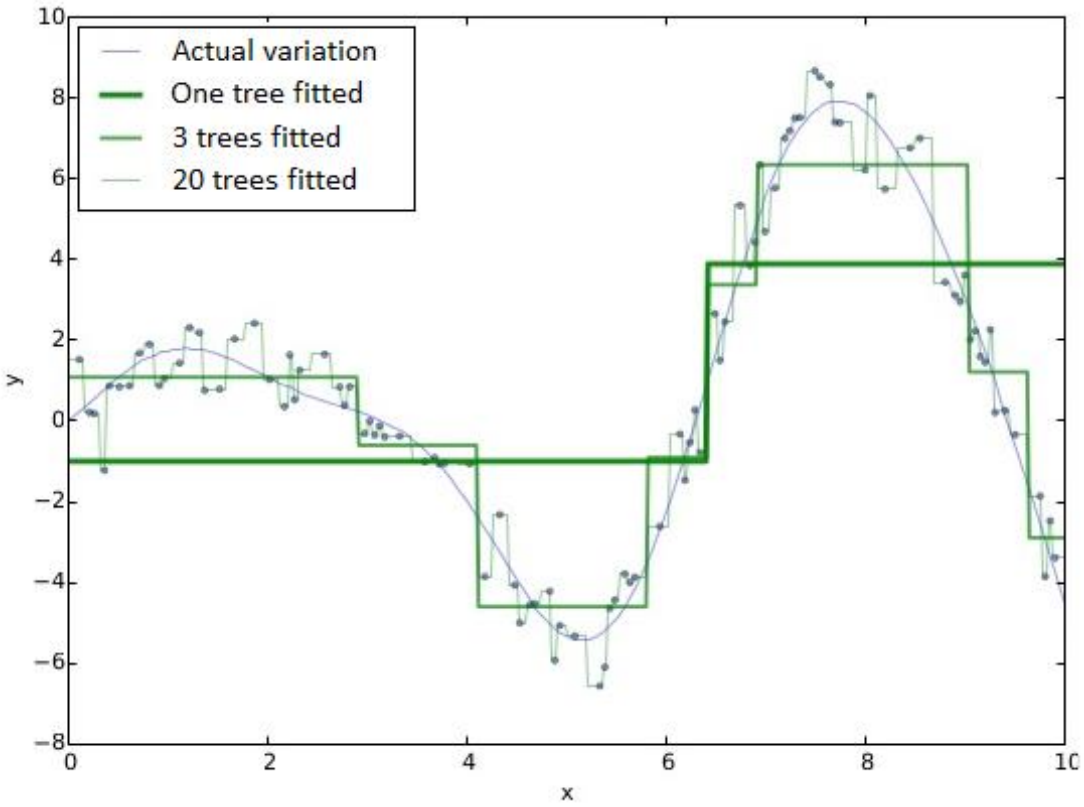

Fig. 1.8. Stagewise development of the Boosted Regression Trees algorithm. The more trees added to the model, the more accurate the prediction becomes. Image adapted from https://www.slideshare.net/DataRobot/gradient-boosted-regression-trees-in-scikitlearn

1.3.2.4. Random Forests

It has been argued that in habitat modelling, the prediction of a precise numerical output is not of much importance and probably, such a 'precise' habitat model would not be trusted by ecologists (Van Broekhoven et al., 2006); a classified output (for example a habitat suitability with classes ranging from 0-unsuitable to 1-excellent) is considered more informative and probably more appropriate. Consequently, regression-based models have been often replaced by classification algorithms. Random Forests (RF) is such an algorithm that, although it can also be used as a curve fitter (regression), it has been often used as an accurate classifier. Similarly to BRT, RF is an ensemble learning model; it creates multiple (internal) outputs and combines them to increase the accuracy of the final prediction (Fig. 1.9). The RF algorithm, simultaneously (unlike the stagewise manner of BRT) generates a large number of decision trees, which are then aggregated to compute the final classification. In detail (Peters et al. 2007; Vezza et al. 2015):

1. A bootstrap subset (resampled with replacement) X_i containing approximately 2/3 of the elements of the original dataset X is selected as the training dataset (the set of observations with known output, from which the algorithm will learn the relationships

between the predictor and the response variables). The elements not included in the training dataset are referred to as out-of-bag (OOB) data for that bootstrap sample.

2. X_i is used to grow an unpruned classification tree (unlike the BRT algorithm, which uses pruning) to the maximum depth but, rather than choosing the best binary split among all predictive variables, m predictor variables are randomly selected and the best binary split is chosen among these variables.
3. Each tree is fully grown and used to predict OOB observations. Prediction is applied according to the majority vote of the ensemble of *k* trees (the predictions from all the trees are combined to predict an observation class as well as a probabilistic prediction output for that observation).

As more trees are added to the forest, the OOB error is reduced and the predictive accuracy of the 'random forest' increases.

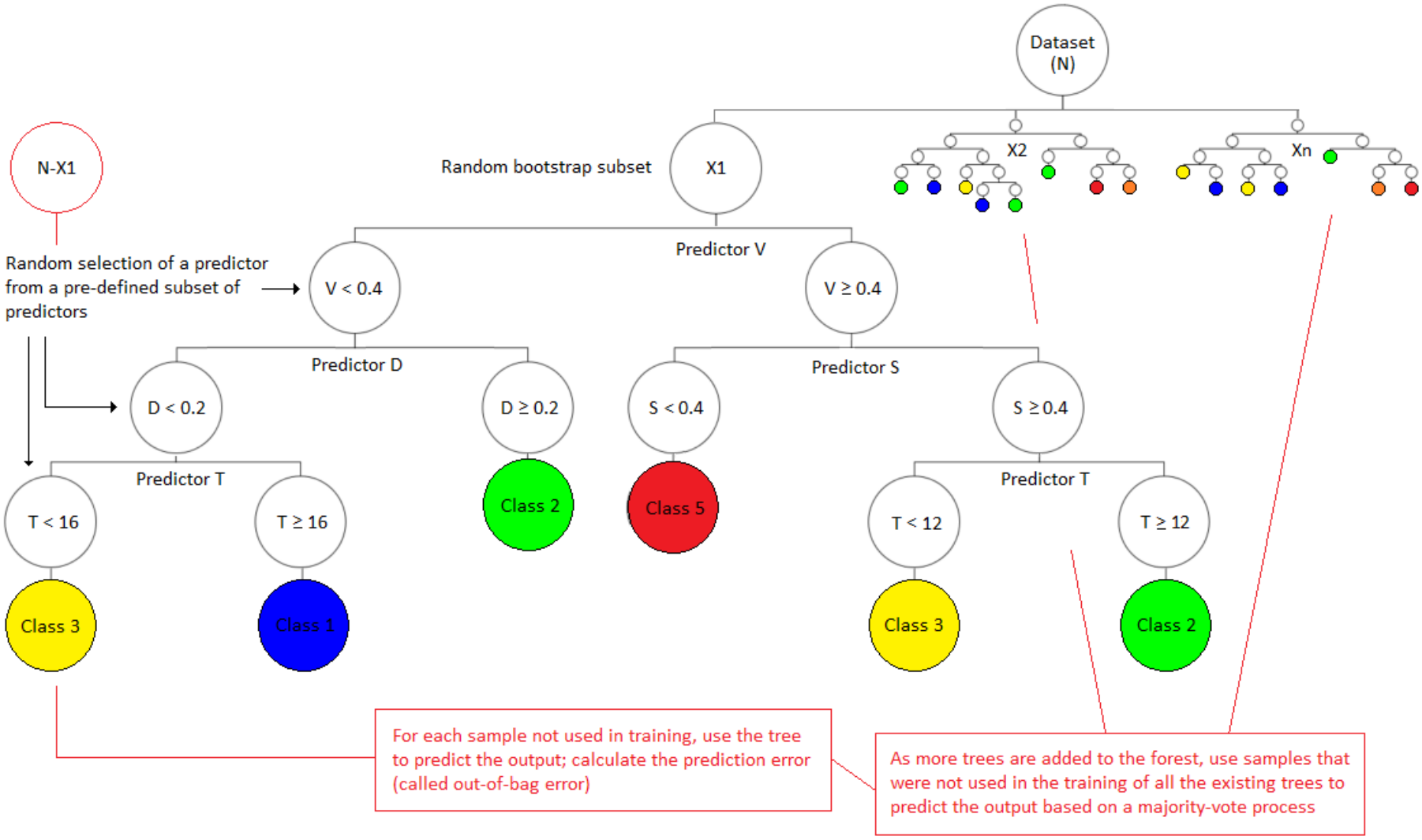

Fig. 1.9. Schematic representation of the Random Forest algorithm

1.3.2.5. Fuzzy logic

In fuzzy logic (Zadeh, 1965) predictions are made based on a rule-based approach. A fuzzy rule-based algorithm can handle the inherent vagueness of the input and output data, as well as the possible interaction between the predictor variables (Ahmadi-Nedushan et al., 2006). The basic concept of a fuzzy rule-based algorithm is that the actual, numerical values of the predictor variables are converted to partially overlapping classes (fuzziness is introduced), which are called membership functions and range from 0 to 1 (Fig. 1.10); a set of IF-THEN rules is developed based on a training dataset and the value of the response variable is predicted by the use of logical operators (AND/OR). Based on the detailed description provided in Ross (2010), the steps of a fuzzy rule-based algorithm are the following:

1. Fuzzification of the input variables (predictors): In this step, partially overlapping classes called membership functions or fuzzy sets are defined for each predictor and the actual, numerical values (called crisp sets) of each predictor are assigned to one or more membership functions. By this process, the crisp sets of each input variable are converted to a fuzzy 'membership degree', ranging from 0 to 1 for each membership function. Then the process continues using the membership degree of each fuzzy set (corresponding to a crisp numerical input) instead of using the crisp input itself. For example, a depth value of 0.14 m may yield a membership degree of 0.7 (out of 1) for the 'shallow' fuzzy set and 0.3 for the 'very shallow' fuzzy set (Fig. 1.10). Then the process continues based on the fuzzy sets instead of the crisp numerical inputs.
2. Application of a fuzzy operator (AND or OR) and development of IF-THEN rules: After the fuzzification of the predictor variables, based on the training dataset (with *a priori* known values of the response variable for each combination of the predictors), logical operators, either the AND (min) or the OR (max), are applied to the membership degree of each fuzzy set (defined in the previous step) and the derived, minimum or maximum value (depending on the selected operator) is assigned to the membership function of the output variable, in this case the habitat suitability (K). If for example, K is classified in five classes (f_1, f_2, f_3, f_4, f_5, which may correspond to bad, poor, moderate, good and high K respectively), the application of a logical operator would result in

   $$f_4(K) = min\,[f_2(V), f_3(D)] \quad (1.46)$$
   $$f_3(K) = min\,[f_3(V), f_2(D)] \quad (1.47)$$
   $$f_4(K) = min\,[f_2(V), f_4(D)] \quad (1.48)$$

   where,
   f_i is the membership function (fuzzy set) of each input and output variable
   V the flow velocity
   D the water depth
   K the habitat suitability

3. Aggregation of outputs: When different combinations of the predictors' fuzzy sets result in the same K class, these outputs are aggregated usually using the OR (max) operator; thus, the membership degree of the combined output (F_j) is the maximum membership degree observed for the specific K class:

   $$F_j = max\,[f_i^1(K), f_i^2(K), \dots, f_i^n(K)]$$

4. Defuzzification: In this step, a final 'crisp' K value is derived from the integration of the fuzzified predictor combinations with the different K classes (the membership degrees of all fuzzy sets are combined). There exist various defuzzification options-methods; among them the most widely used are (i) centroid, (ii) maximum membership, (iii) weighted average and (iv) mean of maximum.

Centroid: $K = \frac{\int xf(x)dx}{\int f(x)dx}$ (1.49)

Maximum membership: $K = \max[f(x)]$ (1.50)

Mean of maximum: $K = \frac{x_a + x_b}{2}$ (1.51)

Weighted average: $K = \frac{\sum_{i=1}^{n} \overline{x_1} f(\overline{x_1})}{\sum_{i=1}^{n} f(\overline{x_1})}$ (1.52)

where,
$f(\overline{x_1})$ is the membership degree at the average value $\overline{x_1}$ of each fuzzy set
x_a is the first value with the highest membership degree of the class with the highest membership
x_b is the last value with the highest membership degree of the class with the highest membership

1.3.2.6. Fuzzy rule-based Bayesian algorithm

This algorithm uses the Bayesian joint probability and a classification system based on an 'expected utility' function (Brookes et al., 2010) and can be summarized in three steps:

1. Fuzzification of the input variables (predictors): This is the same step followed in the fuzzy-logic-based algorithm described previously. The input predictors (crisp values) are fuzzified in user-defined overlapping classes (fuzzy sets).
2. Calculation of the Bayesian joint probability: The joint probability for independent events is calculated as

   $P(A \cap B) = P(A|B)P(B) = P(B|A)P(A)$ (1.53)

   where,
   $P(A \cap B)$ is the joint probability of event A and event B occurring together
   $P(A|B)$ is the conditional probability of event A occurring given that event B occurred
   $P(B|A)$ is the conditional probability of event B occurring given that event A occurred

   In the case of V, D and S predictors, they are considered independent events and their joint probability is calculated by replacing $P(A|B)$ with $P(A)$. For example, the joint probability of V being 0.5 m/s and the D being 0.2 m, given their probabilities P(V:0.5 = 0.8) and P(D:0.2 = 0.3) is 0.8 x 0.3 = 0.24. The fuzzy membership degrees (fuzzified input values) from step 1 are used as the probabilities of occurrence of each input.
3. Classification K in habitat suitability classes: The algorithm applies an expected utility function (Brookes et al., 2010) to determine the final K-class value. A score is assigned to each K class (in our case bad-0.1, poor-0.3, moderate-0.5, good-0.7, high-0.9) and each value is multiplied by the joint probability of occurrence of the specific K class as follows:
   $EU(A) = \sum_{i=1}^{n} P(x_i|A)U(x_i)$ (1.54)

   where,
   $EU(A)$ is the expected utility of action or event A
   $P(x_i|A)$ is the probability of action or event A
   $U(x_i)$ is a utility weight to convert a state to numerical values

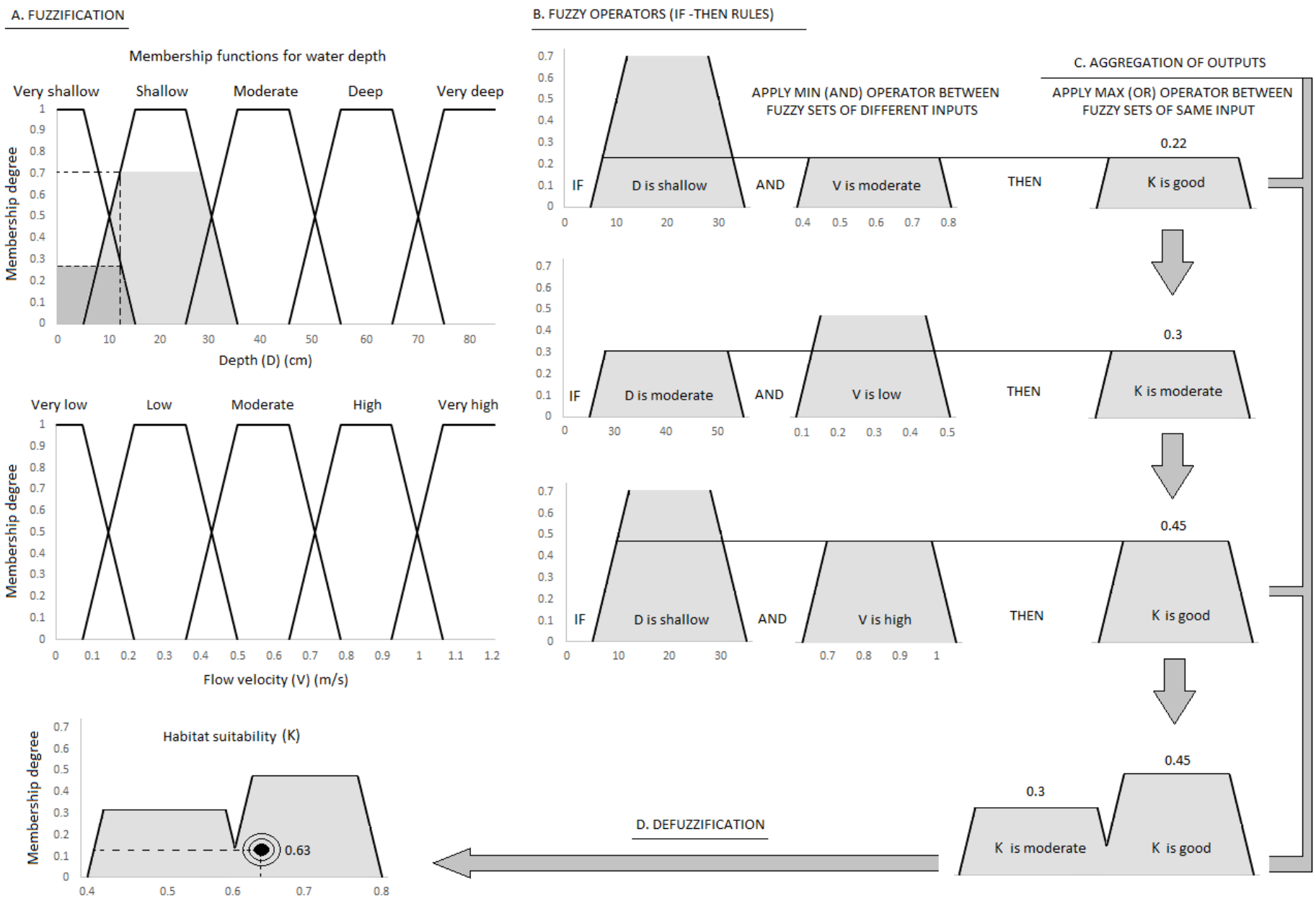

Fig. 1.10. Schematic representation of the Fuzzy Logic algorithm

1.4. Ecological indicators - the benthic macroinvertebrates

Freshwater macroinvertebrates, benthic invertebrates, benthic macroinvertebrates or simply 'macroinvertebrates' are small (approx. 0.5 mm - 2 cm), bottom-dwelling invertebrate animals (including insects -e.g. dragonfly or stonefly larvae-, worms, leeches and snails), which are visible to the naked eye (hence, macroinvertebrates) (Fig. 1.11, 1.12). BMs have long been considered reliable indicators for ecological monitoring (Rosenberg and Resh, 1993). In Europe, they have been used as biological indicators in the ecological monitoring of surface waters within the implementation of the Water Framework Directive 2000/60/EC (European Union Council, 2000), together with the fish fauna, aquatic macrophytes and diatoms. The generic concept of using benthic macroinvertebrates as ecological indicators is that the benthic community of polluted sites will differ from the benthic community of unpolluted sites, with a degree, which is predictable and can be quantified to reflect the relevant pollution load. There are currently numerous studies worldwide, which show that the magnitude of anthropogenic impact in a river reach (either the surrounding land-use patterns or the in-stream chemical pollution) is strongly correlated with benthic-macroinvertebrate metrics reflecting the status of the benthic community (Stephenson and Morin, 2009; Theodoropoulos and Iliopoulou-Georgudaki, 2010; Kappes et al., 2011; Sundermann et al., 2013; Theodoropoulos et al., 2015a).

Fig. 1.11. Some taxa of benthic macroinvertebrates. Image from https://dep.wv.gov/WWE/watershed/bio_fish/Pages/Bio_Fish.aspx

Fig. 1.12. Laboratory analysis of benthic macroinvertebrates (one by one, the benthic macroinvertebrate individuals are transferred from the sample to the Petri dishes and then stored for taxonomic identification).

Benthic macroinvertebrates are categorized in varying levels of similarity (classes, families, genus, species etc.). In ecological monitoring, most BM-based metrics use the family level for analyzing and quantifying ecological alteration and, consequently, anthropogenic impact. The use of benthic macroinvertebrates in hydrodynamic habitat models to develop environmental flow predictions has not been so popular, with the relevant studies being primarily focused on fish (Milhous and Waddle, 2012). However, river habitats appropriate for fish survival and diversity may not benefit macroinvertebrates or other aquatic organisms. Consequently, the integration of all elements of the aquatic ecosystem into habitat modelling is a crucial step towards robust, holistic environmental flow recommendations. Benthic macroinvertebrates are considerably less mobile than fish, with less tolerance to changes in the water volume and a reduced ability to colonize habitat-poor areas (Gore, 1989). Related studies have shown that, in contrary to fish that may be limited or not present in many small streams, a diverse benthic macroinvertebrate fauna is supported and benthic macroinvertebrates are abundant in most low-order streams (Barbour et al., 1999). As several authors have acknowledged that benthic macroinvertebrates are ideal candidates for the development of hydroecological models (Niu and Dudgeon, 2011), they are currently increasingly used in model-based environmental flow assessments (Waddle and Holmquist, 2013; Komínková et al., 2017; Theodoropoulos et al., 2018b, 2018c).

1.5. Purpose of the thesis

The ultimate purpose of this thesis was to develop and demonstrate a hydrodynamic habitat modelling methodology using freshwater macroinvertebrates as ecological indicators. To reach this outcome, specific scientific questions were researched and answered, and the following research gaps were covered:

1. The response of freshwater macroinvertebrates to flow variation was researched (chapter 2)
2. The habitat preferences of benthic macroinvertebrates were developed using habitat suitability curves and BM-metrics-based approaches (chapters 2 and 4)
3. A new command-line software implementing fuzzy logic and fuzzy rule-based Bayesian algorithms to simulate-predict habitat suitability was developed in FORTRAN (chapter 3)
4. The predictive performance of multiple state-of-the-art habitat modelling algorithms was researched for benthic macroinvertebrates (chapter 4)
5. Two case studies using a two-dimensional hydrodynamic model were applied to demonstrate the developed BM-based, hydrodynamic habitat modelling methodological framework (chapters 5 and 6)
6. The use of hydrodynamic habitat models to develop environmental flow scenarios was researched and the results were compared with hydrology-based environmental flows (chapter 6)

Chapter 2

Response of benthic macroinvertebrates to natural flow variation and hydrological alteration

2.1. Overview

Physical habitat, a major 'driver' of the distribution, abundance and diversity of aquatic communities in riverine ecosystems, is fundamentally determined by flow variability (Allan, 1995; Bunn and Arthington, 2002). Instream organisms are affected by hydrological processes, either directly due to the applied hydrodynamic forces of varying magnitude (which depend on the hydraulic properties of the water) (Giller and Malmqvist, 1998) or indirectly, by determining the composition of substrate, the water chemistry and the availability of physical habitat (Hart and Finelli, 1999). As the successful conservation and management of aquatic ecosystems requires deep knowledge of the underlying hydrological-hydroecological processes (Acreman and Ferguson, 2010), research has long been focused on quantifying the response of aquatic communities to natural or anthropogenic hydrological and hydraulic variation (Poff and Zimmerman, 2010; Caiola et al., 2014; Papadaki et al., 2016). Benthic macroinvertebrates (BMs) have often been used as the target aquatic community in such studies (Gibbins et al., 2001; Theodoropoulos et al., 2010; Karaouzas et al., 2011; Armanini et al., 2014) and they have been proven reliable ecological quality indicators (Rosenberg and Resh, 1993; Theodoropoulos et al., 2015). Still, their use in hydroecological studies is limited, and currently, existing literature on the response of benthic macroinvertebrates to flow variability is primarily focused on extreme hydrological events, such as floods (Herbst and Cooper, 2010; Mesa, 2010; Mundahl and Hunt, 2011) and droughts (Lake, 2011; Skoulikidis et al., 2011; Chessman, 2015), occurring either naturally within the seasonal or interannual variation in the hydrological cycle, or artificially due to water regulation by dams and water abstractions. Their response to flow variation of moderate magnitude remains insufficiently researched.

A flood has been defined in the EU Floods Directive as 'the temporary covering by water of land not normally covered by water' (European Commission, 2007). The effects of floods on aquatic communities have been well documented (Leigh et al., 2015); they are related to the alteration of physical habitat provoked by the increased flow velocity/discharge, which in turn alters the composition of the instream assemblages. During and after floods, large amounts of organic and inorganic matter are transferred downstream (Lake, 2000), affecting the water chemistry and as a consequence, community composition. In-stream productivity, retention of particulate organic matter and decomposition are also affected (Hladyz et al., 2012), channel morphology is altered, macrophytes are translocated and other aquatic organisms are dislodged and transferred downstream (Brittain and Eikeland, 1988; Lake, 2000). This results in reduced macroinvertebrate density and diversity (Gjelrov et al., 2003; Melo et al., 2003; Suarez et al., 2017), while taxonomic richness may be reduced or remain constant (Rempel et al., 1999; Effenberger et al., 2008). Macroinvertebrates however have behavioral, morphological and physiological adaptations, evolved over large time scales to resist physical disturbances. Such adaptations to prevent dislodgment include small-sized bodies and specialized structures such as mucilage (Biggs and Hickey, 1994), hooks (Crosskey, 1990) and suckers (Frutiger, 1988), while many animals actively drift to microhabitats which offer protection from floods, usually called refugia (Negishi and Richardson, 2006; Fuller et al., 2010).

Despite the aforementioned assiduous research, studies on ecologically significant habitat features associated with river morphology and flow regime still remain scarce (Belmar et al., 2013). In combination with the lack of studies examining the response of freshwater communities to disturbances of smaller magnitude of hydrological alteration (between 0 - 50% of the naturally occurring flow), the development of quantitative relationships between ecological responses and altered flow regimes is generally inhibited (Poff and Zimmerman, 2010). Such relationships however are of critical importance to develop robust environmental flow recommendations downstream of anthropogenic activities provoking hydrological alteration, while they comprise essential input for advanced hydrodynamic habitat modelling approaches, which offer water managers and stakeholders the ability to select the optimal, among various environmental flow scenarios (Waddle and Holmquist, 2011; Theodoropoulos

et al., 2015a), with the purpose of maintaining the integrity and functionality of freshwater ecosystems.

2.2. Purpose of the chapter

This chapter researches and describes the response of benthic macroinvertebrates to natural flow variability. Hydrological, hydraulic and BM data were collected from four sites in Greek rivers before and after a heavy rainfall event, which in turn resulted in a high flow event of moderate magnitude. Differences in the macroinvertebrate communities between the pre- and post-impact samples (abundance, diversity, taxonomic richness and Ephemeroptera-Plecoptera-Trichoptera richness) were examined. Moreover, hydroecological relationships between hydraulic-habitat variability, in terms of flow velocity, water depth and substrate type, and the BM metrics were researched, with the purpose of calculating optimal (suitable) ranges for the aforementioned parameters and thus developing preliminary habitat suitability criteria for benthic macroinvertebrates.

2.3. Study area

The mountainous reaches of four rivers in central Greece were sampled for hydrological and ecological data (Fig. 2.1). The selected reaches are characterized by natural landscape with no or very minor anthropogenic activities, mountainous relief with altitudes ranging from 407 to 972 m, large areas with evergreen forests mainly composed of firs belonging to the species *Abies cephalonica* and *Abies borisii regis*, which are often mixed with deciduous forests of *Quercus ceris, Cornus sp.* and *Fagus sp.* The riparian vegetation is composed of thick riparian forests including plane trees (*Platanus orientalis*), willows (*Salix alba*), poplars (*Populus nigra*), alders (*Alnus glutinosa*) and ash trees (*Fraxinus angustifolia*).

The study area has a temperate mediterranean climate, characterized by hot, dry summers and cold, wet winters, with temperatures ranging between 0 ^{o}C (or lower) and 35 ^{o}C (or higher during extreme events). The flow regime is highly seasonal, influenced by the amount of precipitation, most of which falls between October and April (maximum in January), with the driest months being July, August and September (minimum rainfall during August). Due to the high variety of climatic subtypes resulting from the influence of the topography on the incoming air masses from the central Mediterranean Sea, we selected meteorological stations, near each sampling area to describe the particular microclimatic conditions (Theodoriana, Pertouli and Koniakos at altitudes of 924, 1170 and 840 m respectively) by deriving mean monthly precipitation values for the period 2010 - 2015 (Fig. 2.2). The maximum and minimum average precipitation for Theodoriana and Koniakos stations was in January (395.7 and 158.2 mm respectively) and August (48.5 and 24 mm respectively). For the Pertouli station, the maximum values were observed in October (212.9 mm) and the minimum in July (23.12 mm).

Sampling was applied prior to (August 2015) and after (October 2015) a heavy rainfall event, which took place between the 21st and 24th of October, 2015. The precipitation observed during the event was 117 mm at the Theodoriana station (40% of the month's average rainfall), 57.6 mm at the Pertouli station (30% of average) and 89.8 mm at the Koniakos station (110% of average).

2.4. Site selection and sampling periods

Four reference sites were selected (Fig. 2.1; Table 2.1) according to the European guidelines for reference site selection (REFCOND - WFD CIS Guidance Document No. 10, 2003) in order to assess only the effects of flow-related changes and avoid possible bias of the results from pressures resulting from water quality degradation. At each site, a maximum of 20 rectangular microhabitats of 0.0625 m^2, (combinations of flow velocity, water depth and substrate type) was sampled prior to (August 2015) and after (October 2015) the high flow event, resulting in a dataset of 142 microhabitats spanning over two periods. Detailed characteristics of each

microhabitat are shown in table A1. Three additional unpolluted sites, not impacted by the high flow event, were sampled during the same periods to account for possible seasonal influence on the results of the study (and as indicated and supported by previous literature (Lazaridou-Dimitriadou, 2002), no seasonal variation was observed).

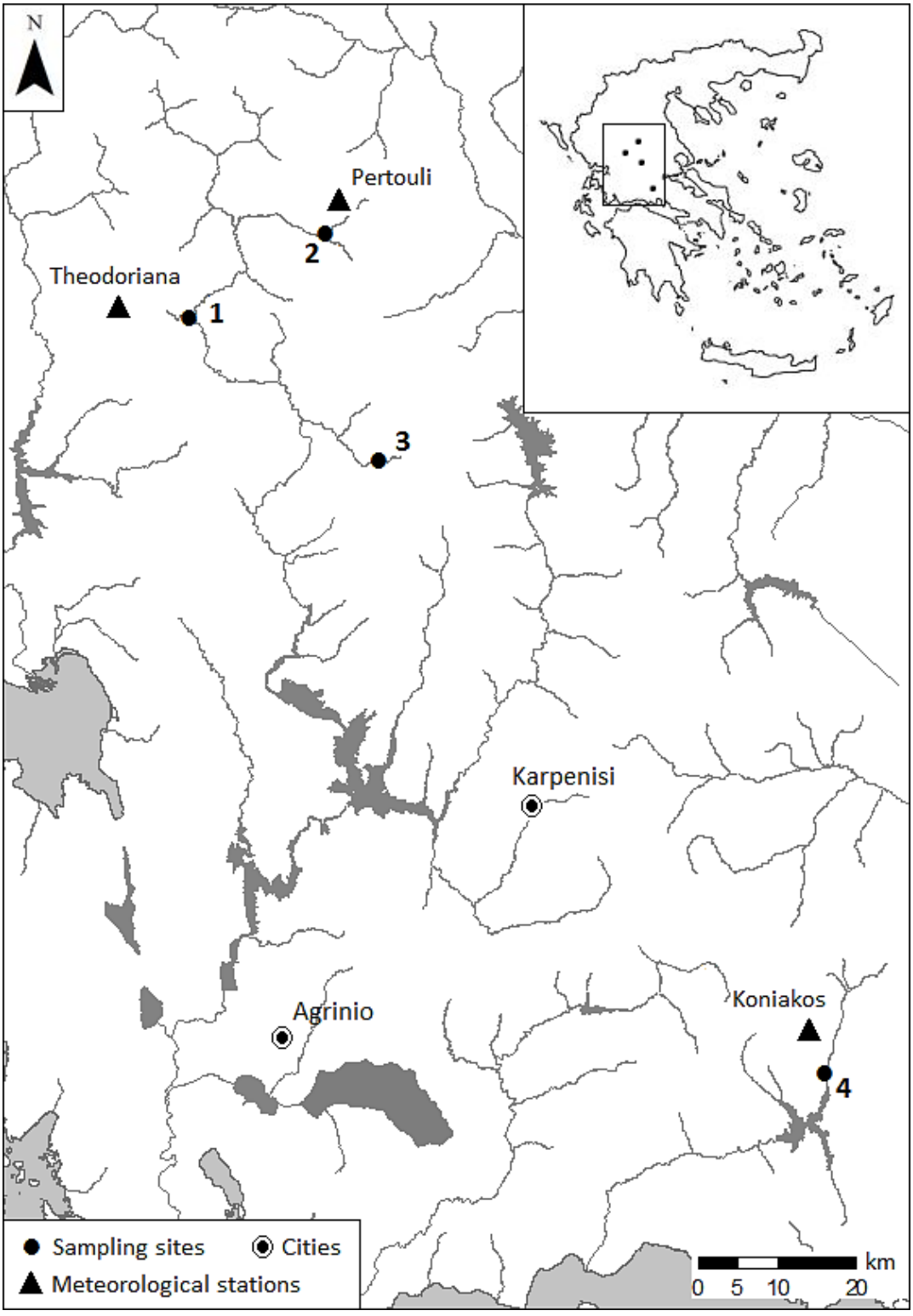

Fig. 2.1. Map of the study area

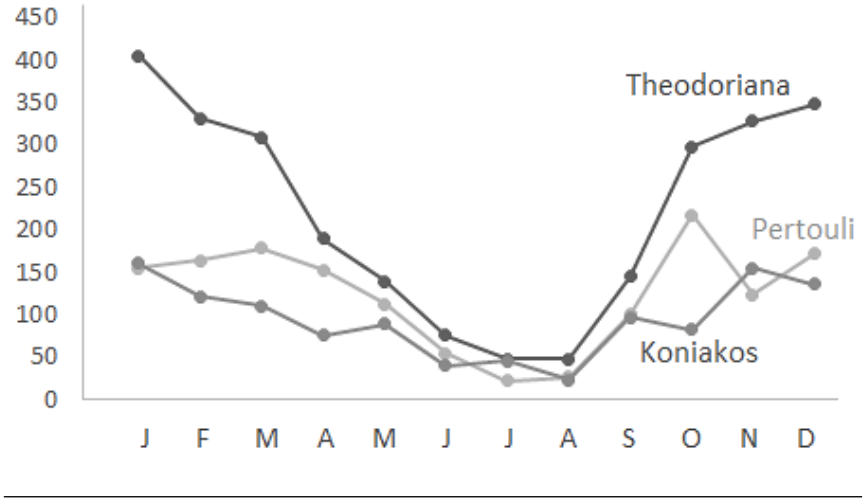

Fig. 2.2. Average monthly precipitation (mm) of the three meteorological stations for the period 2010 - 2015

Table 2.1. Physicochemical characteristics of the selected sites

	Altitude (m)	Catchment area (km^2)	Distance to source (km)	Strahler order	High flow event	Temperature (°C)	pH	DO (mg/L)	DO (%)	Conductivity (µS/cm)	TDS (mg/L)
1	659	56.27	2.8	1	Before	18.9	7.9	7.36	87.1	231	113
					After	9.6	8.2	9.83	92.8	224	113
2	972	49.07	6.68	2	Before	19.9	8.2	9.17	90.7	340	169
					After	8.9	8.1	10.27	95.4	214	108
3	563	81.14	2.64	1	Before	18.5	8.1	9.1	104.3	289	148
					After	9.3	8.2	10.74	98.8	268	134
4	407	221.51	15.46	3	Before	23.8	8	8.79	105	324	162
					After	13	8.3	8.85	88.5	284	142

2.5. Environmental and hydraulic-habitat data

Water temperature, dissolved oxygen (DO), electrical conductivity and total dissolved solids (TDS) were measured using the Aquaread AP-2000 Multiparameter Meter. Water samples were afterwards collected in plastic bottles (250 mL), stored at 4 ^{o}C, transferred to the lab, and analyzed for major ions (NO_3^-, NO_2^-, NH_4^+ and PO_4^{3-}) using the Merck Nova 60 Spectroquant Photometer, with the results indicating that all sites conformed to the REFCOND guidelines for reference site selection (NO_3^-<0.5 mg/L; NO_2^-<0.3 mg/L; NH_4^+<0.01 mg/L; PO_4^{3-}<0.15 mg/L).

At each microhabitat, flow velocity, water depth and substrate were recorded. Flow velocity (V) was measured using the Swoffer 2100 current velocity meter, water depth (D) was measured using a water-depth measurement rod and substrate (S) was visually assessed using the categories defined by Schneider et al. (2010).

2.6. Benthic macroinvertebrates

Immediately after the hydrological-hydraulic measurements, benthic macroinvertebrates were sampled at each microhabitat using a 0.25 x 0.25 m surber sampler with a mesh size of 500 μm. Samples were preserved in plastic bottles containing 70% ethanol. In the lab, all specimens from each sample were sorted and identified at the family level using a stereo microscope and macroinvertebrate identification guides for the Mediterranean region (Campaioli et al., 1994; Tachet et al., 2010; Patsia and Lazaridou, 2011). The relative abundance of Functional Feeding Groups (FFGs) and metrics describing the integrity of benthic communities including macroinvertebrate abundance, taxonomic richness (Ntaxa), diversity (Shannon's index) and EPT richness (EPTtaxa) were calculated using the ASTERICS 3.1.1 software.

2.7. Statistical analysis

Samples were grouped using the Non-metric Multidimensional Scaling (NMDS) procedure with the Bray-Curtis distance measure, implemented in the PRIMER 6 statistical software. NMDS is an ordination technique, in which samples are allocated to a two-dimensional or three-dimensional space based on their ranked dissimilarity, in a concept that distant samples will have more differences than neighboring samples. Count biological variables (abundance, Ntaxa, EPTtaxa, Shannon's diversity index) were square root transformed and percentage variables (%FFGs) were log-transformed to approximate normality and homoscedasticity (Quinn and Keough, 2002; Leps and Smilauer, 2003; George and Mallery, 2010). The transformed data were afterwards re-tested for heterogeneity of variance using the Levene's test (Levene, 1960) and independent sample t-tests were applied to identify macroinvertebrate community differences between the microhabitats sampled prior to and after the high flow event, using the IBM SPSS 22.0 statistical package. For pre- and post-impact groups, failing to meet the Levene-test's criteria, Welch's t-test was used instead of Student's t-test.

To examine preliminary hydroecological relationships, Boosted Regression Tree (BRT) models were developed to investigate the response of the selected BM metrics (abundance, Ntaxa, EPTtaxa and Shannon's diversity index) to the environmental-hydraulic predictors (high flow event, site/location, substrate type, depth, bed flow velocity and average flow velocity). As previously described BRT is a relatively new and powerful statistical model used efficiently to explain and predict the response of aquatic communities to environmental variability (Leathwick et al., 2006; Leclere et al., 2011; Waite et al., 2014; Pilière et al., 2014). The main advantages of BRT are the ability of fitting complex nonlinear relationships and the enhanced reliability in identifying predictors' interactions without being affected by outliers (Elith et al., 2008). BRTs are considered to have increased predictive power against Generalized Linear Models (GLM), Classification and Regression Trees (CART) (Leclere et al., 2011) and Generalized Additive Models (GAM) (Leathwick et al., 2006). BRT models were fitted and run in R version 3.1.0 (the R Foundation for Statistical Computing, 2014), using the dismo package v1.0-15 (Hijmans et al., 2016). A bag fraction of 0.5, a learning rate of 0.002 and a tree complexity of 2

were used to develop the models, which achieved at least 1000 trees (Table A4), following the rule of thumb suggested by Elith et al. (2008). Backwards elimination of variables was performed using the simplification function in dismo. The remaining variables were afterwards used to develop the final BRT model. The BRT models were developed using untransformed data, according to Elith at al. (2008).

2.8. Results

A total of 6905 BM specimens (individuals) belonging to 135 taxa were isolated and identified from the 142 microhabitats collected before and after the high flow event. The allocation of microhabitat samples to the three-dimensional space according to the NMDS procedure showed a clear differentiation between the pre- and post-impact samples, indicating structural differences in their BM communities (Fig. 2.3).

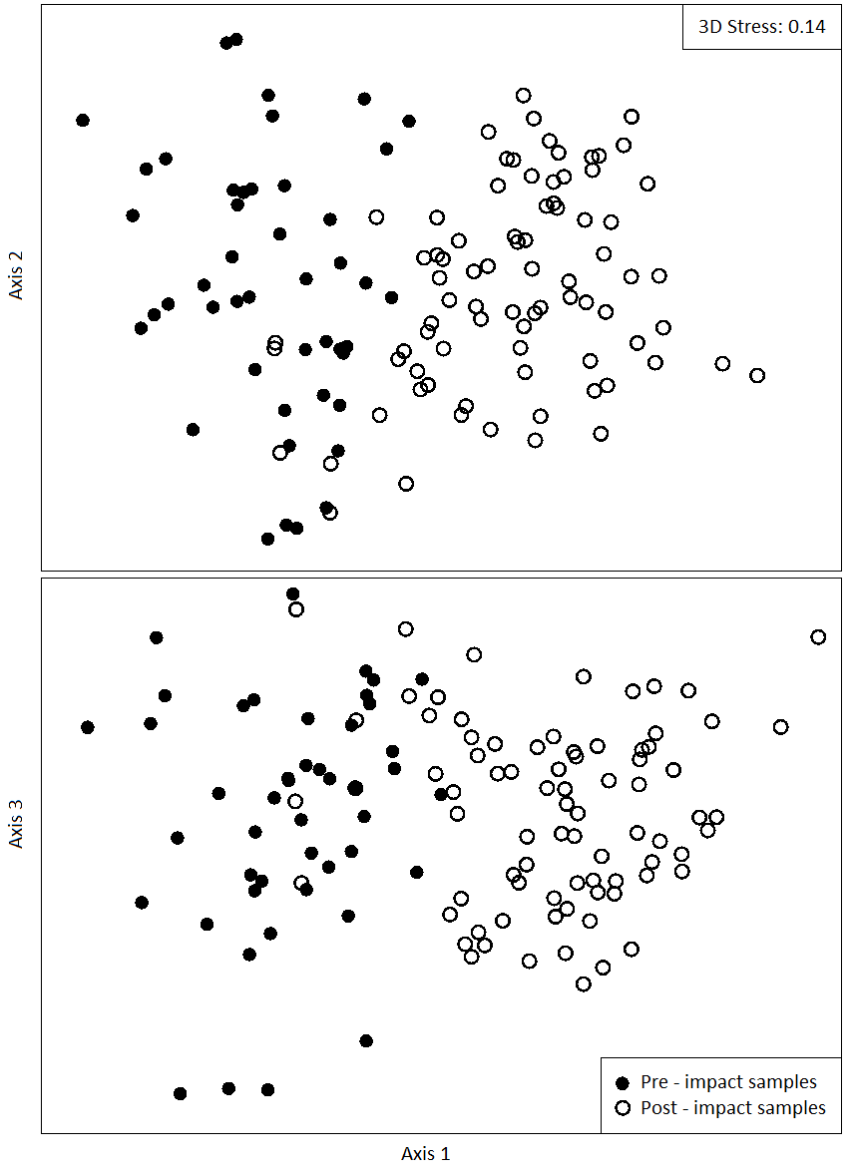

Fig. 2.3. Grouping of microhabitats samples in the three-dimensional space according to the NMDS procedure

On average, macroinvertebrate abundance showed a 9.5-fold decrease between the pre- and post-impact samples (mean ± SE, pre-impact: 80 ± 7 ind, post-impact: 8 ± 1 ind). Taxa

richness decreased by 2.5 times the pre-impact values (mean ± SE, pre-impact: 10 ± 0.4, post-impact: 4 ± 0.4), EPT richness showed a 2-fold decrease (mean ± SE, pre-impact: 6 ± 0.2, post-impact: 3 ± 0.3) and diversity showed a 1.6-fold decrease (mean ± SE, pre-impact: 1.6 ± 0.05, post-impact: 1 ± 0.1), with all differences being statistically significant ($p<0.05$; Table A2). Statistically significant changes were also detected in the relative abundance of all FFGs between the pre- and post-impact samples. The relative abundance of miners decreased by 5 times the pre-impact values (mean ± SE, pre-impact: 2.5 ± 0.28, post-impact: 0.6 ± 0.23). Gatherers/collectors showed a 1.6-fold decrease (mean ± SE, pre-impact: 28.4 ± 1.1, post-impact: 17.8 ± 2.15), active filter feeders showed a 6.1-fold decrease (mean ± SE, pre-impact: 4.9 ± 0.54, post-impact: 0.81 ± 0.4) and the relative abundance of passive filter feeders increased by 3.25 times the pre-impact values (mean ± SE, pre-impact: 4.65 ± 0.8, post-impact: 13.6 ± 2.1). The relative abundance of grazers/scrapers decreased 0.9 times the pre-impact values (mean ± SE, pre-impact: 26.2 ± 0.98, post-impact: 23.9 ± 2), shredders showed a 1.9-fold decrease (mean ± SE, pre-impact: 4.45 ± 0.66; post-impact: 2.89 ± 0.64) and parasites showed a 7-fold decrease (mean ± SE, pre-impact: 2.42 ± 0.27, post-impact: 0.35 ± 0.2) (Table A2).

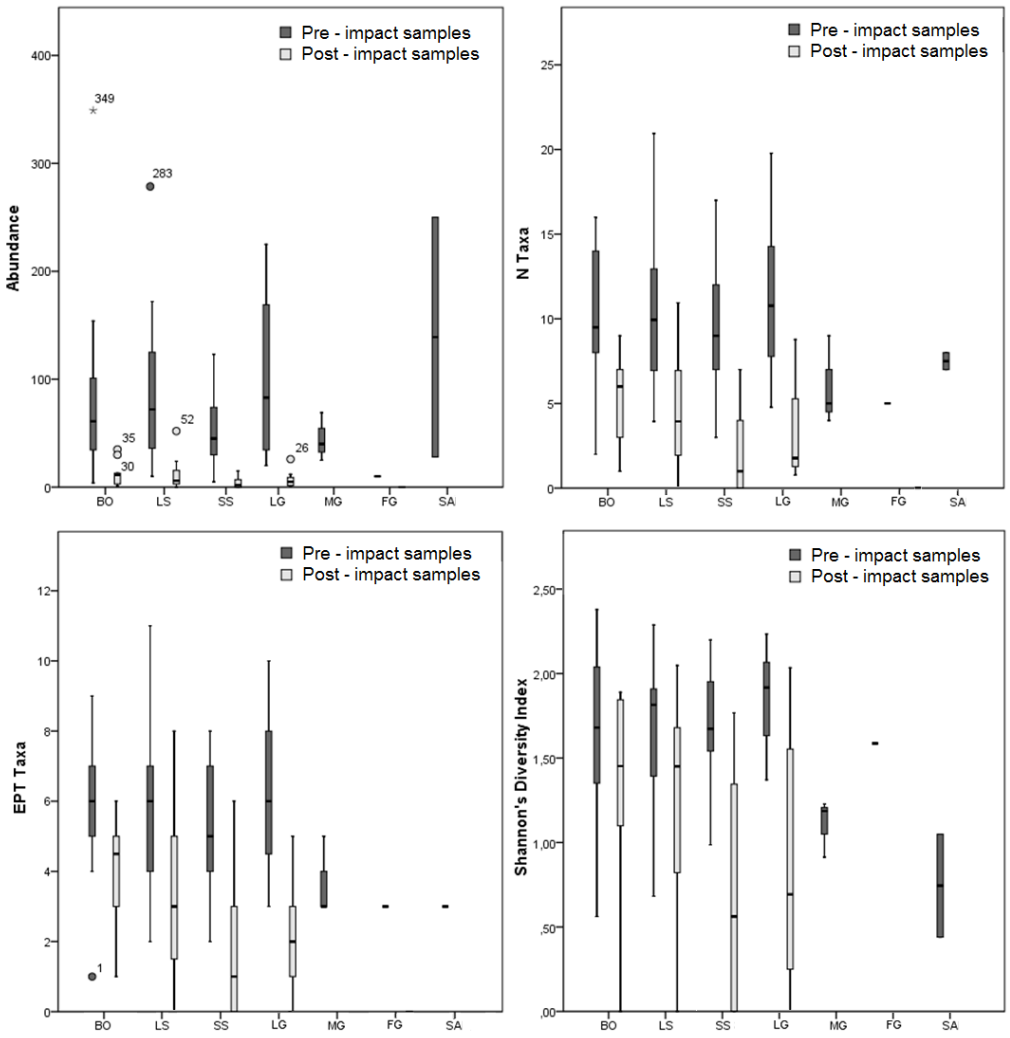

Fig. 2.4. Box plots of the macroinvertebrate metrics per substrate type of the pre- and post-impact samples. Each box shows the median within the box, the 25th and 75th percentile as the upper and lower margins of the box, and the 95% confidence interval as error bars. Dots indicate outliers, asterisks indicate extreme outliers. BO: Boulders, LS: Large stones, SS: Small stones, LG, MG, FG: Large, medium and fine gravel, respectively, SA: Sand

According to the substrate-specific analysis, all macroinvertebrate metrics were significantly reduced for all substrate types prior to and after the moderate-magnitude flow event (Fig. 2.4; Table A3). It must be noted that after the event, no fine substrate microhabitats (medium gravel, fine gravel and sand) were present at the sampling sites. Moreover, prior to the event, higher mean abundance values were observed at the sand and large-gravel microhabitats (139 ind and 105 ind, respectively, comprising 24% of the total invertebrate abundance), while after the event, higher mean values were detected in boulders and large stones (12 ind and 10 ind, respectively, comprising 73% of the total abundance).

The per-substrate relative abundance of FFGs was also altered between the pre- and post-impact samples (Fig. 2.5). Higher relative abundance of predators was detected at all the remaining substrates after the high flow event. The relative abundance of passive filter feeders was higher in coarse substrates (BO, LS, SS) and lower in gravel. Shredders were higher only in boulders, while the relative abundance of all other functional feeding groups was reduced after the event. Despite the overall structural changes, grazers/scrapers, gatherers/collectors predators and passive filter feeders were the most abundant feeding types both in the pre- and post-impact samples.

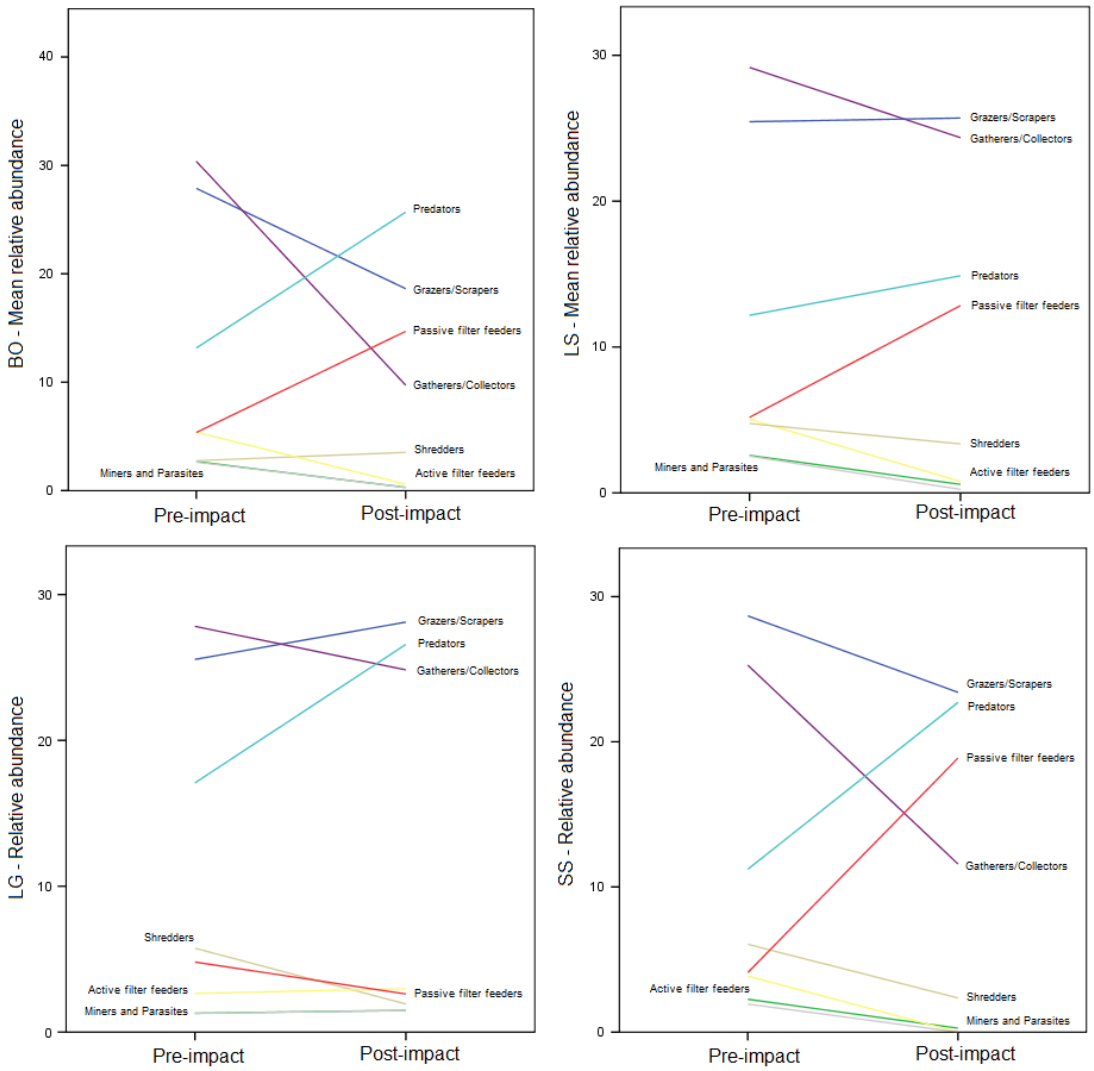

Fig. 2.5. Per-substrate, average relative abundance of the functional feeding groups between the pre- and post-impact samples. BO: Boulders, LS: Large stones, SS: Small stones, LG: Large gravel

According to the BRT models the high-magnitude flow event had the strongest impact on macroinvertebrate abundance, Ntaxa and EPTtaxa (relative influence 36.8%, 42.9% and 27.1%, respectively) (Fig. 2.6). Shannon's diversity index was mostly influenced by the spatial variability, represented by the different sampling sites (relative influence 31.5%) followed by the influence of the high-magnitude flow event itself (27.5%). Spatial variability in general had a great effect on all the modelled macroinvertebrate metrics. Furthermore, partial dependency plots (PDPs) showed a negative influence of depth on the Ntaxa, EPTtaxa, Shannon's diversity index and total macroinvertebrate abundance. Average flow velocity influenced the Ntaxa (8.8%) and the EPTtaxa (13.4%).

Regarding microhabitat-defining, physical-hydraulic variables (flow velocity, water depth and substrate), all macroinvertebrate metrics decreased in finer substrates and in flow velocities higher than 0.7 m/s and depths higher than 0.3 m. The PDPs showed specific optimal values for each metric. Abundance was higher in boulders, large stones and large gravel and in depths lower than 0.2 m. Ntaxa index was optimal in boulders, large stones and large gravel, in flow velocities between approximately 0.25 and 0.65 m/s and in depths approximately lower than 0.2 m. EPTtaxa index was higher in boulders, large stones and large gravel and in average flow velocities between 0.25 and 0.6 m/s. Diversity was higher in boulders, large stones, large and fine gravel, in depths around 0.2 m.

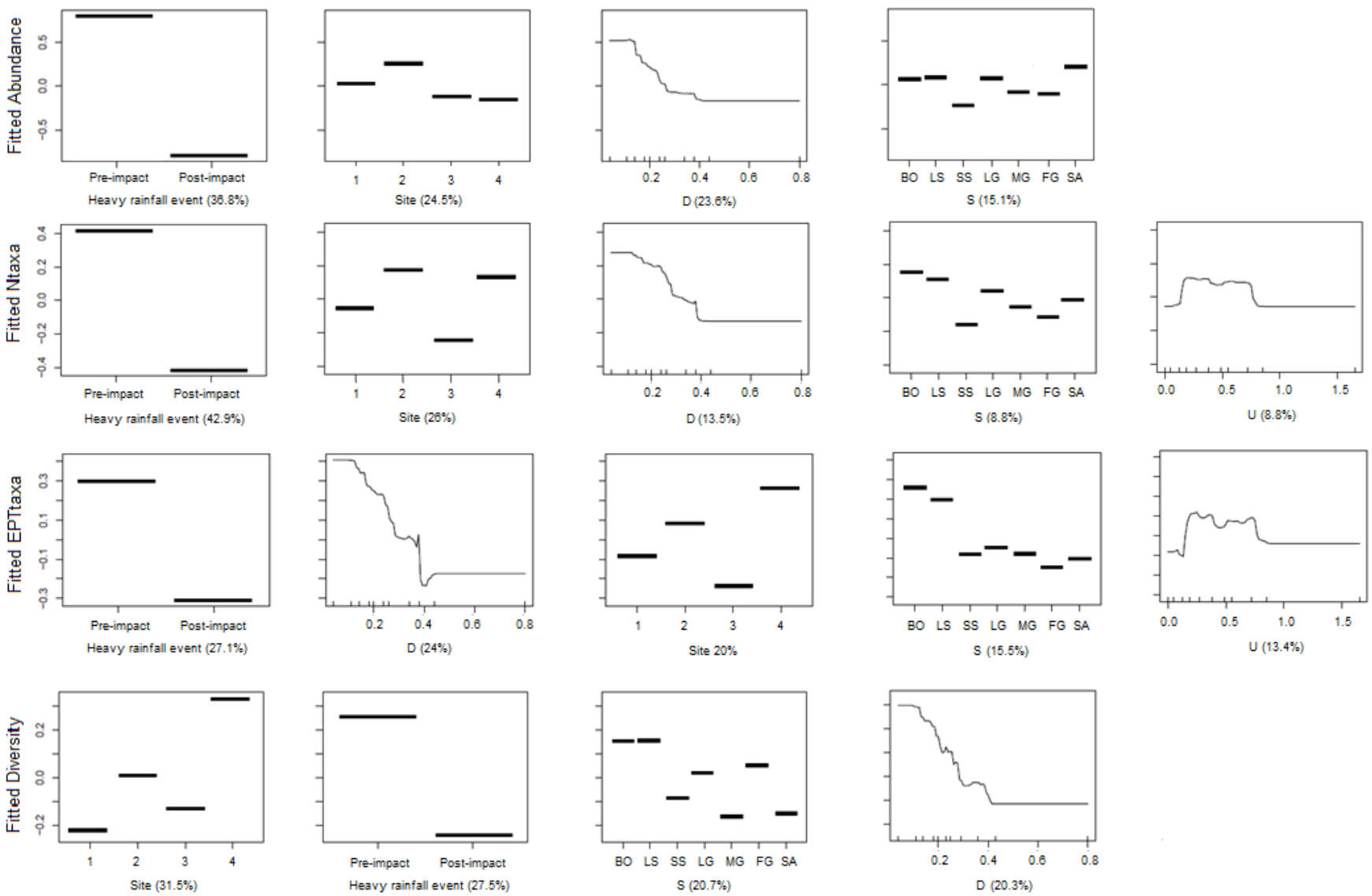

Fig. 2.6. Partial dependency plots for the environmental - hydraulic predictors in BRT models for the macroinvertebrate metrics. Rug plots at inside bottom of 'D' and 'U' plots show the distribution of samples across that variable, in deciles. D: Depth, U: Average flow velocity, S: Substrate

2.9. Discussion

The results of the study suggest that benthic macroinvertebrates do respond to natural flow variation. According to the NMDS plot, the pre- and post-impact microhabitat samples were clearly separated, reflecting the influence of the rainfall-induced moderate-magnitude flow event on their BM-community structure. The results of the BRT model further backed up this influence by showing that the highest portion of the overall variation (27.1% to 42.9%) was explained by the high-flow event itself, which exerted strong influence on all macroinvertebrate metrics studied.

Macroinvertebrate abundance, taxonomic richness, EPT richness and diversity decreased significantly by 90%, 60%, 50% and 25% respectively, between the pre- and post-impact microhabitat samples, as in partial accordance with previous studies, which indicate similar trends, but of varying magnitude and significance. Specifically, the 90% and 60% decrease in macroinvertebrate abundance and taxonomic richness respectively, has been previously reported by Argerich et al. (2004) as a result of an extremely large flood. Mesa (2010) also detected a 70% decrease in macroinvertebrate abundance but no statistically significant differences in the richness and diversity of macroinvertebrate communities, which in contrast, was derived by the results of the current study and those of Rosser and Pearson (1995), as well as those of Jacobsen and Encalada (1998). In contrast, Melo et al. (2003) indicated only a 15% decrease in macroinvertebrate abundance. Despite this variability in the magnitude of structural alteration, attributed to the variety of climatological characteristics of each study area, the different sampling periods (pre- and post-impact) and the methods applied, most studies conclude that macroinvertebrate abundance, diversity and often taxonomic richness and EPT richness decrease due to floods and extreme rainfall events (Poff and Zimmerman, 2010). In addition, our study indicates that even after events of moderate flow-alteration, the benthic communities are critically influenced.

Despite the overall structural degradation, the results of the study, being supported by previous relevant research (Lancaster and Hildrew, 1993; Rempel et al., 1999; Fuller et al., 2010), reveal that during high flow events, specific types of substrate act as flow refugia, providing shelter against macroinvertebrate dislodgment. In our study, these substrate types were mainly boulders and large stones, hosting 73% of the total macroinvertebrate abundance and higher taxonomic richness, compared to finer substrates, after the high flow event. As discussed by Borchardt (1993) and indicated in the current study, benthic macroinvertebrates either actively drift to these refugia or are accidentally protected, being on refugia when flow/hydraulic conditions become critical (provoking dislodgment). This is suggested by the fact that prior to the moderate-magnitude flow event, macroinvertebrates were almost evenly distributed among the various microhabitats (Fig. 2.4), while concentrated in coarser substrates (at the interstitial spaces or underneath boulders and large stones) after the event.

Regarding the response of particular functional feeding groups to elevated flows, the results showed increasing relative abundance of predators and passive filter feeders in flow refugia, while the relative abundances of gatherers/collectors and grazers/scrapers were reduced or remained constant. Nevertheless, these four FFGs were the most dominant, both prior to but especially after the event. Predator macroinvertebrates are favored by the high concentration of prey taxa in flow refugia due to the high retention rates of organic matter at these coarse microhabitats (Dobson and Hildrew, 1992; Haapala et al., 2003). In addition, the increased flow velocity, favors the transport of fine organic material within the water column and thus justifying the increased relative abundance of passive filter feeders (Wallace and Merritt, 1980; Georgian and Thorp, 1992) or the high relative abundance of grazers/scrapers (Pastuchova et al., 2010).

Preliminary quantitative relationships between flow alteration and ecological responses of freshwater macroinvertebrates were developed using BRT models. According to the results, high macroinvertebrate abundance, taxonomic richness, EPT richness and diversity

were detected in flow velocities between 0.3 m/s and 0.75 m/s, in water depths near 0.2 m (with all metrics decreasing rapidly in depths higher than 0.4 m) and in coarser substrates (but with high variability). These results are in accordance with the majority of previous studies, which although originating from different locations with varying climatic and hydrodynamic conditions, indicate similar macroinvertebrate preferences. With minor exceptions for certain macroinvertebrate taxa (Jowett et al., 1991), flow velocities higher than 0.7 m/s are not considered suitable for most macroinvertebrates (Gore et al., 2001; Li et al., 2009; Horta et al., 2009; Shearer et al., 2015), while the optimal range usually varies between 0.1 m/s and 0.6 m/s. However, certain taxa present optimal suitability in higher or lower flow velocities. Regarding water depth, suitability usually peaks at 0.25 m (Jowett et al., 1991; Gore et al., 2001; Li et al., 2009) in accordance with our results, while ranging between 0.1 m and 1 m. Regarding substrate type, large and small stones (6 cm - 25 cm) are generally considered more suitable but with high variation among studies. Our results also suggest that coarser substrates are more suitable, revealing higher abundance and taxonomic richness in large stones, boulders, small stones and large gravel.

Although in the current study, sand was found to host high macroinvertebrate abundance, the limited number of samples (3 out of 142) with the specific substrate type, inhibits any relevant discussion. However, the dominant taxon in the particular substrate was Chironomidae, which is known to thrive in finer substrates (Jowett et al., 1991; Horta et al., 2009; Shearer et al., 2015). A combinational suitability index would indicate that sand is a moderately-suitable substrate, as also concluded in the aforementioned studies and supported by the low EPT richness and diversity of the current study.

This study concluded that the structure of macroinvertebrate communities is critically influenced after a high-flow event, even of moderate magnitude. While derived by a naturally-occurring heavy-rainfall event, this information could explain much of the well-documented structural degradation of macroinvertebrate communities downstream of hydropower dams and reservoirs (Allan and Castillo, 2007; Theodoropoulos et al., 2015b). Macroinvertebrate-derived metrics from such locations indicate degraded ecological quality, attributed, *inter alia,* to the irregular water level fluctuations (Hartmann and Mihuc, 2008), both inter-annual and intra-annual, which prevent healthy benthic macroinvertebrate communities from being established. As the European Union urges for the provisioning of environmental flows downstream of dams to restore the integrity of aquatic ecosystems (WFD CIS Guidance Document No. 31, 2015), the reference data collected in the current study enabled the establishment of preliminary hydroecological relationships (the habitat preferences of benthic macroinvertebrates), with a final aim to ensure robust, biologically-derived environmental flow recommendations. Integrating these preferences in hydrodynamic habitat models (HHMs) (Theodoropoulos et al., 2015a) could be of valuable importance for water managers to select the optimum among various flow scenarios. Further studies collecting combined hydrological-hydraulic-biological data to enrich the current reference dataset would provide HHMs-based environmental flow recommendations with enhanced accuracy, towards the restoration and maintenance of functional aquatic ecosystems.

2.10. Conclusions

1. Benthic macroinvertebrates respond to flow variation.
    - The structure of macroinvertebrate communities is critically influenced by high flow events, even of moderate magnitude.
    - Benthic-invertebrate abundance, diversity, taxonomic richness and EPT richness significantly decreased between the pre- and post-impact samples.
    - The composition of functional feeding groups was altered after the high flow event.

- Boulders and large stones served as flow refugia, concentrating organic matter and thus maintaining less degraded benthic macroinvertebrate communities, but with altered composition of FFGs (increased predators and passive filter feeders).

2. The response of benthic macroinvertebrates to flow variation follows a Gaussian distribution with specific optima.
    - Optimal (suitable) ranges for flow velocity were estimated between 0.3 m/s and 0.75 m/s and for water depth at 0.2 m.
    - Coarser substrates (boulders and large stones) were more suitable but with higher variability between the various substrate types.

Chapter 3

Filling the gaps in BM-based habitat modelling - Development of a command-line habitat module to facilitate the application of two-dimensional hydrodynamic habitat models

3.1. Overview

Hydrodynamic habitat models (HHMs) have long been researched since the mid-1970s for their potential to quantify and predict the response of freshwater biota to hydrological-hydraulic variation (Maddock, 1999; Benjankar et al., 2014; Stamou et al., 2018). HHMs integrate computational fluid dynamics and ecological knowledge into a two-module framework; a hydrodynamic module provides information on the change of physical habitat as a function of flow by predicting water depths (D) and depth-averaged flow velocities (V) at multiple discharges in a computational grid that simulates the area under investigation. A coupled habitat module compares the predicted values of V and D with information on the habitat preferences of aquatic biota to calculate habitat suitability at each simulated discharge (Acreman and Dunbar, 2004; Gopal, 2013).

Over the years and within much 'constructive' debate between researchers (Orth, 1987; Holm et al., 2001; Booker et al., 2004; Lamouroux et al., 2010; Lancaster and Downes, 2010) new methods have been incorporated in HHMs to improve the predictive accuracy of their hydrodynamic and habitat modules. Since the early one-dimensional concept of habitat suitability curves (HSCs) (Bovee, 1986) implemented in the PHABSIM software (Milhous et al., 1989; Waddle, 2001), the hydrodynamic module of HHMs advanced from 1D cross-sectional interpolations to 2D/3D unsteady- and steady-flow simulations of enhanced accuracy (e.g. open TELEMAC-MASCARET - Galland et al., 1991; CASiMiR 2D - Schneider et al., 2001; River2D - Steffler and Blackburn, 2002). The habitat module simultaneously advanced from the initial HSCs concept; habitat suitability is currently modelled based on multivariate statistical methods, machine-learning and fuzzy rule-based algorithms (Van Broekhoven et al., 2006; Dakou et al., 2007; Vezza et al., 2015).

However, it was not until the last few years that two-dimensional HHM applications became more popular than their 1D alternatives; still, 2D HHMs-based research on environmental flows has been focused on fish (Muñoz-Mas et al., 2016; Papadaki et al., 2017); case studies using other biotic elements of the aquatic ecosystem as environmental flow indicators are disproportionately limited. Within this context, the following limitations currently inhibit any effort towards 2D BM-based hydrodynamic habitat modelling applications to inform environmental flow assessments:

1. Integrated HHM software applications have been mostly developed to be used for fish (CASiMiR benthos is the only option currently).
2. The current HHMs mainly combine a 1D hydraulic module and a HSCs-based habitat module (PHABSIM - Milhous et al., 1989; CASiMiR Fish - Schneider at al., 2001), with River2D and CASiMiR 2D being the only available 2D options.
3. Advanced habitat modelling algorithms (machine learning, fuzzy logic, fuzzy rule-based Bayesian inference), which have been proven more accurate than HSCs, especially for other-than-fish biotic elements, are not currently implemented (again, only River2D has a fuzzy-logic option).

Integrated BM-focused software applications are not available. Consequently, the current HHMs-based EFAs, which use other biotic elements as environmental flow indicators, apply the fish-based habitat tools to develop environmental flow scenarios.

3.2. Purpose of the chapter

This chapter describes the HABFUZZ software; a command-line tool, which applies fuzzy logic and fuzzy rule-based Bayesian algorithms to calculate-predict and simulate the BM-based habitat suitability at each node of a computational grid of a previous two-dimensional hydrodynamic simulation of a river reach. It is a habitat module developed in FORTRAN to assist the TELEMAC 2D hydrodynamic model (but it can be also used with other 2D hydrodynamic models) in the development of fuzzy rule-based environmental flow scenarios. HABFUZZ uses the hydrodynamic output of TELEMAC 2D (the V, D and S microhabitat values at each node of

the grid in various discharges) and calculates the habitat suitability at each node (that is, for each V, D and S combination) based on a BM-reference training dataset collected in Greek rivers. The primary output of HABFUZZ is a txt file with the habitat suitability values for each microhabitat combination.

3.3. Description of HABFUZZ

The generic concept of fuzzy logic and fuzzy rule-based Bayesian inference has been described in chapter 1. Here, an example is provided and the algorithms of HABFUZZ are implemented using specific example datasets. HABFUZZ requires two input files, (i) a training dataset of microhabitat combinations (observations) of flow velocity (V), water depth (D) and substrate type (S), associated with an *a priori* calculated specific habitat suitability (K) value and (ii) a test dataset of microhabitat observations (V, D and S) with unknown K, which will be predicted by HABFUZZ. The training and test datasets used in this example are shown in tables 3.1 and 3.2, respectively. For technical details on file preparation to be inputted in HABFUZZ please consult the HABFUZZ manual (https://chtheodoro.wixsite.com/habfuzz/documentation). HABFUZZ can also include the water temperature as a fourth predictor in the calculation of habitat suitability, however, this predictor is not included in the example datasets to ease understanding.

Table 3.1. Example training dataset

Microhabitat	Flow velocity (m/s)	Water depth (m)	Substrate type	Habitat suitability
1	0.20	0.12	Boulders	0.65
2	0.30	0.35	Large stones	0.24
3	0.32	0.05	Boulders	0.45
4	0.73	0.50	Small stones	0.3
5	0.32	0.43	Large stones	0.7
6	0.24	0.98	Large gravel	0.65
7	0.56	0.65	Boulders	0.21
8	1.12	1.10	Medium gravel	0.1
9	0.23	0.32	Sand	0.96
10	0.22	0.05	Large stones	0.5
11	0.01	0.12	Sand	0.4

Table 3.2. Example test dataset

Microhabitat	Flow velocity (m/s)	Water depth (m)	Substrate type
1	0.28	0.29	Boulders
2	0.05	0.08	Large stones
3	0.46	0.80	Small stones

HABFUZZ offers two options, (i) a fuzzy logic process with various defuzzification algorithms (FL) and (ii) a fuzzy rule-based Bayesian algorithm (FRB). In FL, the output habitat suitability is initially a combination of fuzzy sets (five K classes - bad, poor, moderate, good, high) and within the defuzzification process K is converted into a crisp output ranging from 0 to 1. In the FRB algorithm, habitat suitability is expressed using the same five classes. Each class is assigned with a utility score (bad - 0.1, poor - 0.3, moderate - 0.5, good - 0.7, high - 0.9) and multiplied by the joint probability of each combination observed.

In both algorithms, the initial values of the input data (V, D and S) are converted to membership degrees based on a process called fuzzification, which resembles classification but enables the user to account for possible uncertainty in the developed fuzzy sets (which are also called membership functions). For example, if the values of water depth (D) range from 0.03 m to 1.5 m you are pretty sure that D values between 0.03 m and 0.1 m can be defined as LOW, D values between 0.2 m and 0.5 m can be defined as MODERATE etc. But you are not sure if a

value of 0.12 m is LOW or MODERATE. Fuzzy logic lets you numerically say 'I am 70% sure that a value of 0.12 m can be defined as LOW and 30% as MODERATE' by writing 'the membership degree of 0.12 m to the LOW fuzzy class is 0.7 and the membership degree of 0.12 m to the MODERATE class is 0.3'. This process is applied in HABFUZZ for every value of the training and test datasets and for each variable included. HABFUZZ fuzzifies all inputs into trapezoidal-shaped membership functions (Fig. 3.1), with their class boundaries defined by the user (this is the only part of HABFUZZ which requires the user to intervene).

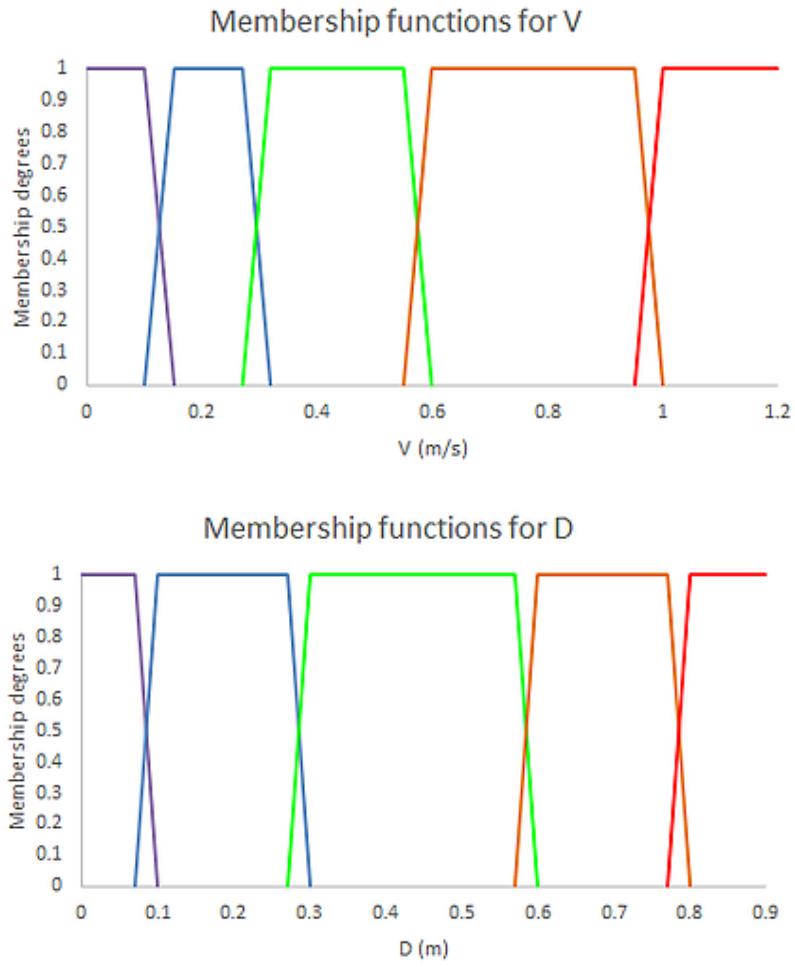

Fig. 3.1. User-defined fuzzy sets (membership functions) for flow velocity (V) and water depth (D)

After reading the training dataset, HABFUZZ develops the rules database based on the classes observed for each microhabitat combination and its relevant K. The value of each variable of each microhabitat combination is classified in one of the following classes (which can be re-defined by the user):

Flow velocity (V)	Water Depth (D)	Temperature (T)
VERY LOW: 0 - 0.075 m/s	VERY SHALLOW: 0 - 0.125 m	VERY LOW: 0 - 12.5 oC
LOW: 0.075 - 0.175 m/s	SHALLOW: 0.125 - 0.325 m	LOW: 12.5 - 14 oC
MODERATE: 0.175 - 0.45 m/s	MODERATE: 0.325 - 0.575 m	MODERATE: 14 -18 oC
HIGH: 0.45 - 0.75 m/s	DEEP: 0.575 - 0.725 m	HIGH: 18 - 24 oC
VERY HIGH: > 0.75 m/s	VERY DEEP: > 0.725 m	VERY HIGH: >24 oC

Substrate type (S)	Habitat suitability (K)
BOULDERS: 0.070	HIGH: 0.8 - 1
LARGE STONES: 0.050	GOOD: 0.6 - 0.8
SMALL STONES: 0.040	MODERATE: 0.4 - 0.6
LARGE GRAVEL: 0.030	POOR: 0.2- 0.4
MEDIUM GRAVEL: 0.026	BAD: 0 - 0.2
FINE GRAVEL: 0.024	
SAND: 0.022	
SILT: 0.020	

The boundaries for each class are the same with those used for fuzzification and can be modified by the user. HABFUZZ creates a matrix with all the class combinations observed and the relevant K for each combination. From this point, HABFUZZ implements the two different algorithms, (i) the fuzzy logic algorithm (Mamdani and Assilian, 1975; Ross, 2010) and (ii) the fuzzy rule-based Bayesian algorithm (Brookes et al., 2010).

3.3.1. The fuzzy logic algorithm (Mamdani and Assilian, 1975)

In FL, when a microhabitat combination is observed more than once with different K (same combination of predictors' values but different K), HABFUZZ calculates the overall K by (a) averaging, (b) deriving the lowest K observed or (c) by deriving the maximum K observed. The user is prompted by HABFUZZ to select one of these three scenarios (called average, worse and optimum scenario, respectively) prior to developing the rules database. The rules are then developed in the following concept:

1. The values of V, D, S (and T) and K of each microhabitat combination in the training dataset are classified based on the classes illustrated above. For the first three rows of table 3.1, HABFUZZ classifies all values and 'translates' them as
   a. IF V is MODERATE AND D is VERY SHALLOW AND S is BOULDERS THEN K is GOOD.
   b. IF V is MODERATE AND D is MODERATE AND S is LARGE STONES THEN K is POOR.
   c. IF V is MODERATE AND D is VERY SHALLOW AND S is BOULDERS THEN K is MODERATE.

   As the combinations (a) and (c) result in the same V, D and S classes but different K, HABFUZZ applies one of the three abovementioned scenarios to calculate a single K for this combination. If for example the average scenario is selected, K would be (0.65+0.45)/2 = 0.55 (classified as MODERATE). This process is repeated for all the microhabitat combinations available in the training dataset. This means that a large number of rules may be developed; in HABFUZZ there are five classes of V, five classes of D, five classes of T and eight classes of S, which equals to 5 x 5 x 5 x 8 = 1000 rules!
2. The model's predictive accuracy is calculated using a 10-fold cross validation process. The training dataset is divided in two parts: 90% of the data (microhabitat combinations) are randomly selected and the rules are developed for this 90% of data. Then, the rules that have been developed based on this 90% are used to predict K for the remaining 10%. This process is repeated 10 times (random selection of 90% and predicting the remaining 10%) and finally the CCI index (correctly classified instances %) is produced to inform the user about the model's predictive accuracy.
3. Prediction of K in the test dataset. To predict the K values of the test dataset (microhabitat combinations with unknown K), HABFUZZ applies the following procedure for each microhabitat:
   a. The V, D and S values of each test microhabitat are fuzzified and each value is replaced by a membership degree for each fuzzy class.

b. The whole training dataset is now used to develop the rules database.
c. HABFUZZ then refers to the rules database to derive the class combinations and the relevant K for each combination.
d. The rules corresponding to each combination are applied using the AND operator (minimum) (Fig. 3.2). The membership degree of each input value is used. For example, if we have a V of 0.18 m/s, which corresponds to a membership degree of 0.3 in the VERY LOW class and a value of D at 0.12 m, corresponding to a membership degree of 0.8 to the SHALLOW class, then the AND operator says that the membership degree of the K (let's say HIGH from the relevant rule) will be 0.3 (minimum value between 0.3 and 0.8).

4. The different K classes observed along with their membership degrees are then aggregated and a defuzzification process is applied to calculate the final HS value (Fig. 3.3). The defuzzification algorithms implemented in HABFUZZ are (i) centroid, (ii) weighted average, (iii) maximum membership and (iv) mean of maximum.

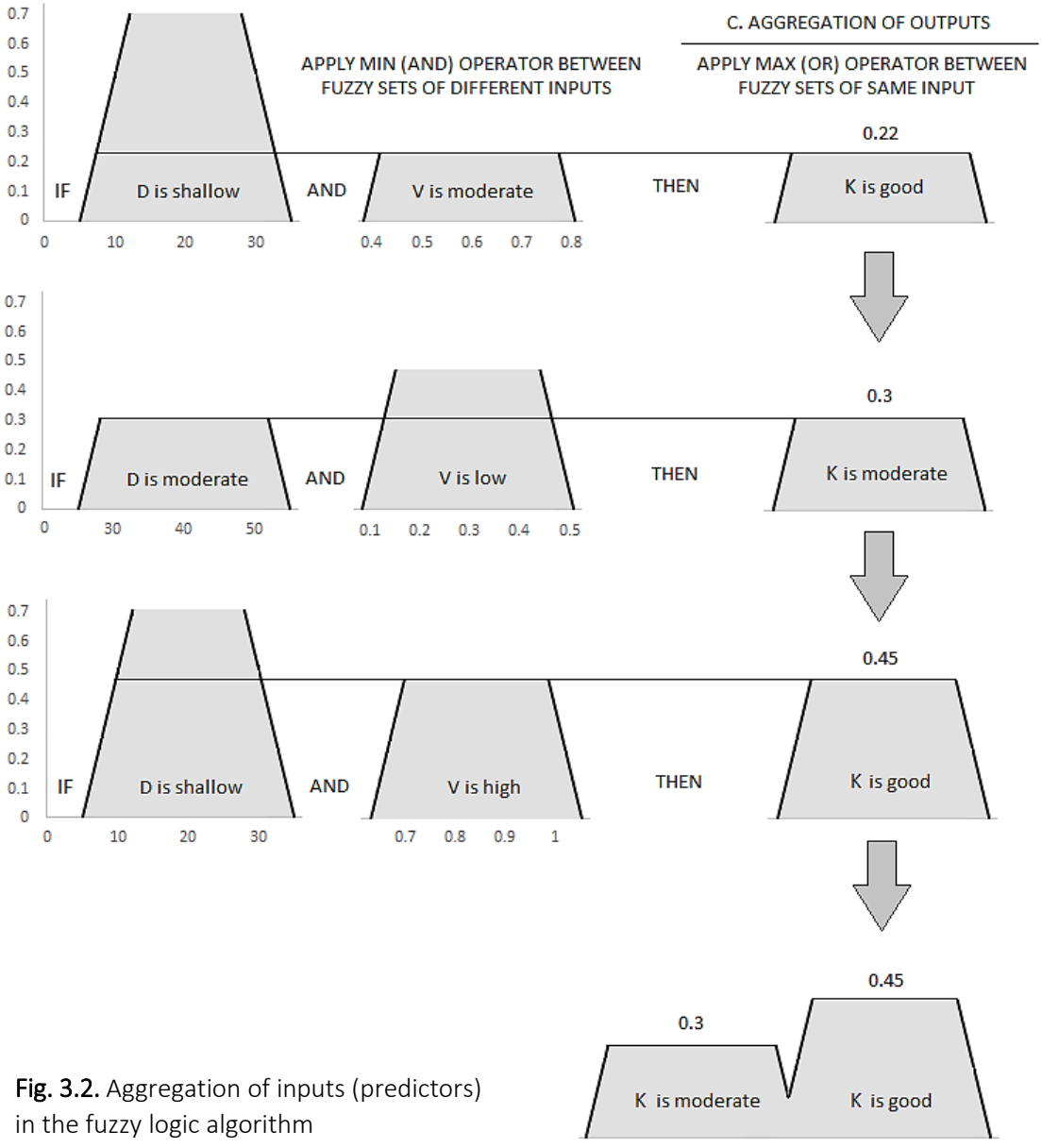

Fig. 3.2. Aggregation of inputs (predictors) in the fuzzy logic algorithm

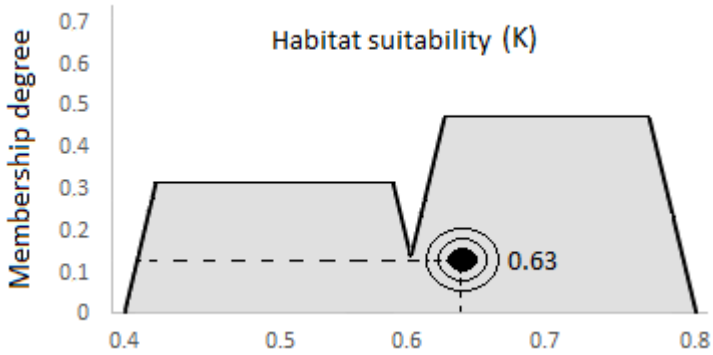

Fig. 3.3. Defuzzification and calculation of the final habitat suitability

3.3.2. The fuzzy rule-based Bayesian algorithm (Brookes et al., 2010)

In FRB, when a microhabitat combination is observed more than once with different K, HABFUZZ keeps a record of both observations and assigns a probability value according to the times that a different K class is observed for the same class combination. The first two steps are the same with the FL algorithm. From step 3, the process goes as follows:

3. To predict the K values of the test dataset (microhabitat combinations with unknown K), HABFUZZ applies the following procedure FOR EACH MICROHABITAT:
    a. The V, D and S values of each test microhabitat are fuzzified and each value is replaced by a membership degree for each fuzzy class.
    b. The whole training dataset is now used to develop the rules database.
    c. HABFUZZ then refers to the rules database to derive the class combinations and the relevant K for each combination.
    d. The rules corresponding to each combination are applied using the membership degree of each class as the probability of occurrence of this class (fig. 3.4). For example, if we have a V of 0.18 m/s, which corresponds to a membership degree of 0.3 in the VERY LOW class and a value of D at 0.12 m, corresponding to a membership degree of 0.8 to the SHALLOW class, then the fuzzy Bayesian algorithm suggests that the membership degree of K (let's say HIGH with a probability of 0.5 from the relevant rule) will be 0.3 x 0.8 x 0.5 = 0.12 (the joint probability of these classes occurring in the specific combination). The Bayesian term is used since we say the probability of K being HIGH GIVEN THAT V is VERY LOW and D is SHALLOW.

3.4. Running HABFUZZ

(Using the training and test datasets of tables 3.1 and 3.2)

The tool runs from the command line window. The command prompt opens and after a short welcome message the software asks for the inference process to be implemented (Fig. 3.4 and 3.5).

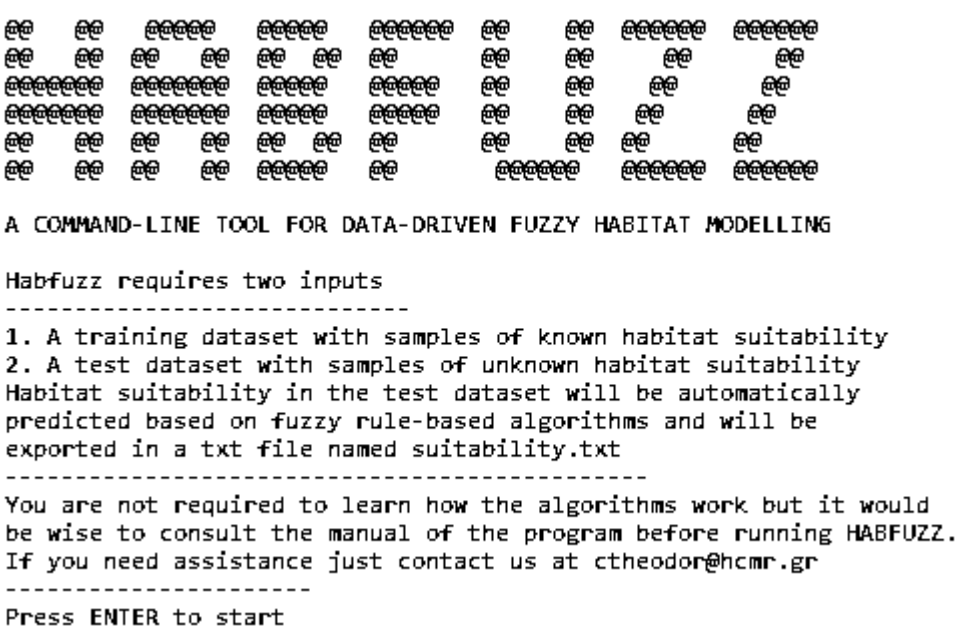

Fig. 3.4. The welcome-screen of HABFUZZ

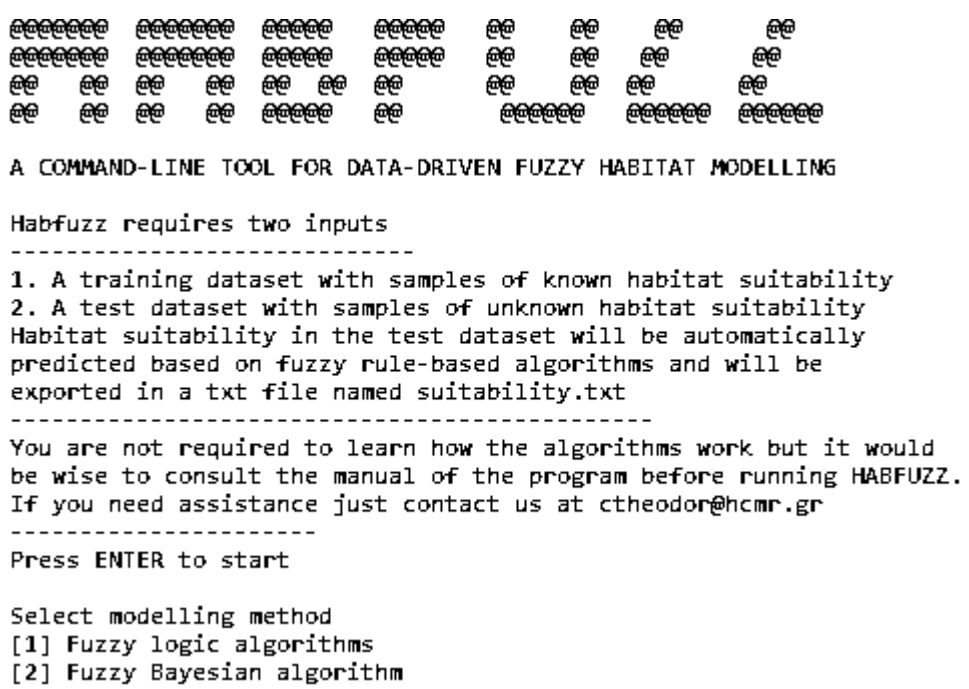

Fig. 3.5. Selection of modelling algorithm in HABFUZZ

After selecting the modelling algorithm, the user is asked to select the cross validation scheme (either Monte Carlo or ten-fold) (Fig. 3.6). In the ten-fold cross validation, the initial dataset is randomly partitioned in ten equal-sized subsamples. Nine subsamples are used as the training

dataset and the remaining subsample is used for model validation. This process is repeated ten times (folds), using a different subsample for validation at each iteration. The Monte Carlo scheme also includes ten iterations but at each iteration the initial dataset is randomly partitioned in two subsamples. The first subsample contains 90% of the initial data and is used for calibration, and the second subsample contains the remaining 10% and is used for validation. At each iteration, the initial data is again randomly partitioned and thus the same data may be randomly included in each subsample more than once, in contrast to the ten-fold cross validation scheme. The performance of each model is evaluated as the average percentage of the correctly classified instances (CCI) between each iteration of the ten-fold cross-validation process

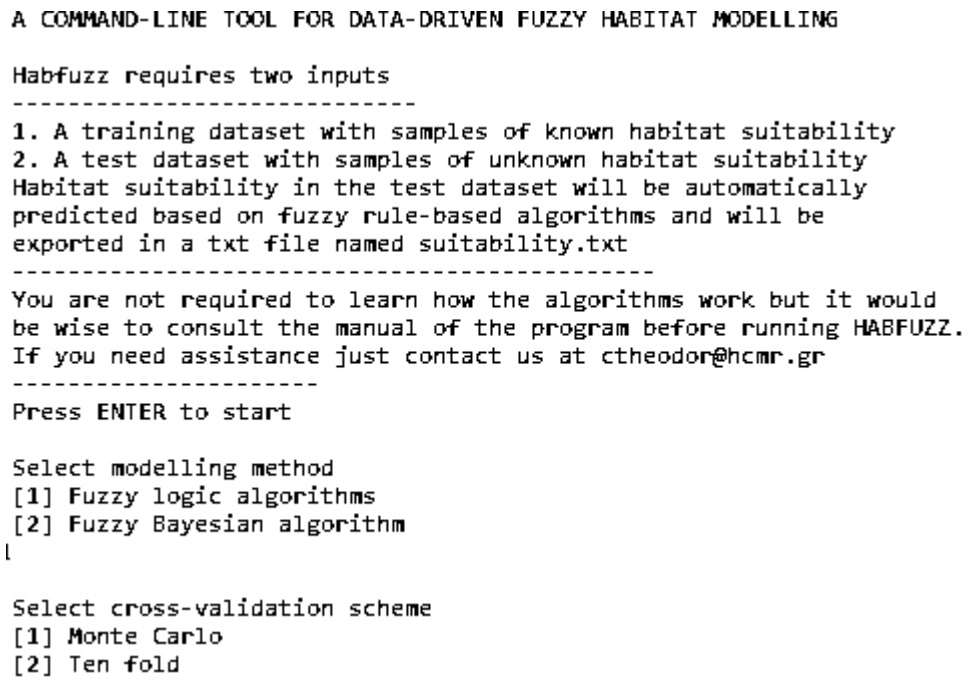

Fig. 3.6. Selection of the cross-validation method

3.4.1. Running the fuzzy logic algorithms

If the FL option is selected, the program, after selecting the cross-validation scheme, prompts the user to select the desired management scenario to implement (Fig. 3.7). There are three available scenarios based on the method used for deriving the outcome of each IF-THEN rule from the training dataset of the program, (i) the average scenario, where the different suitability values for the same combinations of flow velocity, water depth and substrate type are averaged to derive the final habitat suitability, (ii) the worst scenario, where the final suitability is derived from the minimum observed suitability and (iii) the optimum scenario where the final suitability is derived by the maximum observed suitability. A default scenario is also present (the moderate scenario). If a specific combination in the observed data does not match a combination in the reference data, the program returns a value of '-1' for the habitat suitability.

After selecting the desired scenario, the user is asked to select the defuzzification method (Fig. 3.8). A default method (centroid) is available. After selecting the defuzzification method, HABFUZZ calls the relevant subroutines to perform the tasks selected. The program informs the user when the process is completed and indicates the *suitability.txt* file created where the suitability values are stored and the *log.txt* file with the fuzzy membership degrees for each class.

```
predicted based on fuzzy rule-based algorithms and will be
exported in a txt file named suitability.txt
-------------------------------------------
You are not required to learn how the algorithms work but it would
be wise to consult the manual of the program before running HABFUZZ.
If you need assistance just contact us at ctheodor@hcmr.gr
----------------------
Press ENTER to start

Select modelling method
[1] Fuzzy logic algorithms
[2] Fuzzy Bayesian algorithm
1

Select cross-validation scheme
[1] Monte Carlo
[2] Ten fold
1

Select the preferred scenario to implement
[1] Average
[2] Worst
[3] Optimum
[4] Default
```

Fig. 3.7. Selection of the desired scenario

```
Select modelling method
[1] Fuzzy logic algorithms
[2] Fuzzy Bayesian algorithm
1

Select cross-validation scheme
[1] Monte Carlo
[2] Ten fold
1

Select the preferred scenario to implement
[1] Average
[2] Worst
[3] Optimum
[4] Default
3

Select the preferred defuzzification method
[1] Centroid
[2] Max membership
[3] Weighted average
[4] Mean-max membership
[5] Default
```

Fig. 3.8. Selection of the defuzzification method

Assuming that the training dataset has been used for the development of the rules database, for the test data of table 3.2, the crisp input values for V and D, are fuzzified as depicted in table 3.3.

Table 3.3. Fuzzification results for the training dataset (first three rows of table 3.1).

	Fuzzy membership classes						
Crisp inputs	V Very Low	V Low	V Moderate	D Very Shallow	D Shallow	D Moderate	D Very Deep
V = 0.28	0	0.8	0.2				
V = 0.05	1	0	0				
V = 0.46	0	0	1				
D = 0.29				0	0.333	0.667	0
D = 0.08				0.333	0.667	0	0
D = 0.80				0	0	0	1

V: Flow velocity, D: Water depth

HABFUZZ then checks each combination of inputs (their corresponding fuzzy sets) and assigns a membership degree using the AND (min) operator to the relevant K class they belong (based on the IF-THEN rules developed from the training dataset, and depending on the selected management scenario). If the user, for example, selected the moderate scenario, the membership degree of each combination in the relevant K class (including the substrate type) is depicted in table 3.4.

Table 3.4. Checking the relevant IF-THEN rules and assigning membership degrees to the suitability class by applying the AND (min) operator.

V	D	S	K
Moderate (0.2)	Moderate (0.667)	Boulders (1)	-
Moderate (0.2)	Shallow (0.333)	Boulders (1)	High (0.2)
Low (0.8)	Moderate (0.667)	Boulders (1)	Moderate (0.667)
Low (0.8)	Shallow (0.333)	Boulders (1)	Good (0.333)
Very Low (1)	Very Shallow (0.667)	Large stones (1)	Good (0.667)
Very Low (1)	Shallow (0.333)	Large stones (1)	Good (0.333)
Moderate (1)	Very Deep (1)	Small stones (1)	-

V: Flow velocity, D: Water depth, S: Substrate type, K: Habitat suitability

HABFUZZ then combines the same K classes observed (aggregation step) using the OR (max) operator and the different membership degrees of all classes are defuzzified using one of the methods described before. The results of the aggregation and defuzzification processes (in this case the centroid defuzzification method was selected) are depicted in table 3.5.

Table 3.5. Aggregation of outputs using the OR (max) operator. It can be seen that microhabitat 3 is not referred in the IF-THEN rules and a value of -1 is returned by HABFUZZ.

Microhabitat	V	D	S	K
1	0.28	0.29	Boulders	0.622
2	0.05	0.08	Large stones	0.700
3	0.46	0.80	Small stones	-1

V: Flow velocity, D: Water depth, S: Substrate type, K: Habitat suitability

3.4.2. Running the fuzzy rule-based Bayesian algorithm

If the FRB is selected, the program immediately calculates K according to the steps described previously. Again, using the test data of table 3.2, the crisp input values for V and D, are fuzzified as depicted in table 3.3. The process then treats the fuzzified membership degrees as the probability of each observation occurring, suggesting for example that *'the probability of K being high is the joint probability that V is moderate, D is shallow and S is boulders'.* This concept is depicted for the example training dataset for each microhabitat in tables 3.6, 3.7 and 3.8.

Table 3.6. (A) The joint probability table for the fuzzified inputs of microhabitat 1 (S=Boulders, not shown but included). (B) Joint probability after including the probability of the habitat suitability (not shown) class for each combination.

(A) Microhabitat 1	D (P)		
V (P)	Shallow (0.333)	Moderate (0.667)	JP = P(V) x P(D) x P(S) Substrate's P is always 1 since S is not fuzzified.
Low (0.8)	0.2664	0.5336	
Moderate (0.2)	0.0666	0.1334	

(B) Microhabitat 1	D (P)						
V (P)	Shallow (0.333)				Moderate (0.667)		JP = P(V) x P(D) x P(S) x P(K)
Low (0.8)	0.1455	0.0729	0.0239	0.0239	0.2668	0.2668	
Moderate (0.2)	0.0667				-		

V: Flow velocity, D: Water depth, S: Substrate type, JP: Joint probability, K: Habitat suitability; Blue colour: High K, Green colour: Good K; Yellow colour: Moderate K, Red: Bad K

Table 3.7. (A) The joint probability table for the fuzzified inputs of microhabitat 2 (S=Large stones, not shown but included). (B) Joint probability after including the probability of the habitat suitability class for each combination. JP: Joint probability.

(A) Microhabitat 2	D (P)		
V (P)	Very Shallow (0.667)	Shallow (0.333)	JP = P(V) x P(D) x P(S)
Low (1)	0.667	0.333	

(B) Microhabitat 2	D (P)							
V (P)	Very Shallow (0.667)			Shallow (0.333)				Joint Probability = P(V) x P(D) x P(S) x P(K)
Very Low (1)	0.1667	0.3335	0.1667	0.0639	0.1412	0.1022	0.0256	

V: Flow velocity, D: Water depth, S: Substrate type, JP: Joint probability, K: Habitat suitability, Blue colour: High suitability, Green colour: Good suitability, Yellow: Moderate suitability, Orange: Poor suitability

Table 3.8. The joint probability table for the fuzzified inputs of microhabitat 2 (S=Small stones, not shown but included). Since the specific combination is nor present in the training dataset, no further calculations are applied.

Microhabitat 3	D (P)	
V (P)	Very Deep (1)	Joint Probability = P(V) x P(D) x P(S)
Moderate (1)	1	

V: Flow velocity, D: Water depth, S: Substrate type, JP: Joint probability

HABFUZZ then assigns a score at each habitat suitability class to calculate the final suitability output (bad - 0.1, poor - 0.3, moderate - 0.5, good - 0.7, high - 0.9), using the 'expected utility' equation. Each probability from tables 3.6(B) and 3.7(B) is multiplied by the score of each relevant suitability class and all products are summed (for each microhabitat) to derive the final habitat suitability. The results of the fuzzy rule-based Bayesian algorithm are presented in table 3.9.

Table 3.9. The fuzzy Bayesian calculation of habitat suitability using the 'expected utility (EU)' equation

Microhabitats	Joint probability combinations							EU
1 -->	0.1455 x 0.9	0.0729 x 0.7	0.0239 x 0.5	0.0239 x 0.1	0.2668 x 0.7	0.2668 x 0.5	0.0667 x 0.9	0.577
2 -->	0.1667 x 0.9	0.3335 x 0.7	0.1667 x 0.5	0.0639 x 0.9	0.1412 x 0.7	0.1022 x 0.5	0.0256 x 0.3	0.677

3.5. Output

Regardless of the algorithm selected to predict K, the primary output of HABFUZZ is a txt file with the predicted K values for each microhabitat combination in the test dataset. In addition, HABFUZZ calculates the following parameters-indicators to facilitate a possible environmental flow selection process (Fig. 3.9):

1. Overall Suitability Index (OSI): $OSI = \sum_{i=1}^{w} K_i$
2. Normalized OSI (nOSI): $nOSI = \frac{OSI}{w}$
3. where,
   K_i (from 0 to 1) denotes the habitat suitability
   w denotes the total No. of wetted nodes in the computational mesh at each Q scenario
4. Certainty of prediction (COP): The ratio of the No. of microhabitat combinations actually found in the training dataset to the total No. of nodes in the computational mesh; HABFUZZ applies a 'trick' when a microhabitat combination is not found in the training dataset and instead of returning some arbitrary K value for a particular node (e.g. -1), it uses the K value of its neighboring node in the domain.
5. Percentage of wetted nodes in the computational mesh at each Q scenario (w).
6. Habitat connectivity (C): The ratio of connected (neighboring) nodes with K>0.6 to the total number of wetted nodes with K>0.6.
7. Habitat availability (A): The ratio of connected (neighboring) nodes with K>0.6 to the total number of nodes in the study reach (wetted and dry).

```
Habitat suitability calculation for test microhabitat        5169 successful
Habitat suitability calculation for test microhabitat        5170 successful

Habitat suitability calculation successful!

Finished!

Overall model performance       61.58 %
Percent wetted nodes            80.66 %
Certainty of prediction            80 %
Habitat connectivity               94 %
Habitat availability               60 %
Overall Suitability Index - OSI    2825.253
Normalized OSI                     0.701

Writing results to files...

Results ready
End of process
Please check the created file suitability.txt

Thank you for using HABFUZZ!

Press ENTER to exit
```

Fig. 3.9. The parameters calculated in HABFUZZ to facilitate the development of environmental flow scenarios

A schematic representation of the processes of HABFUZZ is illustrated in Fig. 3.10 and Fig. 3.11 (in more detail). A webpage has been developed to support the software (https://chtheodoro.wixsite.com/habfuzz). HABFUZZ is also available for download from SourceForge (https://sourceforge.net/projects/habfuzz) and GitHub (https://github.com/chtheodoro/habfuzz).

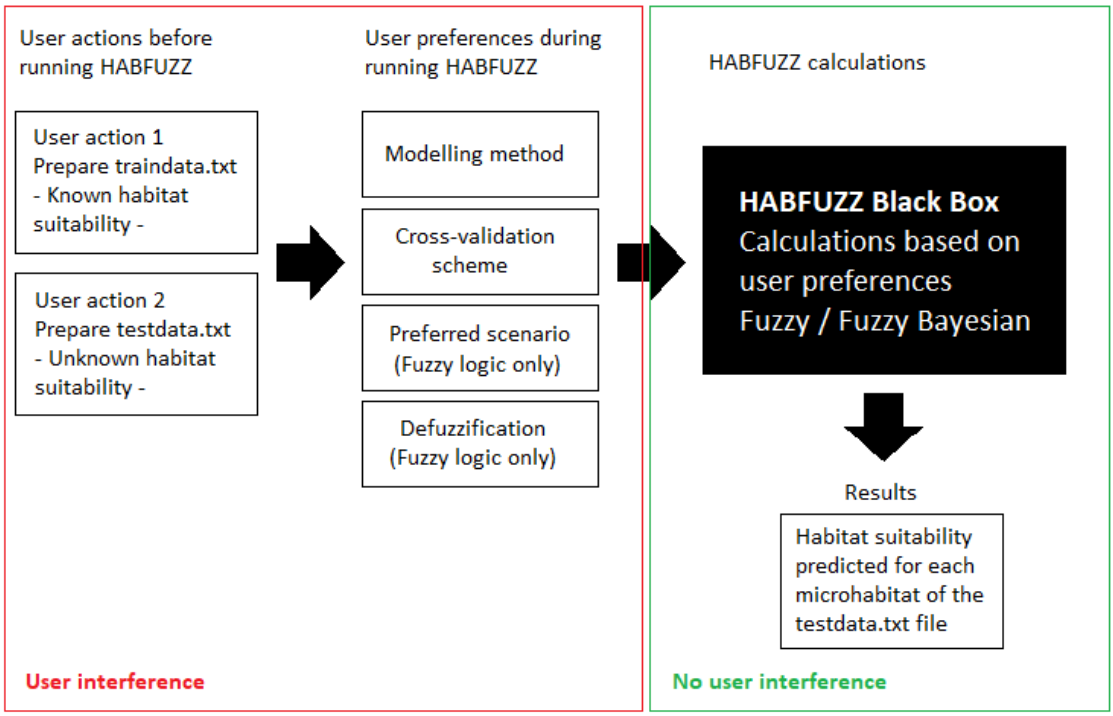

Fig. 3.10. Schematic representation of the HABFUZZ options

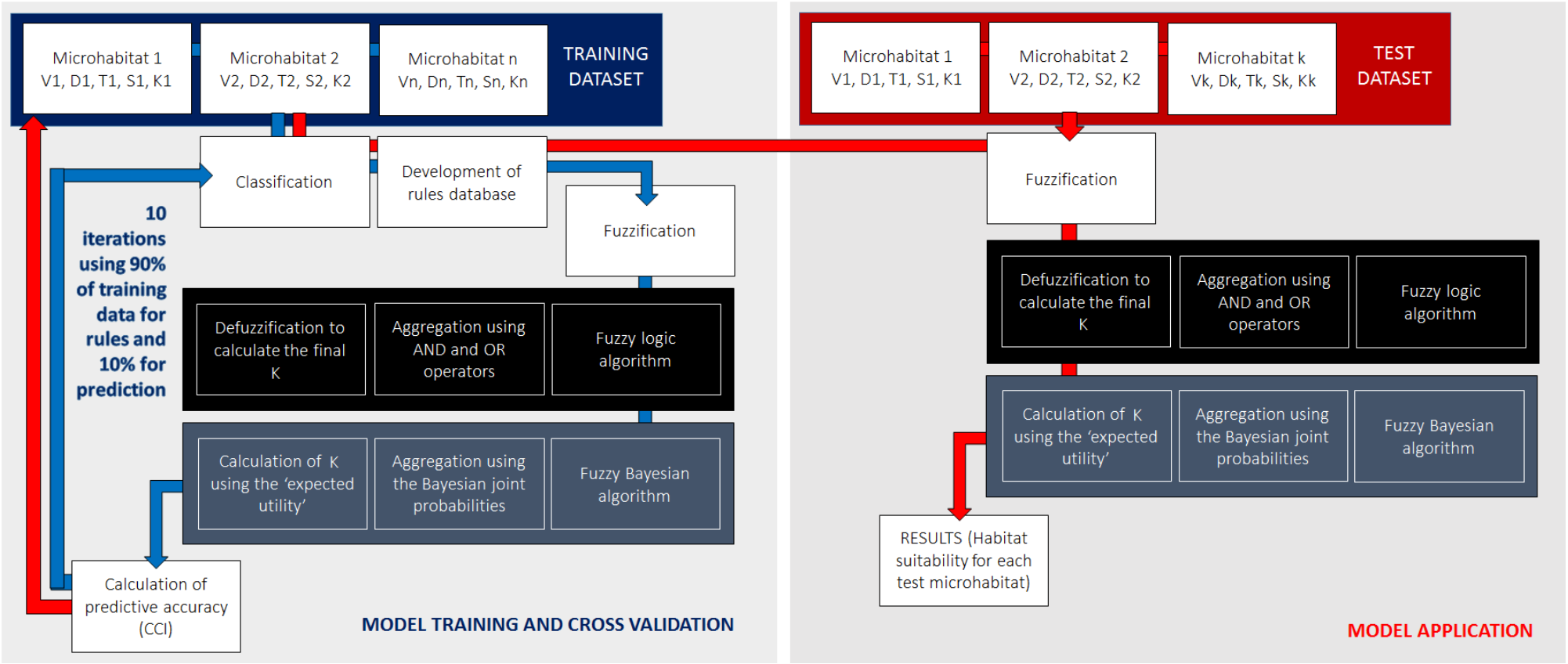

Fig. 3.11. Detailed graphical representation of the HABFUZZ concept

Chapter 4

Researching the predictive accuracy of state-of-the-art algorithms to be used in benthic-invertebrates-based habitat models

4.1. Overview

As previously mentioned, hydrodynamic habitat models (HHMs) include two different modules-components; (i) a hydraulic/hydrodynamic component, which calculates the flow velocity (V) and the water depth (D) for various discharges at each node of the computational grid of a simulated river reach and (ii) a habitat component, which uses the hydrodynamic output to calculate the habitat suitability at each node of the grid and for each discharge. During the past decades, despite the continuous efforts to increase the predictive accuracy of HHMs, there has been much controversy and criticism on the methods applied in their habitat modules to quantify the relationship between the environmental predictor variables and the biological response variables (Ahmadi-Nedushan et al., 2006; Hirzel and Le Lay, 2008; Jowett et al., 2008). The traditional and most widely used approach is the one described by Bovee (1986), which requires the development of three types of univariate habitat suitability curves (HSC) based either on expert knowledge (category I - professional judgment curves), or on actual field data (categories II and III - habitat utilization and habitat preference curves) to quantify the relationship between the abiotic variables -V, D, substrate type (S) and/or water temperature (T)- and the biotic response variables (usually the abundance of target organisms). Based on this rather simplistic approach and in combination with the criticism received, complex mathematical methods evolved and are currently available as 'habitat modelling algorithms'. These methods can be classified in the following categories, based on the conceptual approach they use to predict the habitat suitability:

(1) Multivariate statistical models (usually regression-oriented); the concept of these models is to find a best-fit curve that represents the relationship between the environmental-hydraulic predictors and the biotic response variables, based on specific assumptions about the distribution of data. Over time, these models have been enhanced to include various alternatives of the fundamental curve-fitting concept to avoid the assumptions of linearity between the predictor and response variables (Generalized Linear Models (GLMs) - McCullagh and Nelder, 1989) or to account for the cumulative influence of the predictors on the response variables (Generalized Additive Models (GAMs) - Hastie and Tibshirani, 1990).

(2) Machine learning models; non-parametric algorithms, which combine regression or classification functions based on the characteristics of the available data. These algorithms can deal with complex relationships and interactions between the environmental variables; they are able to handle large amounts of data with possible non-linear relationships between the predictors and process complex and noisy data (Recknagel, 2001). The most widely used examples include Classification and Regression Trees (Breiman et al., 1984; Dakou et al., 2007), Artificial Neural Networks (Broomhead and Lowe, 1988; Tirelli and Pessani, 2009), Random Forests (Breiman, 2001; Vezza et al., 2015; Booker, 2016) and Boosted Regression Trees (Elith et al., 2008; Theodoropoulos et al., 2017).

(3) Fuzzy-rule based models (Zadeh, 1965), often enhanced by Bayesian Belief Networks (BBNs - Pearl, 1988); based on sets of IF-THEN rules, fuzzy models convert the actual values of the predictor and response variables to membership functions ranging from 0 to 1 and calculate the habitat suitability by applying logical operators (AND/OR). These methods can handle the inherent vagueness of the input and output data, as well as the possible interaction between the predictor variables (Ahmadi-Nedushan et al., 2006) and have been applied in habitat modelling, in combination with BBNs to enhance predictive accuracy (van Broekhoven et al., 2006; Liu et al., 2013; Lange et al., 2015).

The available literature indicates that most of the research on HHMs has been carried out using the fish fauna as the target biotic element of the aquatic ecosystem. In contrast, benthic-macroinvertebrate (BM) benchmark datasets and relevant comparative modelling

studies are disproportionately limited (Poff and Zimmerman, 2010; Shearer et al., 2015; Theodoropoulos et al., 2015).

4.2. Purpose of the chapter

In this chapter, the predictive performance of widely applied habitat modelling algorithms is evaluated using a reference hydroecological dataset consisting of microhabitat-defining predictors (V, D, S and T) and BM-related response variables, collected from an extended sampling network in Greek streams and rivers. The primary question, which, based on the aforementioned analysis, needed to be answered is: 'Do the specific distributional properties of this and similar hydroecological datasets -i.e. (i) imbalanced nature, (ii) complex interactions between the microhabitat-defining variables, (iii) high variation of the response BM variables- require the application of specific habitat modelling methods to avoid producing misleading results and enhance the predictive accuracy of HHMs?'. In addition, working solutions are proposed that address the difficulty of working with highly variable hydroecological data in model-based environmental flow assessments.

4.3. Collection of the reference dataset

A total of 380 microhabitat samples (Table A5) was collected from streams and rivers in an extended sampling area surrounded by natural landscapes with no or very minor human influence. Unimpacted sites were deliberately selected with the purpose of eliminating bias originating from water quality degradation and focus only on the influence of the hydraulic properties of the water on the BM communities. Data were collected from perennial streams and rivers in central and southern Greece (Fig. 4.1; Table 4.1), belonging to the RM-1 (10-100 km^2; altitudes between 200-800 m.a.s.l.; mixed geology), RM-2 (100-1000 km^2; altitude < 600 m.a.s.l.; mixed geology) and RM-4 (10-1000 km^2; altitudes between 400-1500 m.a.s.l.; mixed geology) European intercalibration types (Van de Bund et al., 2004). In detail, the study area is characterized by semi-mountainous to mountainous relief with altitudes ranging from 116 to 972 m.a.s.l., large areas with evergreen forests, often mixed with deciduous forests of *Quercus sp., Cornus sp.*, *Pinus sp.* and *Fagus sp.* The riparian vegetation is composed of thick forests including plane trees, willows, poplars, alders and ash trees.

Table 4.1. Geomorphological properties of the study sites. T: Tributary, M: Main stem

Site No.	River	Site coordinates	Altitude (m)	Strahler order	Distance to source (km)	Catchment area (m^2)
1	Acheloos (T)	39°31'24.16"N 21°26'34.88"E	972	2	6.68	49
2	Acheloos (T)	39°25'42.01"N 21°14'51.68"E	563	1	2.81	56
3	Acheloos (T)	39°16'23.11"N 21°31'39.99"E	659	1	2.64	81
4	Evinos (M)	38°43'20.39"N 22°01'08.20"E	774	2	5.16	86
5	Mornos (M)	38°35'53.43"N 22°11'18.01"E	407	3	15.46	222
6	Krathis (M)	38°00'55.29"N 22°15'44.10"E	911	1	7.32	32
7	Alfeios (T)	37°41'36.95"N 21°57'57.87"E	403	1	7.86	27
8	Parapeiros (M)	37°59'47.93"N 21°46'00.27"E	291	2	6.71	39
9	Parapeiros (M)	38°03'07.38"N 21°42'55.96"E	116	2	15.09	108

The climatic conditions are typical of temperate Mediterranean areas, with hot, dry summers and cold, wet winters. Temperatures usually range between 0°C and 30°C. The greatest amount of precipitation falls between October and April, with the driest months being July, August and September. Maximum and minimum precipitation was recorded from nearby meteorological stations for the northern parts of the study area (sites 1, 2 and 3) in January (395.7 mm) and August (48.5 mm). For the sites of central Greece (4 and 5) the amount of precipitation was 158.2 mm in January and 24 mm in August, while in the southern parts of the area (sites 6, 7, 8 and 9), the relevant amount was 211.4 mm in March and 2.8 mm in July, respectively. According to the REFCOND guidelines for reference site selection (WFD CIS Guidance Document No. 10, 2003), nine sites were selected in the study area (Fig. 4.1; Table 4.1).

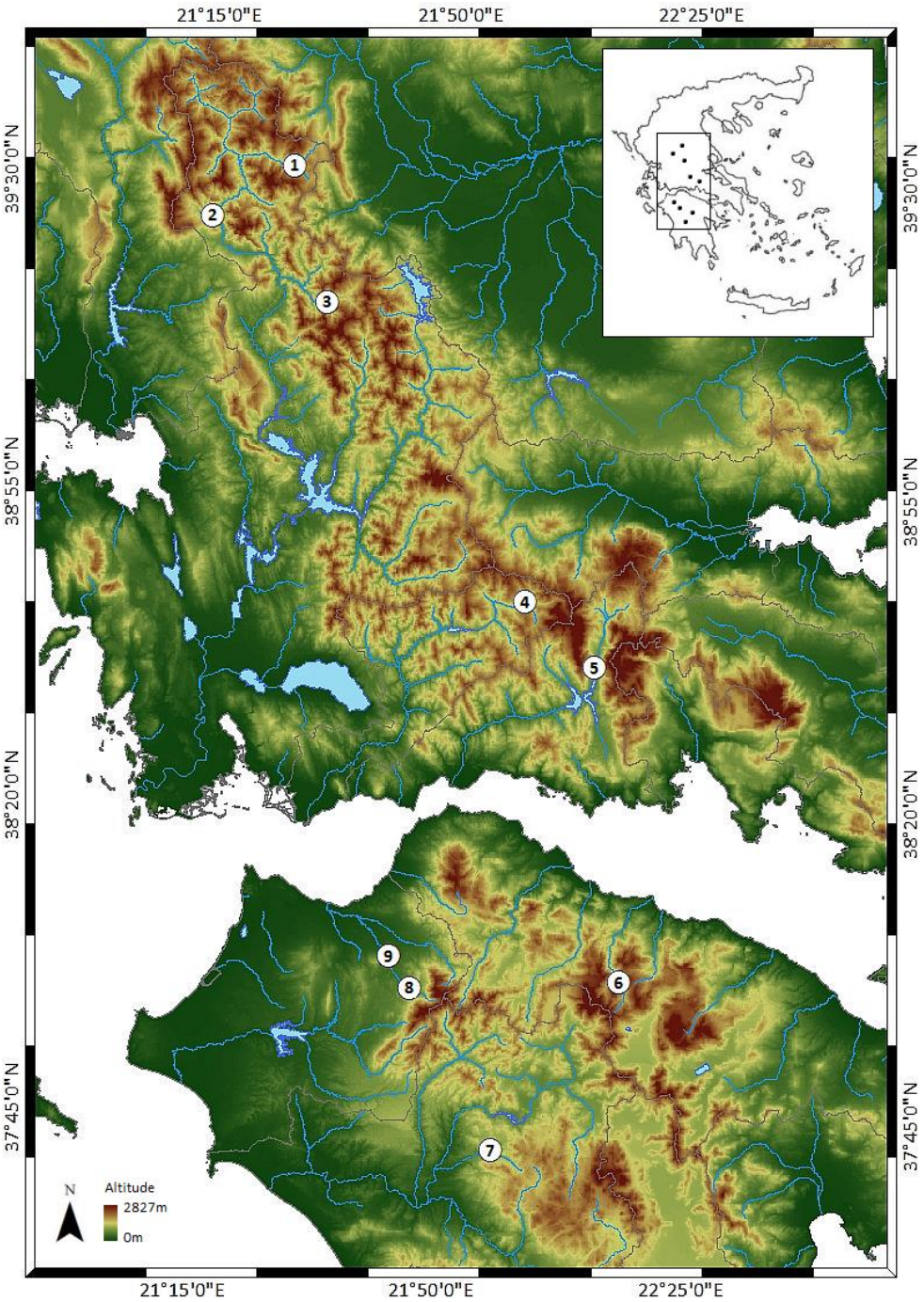

Fig. 4.1. The study area. 380 microhabitat samples were collected from 9 sites in Greek streams and rivers

4.4. Physicochemical data collection

At each site, the Aquaread AP-2000 Multiparameter Meter (https://www.aquaread.com) was used to measure water temperature, electrical conductivity, dissolved oxygen, and total dissolved solids. Water samples were afterwards collected, stored in plastic bottles (250 mL) at 4°C, transferred to the lab and analyzed for major ions (NO_3^-, NO_2^-, NH_4^+ and PO_4^{3-}) using the Merck Nova 60 Spectroquant Photometer (https://www.sigmaaldrich.com/catalog/product/mm/109751), with the results (not shown) indicating that the physicochemical properties of all sites conformed to the REFCOND guidelines (NO_3^- < 0.5 mg/L; NO_2^- < 0.3 mg/L; NH_4^+ < 0.01 mg/L; PO_4^{3-} < 0.15 mg/L).

4.5. Hydraulic-habitat and biological data collection

Benthic macroinvertebrates were collected at each site immediately after the physicochemical measurements. A modified AQEM approach (AQEM Consortium, 2002) was applied, in which benthic macroinvertebrates were sampled from a maximum of 20 rectangular microhabitats (measurement combinations of V, D and S). A Surber sampler was used (area - 0.25 x 0.25 m; mesh size - 500 μm), resulting in a total sampling area of 0.0625 m^2 at each microhabitat. Each BM sample was separately preserved in plastic bottles containing 70% ethanol. At each microhabitat, V, D and S were afterwards recorded. The Swoffer 2100 current velocity meter was used to measure flow velocity at 0.6 x D (measuring from the surface) when D ≤ 0.75 m and by averaging 0.2 x D and 0.8 x D when D > 0.75 m according to Nolan and Shields (2000). A water-depth measurement rod was attached to the current velocity meter and was used to measure the water depth. The type of substrate was visually assessed using the categories defined by Schneider et al. (2010). The final BM dataset collected included 380 microhabitats over three sampling periods (spring, summer and autumn 2015). Detailed characteristics of each microhabitat are shown in Table A5.

4.6. Data analysis

In the lab, all macroinvertebrate specimens from each sample were sorted and identified at the family level using a stereo microscope and macroinvertebrate identification guides for the Mediterranean region (Tachet et al., 2010). The abundance of BMs was calculated and the ASTERICS 3.1.1 software (Wageningen Software Labs, 2004) was then used to calculate commonly used BM metrics: taxonomic richness, diversity (Shannon's index) and EPT richness (Ephemeroptera, Plecoptera, Trichoptera).

4.7. Habitat suitability

The (micro) habitat suitability was calculated based on BM metrics commonly applied to assess the quality-suitability in relevant studies (Englund and Malmqvist, 1996; Monk et al., 2006; Waddle and Holmquist, 2011; Holmquist et al., 2015). Based on a combination of expert judgment, literature review and statistical analysis, including the spatial and temporal variation of the dataset (Table 4.2, Fig. 4.2-4.6), the following multimetric index used:

$$\kappa = 0.4\,\frac{n_{ij}}{n_{jmax}} + 0.3\,\frac{H_{ij}}{H_{jmax}} + 0.2\,\frac{EPT_{ij}}{EPT_{jmax}} + 0.1\,\frac{a_{ij}}{a_{jmax}}$$

where,

κ is the habitat suitability of the i^{th} microhabitat of the j^{th} site, ranging from 0 to 1

n_{ij} denotes the number of BM taxa (families) found at the i^{th} microhabitat of the j^{th} site

H_{ij} denotes the Shannon's diversity index for the i^{th} microhabitat of the j^{th} site

EPT_{ij} is the number of EPT taxa found at the i^{th} microhabitat of the j^{th} site

a_{ij} is the abundance of benthic macroinvertebrates found at the i^{th} microhabitat of the j^{th} site

n_{jmax}, H_{jmax}, EPT_{jmax}, and a_{jmax} denote the maximum value of the relevant variables observed at the j[th] site

It must be noted that the equation used, 'relaxes' any seasonal or site-specific variation in the BM communities due to the particular hydrological and climatological features of each site, since the values of each BM metric are normalized *per site* and *per season* to a range between 0 (unsuitable) and 1 (suitable) by dividing by the maximum observed value of the particular metric at each site for each sampling period.

Table 4.2. Statistically significant correlations (Spearman's coefficient) between the three hydrological-hydraulic variables and the four benthic-invertebrate metrics used to calculate the microhabitat suitability.

Subset		No. of taxa	Diversity	No. EPT taxa	Abundance
	Flow velocity (m/s)			0.109*	0.108*
Pooled (n=380)	Depth (m)	- 0.332**	- 0.235**	- 0.240**	- 0.268**
	Substrate class			0.112*	
	Flow velocity (m/s)				0.180*
Spring (n=160)	Depth (m)	-0.285**	-0.225**	-0.285**	-0.217**
	Substrate class				
	Flow velocity (m/s)			0.199*	0.206**
Summer (n=160)	Depth (m)	-0.352**	-0.261**	-0.234**	-0.307**
	Substrate class				
	Flow velocity (m/s)				
Autumn (n=60)	Depth (m)	-0.305**		-0.261*	
	Substrate class				
	Flow velocity (m/s)			0.252*	
RM1-2 (n=100)	Depth (m)	-0.274**			-0.231**
	Substrate class				
	Flow velocity (m/s)				
RM4 (n=280)	Depth (m)	-0.318**	-0.253**	-0.292**	-0.267**
	Substrate class			0.133*	

*p<0.05, **p<0.01

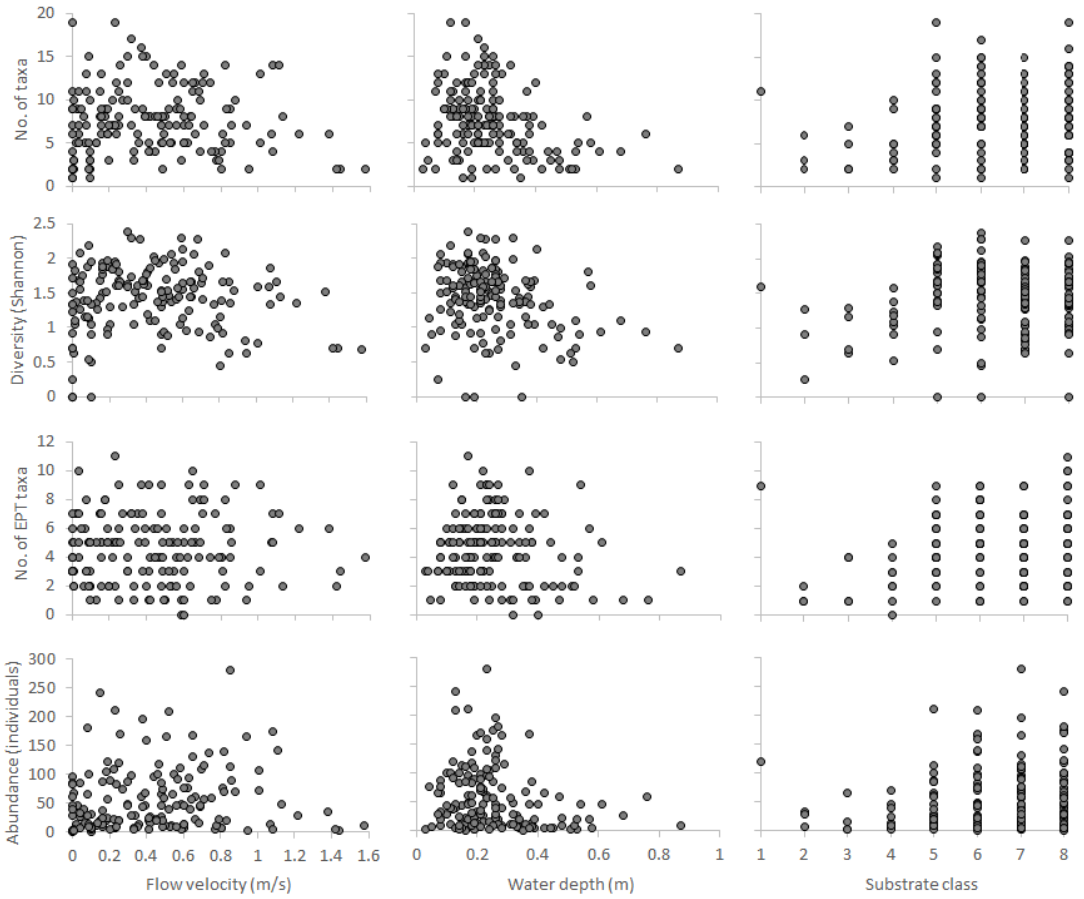

Figure 4.2. Hydroecological relationships developed from the spring samples (n=160) of the dataset between the three abiotic predictors and the four selected biotic response variables-metrics. Substrate classes; 1: Silt, 2: Sand, 3: Fine gravel, 4: Medium gravel, 5: Large gravel, 6: Small stones, 7: Large stones, 8: Boulders. EPT: Ephemeroptera, Plecoptera, Trichoptera

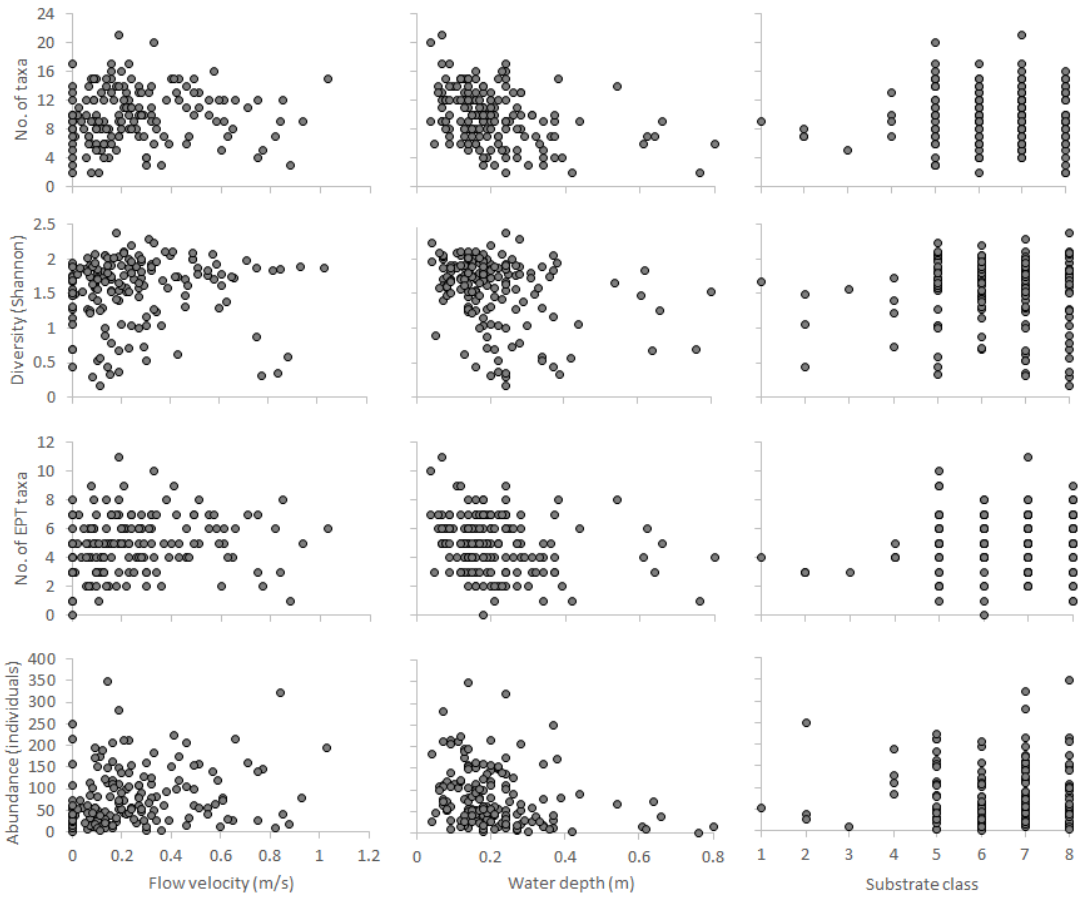

Figure 4.3. Hydroecological relationships developed from the summer samples (n=160) of the dataset between the three abiotic predictors and the four selected biotic response variables-metrics. Substrate classes; 1: Silt, 2: Sand, 3: Fine gravel, 4: Medium gravel, 5: Large gravel, 6: Small stones, 7: Large stones, 8: Boulders. EPT: Ephemeroptera, Plecoptera, Trichoptera.

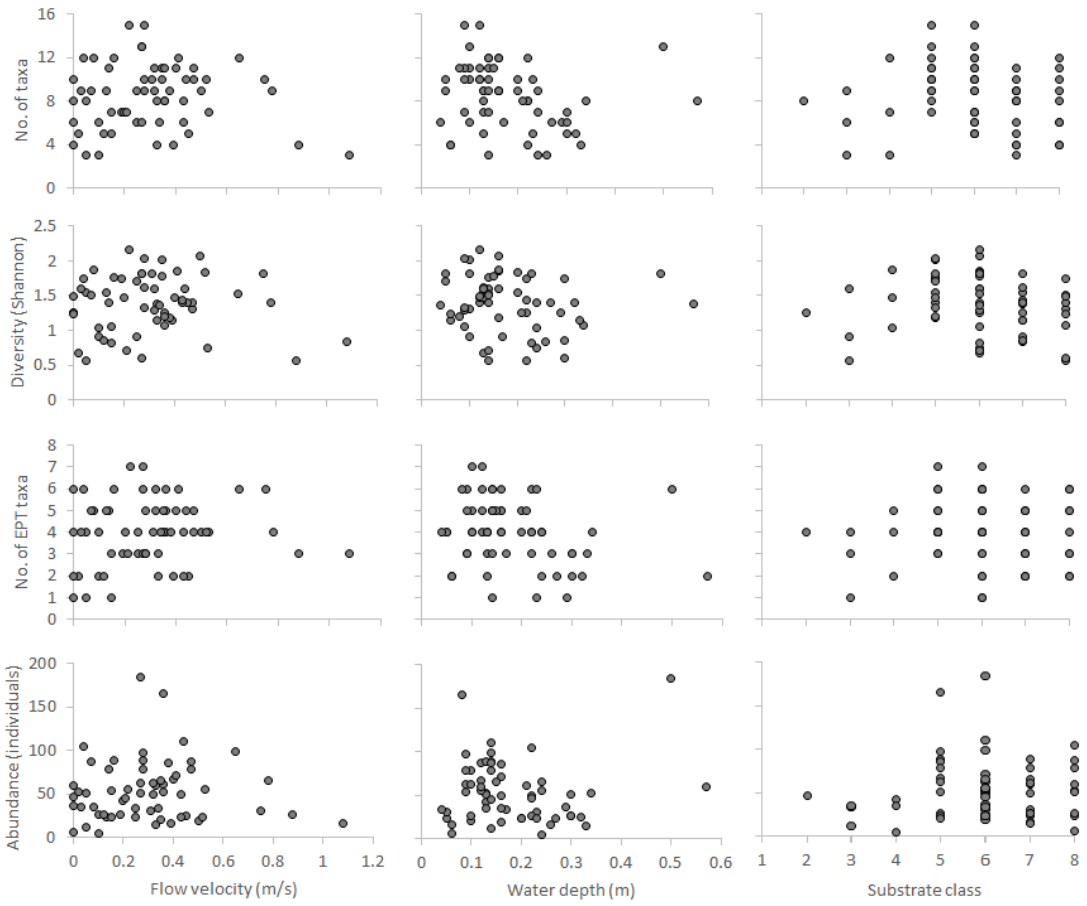

Figure 4.4. Hydroecological relationships developed from the autumn samples (n=60) of the dataset between the three abiotic predictors and the four selected biotic response variables-metrics. Substrate classes; 1: Silt, 2: Sand, 3: Fine gravel, 4: Medium gravel, 5: Large gravel, 6: Small stones, 7: Large stones, 8: Boulders. EPT: Ephemeroptera, Plecoptera, Trichoptera

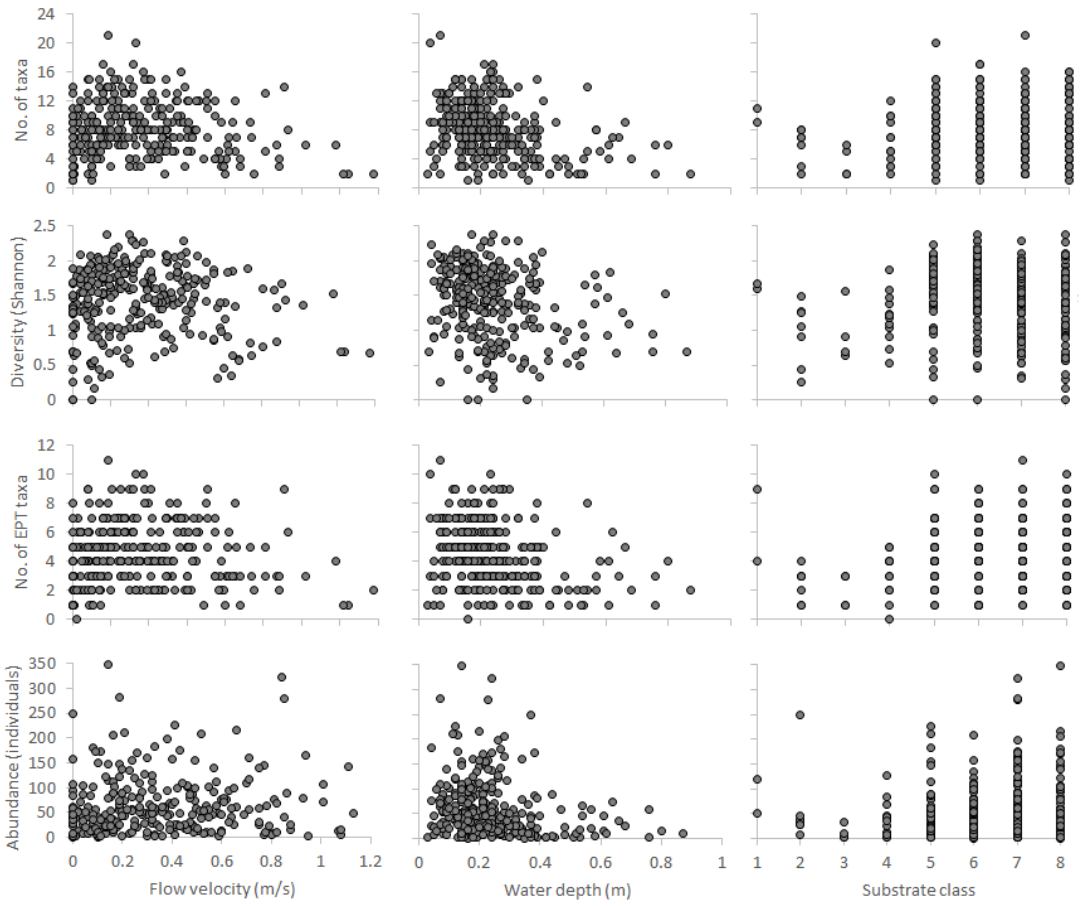

Figure 4.5. Hydroecological relationships developed from the RM4-type samples (n=280) of the dataset between the three abiotic predictors and the four selected biotic response variables-metrics. Substrate classes; 1: Silt, 2: Sand, 3: Fine gravel, 4: Medium gravel, 5: Large gravel, 6: Small stones, 7: Large stones, 8: Boulders. EPT: Ephemeroptera, Plecoptera, Trichoptera.

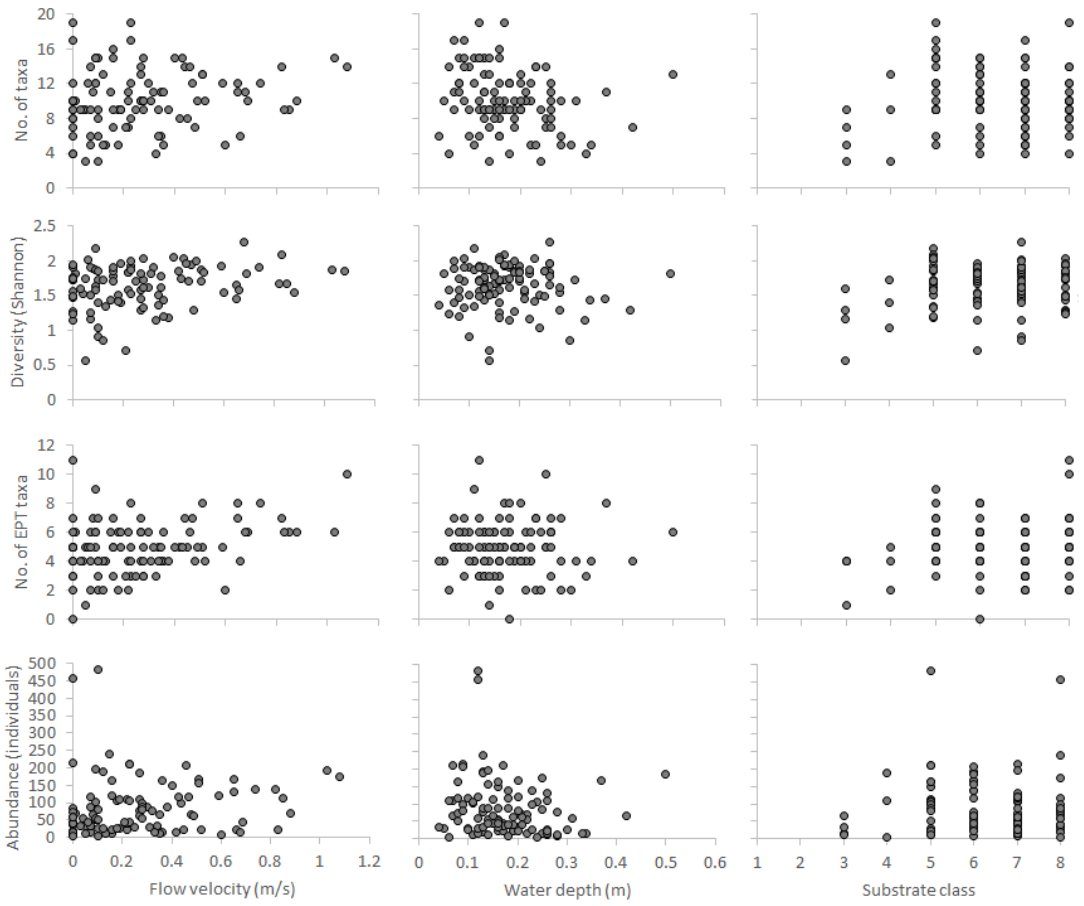

Figure 4.6. Hydroecological relationships developed from the RM1-2-type samples (n=100) of the dataset between the three abiotic predictors and the four selected biotic response variables-metrics. Substrate classes; 1: Silt, 2: Sand, 3: Fine gravel, 4: Medium gravel, 5: Large gravel, 6: Small stones, 7: Large stones, 8: Boulders. EPT: Ephemeroptera, Plecoptera, Trichoptera.

4.8. Hydroecological relationships

The Non-metric Multidimensional Scaling (NMDS) procedure, implemented in the PRIMER 6 statistical software with the Bray-Curtis distance measure was used in order to identify structural similarities between the BM communities. BM data (abundance) were square root transformed prior to the analysis to approximate normality (Quinn and Keough, 2002; Leps and Smilauer, 2003). Hydroecological relationships between the predicted habitat suitability (K) scores and the V, D, S and T hydraulic and environmental predictors were examined using five selected methods: (i) univariate habitat suitability curves (Bovee, 1986), (ii) Boosted Regression Trees (Elith et al., 2008) and (iii) Random Forests (Breiman, 2001), implemented in R version 3.1.0. (R Core Team, 2014), (iv) the Mamdani-Assilian fuzzy inference process with various de-fuzzification algorithms (Zadeh, 1965; Mamdani and Assilian, 1975; Ross, 2010) and (v) a fuzzy Bayesian inference process based on Brookes et al. (2010), both implemented in FORTRAN, using the HABFUZZ software (Theodoropoulos et al., 2016).

4.9. Univariate Habitat Suitability Curves (HSC)

Following the approach of Bovee (1986), habitat utilization curves (category II) were developed to relate the observed habitat suitability (κ) with the predictor variables. The range of values of the continuous predictors was divided into classes, with intervals of 0.1 m/s for V, 0.1 m for D

and 1 °C for T. For each predictor, the average κ of each class was calculated and visualized using histograms. A polynomial regression function (2nd to 4th order) was fitted to each 'predictor-κ' plot-, adjusting it to achieve R^2 values higher than 0.6 and p values lower than 0.05. The categorical predictor (S) was already divided into classes and the average κ for each S class was calculated. Respective polynomial models were used to predict K for each value of the predictor variable (V, D, S and T), thus deriving four different K values (one for each predictor, except for S since it was directly related with the average K), which were then integrated using the following equation:

$$K = \sqrt[4]{K_V \, x \, K_D \, x \, K_S \, x \, K_T}$$

where,
K is the predicted habitat suitability
K_V, K_D, K_S and K_T denote the habitat suitability values derived from the polynomial equation of each predictor variable.

4.10. Boosted Regression Trees (BRT)

BRT is a powerful machine-learning model, which combines two techniques; (i) regression trees, using recursive binary splits to adjust the response to predictor variables and (ii) gradient boosting, a method, which combines several, moderately accurate models to produce a very accurate predictive model. The BRT has been proven to efficiently explain and predict the response of aquatic communities to environmental variability (Leathwick et al., 2006; Leclere et al., 2011; Waite et al., 2014; Pilière et al., 2014). In this study, BRT was used as one of the best available regression-based option because it produces the most reliable best-fit curve among the relevant methods (Elith et al., 2008; Theodoropoulos et al., 2017). The BRT model was fitted using the *gbm.step* function of the 'dismo' package v1.1-4 (Hijmans et al., 2016) in R statistical software version 3.1.0 (R Core Team, 2014). Bag fraction, learning rate and tree complexity were adjusted to develop a model with the lowest cross-validation error. The values of the final model were 0.5, 0.005 and 2 respectively, achieving at least 1000 trees, following the rule of thumb suggested by Elith et al. (2008). The BRT model was developed using untransformed data, according to Elith et al. (2008).

4.11. Random Forests (RF)

RF is an ensemble learning model that generates a large number of decision trees, which are then aggregated to compute the final classification. RF applies the bootstrapping technique (resampling with replacement) and increases the tree diversity by randomly changing the sets of predictor variables over the different tree induction processes. Each classification tree is grown using another bootstrap subset X_i of the original data set X (where i denotes the index of the bootstrap iteration, ranging from 1 to the maximum number of trees k) and the nodes are split using the best split predictor variable among a subset of m randomly selected predictors (Liaw and Wiener, 2002). In detail, the algorithm for growing a RF of k classification trees goes as follows (Peters et al., 2007; Vezza et al., 2015):

(1) A bootstrap subset X_i containing approximately 2/3 of the elements of the original data set X is selected. The elements not included in the training dataset are referred to as out-of-bag (OOB) data for that bootstrap sample.
(2) X_i is used to grow an unpruned classification tree to the maximum depth but, rather than choosing the best split among all predictive variables, m predictor variables are randomly selected and the best split is chosen among these variables.
(3) Each tree is fully grown and used to predict OOB observations. Prediction is applied according to the majority vote of the ensemble of k trees (the predictions from all the trees are combined to predict an observation class as well as a probabilistic prediction

output for that observation). As OOB observations are not used in the fitting of the trees, this procedure is similar to the cross-validation process, which prevents overfitting.

The RF model was built using the *randomForestSRC 2.4.2* package (Ishwaran and Kogalur, 2017) and was further explored using the *ggRandomForests 2.0.1* (Ehrlinger, 2016) and *ggplot2 2.2.1* (Wickham and Chang, 2016) R packages. The parameters in the model were optimized in order to minimize the overall error rate. Specifically, the number of trees was set to 3500 and the number of randomly selected variables to split the nodes was set to 2. Furthermore, since the κ classes were not equally represented in the benchmark dataset, resulting in poor predictive accuracy for the minority class, (i) a weighted RF (W-RF) was applied to increase the probability of the rarely observed κ-class samples to be selected during bootstrapping and (ii) a RF was applied where the majority classes were down-sampled (D-RF) so that all classes were represented equally in each tree. The class-weight and down-sampling balancing were implemented using the *classwt* and the *sampsize* arguments, respectively, in *randomForest 4.6-12* (Liaw and Wiener, 2002) R package.

4.12. Fuzzy logic and fuzzy rule-based Bayesian inference

Fuzzy rule-based models use linguistic descriptions, such as 'low', 'moderate' and 'high' to convert the fixed, numerical values of the predictor and response variables (called crisp sets) to overlapping membership functions (fuzzy sets), usually trapezoidal or triangular-shaped, characterized by four parameters (a_1, a_2, a_3, a_4) (van Broekhoven et al., 2006) (see also chapter 3). By this procedure, called fuzzification, each numerical value of the predictor and the response variables is assigned to one or more membership functions with a specific membership degree ranging from zero to one. In trapezoidal-shaped membership functions, the membership degree linearly increases from 0 to 1 for values between a_1 and a_2, remains constant for values between a_2 and a_3 and linearly decreases from 1 to 0 for values between a_3 and a_4. In triangular-shaped membership functions, a_2 is equal to a_3. The membership functions of the predictor variables (in this case V, D, S and T) are afterwards related with the habitat suitability (note that κ is calculated based on BM community metrics and not the abundance of particular BM taxa) by a set of IF-THEN rules, either data-driven or expert-knowledge-based, such as 'IF V is low AND D is moderate AND S is gravel AND T is moderate THEN K is high'. The 'IF' part is called 'the antecedent' and the 'THEN' part is called 'the consequent'.

In typical fuzzy logic applications, the degree of fulfilment of each IF-THEN rule is afterwards calculated as the minimum of the membership degrees in its antecedent. Finally, to each linguistic habitat suitability value (κ) a fulfilment degree is also assigned, equal to the maximum of the fulfilment degrees of all rules with the output value under consideration in their consequent (van Broekhoven et al., 2006) and the final predicted K is calculated within a defuzzification process, in which the K fuzzy values are converted into a single crisp numerical value. The algorithms used for defuzzification were (i) centroid (FLC), (ii) weighted average (FLWA), (iii) maximum membership (FLMM) and (iv) mean of maximum (FLM) (Ross, 2010).

A fuzzy rule-based Bayesian inference algorithm (FRB) that deviates from the typical approach (Brookes et al., 2010) was additionally applied; the fuzzy membership degree of each predictor variable is considered as the probability of occurrence of the particular fuzzy set. The IF-THEN rules are then combined using the Bayesian joint probability, so that (referring to the previous example) the probability of a microhabitat's K being high is the joint probability that V is low AND D is moderate AND S is gravel AND T is moderate. Since K is also a linguistic output, a score is assigned to each habitat suitability class. Given for example two membership functions $\{X_1, X_2, \dots X_i\}$ and $\{Y_1, Y_2, \dots Y_j\}$ for the predictor variables X and Y, respectively, there are $M_{ij} = X_i Y_j$ cross memberships and the final predicted K is derived as:

$$K = \sum M_{ij} S_{ij}$$

where,
K is the predicted habitat suitability
M_{ij} denotes the joint probability of occurrence of each K class (cross memberships)
S_{ij} denotes the score of each K class

Five-class, trapezoidal-shaped membership functions were used for the fuzzification of V, D and T (Table 4.2). Habitat suitability (both the observed κ and the predicted K) was treated as a crisp input/output and classified using a 3-class scheme, as the minimum acceptable output scheme, and a 5-class scheme following the status classification system of the Water Framework Directive 2000/60/EC (WFD - European Commission, 2000). The substrate type was also treated as a crisp input, keeping the classes of Schneider et al. (2010) and numbering them appropriately (Table 4.3) to be included in the HABFUZZ software.

Table 4.3. Linguistic values of the abiotic (predictor) and biotic (response) variables. V: flow velocity; D: water depth, S: substrate, T: temperature, K: habitat suitability. See Schneider et al. (2010) for substrate-type size. Fuzzy set parameters follow the {a_1, a_2, a_3, a_4} order as explained in the text.

Variable	Linguistic value	Fuzzy set parameters	Variable	Linguistic value	Crisp set parameters
V (m/s)	Very low	{0, 0, 0.05, 0.1}	K (3-class)	Low	{0, 0.2}
	Low	{0.05, 0.1, 0.15, 0.2}		Moderate	{0.2, 0.6}
	Moderate	{0.15, 0.2, 0.4, 0.5}		High	{0.6, 1}
	High	{0.4, 0.5, 0.7, 0.8}	K (5-class)	Bad	{0, 0.2}
	Very high	{0.7, 0.8, 0.8, 0.8}		Poor	{0.2, 0.4}
D (m)	Very shallow	{0, 0, 0.1, 0.15}		Moderate	{0.4, 0.6}
	Shallow	{0.15, 0.2, 0.3, 0.35}		Good	{0.6, 0.8}
	Moderate	{0.3, 0.35, 0.55, 0.6}		High	{0.8, 1}
	Deep	{0.55, 0.6, 0.7, 0.75}	S	Boulders (BO)	0.070
	Very deep	{0.75, 0.8, 0.8, 0.8}		Large stones (LS)	0.050
T (°C)	Very low	{0, 0, 9, 10}		Small stones (SS)	0.040
	Low	{9, 10, 13, 15}		Large gravel (LG)	0.030
	Moderate	{13, 15, 17, 19}		Medium gravel (MG)	0.026
	High	{19, 20, 23, 25}		Fine gravel (FG)	0.024
	Very high	{25, 27, 27, 27}		Sand (SA)	0.022
				Silt (SI)	0.020

4.13. Evaluation of the models' performance and comparison

Ten times repeated ten-fold cross validation was applied to evaluate the predictive accuracy of each algorithm (Kohavi, 1995). The initial dataset was randomly partitioned in ten equal-sized subsamples. Nine subsamples (342 microhabitats) were used as the training dataset and the remaining subsample (38 microhabitats) was used for model validation. This process was repeated ten times (folds), using a different subsample for validation at each iteration. The ten-fold cross validation was repeated ten times to acquire more robust results. The performance of each model was evaluated as the average percentage of the correctly classified instances (CCI) between each iteration of the ten-fold cross-validation process.

4.14. Results and discussion

A total of 26,758 individuals were isolated from the 380 sampled microhabitats and 70 benthic invertebrate families were identified. The allocation of samples to the three-dimensional space

according to the NMDS procedure showed structural community differences based on the typological and geographical grouping applied, mainly for sites 6, 8 and 9 (Fig. 4.7). The microhabitats of these sites were concentrated at specific parts of the 3D plot and were partially isolated from the rest of the samples, indicating increased similarity between them and consequently, increased dissimilarity with the microhabitats of the other sites. This trend suggests that typological variation (site 8: RM-1, site 9: RM-2, site 6: RM-4) results in biological variation, as was initially expected.

While in abundance-based habitat models, the aforementioned dissimilarities may suggest the exclusion of these microhabitats from model training, our working solution links the predictor variables (V, D, S and T) directly to the habitat suitability (κ) using BM metrics instead of the microhabitat's macroinvertebrate abundance. This enables the application of the whole dataset to predict K in sites with varying typological properties, as long as their specific microhabitat characteristics resemble the ones provided in the training dataset. In addition, since the response variable κ is normalized *per site* and *per season* (and consequently *per river type*), typological, geographical, or even seasonal differences can be eliminated (Jowett et al., 2008), as each sample is compared with the samples of the same site.

With the inclusion of all microhabitat samples in the training dataset, the relationship between the predictor variables and the BM-metrics-based κ is depicted in Fig. 4.8. These are the typical distributions of such datasets (Fukuda et al., 2013), and the variation observed reflects the complex interactive relationships between the abiotic predictors (Jowett et al., 1991; Leclerc et al., 2003), which obviously cannot be effectively illustrated in the 2-dimensional space. The ideal visualization scheme to illustrate such complex interactions would require a 5D scatter plot (plotting V, D, S, T and κ simultaneously). However, such a scheme, although scientifically meaningful, would be visually too complex to assimilate and susceptible to common pitfalls related with high dimensionality (Ronan et al., 2016). As a consequence, the 2D scatter plots were only used to enable an initial visualization of the raw dataset and facilitate further analysis.

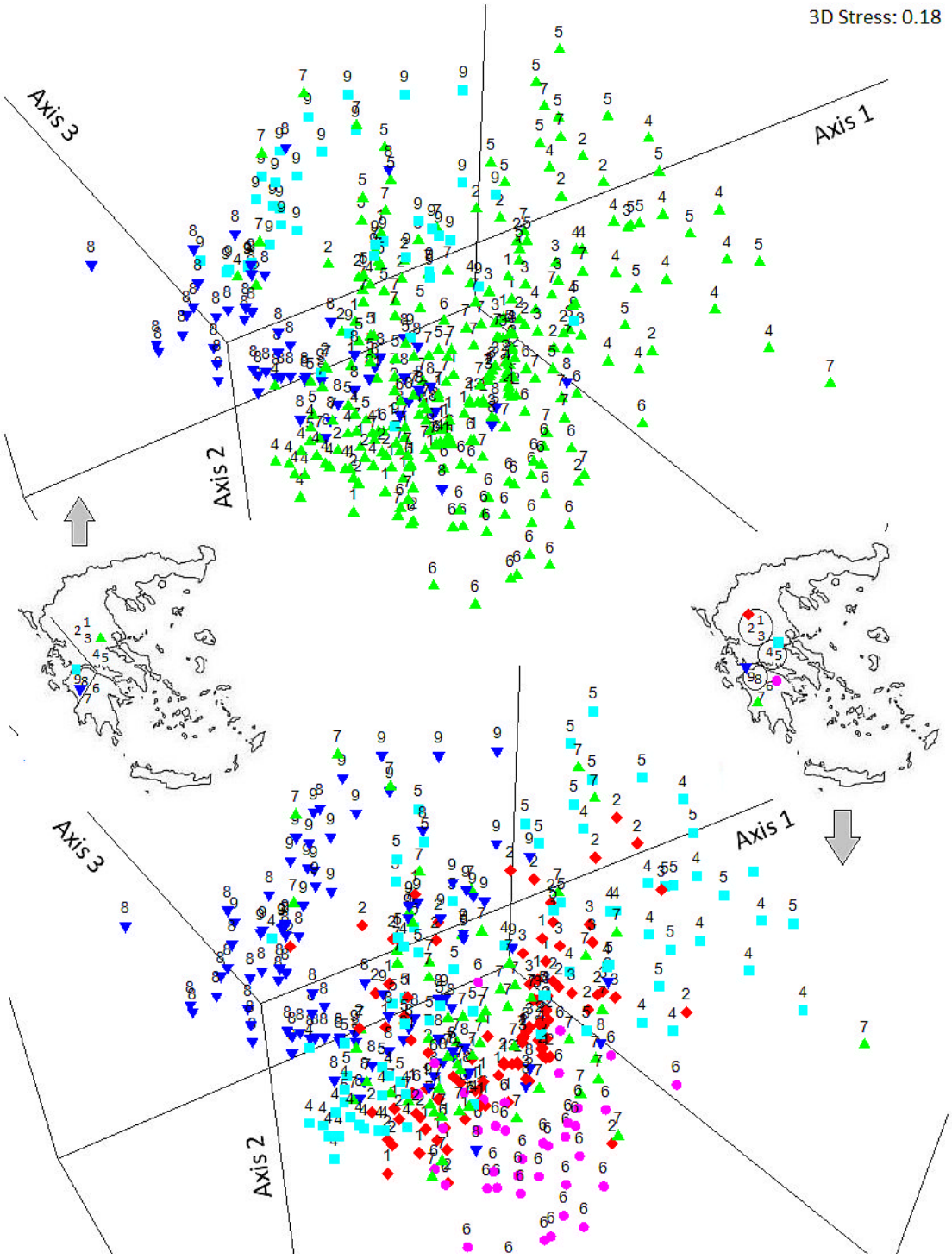

Fig. 4.7. Allocation of microhabitats to the NMDS 3D space. (Top: Grouping based on river type, Bottom: Grouping based on geographical location). The number of each site is also depicted.

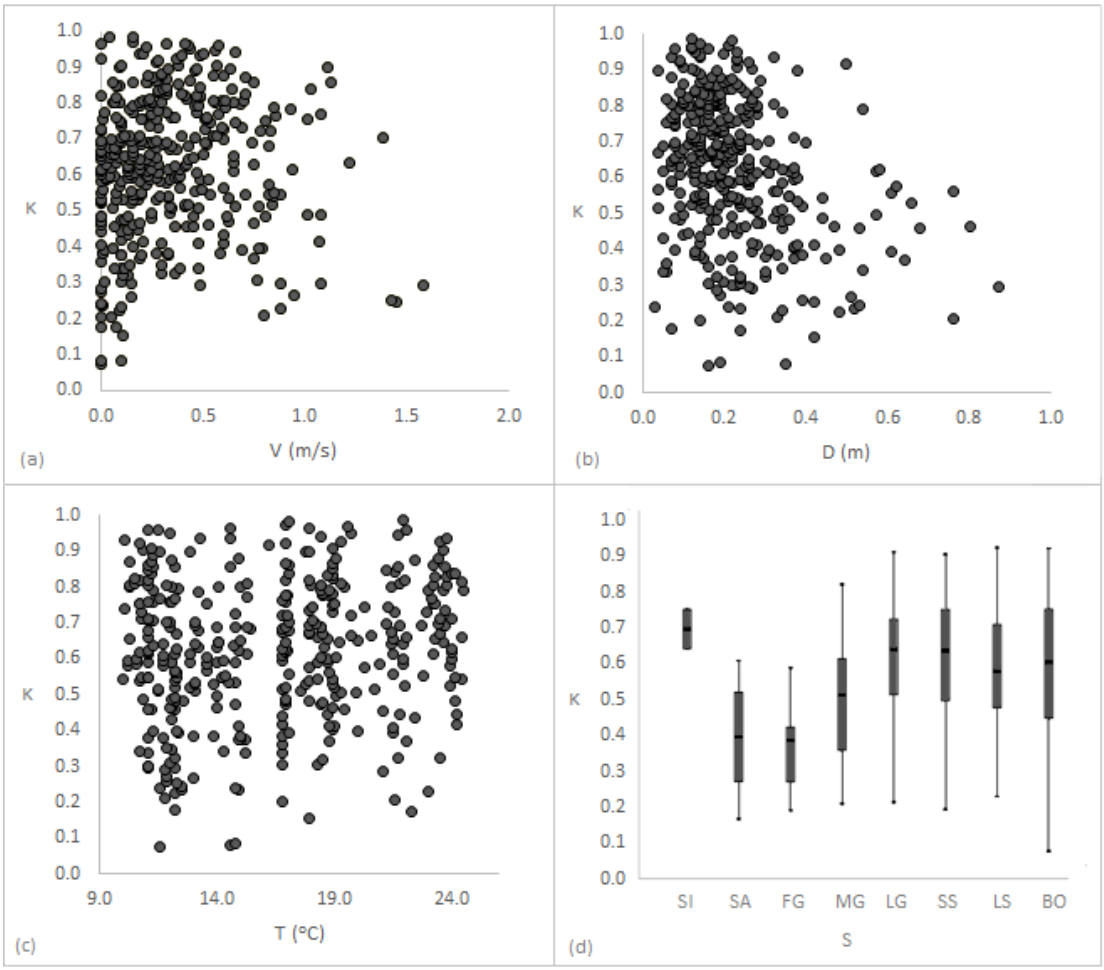

Fig. 4.8. Two-dimensional scatter plots between the predictor and response variables. V: flow velocity, D: water depth, T: temperature, S: substrate type, κ: observed habitat suitability. For S classes see Table 4.3.

According to the habitat suitability curves developed by both the HSC and BRT models (Fig. 4.9), κ values were highest in flow velocities between approximately 0.25 and 0.65 m/s, with the optimal κ values being recorded near 0.6 m/s. Water depths less than 0.3 m showed increased κ, peaking near 0.2 m and decreasing rapidly to minimum in D values greater than 0.4 m. Finer substrates had (in most cases) lower habitat suitability, with the highest κ values being recorded in boulders and large stones. Regarding T, the lowest κ values were recorded in temperatures between 12 and 16°C, increasing in T values less than 12°C and greater than 16°C. However, temperature had the weakest relationship with κ among the four predictor variables.

Similar BM habitat preferences have been indicated in the majority of previous studies from various geographic locations with varying climatic and hydrodynamic conditions. With minor exceptions for certain macroinvertebrate taxa (Jowett et al., 1991), flow velocities higher than 0.7 m/s are not considered suitable for most macroinvertebrates (Gore et al., 2001; Li et al., 2009; Shearer et al., 2015) and, in agreement with our findings, the optimal κ has been recorded in V values between 0.1 m/s and 0.6 m/s. Regarding D, habitat suitability in low-order streams and rivers usually peaks at 0.25 m (Jowett et al., 1991; Gore et al., 2001; Li et al., 2009), ranging between 0.1 m and 1 m. Coarser substrates are generally considered more suitable for benthic macroinvertebrates but with high variation among studies. Our results also suggest that large stones and boulders were more suitable (except for a unique 'silt' sample with high κ values).

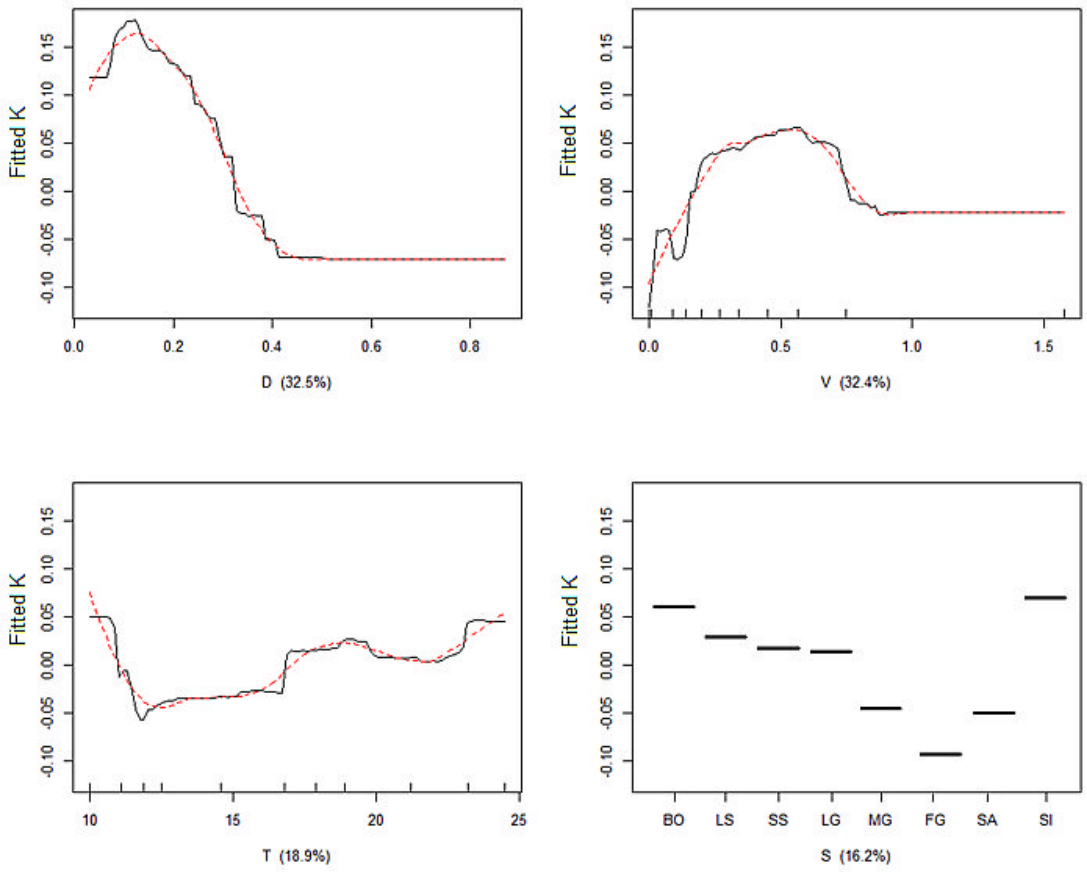

Fig. 4.9. BRT-fitted K in response to the values of the environmental/hydraulic predictors. Y axes are on the logit scale and centered to have zero mean over the data distribution. Marks at the inside bottom of the plots indicate data range and deciles of site distribution across each variable. The solid line is the BRT-modelled response curve. The dashed line (red) is the LOESS smoother (span 0.25) fitted to the response curve. S abbreviations are explained in Table 4.2.

The probability of each K-class in response to the values of the environmental and hydraulic predictors, based on the RF model application, is illustrated in Fig. 4.10. Probability (p) values between the high (H) and moderate (M) K classes showed inverse trends for V, D and T. The p value of H increased above 0.5 in V values between 0.1 and 0.7 m/s, in contrast with the p value of the M class, which decreased below 0.5 in the same V range. Regarding D, p values higher than 0.5 were recorded for D values less than 0.3 m, contrasting to the p values of the M class. T values higher than 15°C resulted in increasing H class p (>0.5) and decreasing M class p (<0.5). With much deviation from the mean values, H-class p increased in boulders, large and small stones and large gravel. The M-class p increased in fine gravel, medium gravel and sand, while the L-class p was higher in sand.

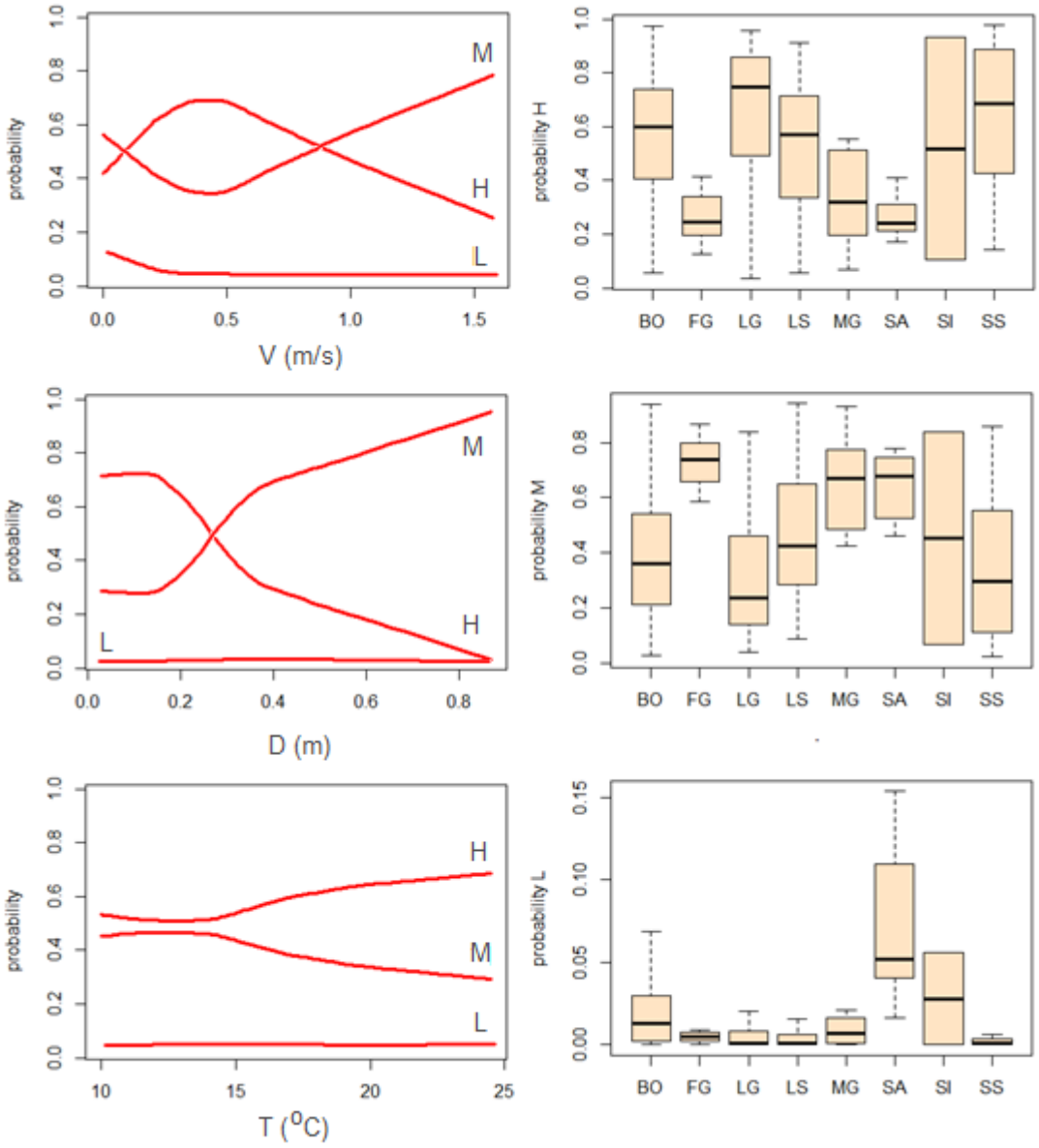

Fig. 4.10. Probability of K in response to the values of the environmental/hydraulic predictors, based on the RF model. V: flow velocity, D: water depth, S: substrate type, T: temperature, H: high K class, M: moderate K class, L: low K class. For S-classes see Table 4.3.

It has to be noted that due to the small representation of the low κ class in the benchmark dataset, its probability of occurrence was very low for all the predictor variables, increasing only to near 0.1 for V values less than 0.2 m/s. This 'weakness' was observed not only in the RF algorithm but also in HSC and BRT and is a common pitfall in imbalanced datasets as many algorithms are constructed to minimize the overall error rate, which often results in poor accuracy for the minority class (Sun et al., 2007; Sun et al., 2009; Ali et al., 2015). However, in our study adjusting the RF model in favor of the 'rare' class, either by class-weight or down-sampling, resulted in a decrease of the major classes' classification accuracy and of the model's overall predictive accuracy. Consequently, the selection of the 'best' model is highly subjective and mostly depends on the purpose of the model's application. For example, in WFD-oriented habitat simulations, the user's interest is mainly focused on accurately predicting -and discriminating between- the M and G K-classes (finding the M-G boundary), since in the WFD's classification system only the 'good' and 'high' K classes are considered acceptable (European Commission, 2000).

Based on the overall performance metrics calculated during the 10-fold cross validation process (Table 4.4), and regarding the 3-class K scheme, the FLC and FLWA models had the lowest performance (50.13% and 49.14% respectively). The remaining fuzzy-logic-based models showed acceptable predictive accuracy (>50% CCI) but were outperformed by the HSC, RF and FRB models, which showed 61.38%, 61.94% and 61.2% accuracy, respectively, while the BRT model had the highest overall performance (67.92%), reaching a maximum of 81.58% during cross-validation. As previously mentioned, in contrast to the fuzzy rule-based algorithms, the HSC, BRT and RF models failed to accurately predict the low-class K (all models had an accuracy lower than 10% for this class). Adjusting the RF model to account for the low κ microhabitats increased the predictive accuracy of the low K class from 0% to 50% and 55% for the W-RF and the D-RF, respectively, but decreased the accuracy of the H class by 10% (W-RF) and 20% (D-RF), while the M class predictions showed varying shifts (+10% for W-RF and -10% for D-RF). The overall predictive accuracy decreased from 61.85% to 57% and 54% for the W-RF and D-RF, respectively.

Table 4.4. Model performance, evaluated as the average percentage of Correctly Classified Instances (%CCI) during the cross validation process.

Model	3-class K			5-class K		
	Performance (%CCI)	Min %CCI	Max %CCI	Performance (%CCI)	Min %CCI	Max %CCI
HSC	**61.38**	55.26	71.68	**35.28**	26.31	43.73
BRT	**67.92**	60.52	81.58	**38.66**	28.94	47.36
RF	**61.85**	-	-	**35.32**	-	-
W-RF	57.23	-	-	-	-	-
D-RF	54.38	-	-	-	-	-
FLC	50.13	46.84	54.47	30.42	26.84	32.11
FLWA	49.74	46.84	52.89	29.63	26.58	32.11
FLMM	**61.16**	58.16	63.95	**35.87**	32.11	40
FLM	**60.68**	55.79	65.26	**34.37**	32.11	38.16
FRB	**61.20**	58.95	64.10	**36.62**	34.47	40

These results suggest the use of the FRB model for reliable applications of habitat suitability modelling in imbalanced datasets, since it had the highest overall predictive accuracy and also performed well in predicting the low K-class samples (71% accurate), without any further adjustment (Fig. 4.11). It must be noted however, that as the detail of the final prediction increased (by applying the 5-class K scheme) the predictive performance of all models, including the FRB, decreased dramatically to unacceptable prediction levels, ranging from 29.63% to 38.66% (again the BRT, RF and FRB models were the most accurate).

Previous studies show varying results regarding the predictive accuracy of habitat models, obviously due to the different methodological approaches applied and the variation of the input datasets. A 5-class K scheme has rarely been previously adopted. As partially discussed in Lange et al. (2015) and our results confirm, the application of habitat suitability modelling within a 5-class K system (according to the WFD classification) is prohibitive due to the low (unacceptable) predictive accuracy of the models. Moreover, existing habitat models relate habitat suitability directly to the abundance of particular aquatic taxa (either fish or benthic macroinvertebrates) or are based on presence-absence schemes. Within this context, 4-class K, BM abundance-based fuzzy models (van Broekhoven et al., 2006; Mouton et al., 2009) showed %CCI values between 50% and 66%. Fish-based presence-absence fuzzy models (Muñoz-Mas et al., 2016) calculated %CCI values between 45% and 48%. In addition, previous fish-based RF model applications (Mouton et al., 2011; Vezza et al., 2015) confirm the increased accuracy of the specific method, calculating %CCI values greater than 70%.

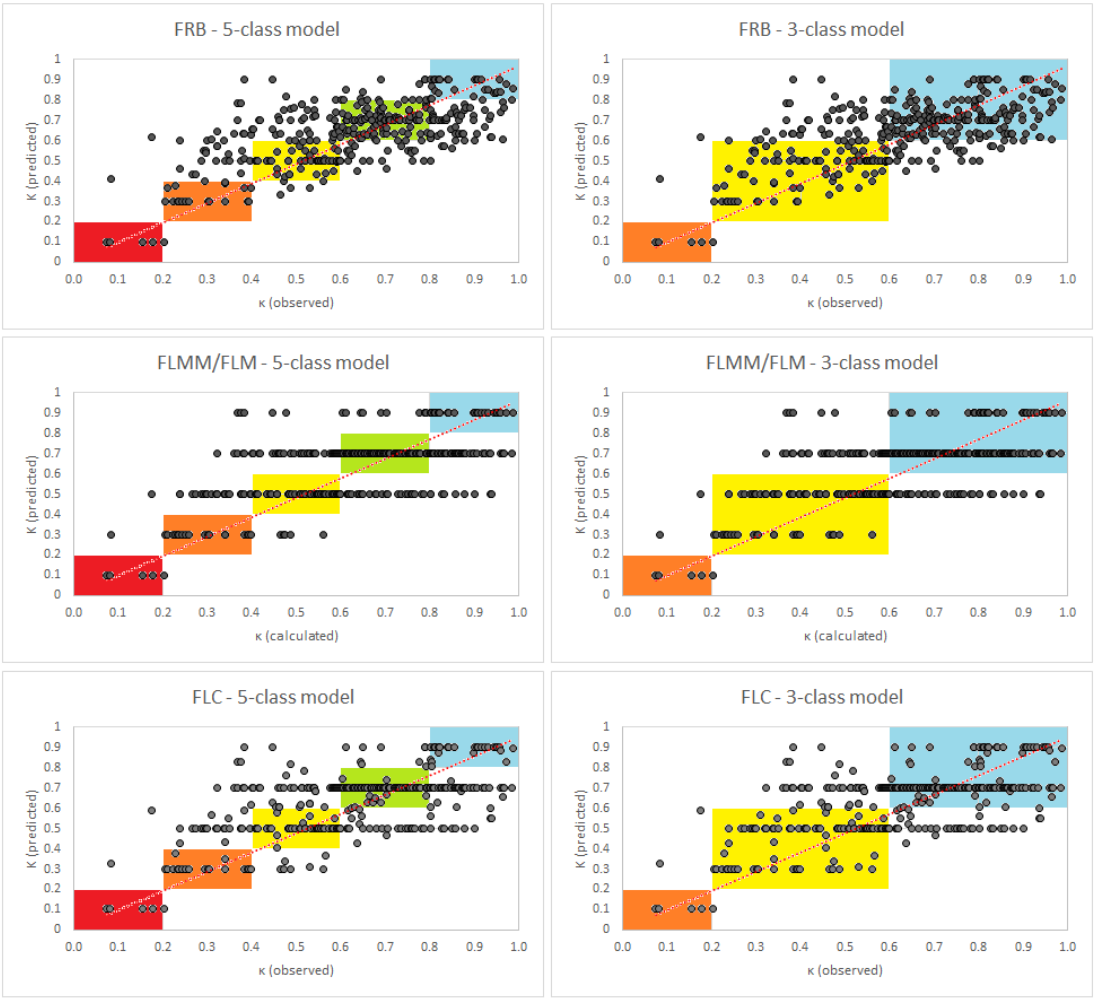

Fig. 4.11. Graphical representation of the fuzzy rule-based models' output. The observed *κ* is plotted against the predicted *K* using the 3-class (Low: [0,0.2], Moderate: (0.2,0.6], High: (0.6,1]) and 5-class (Bad: [0,0.2], Poor: (0.2,0.4], Moderate: (0.4,0.6], Good: (0.6,0.8], High: (0.8,1]) systems to visualize the model's accuracy at each case. The dotted line indicates 100% accuracy.

4.15. Conclusions

BM-based data-driven habitat modelling requires the application of specific algorithms to avoid producing misleading results and enhance the predictive accuracy of the output habitat suitability, depending on the distributional properties of the input hydroecological dataset.

- The complex interactions between the microhabitat-defining predictors and the high variation of the response BM variables did not significantly influence overall model performances. All models including the univariate HSC algorithm (which does not account for interactions between predictors) showed almost equal overall performance.
- In contrast, the imbalanced nature of the dataset, reduced the predictive accuracy of the HSC, BRT and RF algorithms for the low-K class to unacceptable levels. This suggests that the imbalanced nature of a dataset should be the main factor to consider when selecting the most suitable algorithm.
- Random Forests and Boosted Regression Trees can be effectively applied to provide reliable habitat suitability predictions. The predictive accuracy of these models was 61.85% and 67.92% respectively, reflecting the increased predictive capacity of these algorithms. However, both models failed to efficiently predict the microhabitats with low habitat suitability, due to the disproportionately limited number of such microhabitats in the benchmark dataset. The use of W-RF and D-RF overcame this problem but at the cost of decreasing the overall predictive accuracy.
- The FRB, FLM and FLMM models also had high overall predictive accuracy. In addition, due to the intrinsic properties of these algorithms, which, using a set of data-driven IF-THEN rules, process and predict the habitat suitability of each microhabitat one-by-one, these models developed reliable predictions for all classes of habitat suitability.
- It must be noted however that all models failed to efficiently predict the microhabitat suitability when a 5-class scheme was applied, suggesting that as the detail of the final prediction increases, the application of the selected models becomes insufficient. As partially discussed in van Broekhoven et al. (2006) and in agreement with our ecological viewpoint, while a 3-class-based, accurate predictive model is considered sufficient for ecological applications (e.g. for model-based environmental flow assessments), other modelling options could further increase the predictive performance of habitat models.

It is finally concluded that Boosted Regression Trees and Random Forests can be effectively used in habitat modelling, given balanced datasets. However, the fuzzy rule-based algorithms should be preferred when modelling imbalanced datasets. In addition, when the input dataset is large enough to provide sufficient data-driven IF-THEN rules to 'feed' a fuzzy-rule-based algorithm (FRB, FLM, FLMM), these models are likely to produce the most reliable habitat suitability predictions. The application of other machine-learning algorithms should be further investigated because the predictive accuracy of Random Forests and Boosted Regression Trees indicates the high potential of such models for habitat modelling applications.

Chapter 5

Case study 1 - Application of TELEMAC 2D and HABFUZZ to simulate habitat suitability using benthic macroinvertebrates and develop model-based environmental flow scenarios downstream of the Parapeiros River Dam (western Greece)

5.1. Overview

The potential use of hydrodynamic habitat models (HHMs) in environmental flow assessments (EFAs) has long been researched since the mid-1970s (Bovee and Milhous, 1978; Bovee, 1986; Maddock, 1999; Ahmadi-Nedushan et al., 2006; Benjankar et al., 2014; Stamou et al., 2018). During the last decades, the predictive accuracy of HHMs has been highly improved, new algorithms were introduced in their habitat modules and the overall effectiveness of HHMs in providing accurate EFAs has hence been widely recognized. However, in Europe, and to a lesser extent, worldwide, (i) the practical application of HHMs in EFAs remains disproportionately limited compared to their hydrology-based alternatives (Dunbar et al., 2012; Linnansaari et al., 2013; Rivaes et al., 2017), (ii) it has been primarily focused on fish (Waddle and Holmquist, 2011; Arthington, 2012; Leitner et al., 2017), while other components of the aquatic ecosystem have not been equally used (Rivaes et al., 2017; Theodoropoulos et al., 2018a) and (iii) two-dimensional hydrodynamic habitat models only recently became widely used in EFAs (Benjankar et al., 2014; Stamou et al., 2018).

In the European Union, the potential of HHMs to be used for implementing accurate, ecosystem-based EFAs has been officially acknowledged in the Guidance Document No. 31 (WFD CIS, 2015) of the Water Framework Directive 2000/60/EC (WFD - European Union Council, 2000). A three-class hierarchy of EFA methodologies has been suggested, with HHMs being considered as 'level 3', potentially applicable in situations where a high degree of certainty is required to provide water managers with defensible environmental flow recommendations. The low percentage (18%) of European HHMs-based case studies in the relevant WFD Guidance Document is also indicative of this gap between theoretical research/knowledge and practical application of HHMs. Particularly in Greece, HHMs have only recently been incorporated into EFAs and are currently focused solely on fish (Muñoz-Mas et al., 2016; Papadaki et al., 2017), while the legal framework on environmental flows is still based on simplistic and rather arbitrary hydrological criteria (Ministry of Environment, Energy and Climate Change, 2011).

The reasons for this limited application of HHMs in EFAs are mainly associated with cost-effectiveness, time-efficiency, required expertise and availability of hydroecological data (Jorgensen and Bendoricchio, 2001; Conallin et al. 2010). HHMs-based EFAs inevitably require a costly and time-consuming collection of hydraulic and hydrometric data to calibrate and validate the hydrodynamic module (Spense and Hickley, 2000) and usually, additional, carefully designed field visits are necessary to calculate the habitat preferences of aquatic biota (Heggenes et al., 1990). Moreover, the developed hydrodynamic habitat model is usually restricted to an area of 200 or 300 meters, whereas the effects of hydrological alteration may be geographically widespread (Booker, 2016). In addition, most HHMs focus on the habitat preferences of specific (fish) species, while it has long been acknowledged that accurate EFAs, within a holistic framework, must be based on the ecological requirements of different biological communities (Acreman et al., 2009).

5.2. Purpose of the chapter

This chapter describes the application of a two-dimensional hydrodynamic habitat model for the development of ecosystem-based environmental flow recommendations in the downstream route of a regulated river in Greece (Parapeiros, Western Greece). Benthic macroinvertebrates (BMs) were used as the target aquatic community and, based on the conclusions of the previous chapter, a fuzzy rule-based Bayesian algorithm was implemented to accurately assess their habitat preferences. In addition, an analysis of the costs and time required to implement the specific case study is presented. The main purpose of this chapter is (i) to demonstrate the use of benthic macroinvertebrates in model-based EFAs, (ii) to highlight the under-valued features of HHMs that make them ideal candidates for ecosystem-based EFAs, (iii) to discuss on their disadvantages and propose working solutions on how to

properly overcome them and (iv) to point out that HHMs-based environmental flow assessments can be cost-effective and time-efficient and should be ultimately preferred over other options when searching for the fine balance between anthropogenic water demand and long-term ecosystem functionality and integrity.

5.3. Case study

The study reach is located in western Greece, at the downstream route of the river Parapeiros (Fig. 5.1). Parapeiros has a catchment-area size of 118 km^2 (Digga, 2012). It is a large tributary of the Peiros River. Originating in the mountainous upper parts of the basin, after a distance of 25 km it converges with Peiros and empties in the Patraikos Gulf. The basin has a temperate Mediterranean climate with temperatures ranging from 0^{o}C to 35^{o}C. The flow regime is highly seasonal; increased runoff occurs between October and April, while July, August and September are the driest months of the year. Average maximum precipitation over a 30-year period (1961 - 1990) has been recorded in December (121.8 mm) and minimum in August (4.8 mm).

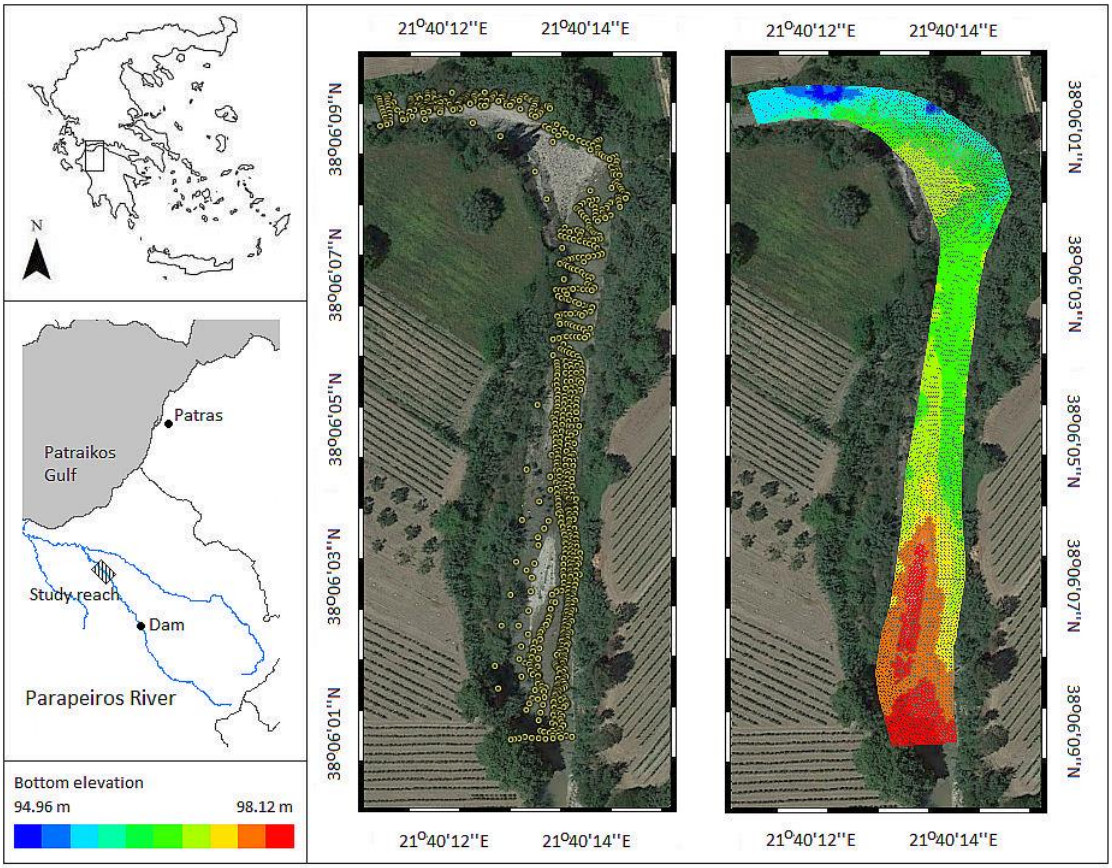

Fig. 5.1. The study area; the Peiros-Parapeiros River Basin is depicted along with the location of the major dam in the river Parapeiros and the GPS-derived topography.

The river basin is currently ungauged. Existing rainfall-runoff models (Digga, 2012) calculate daily discharges, based on average annual values, ranging from 1.22 m^3/s to 1.73 m^3/s, while daily discharge values from a gauged site in a neighboring basin of similar hydrological and climatological characteristics (Glafkos River - Mechleri, 2008) range from 0.3 m^3/s (from June to October) to above 3 m^3/s (from November to May), reaching higher than 6 m^3/s during floods and varying between the years. Two dams have been constructed and will soon be operative in order to supply the nearby city of Patras with drinking water. The largest one is the earthen dam located at the mid-course of the Parapeiros River, with a height of 68 m and a

storage capacity of 38.8 x 10^6 m^3. According to the relevant environmental impact assessment, an environmental flow (baseflow) of 0.2 m^3/s, calculated based on a combination of limited hydrological records and hydrological modelling, will be released during summer to maintain the integrity of the downstream aquatic ecosystem (Digga, 2012).

5.4. Collection of topographic information and mesh generation

The two-dimensional (2D) hydrodynamic simulation was carried out in a 277-m long reach, situated 8 km downstream of the major dam location. Channel topography was mapped with 863 points recording longitude (X), latitude (Y) and bottom elevation (H). A Real-Time Kinematic (RTK) GPS was used, consisting of the 'Spectra Precision SP60 GNSS Receiver' (http://www.spectrapre cision.com/eng/sp60.html) and the 'MobileMapper 10 GIS - GPS Receiver' (http://www.optron. com/spectra/products/Mobile-Mapper-10.html). Slope breaks and similar areas with rapid relief changes were mapped with higher density of points, while fewer points were allocated in flat surfaces. The topographic information (X, Y, H points) was afterwards imported into the BlueKenue software (https://nrc.canada.ca/en/research-development/products-services/software-applications/blue-kenuetm-software-toolhydraulic-modellers) to interpolate channel topography and generate a triangular computational mesh representative of the study reach. The computational mesh that was generated for the study reach is composed of 9,875 elements and 5,170 nodes with a 1 m spatial resolution.

5.5. Hydrometric data, calibration and validation of the hydrodynamic module

Longitude, latitude (using the RTK-GPS) and field measurements of water depth (D) and depth-averaged flow velocity (V) were recorded at 15 randomly selected points at two different discharges (Q) (0.3 m^3/s and 1 m^3/s), and were used to calibrate-validate the hydrodynamic model. Water depth was measured using a water-depth measurement rod. Depth-averaged flow velocity (V) was measured using the Swoffer 2100 current velocity meter (http://www.swoffer.com/products.htm) at 0.6 x D when D ≤ 0.75 m and by averaging 0.2 x D and 0.8 x D when D > 0.75 m according to Nolan and Shields (2000). The type of substrate (S) was visually estimated based on the categories defined by Schneider et al. (2010) and used as a basis to adjust the Manning's roughness coefficient (n) for model calibration based on the values suggested by Chow (1959). At each survey, according to the model's requirements, Q was measured at the upstream boundary and water surface elevation (Z) was measured at the downstream boundary. To reduce the required number of field visits, a stage-discharge curve was developed for the downstream boundary following the suggestions of the US National Resources Conservation Service (2012): V was measured at selected points through the cross section; from these V values and their associated cross-sectional areas, Q was computed for various Z values on the rising and falling side of an elevated flow and the stage-discharge curve was developed.

5.6. Software for hydrodynamic simulation

Prior to running the hydrodynamic simulation, boundary and initial conditions were defined using the FUDAA-PREPRO pre-processor (http://prepro.fudaa.fr). Discharge was prescribed at the upstream boundary and Z was prescribed at the downstream boundary based on a stage-discharge curve developed for the downstream boundary. TELEMAC-2D v6.2 (Galland et al., 1991) was afterwards used to simulate D and depth-averaged V in various discharge scenarios.

The model was calibrated using the data (V and D) from the first hydrometric survey (Q = 0.3 m^3/s) and validated using the hydrometric data from the second survey (Q = 1 m^3/s). Calibration was applied by properly adjusting the Manning's n values at different sections of the study reach (based on the initial visual assessment of the substrate types) until an acceptable combination of R^2 between the predicted and observed V and D values was achieved. The Manning's roughness coefficient in the calibrated model ranged from 0.03 to

0.05. The coefficient of determination (R^2) between the predicted and observed D and depth-averaged V values was greater than 0.8 and ranged from 0.9317 (D) to 0.9338 (V) ($p<0.01$) for the calibration dataset and from 0.8879 (D) to 0.9328 (V) ($p<0.01$) for the validation dataset (Fig. 5.2), suggesting strong, statistically significant correlations and an acceptable model performance. Depths in the wetted nodes of the study reach ranged from 0.1 m to 0.92 m for the lowest discharge (0.01 m^3/s) and from 0.3 m to 3.17 m for the highest discharge simulated (7 m^3/s). Depth-averaged V values, respectively ranged from 0.05 m/s to 0.5 m/s (Q = 0.01 m^3/s) and from 0.05 m/s to 3.2 m^3/s (Q = 7 m^3/s). The validated model was used to simulate 11 discharge scenarios ranging from 0.01 m^3/s to 7 m^3/s.

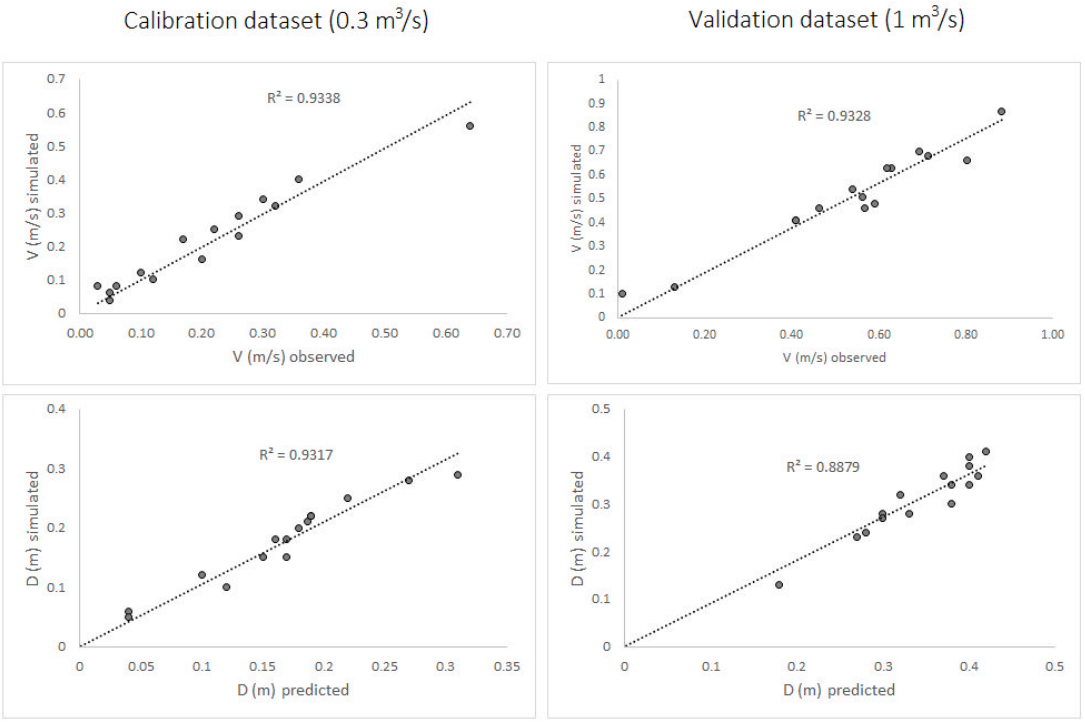

Fig. 5.2. Correlation between observed and simulated data in 15 randomly selected points during calibration (Q = 0.3 m^3/s) and validation (Q = 1 m^3/s). V: flow velocity, D: water depth

5.7. Habitat suitability modelling methods and software

The habitat preferences of benthic macroinvertebrates were assessed using the 'benthos-GR' dataset (https://github.com/chtheodoro/benthos-GR), consisting of 380 microhabitat samples collected from nine sampling sites in Greece (Theodoropoulos et al., 2018a - see chapter 4). Each microhabitat is a combination of V, D and S corresponding to a habitat suitability value (κ), calculated using BM-community metrics commonly applied to assess the quality-suitability in relevant studies (Englund and Malmqvist 1996; Monk et al. 2006; Waddle and Holmquist 2011; Holmquist et al. 2015). Each metric was weighted based on a combination of expert-judgment and previous literature to reflect its relevant contribution-significance to the calculation of κ and the following equation was used:

$$\kappa = 0.4\,\frac{n_{ij}}{n_{jmax}} + 0.3\,\frac{H_{ij}}{H_{jmax}} + 0.2\,\frac{EPT_{ij}}{EPT_{jmax}} + 0.1\,\frac{a_{ij}}{a_{jmax}}$$

where,

κ is the habitat suitability of the ith microhabitat of the jth site, ranging from 0 to 1
n_{ij} denotes the number of BM taxa (families) found at the ith microhabitat of the jth site
H_{ij} denotes the Shannon's diversity index for the ith microhabitat of the jth site
EPT_{ij} is the number of EPT taxa found at the ith microhabitat of the jth site
a_{ij} is the abundance of benthic macroinvertebrates found at the ith microhabitat of the jth site
n_{jmax}, H_{jmax}, EPT_{jmax}, and a_{jmax} denote the maximum value of the relevant variables observed at the jth site

The benthos-GR dataset was used to train and cross-validate the fuzzy rule-based Bayesian algorithm (FRB) described in detail in the previous chapter and implemented in the HABFUZZ software (Theodoropoulos et al., 2016). The numerical values of the input variables (V, D and S) were converted to overlapping, trapezoidal-shaped, membership functions called fuzzy sets (van Broekhoven et al., 2006). By this process, called fuzzification, each numerical value was assigned to one or more fuzzy sets with a membership degree ranging from zero to one; κ values were also classified in five classes (0 ≤ bad ≤ 0.2; 0 < poor ≤ 0.4; 0.4 < moderate ≤ 0.6; 0.6 < good ≤ 0.8; 0.8 < high ≤ 1). The training dataset, with *a priori* calculated κ values, was used to develop sets of data-driven IF-THEN rules, relating the input fuzzy sets with a specific κ class. In the FRB, the fuzzy membership degree (MD) of each input variable (V, D and S) is considered as the probability of occurrence of the particular fuzzy set, such as 'IF V is low with a membership degree of 1 AND D is moderate with a MD of 1 AND S is gravel with a MD of 1 THEN κ is high with a MD of 0.3 and good with a MD of 0.7'. The IF-THEN rules are then combined using the Bayesian joint probability, so that (referring to the previous example) the probability of the specific microhabitat's κ being high is the joint probability that V is low AND D is moderate AND S is gravel AND κ is high (1 x 1 x 1 x 0.3 = 0.3), while the probability of κ being good is the joint probability that V is low AND D is moderate AND S is gravel AND κ is good (1 x 1 x 1 x 0.7 = 0.7). Based on a utility function (Brookes et al., 2010), a score is assigned to each κ class (bad: 0.2, good: 0.4, moderate: 0.6, good: 0.7, high: 0.9) and the habitat suitability for each microhabitat is predicted using the following equation:

$$K = \sum M_{ij} S_{ij}$$

where,
K is the predicted habitat suitability
M_{ij} denotes the joint probability of occurrence of each K class (cross memberships)
S_{ij} denotes the score of each K class
For the previous example, K equals to 0.7 x 0.9 + 0.3 x 0.7 = 0.84 (high).

Since the study reach, typologically belongs to the RM-2 (100-1000 km^2; altitude <600 m.a.s.l.; mixed geology) European intercalibration type (van de Bund, 2009), the model was trained using two datasets, (i) the whole benthos-GR dataset (380 microhabitats) that includes microhabitats from the RM-1, RM-2 and RM-4 river types (T-BGR) and (ii) the microhabitats of the benthos-GR dataset corresponding to samples collected from two reference sites in the same river, upstream of the study site (T-PAR). The output of the hydrodynamic model (D and depth-averaged V values) at each simulated discharge was used as input to the FRB habitat model, which calculated K at each node of the computational mesh of the hydrodynamic model (resulting in 5170 K values x 11 discharge scenarios x 2 training alternatives). The habitat suitability of the study reach at each Q was visualized using the BlueKenue software.

5.8. Environmental flow calculation and selection

The selection of the best Q scenario for each training option (environmental flow) was based on the optimal combination of the below-mentioned calculated parameters/indicators:

i. Overall Suitability Index (OSI): $\boldsymbol{OSI = \sum_{i=1}^{w} K_i}$

ii. Normalized OSI (nOSI): $\boldsymbol{nOSI = \frac{OSI}{w}}$

where,

K_i (from 0 to 1) denotes the habitat suitability

w denotes the total No. of wetted nodes in the computational mesh at each Q scenario

iii. Certainty of prediction (COP): The ratio of the No. of microhabitat combinations actually found in the training dataset to the total No. of nodes in the computational mesh; Habfuzz applies a trick when a microhabitat combination is not found in the training dataset and instead of returning some arbitrary K value for a particular node (e.g. -1), it uses the K value of its neighboring node in the domain.

iv. Percentage of wetted nodes in the computational mesh at each Q scenario (w).

v. Habitat connectivity (C): The ratio of connected (neighboring) nodes with K>0.6 to the total number of wetted nodes with K>0.6.

vi. Habitat availability (A): The ratio of connected (neighboring) nodes with K>0.6 to the total number of nodes in the study reach (wetted and dry).

The optimal combination of the indicators was numerically expressed for each simulated Q using the Optimal Flow Scenario index (OFSi) (with 'i' denoting the different Q scenarios) as follows:

$$OFS_i = nOSI_i \cdot w_i \cdot C_i \cdot A_i \cdot COP_i$$

All OFSi values were normalized in a 0-1 scale by dividing each OFSi with the maximum OFS observed. A useful illustration of the process followed in our case study is shown in Fig. 5.3.

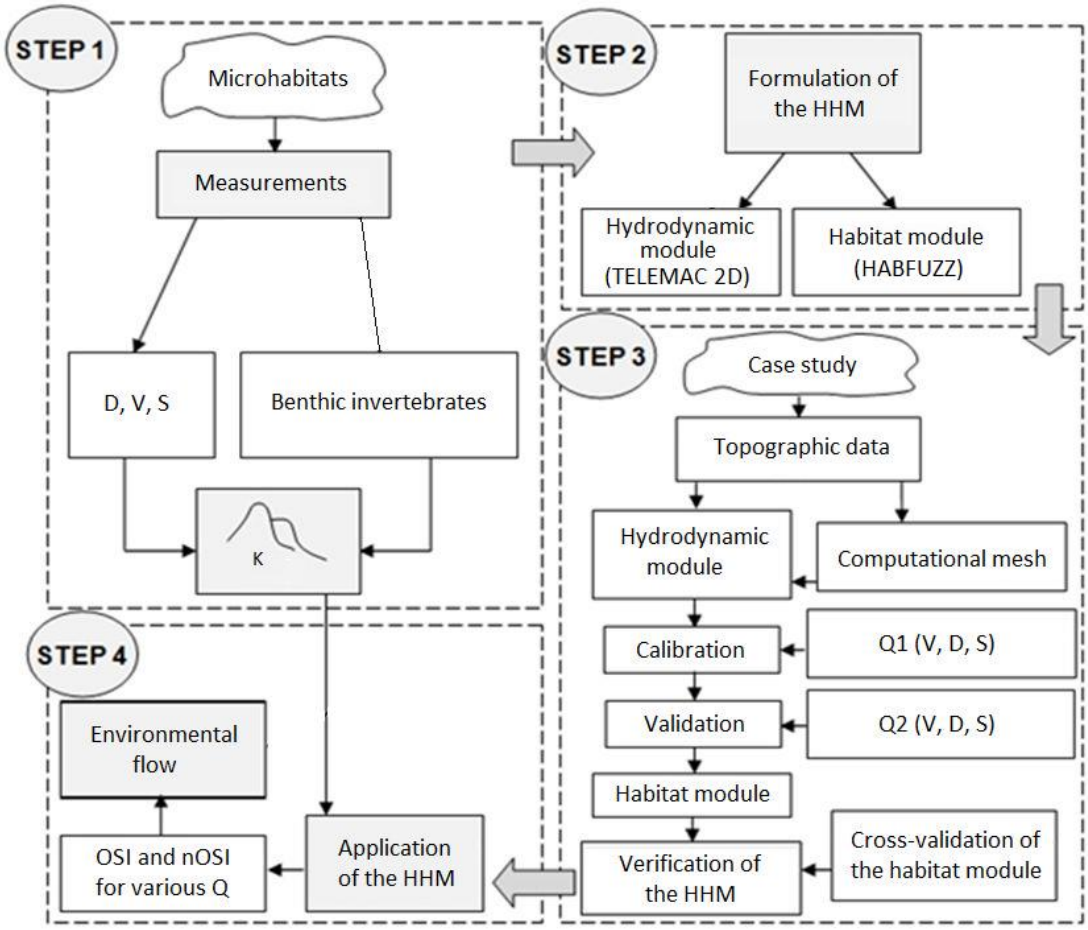

Fig. 5.3. The steps followed to implement the hydrodynamic habitat modelling case study (modified from Theodoropoulos et al., 2015).

5.9. Results

The predicted habitat suitability at each of the 5,170 nodes of the study reach for the various simulated Q scenarios and for each training option (T-BGR) and (T-PAR) is depicted in Fig. 5.4. In addition, table 5.1 shows the suitability indicators calculated for each scenario at each training option. According to the results, the selection of the optimal flow scenario should focus on the Q range between 0.6 m^3/s and 2 m^3/s, since the highest values of the indicators used for the quantification of habitat suitability for both training options were observed in this range. The highest OSI was calculated in Q = 2 m^3/s (T-BGR) and Q = 5 m^3/s (T-PAR); the maximum nOSI was observed in Q = 0.6 m^3/s and Q = 0.8 m^3/s for the T-BGR and the T-PAR training option, respectively; the highest number of wetted nodes was found at Q = 7 m^3/s; maximum connectivity was calculated for Q = 2 m^3/s (T-BGR) and Q = 3 m^3/s (T-PAR); maximum availability was observed in Q = 0.8 m^3/s (T-BGR) and Q = 0.6 m^3/s (T-PAR). The certainty of prediction was also maximum for Q = 0.6 m^3/s and Q = 0.8 m^3/s in T-BGR and for Q = 2 m^3/s and Q = 5 m^3/s. The visual representation of K in Fig. 4 also indicates that, in Q scenarios lower than 0.6 m^3/s and higher than 2 m^3/s, the number of unsuitable habitats (K < 0.6) becomes disproportionately increased and habitat availability reaches unacceptable levels, especially for the T-BGR training option.

According to the OFS values (Fig. 5.5), the optimal flow scenario for freshwater macroinvertebrates corresponds to Q = 2 m^3/s, followed by Q = 0.8 m^3/s (see the discussion for the environmental flow selection). The OFS decrease observed in Q = 1 m^3/s can be explained

through an integrated interpretation of table 5.1, Fig. 5.4 and Fig. 5.5. As the quantity of the water in the study reach increases (from Q = 0.01 m^3/s to 0.8 m^3/s) the habitat indicators increase due to the increase in V and D values until a peak of most indicators is observed from Q = 0.6 m^3/s to Q = 0.8 m^3/s. At Q = 1 m^3/s, the further increase in D and V becomes temporarily suboptimal for benthic invertebrates; the most downstream part of the river becomes deeper while the mid-parts are still too shallow to support high number of optimal habitats. As the discharge increases to 2 m^3/s, new wetted cells are introduced into the reach (mainly in the upper part), with suitable combinations of D and V and the habitat quality indicators increase again (still the most downstream part is continuously deepening and remains unsuitable). In discharges higher than 2 m^3/s the D and V values continuously increase to unsuitable levels.

Table 5.1. The indicators calculated at each simulated discharge and for each training dataset (T-BGR and T-PAR) to facilitate the selection of the optimal flow scenario. The highest values for each indicator have been shaded grey.

T-BGR						
Q (m^3/s)	OSI	nOSI	w (%)	C (%)	A (%)	COP (%)
0.01	1127.624	0.572	46.83	80	13	79
0.1	1684.929	0.625	55.74	86	36	89
0.2	1963.519	0.647	62.03	91	50	90
0.3	2155.988	0.650	67.52	92	54	88
0.6	2487.366	0.685	72.53	93	67	90
0.8	2635.834	0.677	77.37	93	69	90
1	2674.936	0.674	80.66	94	56	88
2	2804.810	0.639	85.83	96	68	88
3	2742.159	0.600	90.91	95	53	79
5	2676.637	0.551	95.61	94	38	77
7	2630.783	0.529	99.21	94	27	55

T-PAR						
Q (m^3/s)	OSI	nOSI	w (%)	C (%)	A (%)	COP (%)
0.01	1123.889	0.671	46.83	92	68	23
0.1	1639.061	0.672	55.74	94	70	38
0.2	1924.067	0.669	62.03	94	73	42
0.3	2112.018	0.669	67.52	95	72	46
0.6	2484.796	0.704	72.53	97	78	62
0.8	2718.057	0.713	77.37	96	77	67
1	2888.461	0.732	80.66	98	75	72
2	3092.51	0.712	85.53	98	72	80
3	3018.117	0.687	90.91	99	58	78
5	3124.756	0.688	95.61	99	45	82
7	3122.387	0.695	99.21	99	29	79

Q: discharge, OSI: overall suitability index, nOSI: normalized OSI, w: wetted cells, C: habitat connectivity, A: habitat availability, COP: certainty of prediction

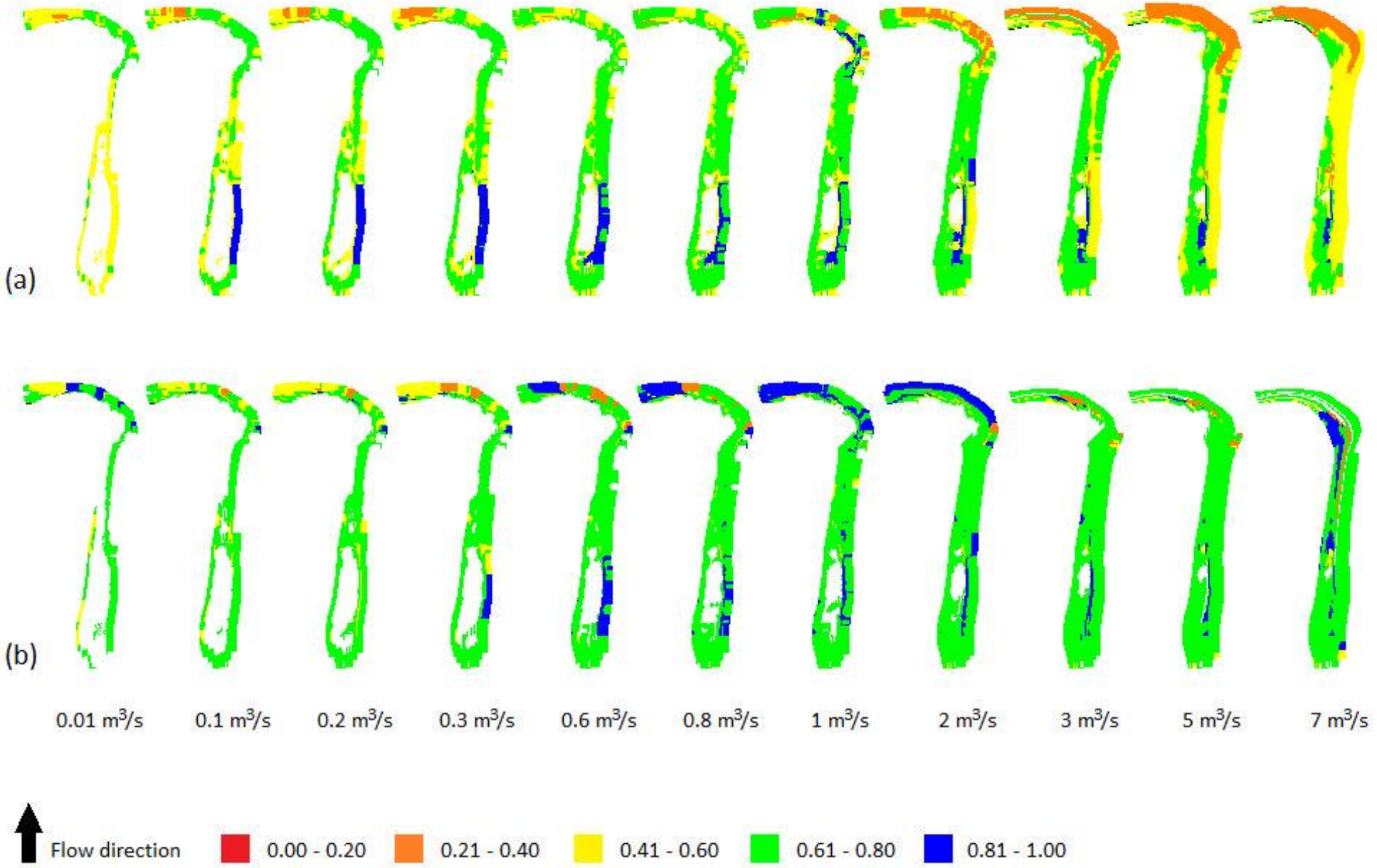

Fig. 5.4. Habitat suitability values for the various simulated discharge scenarios. Values higher than 0.6 are considered acceptable based on the requirements of the Water Framework Directive 2000/60/EC. (a) Model trained using the whole benthos-GR dataset; (b) Model trained using the T-PAR data

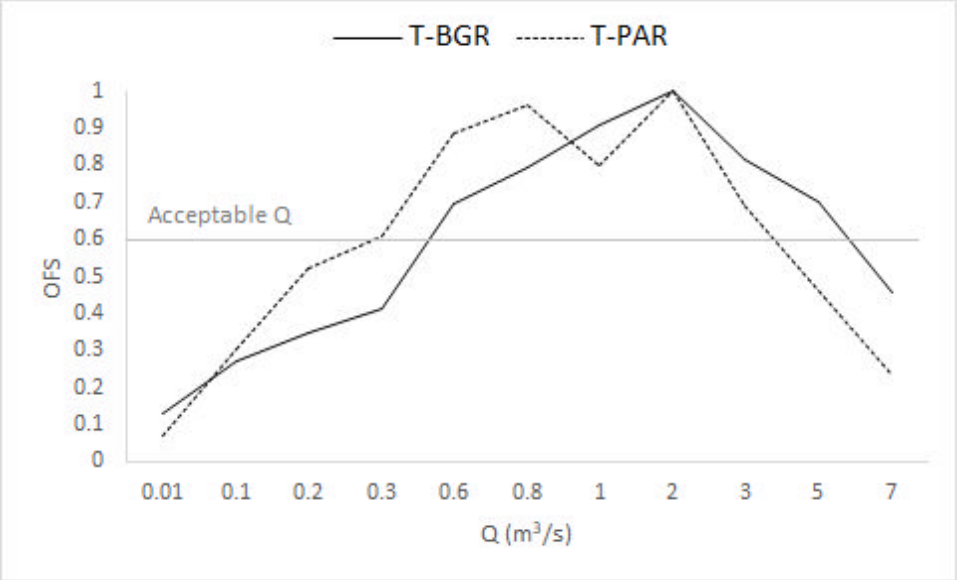

Fig. 5.5. Optimal Flow Scenario (OFS) index values for each discharge (Q) and for each training dataset (T-PAR and T-BGR). Acceptable Q values based on the WFD requirements are indicated.

5.10. Discussion

The results of the study indicate that the hydrology-based environmental flow (eflow) of Q = 0.2 m^3/s, proposed in the relevant environmental impact assessment (EIA) for the Parapeiros River dam, is not sufficient to provide optimal habitat conditions for supporting a functional benthic community. According to the ecosystem-based approach applied in our study, the EIA-proposed eflow ranked between seventh and ninth, based on the OFS values of the two training options (0.521 and 0.348 for the T-BGR and T-PAR, respectively). Habitat suitability was highest at Q = 2 m^3/s for both training alternatives, while acceptable values (OFS ≥ 0.6) included Q = 0.8 m^3/s, Q = 0.6 m^3/s, Q = 1 m^3/s and Q = 3 m^3/s in the T-BGR dataset, extending up to Q = 5 m^3/s in the T-PAR dataset. While optimal BM-habitat can be obviously ensured by providing a 1-m^3/s or 2-m^3/s eflow, water managers and stakeholders may decide to apply another eflow scenario, in search of the fine balance between human and ecosystem water demand. According to the 5-class quality system adopted in the Water Framework Directive 2000/60/EC, for both training options, the eflow scenario of Q = 0.6 m^3/s can be considered acceptable (K > 0.6) to allow for the continuation of the specified use (drinking water supply and water for irrigation), without compromising the long-term functionality of the aquatic ecosystem (WFD CIS, 2003). Since the environmental flow is a negotiated value (Dyson et al., 2003), HHMs provide the most valuable feature in the process, in comparison to their hydrology-based alternatives; the ability to accurately map habitat suitability in various discharge scenarios and offer a simplified visualization of the information required by water managers and stakeholders to reach a consensus.

As mentioned previously, the application of HHMs-based EFAs is disproportionately limited compared to their hydrology-based alternatives, due to reasons mainly associated with time-efficiency, cost-effectiveness, required expertise and availability of hydroecological information (Jorgensen and Bendoricchio, 2001; Conallin et al. 2010).

The expertise required to implement the specific case study may be considered minimal (OWRB, 2011), as all steps of this study including the collection and identification of BM samples, the assessment of their microhabitat preferences and the 2D hydrodynamic habitat simulation were successfully implemented by a small team of environmental biologists and hydraulic-hydrodynamic engineers. Hydrology-based EFAs require teams of almost-equal

size and a similar level of expertise to be adequately implemented and interpreted (Efstratiadis et al., 2014; Zhang et al., 2014).

Hydrodynamic habitat models are considered costly to implement (Lamouroux and Jowett, 2005; Booker, 2016), since they require multiple field visits at the river reach under investigation prior to applying the hydrodynamic habitat simulation. The most cost-intensive step in such implementations is the collection of the hydroecological reference dataset (Theodoropoulos et al., 2018a). However, once the hydroecological dataset has been collected and the reference conditions are established, the hydrodynamic simulation can be carried out by two on-site visits; one visit to collect topographical information and hydrometric data to calibrate the hydrodynamic module and one additional visit to collect a second set of hydrometric data for the validation of the hydrodynamic module. This period of time may be considered rather short, taking into account the valuable final visual representation of an HHM-application, which offers a scientific base for trade-offs between scientists, water managers and stakeholders during the decision-making process. Again, the most time-consuming step is the determination of the hydroecological reference conditions. However, multiple applications can be implemented using the same reference hydroecological dataset in reaches with similar environmental and hydraulic properties.

Based on the aforementioned, the acquisition of a detailed, robust hydroecological dataset is a key step to the application of HHMs-based EFAs. Either as habitat suitability curves or fuzzy rules, habitat preferences of aquatic biota (mainly fish or benthic invertebrates) have been developed worldwide. However, the generalization of these habitat preferences and their transferability to river reaches other than those for which they were developed, has been questioned (Heggenes, 1990; Holm et al., 2001; Lancaster and Downes, 2010) and recently, generalized approaches attempted to overcome this limitation (Lamouroux and Jowett, 2005; Booker, 2016). Based on our application, a useful approach to overcome this 'obstacle' would require:

i. Collection of reference samples (microhabitat observations) from river reaches of the same typology, i.e. similar environmental and hydraulic properties (temperature, flow variability, substrate types). In Greece for example, most rivers belong to the RM-2 (100-1000 km^2 - altitude < 600 m - mixed geology) and RM-4 (10 - 1000 km^2 - altitude between 400 -1500 m - mixed geology) intercalibration types. A reference hydroecological dataset collected from these river types would have a wide application in instream flow studies in Greece.
ii. Calculation of habitat suitability (κ) based on BM metrics and not using specific BM taxa (Theodoropoulos et al., 2018a); as not all BM taxa are found in all river reaches, calculating a κ using BM metrics can be a valuable option.
iii. Normalization of habitat suitability per season and per site (by dividing the calculated κ of each microhabitat with the maximum κ found at each site at each season); this is a key step to eliminate (at least partially) any seasonal and geographical variation; as our results suggested, despite the small variation between the two training datasets, the same environmental flow (Q = 0.6 m^3/s) would be probably selected regardless of the training option applied.

5.11. Conclusion

Ecosystem-based approaches are required to ensure ecosystem integrity and functionality in the long term. Based on the results, the hydrology-based environmental flow of 0.2 m^3/s is not considered suitable to maintain functional benthic communities downstream of the dam; the habitat suitability in Q = 0.2 m^3/s was lower than the ecologically-acceptable limit (OFS ≤ 0.6) and all BM-community metrics were suboptimal (Table 5.2). Cost-effective and time-efficient HHMs-based EFAs can be implemented using advanced surveying-mapping methods and by following specific methodological steps during the process. The establishment of a robust

reference hydroecological dataset is of paramount importance, but once such a dataset has been developed, there are options available to properly treat the dataset and enable its use (as a habitat-module training dataset) in multiple model-based EFAs.

Chapter 6

Case study 2 - Hydrodynamic simulation of habitat suitability using benthic macroinvertebrates; development of model-based environmental flow scenarios and comparison with hydrology-based predictions downstream of the Marathon Reservoir (Attica, Greece)

6.1. Overview

In the last 40 years of research on environmental flow assessments (EFAs), more than 200 EFA methods emerged worldwide (Tharme, 2003) and have been categorized in three groups depending on the type of data they use to calculate environmental flows (eflows):

1. Hydrological methods, which develop environmental flow scenarios based on long-term historical hydrological information (Tennant, 1976; Richter et al., 1996)
2. Habitat simulation methods (also known as hydraulic/hydrodynamic habitat models, which develop environmental flow scenarios based on the interaction between habitat suitability-availability and the distribution of aquatic biota (Vezza et al., 2015; Leitner et al., 2017; Koutrakis et al., 2018; Theodoropoulos et al., 2018a)
3. Holistic methods, which combine hydrological and hydroecological-habitat information to define environmental flows for multiple biotic elements of the aquatic ecosystem (WFD CIS, 2015), including fish, benthic macroinvertebrates, aquatic and riparian vegetation (King et al., 2008; Poff et al., 2010; Solans and Jalón, 2016).

The Tennant method (Tennant, 1976) and the Indicators of Hydrologic Alteration (IHA - Richter et al., 1996) have been the most widely applied hydrological methods. The environmental flow according to the Tennant method is calculated as a percentage of the average annual flow, based on specific eflow classes provided by Tennant (1976) and depicted in Table 6.1. The IHA method applies more complex hydrological indices including annual minimum and maximum flows, magnitude, frequency and duration of high and low flow pulses etc. and calculates/predicts multiple environmental flow components rather than just a baseflow, thus defining a variable annual environmental flow regime, instead of a fixed annual eflow value. These 'desktop' approaches require low effort (regarding time, costs and data processing) to be implemented and have long been preferred over the other two groups when long-term hydrological information is available.

Table 6.1. The hydrology-based environmental flow classes provided by Tennant (1978)

Environmental flow class	Recommended baseflow from Oct to Mar	Recommended baseflow from Apr to Sep
Flushing or maximum	200% of the average flow	
Optimum range	60%-100% of the average flow	
Outstanding	40%	60%
Excellent	30%	50%
Good	20%	40%
Fair or degrading	10%	30%
Poor or minimum	10%	10%
Severe degradation	10% of average flow to zero flow	

Hydrodynamic habitat models (HHMs) have long been researched worldwide, but their real-life applications have not been as popular as their hydrology-based alternatives. As previously explained, these methods quantify and predict the response of aquatic biota to gradients of hydraulic-habitat alteration. A hydrodynamic module provides information on the change of physical habitat as a function of discharge by predicting water depths (D) and depth-averaged flow velocities (V) at multiple discharges in a computational mesh, which simulates the area under investigation (Theodoropoulos et al., 2015). A coupled habitat module compares the predicted values of V and D with information on the habitat preferences of aquatic biota to calculate habitat suitability at each simulated discharge (Acreman and Dunbar, 2004; Gopal, 2013). Environmental flow scenarios are developed based on the interaction between habitat alteration and ecological response.

Both hydrological and HHMs-based methods have been criticized for various aspects of their practical application. Hydrology-based methods lack ecological validation (Acreman and Dunbar, 2004) and thus, their credibility to provide ecologically appropriate flow regimes

has often been questioned (Linnansaari et al., 2013). On the other hand, habitat simulation methods require considerable amount of fieldwork and relevant expertise to be successfully implemented (Linnansaari et al., 2013), while the fundamental concept on which these methods are based (the relationship between the instream flow -or habitat- and the abundance or biomass of aquatic organisms) has also been questioned (Moyle et al., 2011). Recently in Europe, and as Caissie and El-Jabi (2003) had previously concluded, the Guidance Document No. 31 (WFD CIS, 2015) supporting the Water Framework Directive 2000/60/EC (WFD - European Union Council, 2000), suggested a three-tiered hierarchy of the eflow methods' application, depending on the detail/accuracy of the eflow prediction required and on the magnitude of the (possible) hydrological alteration due to the upstream water use (e.g. small-scale water abstraction or the presence of a large water-supply dam). However, environmental flows have often been calculated using only hydrological methods (e.g. Ye at al., 2012; Efstratiadis et al., 2014; Fuladipanah et al., 2015; Chen and Weisbrod, 2016), while studies implementing and comparing eflow scenarios based on a combination of different methods in the same study area are limited (Li et al., 2009; Davis and Hirji, 2003; Shokoohi and Amini, 2013; Papadaki et al., 2017; Nikghalb et al., 2016; Tare et al., 2017; Stamou et al., 2018).

6.2. Purpose of the chapter

This chapter compares environmental flow scenarios developed from hydrological and HHM-based methods, downstream of the Marathon Reservoir (Oinoi Stream - Attica, Greece). Based on historical hydrological information available for the area, five eflow scenarios were developed using three hydrology-based methods, and three eflow scenarios based on the requirements of the national legislation. A two-dimensional hydrodynamic habitat model was additionally applied to develop ecosystem-based eflows using freshwater macroinvertebrates as the target aquatic community. The ultimate focus of this chapter is to explore if the application of HHM-based environmental flow assessments yields similar recommendations to the hydrological methods, and comment on the possible application of the hydrology-based methods as stand-alone tools, thus avoiding the costs and time required to apply the ecosystem-oriented HHM-based methods. With reference to previous literature, the possibility of integrating the two approaches to increase the confidence on predicting and selecting environmental flows is also discussed.

6.3. Case study

The study reach is located in the Region of Attica (central Greece) (Fig. 6.1), downstream of the Marathon Dam. The dam is 54-m high and concentrates the inflows from the Charadros and Varnavas streams, supplying drinking water to the city of Athens and the surrounding areas. With a catchment area of 118 km^2, the two streams converge at the Marathon Dam and form the Oinoi Stream, which empties in the Aegean Sea after a distance of approximately 10 km. The area has a temperate Mediterranean climate characterized by mild winters and hot, dry summers. The mean annual minimum and maximum temperatures are 5 ^oC and 29 ^oC, reaching below 0 ^oC and above 33 ^oC during extreme winter and summer events, respectively. The mean annual precipitation is low, compared to the one recorded in the western and northern parts of the Greek territory (567 mm over a 70-year period). July, August and September are the driest months of the year.

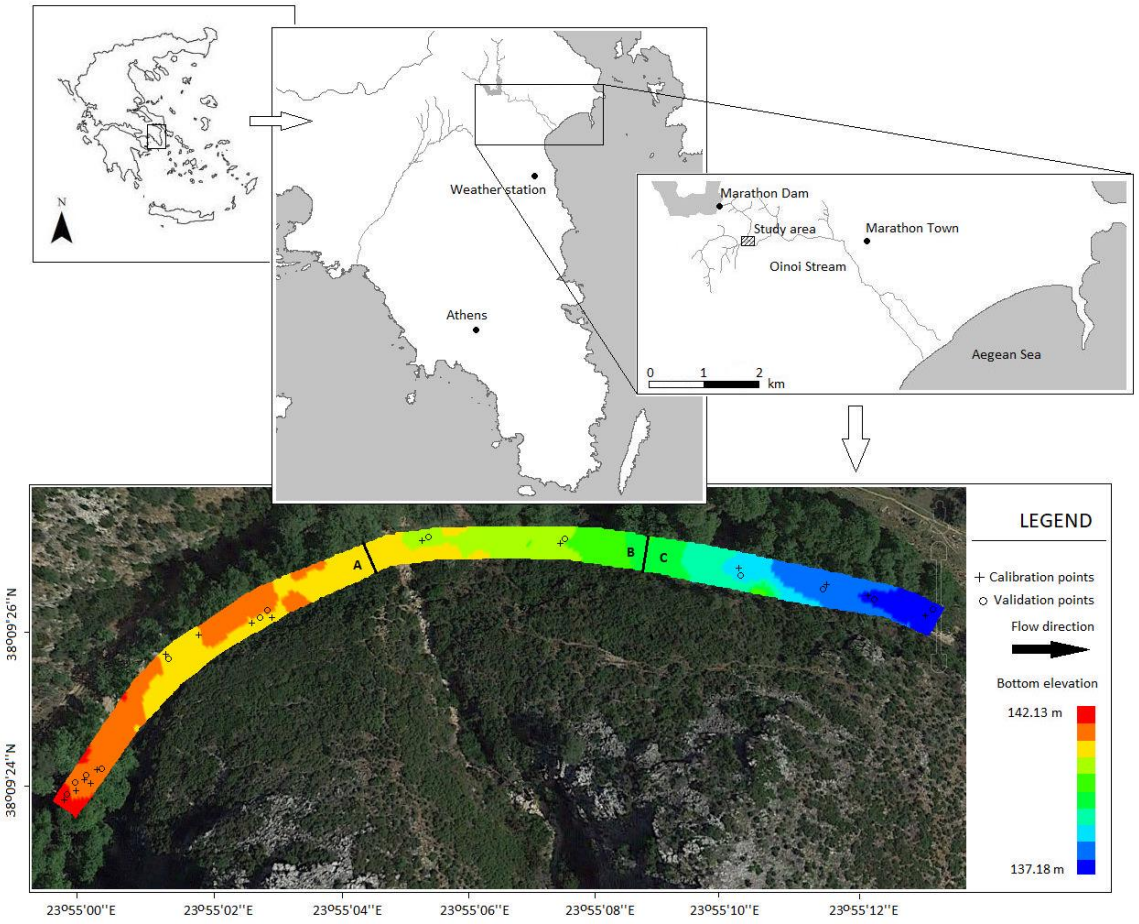

Fig. 6.1. The study area; the Oinoi Stream, the town and the reservoir of Marathon are depicted.

The Oinoi Stream initially flows through a mixture of sclerophyllous vegetation and coniferous forests, which is gradually replaced by agricultural land and urban areas after a distance of almost 6 km. The stream afterwards passes through the town of Marathon, being surrounded by complex cultivation patterns and urban areas until it empties in the Aegean Sea. The water flow downstream of the dam is ungauged. The Marathon Dam was built in 1929 without an environmental flow valve and consequently, there is no outflowing water in the Oinoi Stream. Currently, the minor quantity of spring-fed water flowing through the stream is pumped for irrigation, leaving no flow in the river for almost throughout the year.

6.4. Hydrological data, hydrology-based and legislation-based environmental flows

Daily hydrological data from the operation of the Marathon Dam were obtained for an 11-year period (2002-2013) from the Athens Water Supply and Sewerage Company (EYDAP S.A.). These daily data were used to calculate the inflowing water discharge from the upstream watershed (Charadros and Varnavas streams converging upstream of the reservoir) and they included (i) reservoir water level fluctuation, (ii) precipitation, (iii) lake evaporation, (iv) the water volume transferred from the reservoir to the city of Athens. As in Efstratiadis et al. (2014), a water balance model was developed and applied to the aforementioned data; the inflows considered were the water discharge from the upstream watershed and the daily volume of precipitation, and the outflow was the water volume abstracted for the Athens drinking water supply. The calculated daily discharges from the Varnavas and Charadros streams inflowing to the dam for the period 2002 - 2013 were considered as the natural river flows (the mean monthly discharge

values are shown in Fig. 6.2) from which the hydrology-based environmental flows were calculated using the following methods:

i. Tennant method (Tennant, 1976); in this method, mean annual flows for each hydrological year are calculated and the average value for the whole period of study (QAA) is derived. Environmental flow scenarios are afterwards developed based on the percent deviation from QAA. Based on the method's recommendations, we considered the 10% QAA, 20% QAA and 30% QAA values as potential environmental flow candidates, reflecting the 'fair', 'good' and 'excellent' categories provided in Tennant (1976) (Table 6.1).
ii. Lyons method (Bounds and Lyons, 1979); in this method monthly median flow (MMF) values are derived from long-term hydrological records and used as monthly environmental flow recommendations, weighted between the wet and dry periods of the year. Based on the method's requirements, the 60% MMF was considered as the minimum environmental flow for the period between March and September, and 40% MMF as the minimum eflow during October-February.
iii. Basic Maintenance Flow (QBM - Alcácer-Santos, 2004); the QBM method analyses the variation in the distribution of minimum flows that have occurred for time periods ranging from one to one-hundred consecutive days (in total, 100 intervals). A moving average of daily flows is calculated for each interval, and the minimum value of each interval and for each year is afterwards derived. The relative increment between each pair of consecutive minima is calculated using the following equation:

$$b_i^k = \frac{(q_i^k - q_i^{k-1})}{q_i^{k-1}}$$

where
b_i^k is the relative increment for the i^{th} year and for the k^{th} interval
q_i^k is the minimum flow value of the k^{th} interval for the i^{th} year

The minimum flow value with the highest relative increment q_i^{kmax} is selected for each year and the average value of all q_i^{kmax} is the final environmental flow.

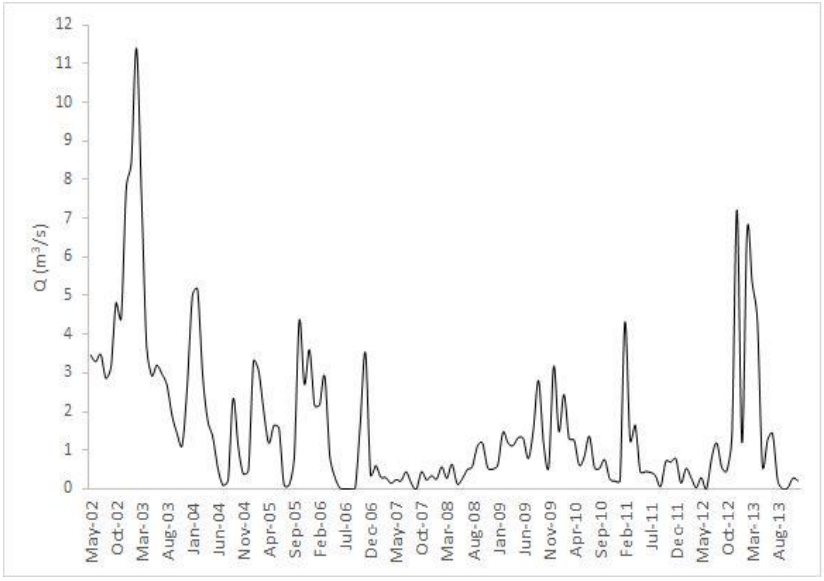

Fig. 6.2. Mean monthly inflows to the Marathon Reservoir for the years 2002-2013, calculated based on a water balance equation.

According to the requirements of the Greek legislation, three environmental flow scenarios were developed for the 11-year study period, based on the following: (a) 30% of the mean monthly flows of June, July and August, (b) 50% of the mean monthly flow of September, (c) 0.03 m^3/s minimum acceptable flow when the previous values are lower.

6.5. Collection of topographic information and mesh generation

A 370-m long reach (3731 m^2) was simulated using a two-dimensional (2D) hydrodynamic model. Channel topography was mapped with 459 points recording longitude (X), latitude (Y) and bottom elevation (H). A Real-Time Kinematic (RTK) GPS was used, consisting of the 'Spectra Precision SP60 GNSS Receiver' (http://www.spectraprecision.com/eng/sp60.html) and the 'MobileMapper 10 GIS - GPS Receiver' (http://www.optron.com/spectra/products/Mobile-Mapper-10.html). The Blue Kenue software (http://www.nrc-cnrc.gc.ca/eng/solutions/advisory/blue_kenue_index.html) was then used to import the topographic X, Y, H data and linearly interpolate channel topography, generating a triangular computational grid composed of 3,938 nodes and 7,140 triangular elements with a 0.9 m spatial resolution. In the rarely occurring cases where dense canopy cover restricted the communication between the RTK-GPS and the satellites (and consequently, spatial coordinates could not be accurately acquired), relief changes were manually measured from the nearest accurate point measurement (measuring the change in X, Y and H) and the missing points were manually inserted to the topography file in the Blue Kenue software.

6.6. Hydrometric data, calibration and validation

Two surveys at different discharges (Q), commonly occurring in the study reach, were carried out to calibrate and validate the hydrodynamic simulation. The model was calibrated using the data from the first hydrometric survey (Q = 0.03 m^3/s) and validated using the hydrometric data from the second survey (Q = 0.3 m^3/s). Following a 2D-adapted, widely applied approach (Leclerc et al., 1995; Lee et al., 2010; Lin et al., 2015), and using the Swoffer 2100 current velocity meter (http://www.swoffer. com/products.htm), water depths (D) and depth-averaged flow velocities (V) were measured at 0.6 x D when $D \leq 0.75$ m, and by averaging 0.2 x D and 0.8 x D when $D > 0.75$ m, based on Nolan and Shields (2000). These field measurements of V and D were recorded at 15 randomly selected points across the river reach at each survey. Longitude and latitude coordinates (using the RTK-GPS) were additionally recorded for each point and the two datasets were afterwards imported into the BlueKenue software. Calibration and validation were applied by manually adjusting the Manning's roughness coefficient (n), based on an initial visual field estimation of the type of substrate, until an acceptable combination of R^2 values between the predicted and observed V and D was achieved. Specifically, the study area was divided in three sections and the Manning's n in the validated model was 0.035 in the upper part, 0.05 in the mid-reach and 0.07 in the downstream part (Fig. 6.1). The R^2 between the predicted and observed D and depth-averaged V values was greater than 0.9 and varied from 0.9577 for D to 0.9795 for V ($p<0.01$) in the calibration dataset and from 0.8954 for D to 0.9591 for V ($p<0.01$) in the validation dataset (Fig. 6.3), suggesting strong, statistically significant correlations and an acceptable model performance. The validated model was used to simulate 16 discharge scenarios ranging from 0.01 m^3/s to 5 m^3/s.

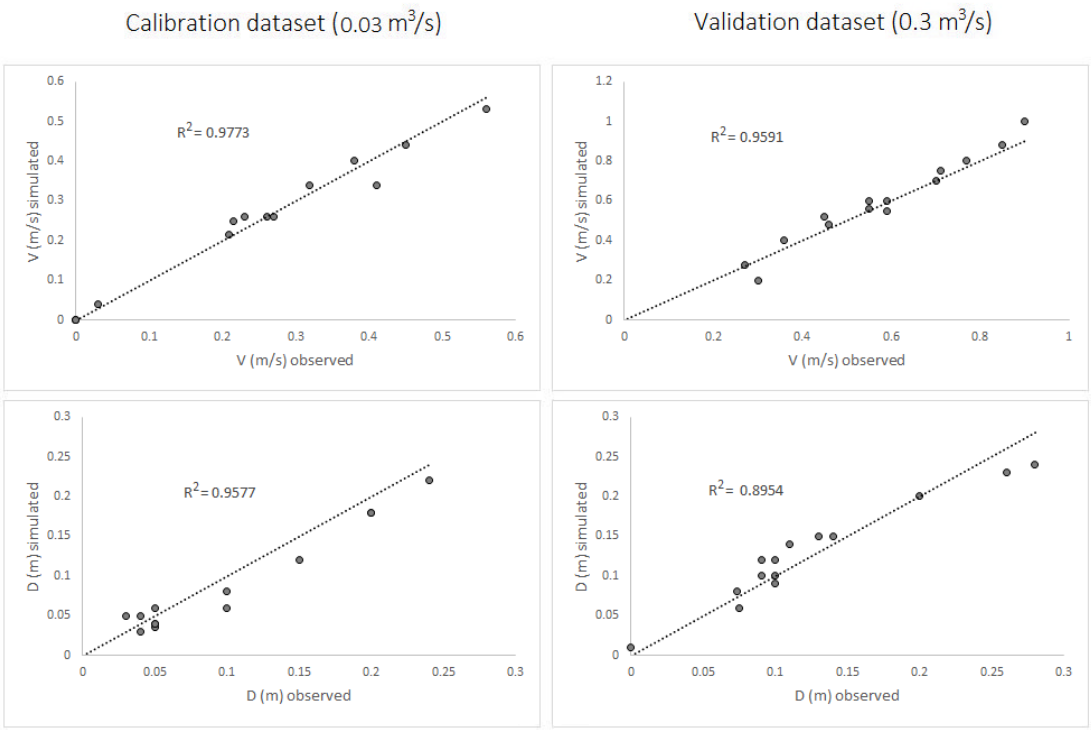

Fig. 6.3. Correlation between the simulated and observed data (V: flow velocity, D: water depth) in 15 randomly recorded points during calibration and validation. Dotted lines represent 100% accuracy (observed values = simulated values).

6.7. Hydrodynamic simulation

The TELEMAC-2D v6.2 (Galland et al., 1991) was used to simulate D and depth-averaged V in various discharge scenarios. Prior to running the hydrodynamic simulation, boundary and initial conditions were defined using the FUDAA-PREPRO pre-processor (http://prepro.fudaa.fr). Q was prescribed at the upstream boundary and water surface elevation (Z) was prescribed at the downstream boundary, according to the software's requirements. The TELEMAC-2D code applies the finite element method (Hervouet, 2007; Liu and Quek, 2014) to solve the depth-averaged St-Venant equations (conservation of mass, x-wise momentum, y-wise momentum).

We simulated D and depth-averaged V values in 16 discharge scenarios. Apart from the upstream inflow boundary, no other sources of incoming water exist in the study reach and, taking into account the short channel length (370 m) and the geology of the reach, no 'sink terms' were introduced in the model, assuming a constant discharge at the whole length of the study reach. Each simulation was run until a steady state was reached; the V and D values at each Q scenario (steady state) were afterwards used as inputs to the habitat model.

6.8. Habitat suitability modelling

In the absence of well-established fish communities in the Oinoi stream (possibly due to the extreme long-term hydrological alteration caused by the presence of the upstream reservoir), we used benthic macroinvertebrates (BM) as our target aquatic community, which have been found to be more widely distributed (Monk et al., 2006) and are commonly used in such cases elsewhere (Waddle and Holmquist, 2013). Their habitat preferences were acquired from the benthos-GR dataset (Theodoropoulos et al., 2018a), which consists of 380 microhabitat observations sampled in Greek streams and rivers of similar environmental and hydraulic properties. The benthos-GR dataset calculates habitat suitability (K) using benthic-community metrics (No. of families, No. of Ephemeroptera-Plecoptera-Trichoptera families, Shannon-

Wiener diversity and total community abundance) rather than just the abundance of individual taxa, thus describing the habitat suitability of the whole benthic-invertebrate community.

The dataset was used to train and cross-validate a fuzzy Bayesian algorithm (FRB), described in detail in Theodoropoulos et al. (2018a) and implemented using the HABFUZZ software (Theodoropoulos et al., 2016). In the FRB, the numerical inputs of V and D are converted to overlapping, five-class, trapezoidal-shaped membership functions (called fuzzy sets). The K values are also classified; in our case we used five, non-overlapping suitability classes (0 ≤ bad ≤ 0.2; 0.2 < poor ≤ 0.4; 0.4 < moderate ≤ 0.6; 0.6 < good ≤ 0.8; 0.8 < high ≤ 1). Each numerical input value of V and D is assigned to one or more fuzzy sets with a membership degree between zero and one (in our application, the type of substrate was treated as a crisp input and classified based on Schneider et al. (2010)). The training dataset (benthos-GR), with *a priori* calculated K values, is used to develop sets of data-driven IF-THEN rules, relating the input fuzzy sets with a specific K class. The fuzzy membership degree (MD) of each input variable (V, D and S) is considered as the probability of occurrence of the particular fuzzy set, such as 'IF V is low with a membership degree of 1 AND D is moderate with a MD of 1 AND S is gravel with a MD of 1 THEN K is high with a MD of 0.3 and good with a MD of 0.7'. The IF-THEN rules are then combined using the Bayesian joint probability, so that (referring to the previous example) the probability of the specific microhabitat's K being high is the joint probability that V is low AND D is moderate AND S is gravel AND K is high (1 x 1 x 1 x 0.3 = 0.3), while the probability of K being good is the joint probability that V is low AND D is moderate AND S is gravel AND K is good (1 x 1 x 1 x 0.7 = 0.7). Based on a utility function (Brookes et al., 2010), a score is assigned to each K class (bad: 0.2, good: 0.4, moderate: 0.6, good: 0.7, high: 0.9) and the habitat suitability for each microhabitat is predicted using the following equation:

$$K = \sum M_{ij} S_{ij}$$

where,
K is the predicted habitat suitability
M_{ij} denotes the joint probability of occurrence of each κ class
S_{ij} denotes the score of each κ class
For the previous example, K equals to 0.7 x 0.9 + 0.3 x 0.7 = 0.84 (high).

We applied a ten-times-repeated ten-fold cross validation process (Kohavi 1995), in which the initial dataset was randomly partitioned in ten equal-sized subsamples. Nine subsamples (90% of data) were used as the training dataset and the remaining subsample (10%) was used for model validation. This procedure was repeated ten times (folds), using a different subsample for validation at each iteration. The whole 10-fold iterations were repeated ten times to acquire more robust results. The performance of the cross-validated habitat model (calculated as the average percentage of correctly classified instances (CCI) between each iteration of the ten-fold cross-validation process) was 61.2% (min: 58.95%; max: 64.1%).

The output of the hydrodynamic model (D and depth-averaged V values) at each simulated discharge was used as input to the habitat model, which calculated *K* at each node of the computational grid of the hydrodynamic model (resulting in 3938 *K* values x 16 discharge scenarios). The habitat suitability of the study reach at each Q was visualized using the Blue Kenue software.

6.9. Environmental flow selection

Following the approach of Theodoropoulos et al. (2018a), the optimal ecosystem-based environmental flow scenario was selected based on the combination of the following indicators-variables:

i. Overall Suitability Index (OSI): $OSI = \sum_{i=1}^{w} K_i$

ii. Average OSI (nOSI): $$nOSI = \frac{OSI}{w}$$

where,
K_i (from 0 to 1) denotes the habitat suitability
w denotes the total No. of wetted nodes in the computational grid at each Q scenario

iii. Certainty of prediction (COP): The ratio of the No. of microhabitat combinations actually found in the training dataset to the total No. of nodes in the computational grid; HABFUZZ applies a trick when a microhabitat combination is not found in the training dataset and instead of returning some arbitrary K value for a particular node (e.g. -1), it uses the K value of its neighboring node in the domain.
iv. Percentage of wetted nodes in the computational grid at each Q scenario (w).
v. Habitat connectivity (C): The ratio of connected (neighboring) nodes with K>0.6 to the total number of wetted nodes with K>0.6.
vi. Habitat availability (A): The ratio of connected (neighboring) nodes with K>0.6 to the total number of nodes in the study reach (wetted and dry).

The optimal combination of the indicators was numerically expressed for each simulated Q using the Optimal Flow Scenario index (OFS):

$$OFS = nOSI \cdot w \cdot C \cdot A \cdot COP$$

All OFSi values were normalized in a 0-1 scale by dividing each OFSi with the maximum OFS observed. As the environmental flow is usually a negotiated value (Dyson et al., 2003), in addition to the best Q scenario, evaluated according to the maximum calculated OFS value, a 5-class system was applied based on the status classification system of the Water Framework Directive 2000/60/EC including the following classes; bad ($0 \leq OFS \leq 0.2$), poor ($0.2 < OFS \leq 0.4$), moderate ($0.4 < OFS \leq 0.6$), good ($0.6 < OFS \leq 0.8$) and high ($0.8 < OFS \leq 1$). A polynomial curve was applied to encompass the OFS values. Based on the polynomial function, environmental flow scenarios with OFS values higher than 0.6 (good and high classes) were considered acceptable and, therefore, potential ecosystem-based eflow candidates in possible negotiation schemes between scientists, stakeholders and managers.

6.10. Results

The results of the hydrology-based environmental flow calculations are depicted in Fig. 6.4. According to the Tennant method, the mean annual flow for the 11-year period was 0.61 m^3/s, and the 'fair', 'good' and 'excellent' classes were 0.06 m^3/s, 0.12 m^3/s and 0.18 m^3/s, respectively. Due to the high number of consecutive days with extremely low flows or zero values, the Lyons and QBM methods yielded the lowest environmental flow values (0.0006 m^3/s and 0.011 m^3/s, respectively). Varying outcomes ranging from 0.03 m^3/s to 0.135 m^3/s were obtained based on the requirements of the Greek legislation.

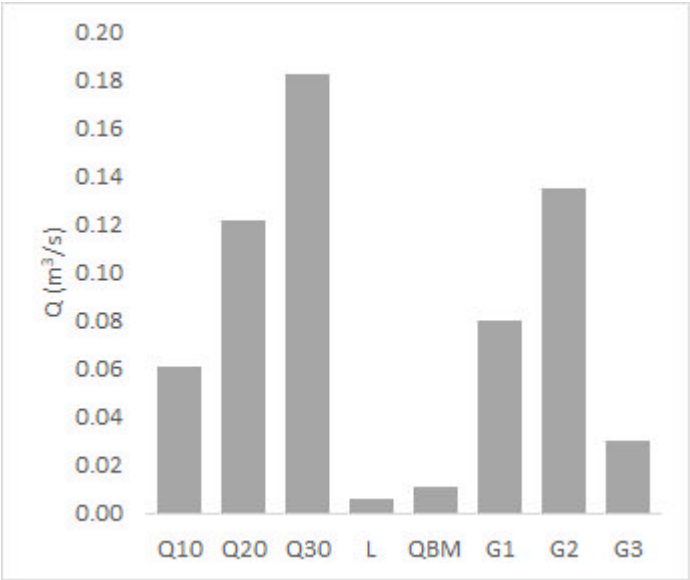

Fig. 6.4. Minimum environmental flows calculated over an 11-year period using the Tennant's 10%, 20% and 30% QAA (Q10, Q20 and Q30, respectively), the Lyons method (L) and the Basic Maintenance Flow (QBM). Environmental flows according to the Greek legislation are also depicted (G1: 30% of mean monthly flows of June, July and August, G2: 50% of the mean monthly September flow, G3: 30 L/s).

Table 6.2: The indicators calculated at each simulated discharge to facilitate the selection of the optimal flow scenario. The highest values for each indicator have been shaded grey.

Q (m^3/s)	OSI	nOSI	w (%)	C (%)	COP (%)	A (%)
0.01	1005.131	0.671	41.39	90	82	18
0.03	1255.029	0.635	50.15	92	84	25
0.05	1414.633	0.651	55.2	92	85	31
0.07	1542.871	0.66	59.35	93	87	36
0.09	1673.573	0.666	63.81	94	87	41
0.1	1684.227	0.671	63.83	94	88	42
0.2	1966.497	0.68	73.46	96	88	53
0.3	2126.507	0.689	78.34	96	89	61
0.5	2267.52	0.694	83	96	88	65
0.7	2344.797	0.671	88.75	95	88	62
0.9	2409.26	0.668	91.6	95	88	60
1.1	2424.688	0.662	93.04	93	90	58
1.5	2379.135	0.638	94.67	92	90	49
2	2293.715	0.605	96.32	91	88	40
3	2041.351	0.529	98	87	89	23
5	1674.186	0.431	98.67	72	82	6

Q: discharge, OSI: overall suitability index, nOSI: average OSI, w: wetted nodes, C: habitat connectivity, A: habitat availability, COP: certainty of prediction

Based on the hydrodynamic simulation, the depths in the wetted nodes of the study reach (data not shown) ranged from 0 m to 0.52 m for the lowest discharge (0.01 m^3/s) and from 0.1 m to 1.23 m for the highest discharge simulated (5 m^3/s). Depth-averaged V values, respectively ranged from 0 m/s to 0.59 m/s (Q = 0.01 m^3/s) and from 0.1 m/s to 3 m/s (Q = 5

m^3/s). The simulated habitat suitability (K) values at each node of the computational grid and at each Q scenario are depicted in Fig. 6.5. According to the results, maximum habitat connectivity (C), availability (A) and nOSI values were recorded at Q = 0.5 m^3/s (Table 6.2), indicating this value as the optimal environmental flow (Fig. 6.6). Based on the WFD classification scheme however (Fig. 6.6a), in combination with the polynomial curve fitted (Fig. 6.6b), Q values ranging from 0.17 m^3/s to 1.5 m^3/s can be considered acceptable (OFS > 0.6; good-high WFD classes). The highest OSI was observed in Q = 1.1 m^3/s, followed by 0.9 m^3/s and 1.5 m^3/s. The highest nOSI and habitat connectivity values were calculated for Q = 0.5 m^3/s, 0.3 m^3/s and 0.2 m^3/s respectively. As expected, more wetted nodes were recorded in higher discharges, while habitat availability peaked at Q = 0.5 m^3/s, followed by 0.7 m^3/s and 0.3 m^3/s.

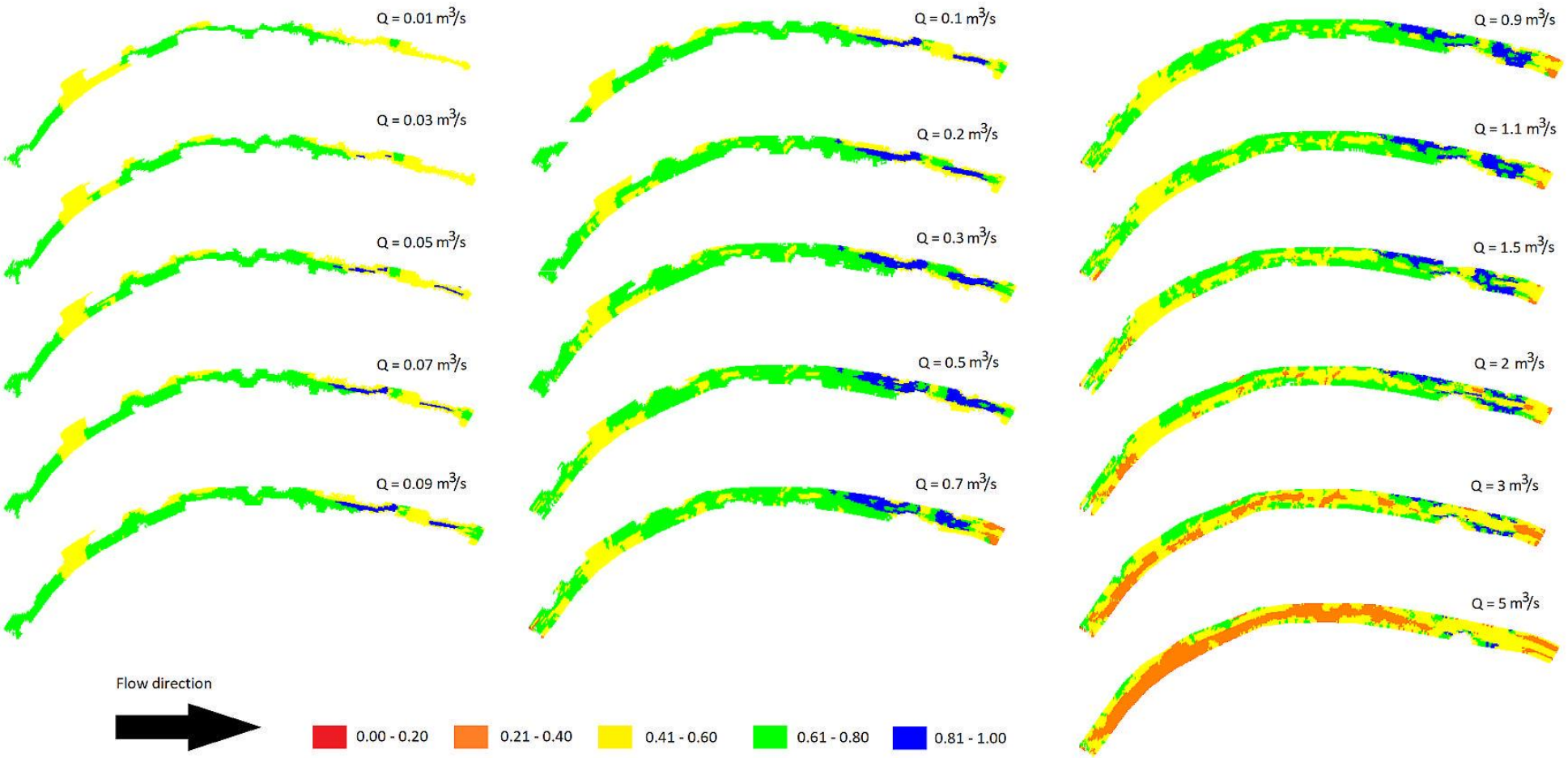

Fig. 6.5. Habitat suitability values for each simulated discharge scenario. Values higher than 0.6 are considered acceptable according to the requirements of the Water Framework Directive 2000/60/EC.

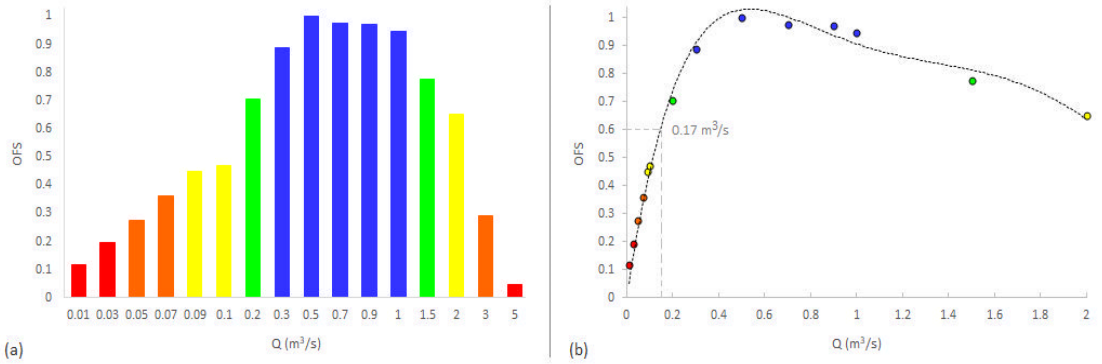

Fig. 6.6. Optimal Flow Scenario (OFS) index for each discharge scenario (Q). (a) Acceptable discharge scenarios range from 0.2 m^3/s to 1.5 m^3/s based on the WFD requirements. (b) Q-OFS scatterplot and polynomial regression curve to select the minimum flow with OFS > 0.6 (0.17 m^3/s).

6.11. Discussion

The results of the study suggest that ecosystem-based environmental flows ranging from 0.17 m^3/s to 1.5 m^3/s are appropriate for maintaining functional benthic-invertebrate communities downstream of the Marathon Reservoir (Fig. 6.6). In lower and higher discharges, respectively, habitat suitability becomes unacceptable based on the requirements of the Water Framework Directive 2000/60/EC, and as a result, the long-term ecological integrity and functionality of the BM communities may be compromised. The aforementioned information could be a valuable reference in negotiations between scientists, water managers and stakeholders (Acreman and Dunbar, 2004), in their effort to balance anthropogenic water demand and ecosystem conservation, within a sustainable water resources management framework (Loucks, 2000).

Theoretically, based on the ecological results, a variety of discharges ranging from 0.17 m^3/s to 1.5 m^3/s, could be considered appropriate for benthic-invertebrate communities. In practice however, water managers and stakeholders would probably select Q = 0.17 m^3/s as the optimal baseflow, being the lowest discharge capable of maintaining an acceptable ecological status of the aquatic ecosystem according to the WFD requirements. In contrast, according to the hydrological results, this value was among the highest calculated eflows; the hydrology-based environmental flows ranged from 0.0006 m^3/s according to the Basic Maintenance Flow method, to 0.18 m^3/s based on the 30% QAA ('excellent' class) of the Tennant method, while according to the national legislation, the environmental flow in the Oinoi Stream should range between 0.03 m^3/s and 0.135 m^3/s.

Nearly all hydrological methods applied, including the most popular Tennant method (Tennant, 1976), calculated lower environmental flows than the ones required to ensure ecosystem integrity and functionality according to the HHM-based, ecosystem-oriented approach followed in our study. Previous comparative studies in various reaches (Shokoohi and Amini, 2013; Nikghalb et al., 2016; Stamou et al., 2018; Theodoropoulos et al., 2018b) showed similar trends (but see Papadaki et al., 2017); Nikghalb et al. (2016) used the habitat preferences of *Luciobarbus capito* and calculated 3-fold increased environmental flows in comparison to those calculated using the Tennant method. Stamou et al. (2018) used the habitat preferences of *Squalius peloponnensis* and calculated eflows two times higher than the hydrology-based eflows, and ten times higher than those required by the Greek legislation on environmental flows. Theodoropoulos et al. (2018b) used benthic macroinvertebrates and calculated environmental flows three times higher, compared to those required by the Greek legislation. However, in the comparative study of Papadaki et al. (2017) carried out in two sites

in Greece, the optimal hydrology-based environmental flows in the first site were between 29% and 45% lower than the habitat-based eflows, while they were between 50% and 58% higher in the second site. Based on the results of our application and as nearly all previous studies suggest lower hydrology-based eflows, compared to the ecosystem-based methods, we could infer that hydrological methods often tend to under-estimate the environmental flows required to ensure healthy aquatic ecosystems.

Based on the aforementioned, the hydrology-based environmental flows in our study were lower than the lowest acceptable ecosystem-based environmental flow. Only the 30% QAA eflow of the Tennant method (0.18 m^3/s) coincided with the ecosystem-based eflow of 0.17 m^3/s (one out of eight hydrological scenarios - 12.5% probability of agreement). However, since the 30% QAA value reflects excellent ecosystem status based on the Tennant method's recommendations, in the absence of a respective ecosystem-based study, water managers and stakeholders would probably prefer to apply the 20% QAA or the 10% QAA scenario, corresponding to the good and fair status respectively. Therefore, hydrological methods should be used with caution, when ecological information is not available. Since a thriving benthic-invertebrate community in the Oinoi Stream is ensured in Q = 0.5 m^3/s, delivering environmental flows based solely on hydrological methods would probably (with a probability of 87.5%) stress the benthic community to unsustainable levels. These results are in accordance with previous literature questioning the use of hydrological methods as stand-alone EFAs (Acreman and Dunbar, 2004; Linnansaari et al., 2013; Arthington 2012; Papadaki et al., 2017), while, in their case study, Shokoohi and Amini (2013) reached the same conclusion, suggesting that delivering hydrology-based environmental flows would degrade the aquatic ecosystem in the long term.

It has been widely acknowledged that integrated frameworks, incorporating hydrological methods in HHM-based EFAs, could be a valuable option when different stakeholders attempt to communicate within an environmental flow assessment (Arthington, 1998; Linnansaari et al., 2013). A three-tiered hierarchy including hydrological, holistic and hydrodynamic habitat modelling methods has been recently proposed in the Guidance Document No. 31 of the Water Framework Directive 2000/60/EC (WFD CIS, 2015), and as Stamou et al. (2018) conclude, integrated methods could result in more 'realistic' eflow values based on the historical hydrological conditions of the study area and considering what can be 'socially' delivered. This conclusion however should not be misconceived as 'downgrading the ecosystem-based environmental flows to maximize possible short-term human benefits in the upstream' (Homa et al., 2005; Jager and Smith, 2008). Acreman (2016) indicates that the desired future condition of an ecosystem depends on what a society considers acceptable; the society-based ecosystem condition however, should not be much deviating from the ecosystem-based standards to ensure long-term ecosystem functionality.

Within this concept, integrated hydrological-HHM frameworks may be useful for providing detailed reference on what is ecologically acceptable and hydrologically-socially feasible (Stamou et al., 2018), and for delivering environmental flows, which partially meet the needs of everyone and fully meet the needs of no one (Pitt and Kendy, 2017). However, the concept of integrating itself requires further explanation, as there is actually no way to literally integrate the two methods; as our application showed and the previous literature indicates, hydrological methods provide historical hydrological information on a study area, whereas HHM-based methods use the habitat preferences of aquatic communities to develop ecosystem-based environmental flow scenarios. Consequently, the use of integrative frameworks combining hydrological and ecological methods bears an inherent insufficiency to increase the confidence on predicting and selecting environmental flows since they comprise different, non-interacting concepts. Nevertheless, as Stamou et al. (2018) imply, information from different sources (hydrological and ecological) is a useful basis for scientists, water

managers and stakeholders towards the development of socially-accepted and ecologically appropriate environmental flow recommendations.

6.12. Conclusion

Different environmental flow methods can yield different eflow predictions, suggesting a specific trend, which was further supported by most previous studies available; that hydrological methods tend to under-estimate the actual environmental flows required to maintain functional aquatic communities. Except for one hydrological eflow scenario (30% QAA - Tennant method) the lowest acceptable ecosystem-based environmental flow was higher than the hydrology-based environmental flows, with varying deviation depending on the hydrological method followed. This is translated to a coincidence probability of 20% (one agreement out of five hydrology-based scenarios), being reduced to 12.5% if we additionally include the results of the Greek legislation guidelines. As a consequence, the hydrology-based methods should not be applied as stand-alone methods, as the risk of delivering ecologically-unacceptable environmental flows is high (with a probability of 80% to 87.5% based on the results of the study). This has also been highlighted in previous literature and further confirmed in this study, which showed that the ecosystem requirements may be slightly, but also highly different.

Chapter 7

Discussion

The purpose of this thesis was to explore the possibility of using benthic macroinvertebrates (BMs) in hydrodynamic habitat models, to facilitate the development of environmental flow scenarios in river reaches impacted by hydrological alteration. It was shown that BMs do respond to hydrological variation and have specific preferences for particular habitat-defining variables (flow velocity, V; water depth, D; type of substrate, S; water temperature, T); these habitat preferences were estimated and state-of-the-art modelling algorithms were explored for their potential to accurately predict the BM-based habitat suitability in test river reaches based on a BM training dataset collected from nine sites in three seasons in Greece. A fuzzy rule-based Bayesian algorithm was ultimately selected, a modelling software (HABFUZZ) was developed to implement this algorithm and a two-dimensional hydrodynamic model (TELEMAC 2D) was used to simulate V and D in two hydrologically altered river reaches (Parapeiros River, western Greece; Oinoi Stream, Attica, Greece). The main outcome of this thesis has been the conceptualization, development and pilot-application of a new, BM-based hydrodynamic-habitat modelling, environmental flow assessment (EFA) framework. Accurate model-based, BM-adapted EFAs can be now implemented in Greece and, upon relevant hydroecological-data availability, worldwide, to facilitate the sustainable management of freshwater resources.

7.1. Response of benthic macroinvertebrates to hydrological variation

The first step towards a BM-based hydrodynamic habitat model (HHM) was to explore whether or not the benthic macroinvertebrates respond to hydrological variation and, consequently, to changes in the major, habitat-defining hydraulic and environmental variables (V, D, S and T). Previous studies have focused on the response of benthic macroinvertebrates to extreme hydrological events -droughts and floods- (Herbst and Cooper, 2010; Mesa, 2010; Lake, 2011; Mundahl and Hunt, 2011, Skoulikidis et al., 2011; Chessman, 2015). The new information that this study offers (described in detail in Chapter 2), is that BMs also respond to natural hydrological variation of moderate magnitude (in comparison to the hydrological extremes of droughts and floods). The distribution, abundance and diversity of BMs before and after a rainfall-induced high flow event was clearly-significantly different; this hydrological variation explained up to 42.9% of the overall BM community variation. In accordance with previous studies on extreme events (Rosser and Pearson, 1995; Argerich et al., 2004; Mesa, 2010) macroinvertebrate abundance, taxonomic richness, richness of Ephemeroptera, Plecoptera and Trichoptera and diversity decreased significantly by 90%, 60%, 50% and 25% respectively, between the pre- and post-impact microhabitat samples. Moreover, specific types of substrate acted as flow refugia, providing shelter against the dislodgment of macroinvertebrates (Lancaster and Hildrew, 1993; Rempel et al., 1999; Fuller et al., 2010). These substrate types were mainly boulders and large stones, hosting 73% of the total BM abundance and higher taxonomic richness, compared to finer substrates, after the high flow event. As discussed by Borchardt (1993) and indicated in the current study, benthic macroinvertebrates either actively drift to these refugia or are accidentally protected, being on refugia when flow-hydraulic conditions become critical, provoking dislodgment.

In addition, the study showed that the response of BMs to the hydrological-hydraulic, habitat-defining variables of V, D, S and T follows a Gaussian distribution with specific optimal values. The results (chapter 2) showed that high macroinvertebrate abundance, taxonomic richness, EPT richness and diversity can be found in V between 0.3 m/s and 0.75 m/s, in D values near 0.2 m and in coarse substrates (higher abundance and taxonomic richness in large stones, boulders, small stones and large gravel). The majority of previous research shows similar BM-habitat-preference trends, although originating from different locations with varying climatic and hydrodynamic conditions (Jowett et al., 1991; Gore et al., 2001; Li et al., 2009; Horta et al., 2009; Shearer et al., 2015).

7.2. Towards a benthic-invertebrates-based hydrodynamic habitat modelling framework

The aforementioned information suggests that benthic macroinvertebrates can be effectively used in HHMs. However, until now, HHMs-based environmental flow assessments have been primarily focused on fish; BM-based frameworks have not been commonly applied (Waddle and Holmquist, 2011; Arthington, 2012; Muñoz-Mas et al., 2016; Leitner et al., 2017; Papadaki et al., 2017). The main reasons for this are mainly associated with cost-effectiveness, time-efficiency, required expertise and availability of hydroecological information (Jorgensen and Bendoricchio, 2001; Conallin et al., 2010). HHMs-based EFAs, either BMs- or fish-focused, inevitably require a costly and time-consuming collection of hydraulic and hydrometric data to calibrate and validate the hydrodynamic module (Spense and Hickley, 2000) and usually, additional, carefully designed field visits are necessary to calculate the habitat preferences of aquatic biota (Heggenes et al., 1990). Moreover, the developed hydrodynamic habitat model is usually restricted to an area of 200 or 300 meters, whereas the effects of hydrological alteration may be geographically widespread (Booker, 2016). In this thesis, it was shown that cost-effective and time-efficient BM-based HHMs can be accurately applied by small teams of hydraulic-environmental engineers and ecologists; the conceptual framework and the relevant technical information to implement-replicate such model-based EFAs from scratch, with the use of state-of-the-art tools, has been also provided.

7.3. The predictive performance of habitat modelling algorithms

As shown in Chapter 4, not all habitat modelling algorithms are appropriate for predicting the habitat suitability for benthic macroinvertebrates in HHM simulations. The main outcome from the performance tests applied in this study between multivariate statistical models -including the traditional habitat suitability curves (HSCs) approach of Bovee (1986)-, machine-learning algorithms and fuzzy-rule-based (FL) models was the following: (i) Several but not all algorithms can be used for accurate predictions; (ii) machine learning models -Boosted Regression Trees (BRT) and Random Forests (RF)- can be used within balanced hydroecological datasets but adjustments are required if they are to be applied within imbalanced datasets; (iii) specific FL models (centroid and weighted average defuzzification) failed to reach acceptable predictions; the models, which developed accurate predictions within imbalanced datasets, without requiring any pre-treatment or adjustment, were the FL maximum-membership-defuzzified and the fuzzy rule-based Bayesian algorithm (FRB). Based on the cross-validation process applied, the mean accuracy of the FRB model was 61.2%, which is considered accurate enough to proceed to 'safe' habitat suitability (K) predictions. Existing literature, although using various K-calculation approaches, shows that the predictive performance of habitat models varies between 45-48% (Muñoz-Mas et al., 2016) and 70% (Mouton et al., 2011; Vezza et al., 2015). Thus, this study favored the use of the FRB algorithm for accurate BM-based predictions.

7.4. Development of a benthic-invertebrates-specific, habitat modelling software

Based on the aforementioned, a command-line tool (HABFUZZ - Theodoropoulos et al., 2016) has been developed in FORTRAN to implement the FRB algorithm (described in detail in chapter 3). HABFUZZ is a one-click tool; the user provides the reference hydroecological dataset with microhabitat observations-combinations of V, D, S, T and K, similar to the one collected in this study, and the relevant test dataset containing microhabitats with known V, D, S and T and unknown K, and the software produces a file with the predicted K values for each microhabitat. HABFUZZ is open source and can be easily integrated with the open-source TELEMAC 2D (Galland et al., 1991). Currently, the only fuzzy-based alternative to HABFUZZ is the CASiMiR software (Schneider et al., 2001), which however includes a one-dimensional hydrodynamic module for the simulation of the study area. HABFUZZ uses the output of the two-dimensional TELEMAC 2D and thus, comparatively more accurate simulations and more detailed representation of the final habitat suitability can be achieved. In addition, HABFUZZ is BM-

specific; the output of HABFUZZ includes various BM habitat-related variables to facilitate accurate K predictions (chapter 4). In this study, HABFUZZ was integrated with TELEMAC 2D and applied to assess the environmental flows (eflows) in two hydrologically altered river reaches in Greece (chapters 5 and 6).

7.5. Key issues considered and addressed during implementation

7.5.1. Abundance- vs metrics-based habitat suitability calculation

It was previously mentioned that a reference hydroecological dataset, as the one collected in this study, includes microhabitat samples relating the V, D, S -and T (optional)- abiotic habitat predictors to the habitat suitability of each microhabitat. But this is not totally true; the raw dataset does not include K values but a BM taxalist (BM families and their abundance at each microhabitat) from which K is calculated. In fish-based studies, K is usually directly related to the abundance of fish species (Mouton et al., 2011; Vezza et al., 2015; Papadaki et al., 2017). BM-based studies have also applied this approach (Li et al., 2009), but in this study we favored a community-metrics-based approach, using metrics that have been well studied for their 'sensitivity' to describe the status-suitability of a benthic-invertebrate community (Englund and Malmqvist, 1996; Buffagni et al., 2006; Monk et al., 2006; Waddle and Holmquist, 2011; Jun et al., 2012; Holmquist et al., 2015). Considering that the numerous BM taxa found in a microhabitat may have partially contrasting K preferences, they should be either treated as a community or only use the habitat preferences of specific taxa. Moreover, a community-metrics approach enables the use of a particular hydroecological dataset in test cases where a taxon may not be present, as the habitat suitability is not directly related to a specific taxon.

7.5.2. How were the different metrics combined into a BM-community K index?

The individual metrics were statistically treated to find correlations between them and the abiotic variables and they were afterwards combined in a single multimetric habitat suitability index, also taking into account the following considerations:

1. *Number of taxa:* A site with high taxonomic richness, is almost certainly more suitable than a site with lower number of taxa.
2. *Diversity index:* A site with increased diversity (Shannon's index) most probably has a healthy BM community and should be considered more suitable than a site with lower diversity index.
3. *EPT index:* A site with higher EPT taxa richness is very likely to be more suitable for the whole BM-community than a site with lower number of EPT taxa.
4. *Abundance:* A site with high abundance of benthic macroinvertebrates may also be more suitable than a site with low abundance. However, abundance alone is not a reliable suitability indicator; a site with 50 Perlidae, for example, is considered more suitable than a site with 3000 Chironomidae and thus, all four metrics were multiplied by a weighting value to account for the experts' certainty about their potential to accurately quantify the 'real' habitat suitability.

Previous studies developing multimetric macroinvertebrate indexes mostly include the number of taxa, the number of EPT taxa and the Shannon's diversity index (Buffagni et al., 2006; Gabriels et al., 2010; Jun et al., 2012). The abundance of the BM community is usually not included due to the aforementioned deficiency. In our study, we included the abundance metric as it was well correlated with the abiotic V, D, and S variables (chapter 4) but weighted it with the lowest score (0.1) to address this issue without totally excluding it. Weighting the individual metrics prior to aggregation to account for such issues is common in multimetric approaches (Buffagni et al., 2006).

7.5.3. The traditional HSCs approach and the fuzzy alternative

Another critical issue that was, and should be, taken into account when relating the V, D, S and T values of a hydroecological dataset with the habitat suitability (either abundance- or metrics-based) is the interaction between the habitat variables to define suitable or not suitable microhabitats based on BMs. Previous literature (Nykanen et al., 2001; Rydgren et al., 2003; Hirzel and Le Lay, 2008) suggests that 'habitat selection by benthic macroinvertebrates is a multivariate process where location (microhabitat) is selected based on several interacting variables'. BM taxa select the values of the habitat-defining predictors simultaneously. If V is suitable but D is not, then the specific microhabitat (interaction of V and D) is not suitable (the taxon will almost certainly avoid being there) and consequently, its K will be low, despite the high suitability of V. If we simultaneously include the variables of S and T, then the interaction between the abiotic predictors seems the primary factor for selecting a model to ensure reliable predictions.

Within this perspective, regression-based univariate modelling methods (HSCs or univariate Generalized Linear Models, GLMs), which assess the influence of each predictor on K independently, resulting in a single best-fit curve, were not considered likely to yield accurate predictions. In addition, the assumption of GLMs for linear combination of the abiotic predictors further restricts the applicability of the particular method in hydroecological studies (Ahmadi-Nedushan et al., 2006; Yi et al., 2017). Machine-learning methods can, at least partially, handle the complex interactive relationships between the predictor variables, since they address non-linearity and explore non-intuitive hydroecological relationships (Olden et al., 2008). As suggested by the performance comparison of the habitat modelling algorithms (chapter 4), FL algorithms are considered advantageous; the inherent design of these algorithms -the IF-THEN-rules based concept- enables them to handle complex interactions between the predictor variables, given that a sufficient set of rules is provided. The advantages of fuzzy-rule-based models, which take into account the inherent uncertainty of ecological variables and handle non-linear interactions, have been previously well documented (Jorde et al., 2001; Mouton et al., 2011; Muñoz-Mas et al., 2012). For the hydroecological dataset collected in this study, the differences between the univariate and multivariate graphical representation of K against V, D, S and T are shown in Fig. 7.1 and 7.2, respectively.

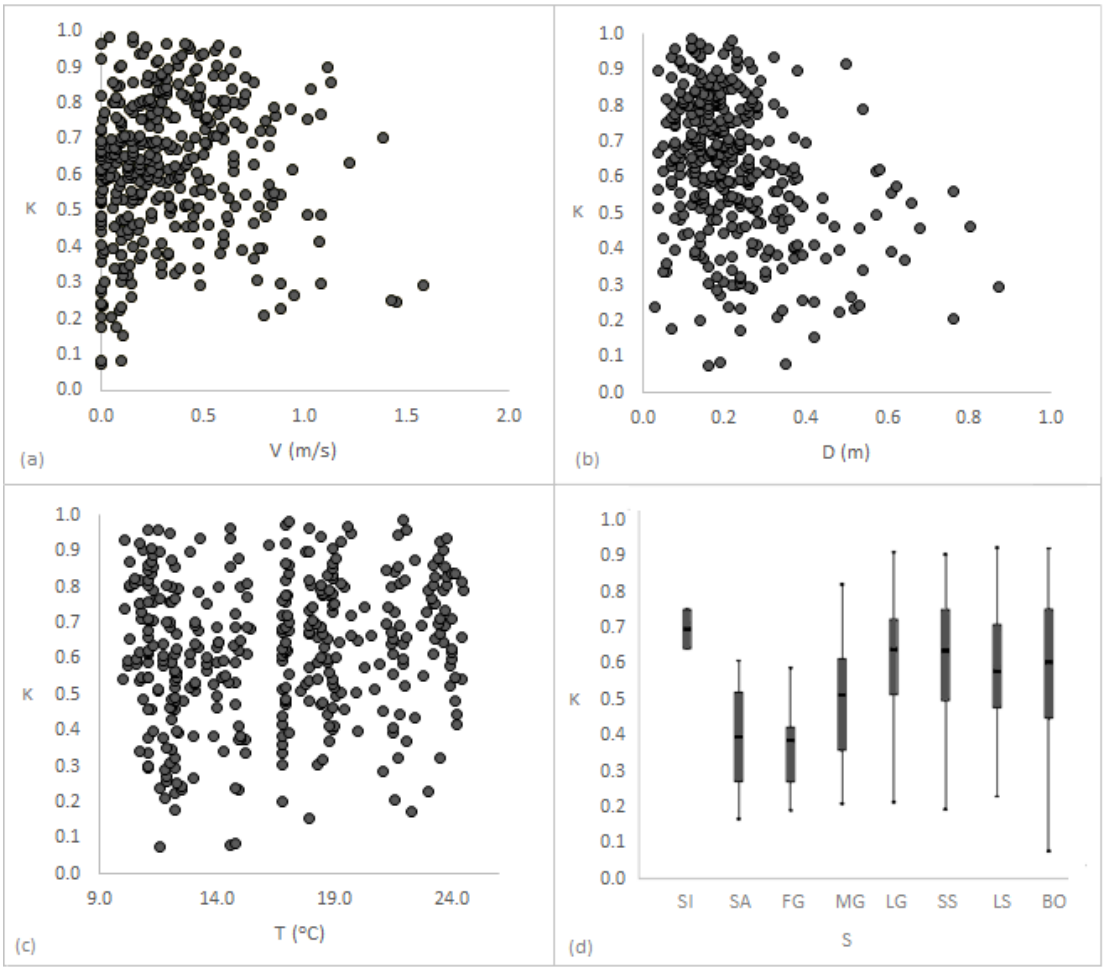

Fig. 7.1. Two-dimensional scatter plots between the abiotic predictors and the habitat suitability (K). V: flow velocity, D: water depth, T: temperature, S: substrate type, κ: observed habitat suitability.

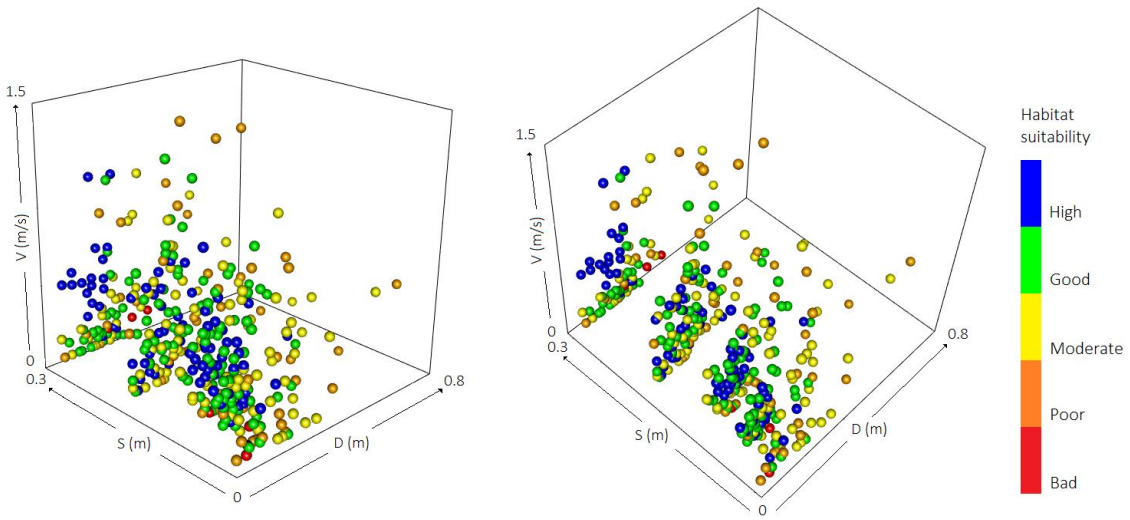

Fig. 7.2. Multivariate, three-dimensional scatter plot between V, D, S and K. V: flow velocity, D: water depth, S: substrate type, K: observed habitat suitability.

7.5.4. The OFS multimetric environmental flow index - is it necessary?

The habitat suitability (K multimetric index) developed in this thesis describes the suitability of a microhabitat based on the status of the macroinvertebrate community. This index was the basis for the HHM-based environmental flow assessment case studies in the two selected reaches in Greece. However, for the final selection of the environmental flow, this index was combined with specific non-BM-related metrics to facilitate its use from the microhabitat- to the reach-scale. Thus, the K index refers to the microhabitat's suitability whereas the OFS index refers to the selection of the discharge, which is the most suitable for the BM community of the whole study reach. The rationale for using each metric of the OFS index was the following:

1. Discharges with high average microhabitat suitability would be potential environmental flow candidates; thus, the K-based, nOSI index was included.
2. Discharges for which the prediction was based on the actual data should be favored as environmental flows against those with increased uncertainty (due to the absence of specific microhabitats from the reference dataset); that is why the COP index was calculated. Ideal datasets would yield a COP of 1. In contrast, if no microhabitat was found in the reference dataset, and consequently, in the fuzzy-rules database, this would result in COP = 0.
3. The more water in the river, the more microhabitats will be available for the BM community; thus, the w index was included.
4. Let's assume that in two different discharges, 60% microhabitats (computational nodes) had good suitability. The discharge with the highest percent of good-K neighboring nodes should be preferred; this was reflected in the C index, the ratio of connected -neighboring- good-K nodes to the total number of good-K nodes.
5. Similarly, the discharge with the highest percent of good-K connected nodes to the total number of nodes (wetted and dry) in the study reach, reflecting habitat availability, should be favored; this is reflected in the A index.

Consequently, the discharge with the highest aforementioned values, combined within the OFS index should be selected as the environmental flow of the study reach. As previous studies are mostly fish-based, they use the Weighted Usable Area (WUA - Bovee, 1986) to incorporate the microhabitat suitability in developing reach-scale environmental flow scenarios. But as benthic macroinvertebrates are less mobile than fish, a WUA approach would not be of much meaning. That is why the OFS index was developed; in a similar to the WUA concept, the BM-focused OFS index incorporates metrics which are most important for the BM community.

7.5.5. Spatial and temporal variation in the habitat preferences of benthic macroinvertebrates

Spatiotemporal variation has long been a subject of discussion in physical habitat modelling (Glozier et al., 1997; Gore at al., 2001; Vismara et al., 2001; Lamouroux et al., 2013; Everaert et al., 2014; Shearer et al., 2015; Booker, 2016). Research suggests that aquatic organisms often shift their habitat preferences among seasons and may have different requirements in different geographical locations. This has been repeatedly confirmed for fish, as there is a complete agreement between studies on different species and from different regions [Glozier et al., 1997; Maki-Petäys et al., 1997; Mérigoux and Dolédec, 2004; Studdert and Johnson, 2015), and thus, in fish-based studies, site- and season-specific habitat suitability criteria have been preferred over generic ones (Heggenes and Saltveit, 1990; Greenberg et al., 1996). In contrast, the fewer available studies BM-based studies reach contrasting conclusions; although most studies suggest increased performance of habitat models when local and season-specific criteria are applied (Mérigoux and Dolédec, 2004; Everaert et al., 2014; Shearer et al., 2015; Kelly et al., 2015), others conclude that the observed differences are not significant enough to inhibit the application of generic habitat suitability criteria (Jowett et al., 1991; Gore et al., 2001; Lamouroux et al., 2013).

As our reference dataset spans three seasons and three river types, it was expected (and partially evident in Fig. 4.2-4.6) to have increased spatiotemporal variation, which should be incorporated in the K index to provide robust results. This could be applied only within the K-normalization process. From the various normalization options available -dividing the observed K by the maximum observed value (i) in the dataset, (ii) in the season, (iii) in the river type, (iv) in the site and (v) within the metric- we excluded the first three options considering that (i) normalizing a spatially variable dataset, that includes multiple river types, only by season, does not take into account the geographical-typological variation and (ii) normalizing a temporally variable dataset, that includes multiple seasons, only by type, does not take into account the seasonal variation. The per-site and per-metric options however account for the spatiotemporal variation, as the observed K at each sample is compared with the maximum K at the site (per-site K normalization) or in more detail, each observed metric is compared with the maximum value of this metric at each site (per-metric K normalization). While both options seemed acceptable, we selected the per-metric normalization to develop the K and OFS indexes.

7.6. Application of the developed HHM-based EFA methodology in two test river-reaches

The developed methodology was successfully implemented in two river reaches in Greece (Parapeiros River, Western Greece; Oinoi Stream, Attica). The most valuable outcome of these applications has been the development of habitat suitability maps in various simulated discharges; with these maps as a basis, scientists, water managers and the local community can 'speak a common language' and negotiate on what each stakeholder considers acceptable. As it has been previously highlighted, environmental flow assessments are required to build the scientific evidence for the selection of ecologically acceptable flow regimes (Dyson, 2003; Acreman and Dunbar, 2004). The actual environmental flow, which will be finally delivered is a negotiated consensus on flow allocation for all stakeholders (Dore et al., 2010), a trade-off value between ecologically and socially acceptable and technically feasible discharges (Stamou et al., 2018). The results from both river reaches showed that the ecologically acceptable environmental flow can be flexible enough (ranging from 0.6 m^3/s to 2 m^3/s for the Parapeiros reach and from 0.17 m^3/s to 1.5 m^3/s for the Oinoi reach) to provide a variety of ecologically acceptable options to negotiate upon.

7.7. Future challenges - From here to where?

In this thesis, a robust BM-focused HHM-based environmental flow assessment methodology was developed. What was not feasible before 2015, is now an option and was twice piloted in two river reaches in Greece; benthic-invertebrate-community indicators can now be integrated with the output of hydrodynamic models to develop environmental flow recommendations downstream of hydrologically altered river reaches. But despite the progress made, there are yet specific challenges that need to be addressed towards the development of accurate model-based EFAs:

1. **Field validation of the habitat module of HHMs;** in this thesis, the hydrodynamic predictions of V and D in various discharges were field-validated with independent observations. V and D values were recorded in two or three different discharges and the hydrodynamic-model's predictive accuracy was assessed based on the divergence between observed and predicted V and D values. In contrast, the habitat module was cross-validated, not field-validated; field-validation of a habitat module requires additional sampling of BM microhabitats in the river reaches of interest in various discharges, additional analysis of BM samples and thus additional time, effort and costs. Thus, a cross-validation process is often followed instead of the field validation. In addition, there is a major issue when attempting to field-validate a habitat model: Environmental flow assessments are applied in hydrologically altered river reaches,

which in addition, are often degraded by point or non-point sources of pollution. A field validation of a habitat model in such polluted reaches would be scientifically meaningless because the aquatic communities would be degraded due to pollution, even if an environmental flow had been delivered. Ideally, field validation should be applied in a hydrologically altered, unpolluted site, where the environmental flow would be delivered as predicted by the habitat model and a field sampling would be afterwards applied to evaluate the habitat suitability in a given number of microhabitats and assess the divergence of the observed suitability values from the predicted ones. Applying this process in polluted sites is wrong; the observed values would be much different from the predicted ones due to the pollution, which is not accounted in the habitat models.

2. Spatiotemporal variation in the BM habitat preferences; spatially and temporally variable hydroecological datasets are often aggregated to increase sample size and enable statistical analysis of the hydroecological results. In this study, we aggregated data from three seasons and two rivers types (nine sites), using a normalization process, which partially accounted for the error that would occur due to the spatiotemporal aggregation of the dataset. However, further research is required to fine-tune the normalization process or compare various alternatives towards minimizing the error from spatiotemporal pooling of data.
3. Collection of reference datasets; model-based, data-driven assessments cannot be applied without the presence of robust hydroecological datasets. Despite the increasing use of hydrodynamic habitat models in environmental flow assessments, reference datasets, from sites of no or very minor anthropogenic influence are currently scarce worldwide due to the costs and time required for them to be collected. However, such datasets are valuable to provide a reference, not only for environmental flow assessments but for future comparisons, assessing changes in aquatic community composition due to climate change in the long-term.

Extended abstract in Greek | Περίληψη στα Ελληνικά

Η χρήση των υδροδυναμικών μοντέλων καταλληλότητας ενδιαιτήματος για την εκτίμηση της οικολογικής παροχής κατάντη ανθρωπογενών παρεμβάσεων θεωρείται η πιο 'ασφαλής' επιλογή σε περιπτώσεις όπου απαιτείται υψηλή ακρίβεια πρόβλεψης, ώστε οι σχετικοί διαχειριστές και ενδιαφερόμενοι να έχουν μία ισχυρή βάση για διαπραγμάτευση κατά τη διαδικασία κατανομής των αδειών χρήσης νερού. Παρά τη γενικότερη αποδοχή της αποτελεσματικότητας των σχετικών μεθόδων από την επιστημονική κοινότητα, η πρακτική τους εφαρμογή και χρήση είναι περιορισμένη σε σύγκριση με τις αντίστοιχες υδρολογικές μεθόδους. Επιπλέον, οι περισσότερες έως τώρα έρευνες εστιάζουν στα ψάρια, ενώ μεθοδολογίες, μοντέλα και λογισμικά που χρησιμοποιούν άλλους οργανισμούς-δείκτες του υδάτινου οικο-συστήματος δεν υπάρχουν. Εντός μιας ολιστικής όμως προσέγγισης της διαχείρισης των βιολογικών και υδάτινων πόρων, οι προτιμήσεις ενδιαιτήματος όλων των οργανισμών θα πρέπει να λαμβάνονται υπόψη κατά την υλοποίηση μελετών εκτίμησης της οικολογικής παροχής. Στη συγκεκριμένη έρευνα, αναπτύχθηκε μεθοδολογία εκτίμησης της οικολογικής παροχής με τη χρήση υδροδυναμικών μοντέλων καταλληλότητας ενδιαιτήματος βενθικών μακροασπονδύλων (ΒΜ) ως βιολογικών δεικτών. Συλλέχθηκαν υδρο-οικολογικά δεδομένα αναφοράς από εννέα μη ρυπασμένες θέσεις δειγματοληψίας σε τρεις εποχές στην Ελλάδα. Βάσει αυτών των δεδομένων, αναλύθηκαν και ποσοτικοποιήθηκαν οι προτιμήσεις ενδιαιτήματος των ΒΜ. Αναπτύχθηκε σχετικός δείκτης καταλληλότητας ενδιαιτήματος ΒΜ (K) ο οποίος ενσωματώνει τέσσερεις βασικές μετρικές-δείκτες της κατάστασης της κοινότητας των ΒΜ και ο οποίος συμπεριελήφθη σε σχετικό δείκτη βέλτιστης οικολογικής παροχής (OFS). Χρησιμοποιώντας τους ανωτέρω δείκτες εκτιμήθηκε η ακρίβεια πρόβλεψης διαφόρων αλγορίθμων-μεθόδων προσομοίωσης ενδιαιτήματος και επιλέχθηκε ως καταλληλότερη η μέθοδος της Μπεϋζιανής Πιθανολογικής Ανάλυσης Ασαφούς Λογικής (FRB). Αναπτύχθηκε σχετικό λογισμικό (HABFUZZ) το οποίο υλοποιεί τον σχετικό FRB αλγόριθμο και χρησιμοποιήθηκε δισδιάστατο υδροδυναμικό μοντέλο (TELEMAC 2D) βάσει του οποίου προσομοιώθηκαν η ταχύτητα ροής (V) και το βάθος (D) σε ποικίλα σενάρια παροχής σε δύο περιοχές μελέτης στην Ελλάδα. Τα αποτελέσματα έδειξαν ότι τα ΒΜ αποκρίνονται στις υδρολογικές μεταβολές-αλλοιώσεις. Η κατανομή, αφθονία και ποικιλότητα της βιοκοινωνίας των ΒΜ πριν και μετά από μια φυσική, μετρίου μεγέθους υδρολογικής διαταραχή (μέτριας έντασης πλημμύρα) παρουσίασαν στατιστικά σημαντικές διαφορές, και η σχετική διαταραχή 'εξήγησε' το 42.9% της βιολογικής απόκρισης-διακύμανσης. Οι προτιμήσεις ενδιαιτήματος των ΒΜ ακολουθούν την κανονική (Γκαουσιανή) κατανομή με συγκεκριμένες βέλτιστες τιμές καταλληλότητας για κάθε υδρολογική-υδραυλική παράμετρο: V, D, τύπο υποστρώματος (S) και θερμοκρασία νερού (T). Παρατηρήθηκε ότι δεν είναι όλοι οι αλγόριθμοι κατάλληλοι για την προσομοίωση των προτιμήσεων ενδιαιτήματος των ΒΜ. Η ακρίβεια πρόβλεψης των διαφόρων μεθόδων συσχέτισης, μηχανικής εκμάθησης και ασαφούς λογικής κυμάνθηκε από 49.74% έως 67.92%, και ο FRB αλγόριθμος παρουσίασε ακρίβεια 61.2%. Βάσει αυτού του αλγόριθμου χαρτογραφήθηκε η καταλληλότητα ενδιαιτήματος σε δύο περιοχές μελέτης. Οι οικοσυστημικής προσέγγισης οικολογικές παροχές που εκτιμήθηκαν με τη χρήση υδροδυναμικών μοντέλων ενδιαιτήματος ήταν υψηλότερες αυτών που εκτιμήθηκαν με τη χρήση υδρολογικών μεθόδων. Ως εκ τούτου, η διάθεση οικολογικών παροχών θα πρέπει να αναθεωρηθεί προς τα άνω ώστε να διασφαλιστεί η μακροχρόνια λειτουργικότητα-ακεραιότητα των υδρόβιων κοινοτήτων. Εκτός από τη σχετική μεθοδολογία, η συγκεκριμένη μελέτη έδειξε ότι (α) περίπλοκες, στοχαστικού τύπου υδρο-οικολογικές σχέσεις μπορούν να περιγραφούν και να προσομοιωθούν με σχετική ασφάλεια με τη χρήση αλγόριθμων ασαφούς λογικής και (β) η χρήση πολυπαραμετρικών δεικτών παρέχει αξιοπιστία κατά την εκτίμηση της κατάστασης-καταλληλότητας των υδρόβιων κοινοτήτων σε ποικίλα σενάρια παροχής. Μελλοντικές έρευνες θα πρέπει να εστιάσουν (α) στη συλλογή σχετικών υδροοικολογικών δεδομένων αναφοράς, (β) στη ανάλυση-διαχείριση της διακύμανσης σειρών δεδομένων από διαφορετικές εποχές και γεωγραφικές θέσεις και (γ)

στην επαλήθευση των προβλέψεων με χρήση ανεξάρτητων δεδομένων πεδίου, ώστε να διασφαλιστεί ακόμη μεγαλύτερη ακρίβεια πρόβλεψης κατά τη διαδικασία εκτίμησης και προσομοίωσης της οικολογικής παροχής κατάντη ανθρωπογενών παρεμβάσεων.

Κεφάλαιο 1 | Εισαγωγή

Η συγκεκριμένη έρευνα αποτελεί συνδυασμό δύο διαφορετικών επιστημονικών κλάδων, της Περιβαλλοντικής Μηχανικής-Υδραυλικής-Υδροδυναμικής και της Βιολογίας-Οικολογίας, υπό την κοινή ονομασία Υδρο-οικολογία (Hydroecology) ή Οικο-υδραυλική (Ecohydraulics). Η Υδροδυναμική είναι ο κλάδος της Μηχανικής των Ρευστών που έχει ως αντικείμενο έρευνας την περιγραφή της κίνησης των ασυμπίεστων υγρών. Η Οικολογία είναι ο κλάδος των φυσικών επιστημών που μελετά την κατανομή και διάδοση των πληθυσμών των ζωντανών οργανισμών, καθώς και του τρόπου με τον οποίο οι ιδιότητες αυτές επηρεάζονται από την αλληλεπίδραση των οργανισμών μεταξύ τους και με το αβιοτικό τους περιβάλλον.

1.1. Υδροδυναμική: Μαθηματική προσομοίωση υδροδυναμικής συμπεριφοράς

Η κίνηση των ασυμπίεστων υγρών, έχει περιγραφεί από το 1822 με ιδιαίτερη ακρίβεια από τις εξισώσεις των Claude-Louis Navier (Γαλλία), και George Gabriel Stokes (Αγγλία) οι οποίες ονομάστηκαν και εξισώσεις Navier-Stokes. Και ενώ μέχρι και τις αρχές του 1900 οι μηχανικοί επιστήμονες απλοποιούσαν τις πολύπλοκες Μερικές Διαφορικές Εξισώσεις σε αλγεβρικές ώστε να μπορούν εύκολα να 'λυθούν με το χέρι', η ραγδαία αύξηση της ταχύτητας και της αποθηκευτικής ικανότητας των ηλεκτρονικών υπολογιστών μετά το 1950 οδήγησε στη δημιουργία υπολογιστικών μοντέλων-λογισμικών τα οποία επιλύουν τις αρχικές διαφορικές εξισώσεις ώστε να περιγράψουν, να προβλέψουν και να προσομοιώσουν τελικά την κίνηση των υγρών. Τα λογισμικά αυτά ονομάζονται πλέον υδροδυναμικά μοντέλα (ή και υδραυλικά μοντέλα).

Για τους οικολόγους από την άλλη, όλα άρχισαν το 1910 όταν ο Roswell Hill Johnson πρώτος χρησιμοποίησε τον όρο 'θώκος' για να προτείνει ότι τα διαφορετικά είδη καταλαμβάνουν διαφορετικούς χώρους στη φύση (Johnson, 1910). Έκτοτε, αρκετοί οικολόγοι εργάστηκαν στην κατεύθυνση της ποσοτικοποίησης των θώκων για κάθε είδος-οργανισμό. Η έννοια του οικολογικού θώκου έδωσε στη συνέχεια αρχή για χρήση της περισσότερο ευρύτερης έννοιας του 'ενδιαιτήματος', ήτοι τη φυσική θέση όπου ένας οργανισμός, είδος ή πληθυσμός επιλέγει για να ζήσει και να αναπαραχθεί. Με τη συνεχή αύξηση της χωρητικότητας και της υπολογιστικής ικανότητας των σύγχρονων υπολογιστών, άρχισαν να εμφανίζονται και σχετικά λογισμικά τα οποία προβλέπουν και προσομοιώνουν τις προτιμήσεις ενδιαιτήματος των οργανισμών, σε σχέση με συγκεκριμένες αβιοτικές παραμέτρους. Τα μοντέλα αυτά ονομάστηκαν μοντέλα καταλληλότητας ενδιαιτήματος και σε ότι αφορά στα υδρόβια οικοσυστήματα, οι αβιοτικές παράμετροι που συνήθως επιλέγονται είναι η ταχύτητα ροής, το βάθος και το υπόστρωμα (και σε μικρότερο βαθμό η θερμοκρασία του νερού) (Bovee and Milhous, 1978; Bradley et al., 2012).

Παρά την αρχικά διαφορετική προέλευση και πορεία των ανωτέρω κλάδων της Υδροδυναμικής και της Οικολογίας, το 1978 άρχισαν οι πρώτες κοινές προσπάθειες για τη δημιουργία 'υδροδυναμικών μοντέλων καταλληλότητας ενδιαιτήματος', λογισμικών δηλαδή που θα συνδυάζουν τα διαφορετικά μοντέλα (υδροδυναμικά και ενδιαιτήματος) σε ένα κοινό προϊόν, ειδικά φτιαγμένο για την πρόβλεψη της καταλληλότητας ενδιαιτήματος σε ποταμούς σε διαφορετικά σενάρια παροχών, ώστε να γίνει επιλογή του καταλληλότερου σεναρίου (αυτού με την υψηλότερη καταλληλότητα). Και τελικά αναπτύχθηκε η έννοια της οικολογικής παροχής, της βέλτιστης δηλαδή παροχής η οποία, βασιζόμενη στα ανωτέρω θα διασφαλίζει τη βιώσιμη διατήρηση των υδρόβιων οικοσυστημάτων.

Τα υδροδυναμικά μοντέλα καταλληλότητας ενδιαιτήματος αποτελούνται από δύο υπομοντέλα, το υδροδυναμικό υπομοντέλο και το υπομοντέλο ενδιαιτήματος. Το υδροδυνα-

μικό υπομοντέλο χρειάζεται κάποιου είδους αποτύπωση της τοπογραφίας μιας περιοχής, η οποία αποτελεί τη βάση για τη δημιουργία ενός υπολογιστικού πλέγματος, επί του οποίου επιλύονται οι εξισώσεις κίνησης του νερού. Η τοπογραφική αποτύπωση μπορεί να γίνει με δύο τρόπους. Ο πρώτος είναι με τη χρήση διατομών κάθετων στην κίνηση του νερού όπου το βάθος του νερού, η στάθμη, η μέση ταχύτητα και το υπόστρωμα καταγράφονται ανά διαστήματα από τη μία όχθη του ποταμού έως την άλλη. Μεγαλύτερος αριθμός διατομών οδηγεί και σε αναλυτικότερη περιγραφή της τοπογραφίας της περιοχής. Ο δεύτερος τρόπος είναι με τη χρήση γεωγραφικών συντεταγμένων (μήκος, πλάτος, υψόμετρο). Αυτού του είδους οι συντεταγμένες μπορούν να καταγραφούν με τη χρήση συσκευών που διαθέτουν GPS υψηλής ακρίβειας (απόκλισης μερικών εκατοστών), όπως RTK-GPS ή drones. Τα μοντέλα τα οποία χρησιμοποιούν τον πρώτο τρόπο τοπογραφικής αποτύπωσης ονομάζονται μονοδιάστατα (1D) σε αντιδιαστολή με τα δισδιάστατα (2D) τα οποία χρησιμοποιούν τον δεύτερο τρόπο αποτύπωσης της τοπογραφίας.

Στα 1D μοντέλα για την περίπτωση μη μόνιμης ροής (unsteady flow) επιλύεται η απλοποιημένη μορφή (Reynold's averaged) των εξισώσεων Navier-Stokes και υπολογίζεται η μέση τιμή της στάθμης και η μέση τιμή, επί του άξονα x, της ταχύτητας ροής για κάθε διατομή. Τα τοπικά βάθη εντός της κάθε διατομής υπολογίζονται αφαιρώντας το τοπικό υψόμετρο από τη μέση στάθμη για την κάθε διατομή, ενώ οι τοπικές ταχύτητες ροής υπολογίζονται χρησιμοποιώντας τα τοπικά βάθη και επιλύοντας απλές εξισώσεις ομοιόμορφης ροής (Bovee, 1982; Benjankar, 2014). Για την περίπτωση μόνιμης ροής (steady flow) τα μοντέλα επιλύουν την εξίσωση συνέχειας και μία εξίσωση για τον δείκτη Manning ώστε να υπολογίσουν το μέτρο της κατά χ κατεύθυνσης της ταχύτητας ροής και τη στάθμη του νερού. Συνήθη χρησιμοποιούμενα 1D υδραυλικά μοντέλα είναι τα PHABSIM (Milhous et al., 1989; Waddle, 2001), CASiMiR (Schneider et al., 2001), HEC RAS (USACE, 2016) και MIKE11 (DHI, 2017).

Στα 2D μοντέλα, δημιουργείται ένα λεπτομερές υπολογιστικό πλέγμα αποτελούμενο από κόμβους και στοιχεία και σε κάθε κόμβο υπολογίζεται (α) το μέτρο της κατά x κατεύθυνσης του διανύσματος της ταχύτητας ροής, (β) το μέτρο της κατά y ταχύτητας και (γ) το βάθος του νερού. Οι υπολογιζόμενες ταχύτητες αποτελούν μέσες ως προς το βάθος ταχύτητες (και αυτή είναι και η διαφορά των 2D με τα 3D μοντέλα τα οποία υπολογίζουν την ταχύτητα και κατά τον z άξονα, ανιχνεύοντας έτσι και τις ως προς το βάθος μεταβολές της). Οι εξισώσεις που επιλύονται από τα 2D μοντέλα προέρχονται από τις εξισώσεις Navier-Stokes, ονομάζονται εξισώσεις ρηχών νερών (shallow water equations) ή εξισώσεις St. Venant και αναπτύχθηκαν το 1871 από τον Adhémar Jean Claude Barré de Saint-Venant. Για την επίλυσή τους τα 2D μοντέλα ακολουθούν μια διαδικασία που ονομάζεται διακριτοποίηση. Η δημιουργία του υπολογιστικού πλέγματος είναι ουσιαστικά η διακριτοποιημένη βάση επί της οποίας επιλύονται οι ανωτέρω εξισώσεις επιλέγοντας μία από τρεις μεθόδους (α) Μέθοδος Πεπερασμένων Διαφορών, (β) Μέθοδος Πεπερασμένων Στοιχείων και (γ) Μέθοδος Πεπερασμένων Όγκων.

1.2. Προσομοίωση (καταλληλότητας) ενδιαιτήματος

Τα αποτελέσματα του υδροδυναμικού υπομοντέλου (έξοδος) αποτελούν τελικά είσοδο για τα μοντέλα προσομοίωσης καταλληλότητας ενδιαιτήματος. Τα τελευταία ποσοτικοποιούν τις σχέσεις μεταξύ επιλεγμένων αβιοτικών παραμέτρων (V, D, S, T) και της κατανομής των υδρόβιων οργανισμών (βιοτικές παράμετροι). Αυτή η διαδικασία προϋποθέτει τα παρακάτω:

1. Ένα σετ δεδομένων 'αναφοράς', δηλαδή ένα σύνολο δεδομένων, συλλεχθέντων από καθαρές (μη ρυπασμένες) θέσεις που θα συσχετίζουν τις αβιοτικές παραμέτρους ενδιαιτήματος με τις βιοτικές.
2. Μία μέθοδο εκτίμησης της καταλληλότητας ενδιαιτήματος βάσει της κατανομής των οργανισμών. Για τα ψάρια, συνήθως τα πιο άφθονα ενδιαιτήματα είναι και τα πιο κατάλληλα (Li et al., 2009; Muñoz-Mas et al., 2016). Για τα βενθικά μακροασπόνδυλα η

ανάλυση είναι λίγο διαφορετική (Waddle and Holmquist, 2011; Theodoropoulos et al., 2018) (βλέπε κεφ. 3).

3. Έναν αλγόριθμο ο οποίος θα εντοπίσει συσχετίσεις και τελικά θα προβλέψει την καταλληλότητα σε νέα ενδιαιτήματα βάσει του συνδυασμού των αβιοτικών παραμέτρων σε αυτά. Συνήθως, με τον όρο 'μοντέλο ενδιαιτήματος' περιγράφεται αυτό το τρίτο στάδιο στην όλη διαδικασία. Το πρώτο μοντέλο ενδιαιτήματος αναπτύχθηκε από τον Bovee (1986) για τα ψάρια. Έκτοτε, οι διάφορες μέθοδοι-αλγόριθμοι εξελίχθηκαν και πλέον περιλαμβάνουν μεθόδους (α) πολυπαραγοντικής στατιστικής ανάλυσης, (β) μηχανικής εκμάθησης και (γ) μεθόδους εκμάθησης ασαφούς λογικής.

Όλες οι μέθοδοι τελικά, ανεξάρτητα από τις εσωτερικές τους διαδικασίες, καταλήγουν σε κάποιου είδους συσχέτιση της καταλληλότητας του ενδιαιτήματος για κάθε αβιοτική μεταβλητή και βάσει αυτών των συσχετίσεων γίνονται οι προβλέψεις σε νέα ενδιαιτήματα άγνωστης καταλληλότητας. Η συνδυαστική χρήση των υδροδυναμικών μοντέλων και των μοντέλων καταλληλότητας ενδιαιτήματος προσφέρει τελικά τη δυνατότητα προσομοίωσης της ταχύτητας ροής και βάθους σε κάθε κόμβο του υπολογιστικού πλέγματος σε διάφορα σενάρια παροχών (υδροδυναμικό υπομοντέλο) και την εκτίμηση της καταλληλότητας σε κάθε κόμβο αλλά και της συνολικής καταλληλότητας της περιοχής για κάθε σενάριο παροχής βάσει των τιμών των V και D (υπομοντέλο ενδιαιτήματος). Προσφέρεται έτσι η δυνατότητα επιλογής της βέλτιστης παροχής ως η οικολογική παροχή που θα πρέπει να διατηρείται ώστε να διατηρείται η υγεία των υδρόβιων βιοκοινοτήτων κατάντη ανθρωπογενών παρεμβάσεων.

1.3. Βενθικά μακροασπόνδυλα

Τα βενθικά μακροασπόνδυλα αποτελούν οργανισμούς που διαβιούν στον βυθό των ποταμών και περιλαμβάνουν προνύμφες εντόμων που περνούν ένα στάδιο της ζωής τους υδρόβια, ενήλικα υδρόβια έντομα, σκώληκες, βδέλλες και σαλιγκάρια κ.α. Εδώ και αρκετές δεκαετίες, τα ΒΜ θεωρούνται αξιόπιστοι δείκτες της ποιότητας των επιφανειακών υδάτων (Rosenberg and Resh, 1993). Στην Ευρώπη χρησιμοποιούνται από το 2000 στα πλαίσια της Οδηγίας για τα Νερά 2000/60/ΕΕ (ΟΠΥ - European Union Council, 2000) μαζί με την ιχθυοπανίδα, τα υδρόβια μακρόφυτα και τα διάτομα. Υπάρχουν πλέον αρκετές έρευνες που δείχνουν ότι το μέγεθος της ανθρωπογενούς επίδρασης σε έναν ποταμό συσχετίζεται σημαντικά με συγκεκριμένες μετρικές-δείκτες βενθικών μακροασπονδύλων, οι οποίες αντανακλούν τελικά την κατάσταση της κοινότητας των ΒΜ (Stephenson and Morin, 2009; Theodoropoulos and Iliopoulou-Georgudaki, 2010; Kappes et al., 2011; Sundermann et al., 2013; Theodoropoulos et al., 2015a).

Τα ΒΜ κατηγοριοποιούνται σε διάφορες ομάδες ποικίλου επιπέδου ομοιότητας (τάξεις, οικογένειες, γένη, είδη κ.α.). Για τους σκοπούς της οικολογικής παρακολούθησης των υδάτων τα ΒΜ αναλύονται συνήθως ως το επίπεδο της οικογένειας. Η χρήση των ΒΜ ως δείκτες καταλληλότητας στα υδροδυναμικά μοντέλα ενδιαιτήματος δεν είναι ιδιαίτερα διαδεδομένη και οι σχετικές έρευνες έχουν επικεντρωθεί στην ιχθυοπανίδα (Milhous and Waddle, 2012). Τα μακροασπόνδυλα όμως είναι λιγότερο κινητικά σε σχέση με τα ψάρια, με μεγαλύτερη ευαισθησία σε απότομες αυξομειώσεις του όγκου του νερού και με μειωμένη ικανότητα εποίκησης περισσότερο δυσμενών ενδιαιτημάτων (Gore, 1989). Επομένως, τα ενδιαιτήματα που είναι κατάλληλα για τα ψάρια δεν είναι κατ' ανάγκη κατάλληλα και για τα μακροασπόνδυλα. Επιπλέον, μικρής τάξης ποταμοί των οποίων η ιχθυοπανίδα μπορεί να είναι ιδιαίτερα περιορισμένη ή και απούσα, φιλοξενούν πλούσια πανίδα βενθικών μακροασπονδύλων (Barbour et al., 1999). Ως εκ τούτου, ο συνδυασμός όλων των κρίκων του υδρόβιου οικοσυστήματος σε σχετικές εφαρμογές υδροδυναμικής προσομοίωσης καταλληλότητας ενδιαιτήματος είναι ένα απαραίτητο βήμα προς την ανάπτυξη αξιόπιστων, ολιστικών σεναρίων οικολογικής παροχής. Όπως έχει επισημανθεί, τα ΒΜ αποτελούν ιδανικούς δείκτες για την ανάπτυξη υδρο-οικολογικών μοντέλων (Niu and Dudgeon, 2011) και η χρήση τους σε μελέτες εκτίμησης οικολογικής παροχής αυξάνεται συνεχώς (Waddle and Holmquist, 2013; Komínková et al., 2017; Theodoropoulos et al., 2018b, 2018c).

Κεφάλαιο 2 | Απόκριση των βενθικών μακροασπονδύλων σε φυσικές και μη υδρολογικές διακυμάνσεις και αλλοιώσεις

Η χρήση των ΒΜ σε υδρο-οικολογικές αναλύσεις είναι σχετικά περιορισμένη και η έως τώρα βιβλιογραφία μελετά κυρίως την απόκρισή τους σε ακραία υδρολογικά φαινόμενα, όπως οι πλημμύρες (Herbst and Cooper, 2010; Mesa, 2010; Mundahl and Hunt, 2011) και οι ξηρασίες (Lake, 2011; Skoulikidis et al., 2011; Chessman, 2015) που οφείλονται είτε σε φυσικές υδρολογικές διακυμάνσεις στα πλαίσια του υδρολογικού κύκλου ή λιγότερο ή και περισσότερο σε ανθρωπογενή επίδραση. Η εκτίμηση της απόκρισης όμως των ΒΜ σε μετρίου μεγέθους υδρολογικές διαταραχές είναι λιγότερο μελετημένη, αλλά πολύ σημαντική για την ανάπτυξη σχετικών μεθόδων εκτίμησης της οικολογικής παροχής.

Στο συγκεκριμένο κεφάλαιο περιγράφεται μία περιπτωσιακή μελέτη εκτίμησης της απόκρισης των ΒΜ σε μία μετρίου μεγέθους φυσική υδρολογική διαταραχή (αύξηση παροχής κατά <50% από τη μέση φυσιολογική παροχή). Υδρολογικές και υδραυλικές παράμετροι καθώς και δεδομένα βενθικών μακροασπονδύλων συλλέχθηκαν σε τέσσερεις θέσεις δειγματοληψίας πριν και μετά τη διαταραχή και διερευνήθηκαν οι πιθανές διαφορές στη σύνθεση και κατανομή των βιοκοινοτήτων ΒΜ (αφθονία, ποικιλότητα, αριθμός taxa). Επιπλέον μελετήθηκαν οι υδρο-οικολογικές σχέσεις μεταξύ της ταχύτητας ροής, του βάθους και του υποστρώματος και συγκεκριμένων μετρικών βενθικών μακροασπονδύλων με στόχο την εύρεση των βέλτιστων τιμών για κάθε υδραυλική παράμετρο.

2.1. Περιοχή μελέτης και μεθοδολογία

Υδρολογικά και οικολογικά δεδομένα συλλέχθηκαν σε τέσσερεις μη ρυπασμένες θέσεις δειγματοληψίας. Σε κάθε θέση, επιλέχθηκαν 20 σημεία εντός του ποταμού όπου καταγράφηκαν η ταχύτητα ροής, το βάθος ροής και το υπόστρωμα, ενώ παράλληλα συλλέχθηκαν και βενθικά μακροασπόνδυλα, πριν (Αύγουστος 2015) και μετά (Οκτώβριος 2015) την υδρολογική διαταραχή. Συνολικά συλλέχθηκαν 142 δείγματα-μικροενδιαιτήματα. Τα δείγματα ΒΜ αναγνωρίστηκαν μέχρι το επίπεδο της οικογένειας και υπολογίστηκαν σχετικοί δείκτες της κατάστασης της κοινότητας των ΒΜ, ήτοι η σχετική αφθονία διαφόρων τροφικών ομάδων (FFG), η αφθονία των ΒΜ, ο αριθμός των taxa, η ποικιλότητα (δείκτης Shannon) και ο αριθμός taxa Εφημερόπτερων, Πλεκόπτερων και Τριχόπτερων (EPT). Τα δείγματα ομαδοποιήθηκαν με τη χρήση της τεχνικής της Μη-Μετρικής Πολυδιάστατης Ομαδοποίησης (NMDS - Bray-Curtis distance measure). Οι τιμές των μετρικών των ΒΜ μετασχηματίστηκαν με τη χρήση της τετραγωνικής ρίζας ώστε να παρουσιάζουν κανονική κατανομή. Τα δεδομένα ελέγχθηκαν για ομοιογένεια διασποράς με τη χρήση του Levene's test (Levene, 1960) και χρησιμοποιήθηκαν t-test ανεξάρτητων δειγμάτων για να ελεγχθούν πιθανές διαφορές στις βιοκοινότητες των ΒΜ πριν και μετά τη διαταραχή. Επιπλέον, χρησιμοποιήθηκε η τεχνική Boosted Regression Trees στη γλώσσα R (Elith et al., 2008) ώστε να βρεθούν συσχετίσεις μεταξύ των αβιοτικών και βιοτικών παραμέτρων και να εντοπιστούν οι βέλτιστες τιμές των βιοτικών μετρικών ανά υδρολογική-υδραυλική παράμετρο.

2.2. Αποτελέσματα - Συζήτηση

Από τα 142 μικροενδιαιτήματα συλλέχθηκαν συνολικά 6905 άτομα ΒΜ που ανήκαν σε 135 οικογένειες. Η κατανομή των μικροενδιαιτημάτων στον τρισδιάστατο χώρο του NMDS έδειξε σαφή διαχωρισμό μεταξύ των δειγμάτων πριν και μετά τη διαταραχή, φανερώνοντας θεμελιώδεις διαφορές στη σύνθεση των βιοκοινοτήτων τους. Κατά μέσο όρο, η αφθονία των ΒΜ υποδεκαπλασιάστηκε μετά τη διαταραχή, ο αριθμός των taxa μειώθηκε κατά 2,5 φορές, ο αριθμός των EPT υποδιπλασιάστηκε και η ποικιλότητα (Shannon) μειώθηκε κατά 1,6 φορές. Όλες οι διαφορές ήταν στατιστικά σημαντικές ($p<0.05$). Σημαντικές διαφορές επίσης

παρατηρήθηκαν στη σχετική αφθονία των FFG. Σε ότι αφορά στους διαφορετικούς τύπους υποστρώματος, όλες οι ανωτέρω μετρικές μειώθηκαν σε όλους τους τύπους. Μετά τη διαταραχή, λεπτόκοκκα υποστρώματα (μέτριας και μικρής διαμέτρου χαλίκια και άμμος) δεν παρατηρήθηκαν. Επιπλέον, πριν τη διαταραχή υψηλότερη αφθονία καταγράφηκε στην άμμο και σε μεγάλης διαμέτρου χαλίκια ενώ μετά τη διαταραχή η μεγαλύτερη αφθονία καταγράφηκε σε μεγάλες πέτρες και βράχους.

Σύμφωνα με την BRT ανάλυση, η υδρολογική διαταραχή είχε τη μεγαλύτερη επίδραση στις βιοκοινότητες ΒΜ. Όλες οι μετρικές ήταν μειωμένες στα λεπτόκοκκα υποστρώματα, σε ταχύτητες ροής μεγαλύτερες των 0,7 m/s και σε βάθη μεγαλύτερα των 0,3 m. Η αφθονία ήταν μεγαλύτερη σε βράχους, μεγάλες πέτρες και μεγάλα χαλίκια και σε βάθη μέχρι 0,2 m. Ο αριθμός των taxa ήταν βέλτιστος σε βράχους, μεγάλες πέτρες και μεγάλα χαλίκια, σε ταχύτητες μεταξύ περίπου 0,25 και 0,65 m/s και σε βάθη μέχρι 0,2 m. Ο αριθμός των EPT ήταν μεγαλύτερος σε βράχους, μεγάλες πέτρες και μεγάλα χαλίκια και σε ταχύτητες ροής μεταξύ 0,25 m/s και 0,6 m/s. Οι ποικιλότητα ήταν μεγαλύτερη σε βράχους, μεγάλες πέτρες, μεγάλα και μικρά χαλίκια και σε βάθη μέχρι 0,2 m.

Η αφθονία των ΒΜ, ο αριθμός taxa, ο αριθμός των EPT taxa και η ποικιλότητα μειώθηκαν σημαντικά κατά 90%, 60%, 50% και 25% αντιστοίχως μεταξύ των δειγμάτων πριν και μετά τη διαταραχή, αποτελέσματα που επί το πλείστον συμφωνούν και με προηγούμενες μελέτες. Μείωση κατά 90% και 60% της αφθονίας των μακροασπονδύλων και του αριθμού των taxa αντίστοιχα, έχει προηγουμένως αναφερθεί από τους Argerich et al. (2004) ως αποτέλεσμα μιας εξαιρετικά μεγάλης πλημμύρας. Ο Mesa το 2010 παρατήρησε επίσης μείωση κατά 70% στην αφθονία των μακροασπονδύλων, αλλά όχι στατιστικά σημαντικές διαφορές στον αριθμό των taxa και την ποικιλότητα. Τέτοιες διαφορές όμως προέκυψαν από τα αποτελέσματα της παρούσας μελέτης και υποστηρίζονται από τα αποτελέσματα των Rosser και Pearson (1995) καθώς και των Jacobsen και Encalada (1998). Αντίθετα, οι Melo et al. (2003) έδειξαν μόνο 15% μείωση της αφθονίας των μακροασπονδύλων. Παρά την ποικιλία των αποτελεσμάτων-παρατηρήσεων που εν μέρει οφείλεται στην ποικιλία των κλιματολογικών χαρακτηριστικών κάθε περιοχής μελέτης και στις εφαρμοζόμενες μεθόδους, οι περισσότερες μελέτες καταλήγουν στο συμπέρασμα ότι η αφθονία των ΒΜ, η ποικιλότητα και συχνά ο αριθμός των taxa και ο αριθμός των EPT taxa μειώνονται λόγω των πλημμυρών και των ακραίων βροχοπτώσεων (Poff and Zimmerman, 2010). Η συγκεκριμένη περιπτωσιακή μελέτη έδειξε επιπλέον ότι ακόμη και μετά από μέτριας έντασης υδρολογικές διαταραχές οι κοινότητες των ΒΜ επηρεάζονται σημαντικά.

Παρά την συνολική οικολογική υποβάθμιση, τα αποτελέσματα της μελέτης, σε συμφωνία με προηγούμενες σχετικές έρευνες (Lancaster και Hildrew, 1993, Rempel et al., 1999, Fuller et al., 2010), έδειξαν ότι συγκεκριμένοι τύποι υποστρώματος παρέχουν καταφύγιο κατά τη διάρκεια υδρολογικών διαταραχών, προφυλάσσοντας τα ΒΜ από το να παρασυρθούν εξαιτίας της έντονης ροής. Από τη συγκεκριμένη έρευνα, αυτοί οι τύποι υποστρώματος ήταν κυρίως ογκόλιθοι-βράχοι και μεγάλες πέτρες, που φιλοξένησαν το 73% της συνολικής αφθονίας των ΒΜ και υψηλότερο αριθμό taxa, σε σύγκριση με τα λεπτόκοκκα υποστρώματα, μετά τη διαταραχή. Όπως αναφέρθηκε από τον Borchardt (1993) και υποδεικνύεται και στην τρέχουσα έρευνα, τα ΒΜ είτε μετακινούνται ενεργά σε αυτά τα καταφύγια, είτε προστατεύονται τυχαία, ευρισκόμενα εκεί όταν η ροή και οι υδραυλικές συνθήκες γίνονται κρίσιμες (προκαλώντας παράσυρση-μετατόπιση). Αυτό φάνηκε από το γεγονός ότι πριν από τη διαταραχή, τα ΒΜ ήταν σχεδόν ομοιόμορφα κατανεμημένα μεταξύ των διαφόρων μικροενδιαιτημάτων, ενώ μετά τη διαταραχή βρέθηκαν συγκεντρωμένα στα χονδρόκοκκα υποστρώματα (στους ενδιάμεσους χώρους ή κάτω από τους ογκόλιθους και τις μεγάλες πέτρες).

Σε ότι αφορά στις υδρο-οικολογικές σχέσεις (μεταξύ V, D, S και K), με ελάχιστες εξαιρέσεις για ορισμένα taxa (Jowett et al., 1991), ταχύτητες ροής μεγαλύτερες από 0,7 m/s δεν θεωρούνται κατάλληλες για τα περισσότερα ΒΜ (Gore et al., 2001; Li et al., 2009; Horta et al. , 2009; Shearer et al., 2015), ενώ η βέλτιστη περιοχή συνήθως κυμαίνεται μεταξύ 0,1 m/s

και 0,6 m /s. Ωστόσο, ορισμένα taxa παρουσιάζουν βέλτιστη καταλληλότητα σε υψηλότερες ή χαμηλότερες ταχύτητες ροής. Αναφορικά με το βάθος του νερού, η καταλληλότητα συνήθως κυμαίνεται στα 0.25 m (Jowett et al., 1991; Gore et al., 2001; Li et al., 2009) σύμφωνα με τα αποτελέσματά μας, ενώ κυμαίνεται μεταξύ 0,1 m και 1 m. Όσον αφορά στον τύπο του υποστρώματος, οι μεγάλες και μικρές πέτρες (6 cm - 25 cm) θεωρούνται γενικά πιο κατάλληλες αλλά με μεγάλες διαφορές στις μελέτες. Τα αποτελέσματά της έρευνας υποδεικνύουν επίσης ότι πιο χονδρόκοκκα υποστρώματα είναι πιο κατάλληλα, με υψηλότερη αφθονία και αριθμό taxa σε μεγάλες πέτρες, ογκόλιθους, μικρές πέτρες και μεγάλα χαλίκια.

2.3. Συμπεράσματα

Η μελέτη αυτή κατέληξε στο συμπέρασμα ότι η δομή των βιοκοινοτήτων των ΒΜ επηρεάζεται σημαντικά ακόμη και μετά από μια μέτριας έντασης υδρολογική διαταραχή. Παρότι η μελέτη αφορούσε σε φυσική διαταραχή, τα αποτελέσματα μπορούν να εξηγήσουν ένα μεγάλο μέρος της παρατηρούμενης υποβάθμισης των κοινοτήτων των ΒΜ κατάντη υδροηλεκτρικών φραγμάτων και ταμιευτήρων (Allan and Castillo, 2007; Theodoropoulos et al., 2015b). Οι ανωτέρω έρευνες έδειξαν υποβαθμισμένη οικολογική ποιότητα που οφείλεται, μεταξύ άλλων, στις συνεχείς και ακανόνιστες διακυμάνσεις της στάθμης των υδάτων (Hartmann and Mihuc, 2008), οι οποίες εμποδίζουν την εγκατάσταση υγιών πληθυσμών ΒΜ. Καθώς η Ευρωπαϊκή Ένωση προτρέπει για την εκτίμηση οικολογικών παροχών κατάντη φραγμάτων για την αποκατάσταση της ακεραιότητας των υδρόβιων οικοσυστημάτων (WFD CIS Guidance Document No. 31, 2015), τα δεδομένα αναφοράς που συλλέχθηκαν στην παρούσα μελέτη επέτρεψαν την ανάπτυξη προκαταρκτικών υδρο-οικολογικών σχέσεων (προτιμήσεων ενδιαιτήματος) με απώτερο στόχο την ανάπτυξη αξιόπιστων σεναρίων οικολογικής παροχής. Η ενσωμάτωση αυτών των προτιμήσεων στα υδροδυναμικά μοντέλα καταλληλότητας ενδιαιτήματος (Theodoropoulos et al., 2015a) έχει ιδιαίτερη σημασία για τους διαχειριστές των υδατικών πόρων ώστε να μπορούν να επιλέξουν το βέλτιστο μεταξύ διαφόρων σεναρίων παροχής.

Κεφάλαιο 3 | Προγραμματισμός-ανάπτυξη λογισμικού υλοποίησης αλγόριθμων ασαφούς λογικής για τη χρήση τους ως μοντέλα καταλληλότητας ενδιαιτήματος: Το λογισμικό HABFUZZ

Κατά τις τελευταίες δύο δεκαετίες, η εφαρμογή δισδιάστατων υδροδυναμικών μοντέλων άρχισε να γίνεται ολοένα και μεγαλύτερη έναντι των αντίστοιχων μονοδιάστατων μοντέλων. Ωστόσο, οι περισσότερες σχετικές 2D περιπτωσιακές μελέτες επικεντρώνονται στη χρήση των ψαριών ως δείκτη καταλληλότητας ενδιαιτήματος (Muñoz-Mas et al., 2016, Papadaki et al., 2017). Εφαρμογές που χρησιμοποιούν άλλα βιοτικά στοιχεία του υδάτινου οικοσυστήματος ως δείκτες οικολογικής παροχής είναι δυσανάλογα λιγότερες. Αναφορικά με τη χρήση των ΒΜ σε υδροδυναμικά μοντέλα καταλληλότητας ενδιαιτήματος (HHMs), αυτή είναι επίσης περιορισμένη, κυρίως λόγω των κατωτέρω:

1. Τα υπάρχοντα λογισμικά HHM έχουν αναπτυχθεί με επίκεντρο τα ψάρια (το πρόγραμμα CASiMiR Benthos είναι η μοναδική επιλογή εστιασμένη στα ΒΜ σήμερα).
2. Τα υπάρχοντα λογισμικά συνδυάζουν ένα μονοδιάστατο υδραυλικό υπομοντέλο και ένα υπομοντέλο ενδιαιτήματος βασισμένο στις καμπύλες καταλληλότητας ενδιαιτήματος (HSCs) (PHABSIM - Milhous et al., 1989, CASiMiR Fish - Schneider at al., 2001), με τα λογισμικά River 2D και CASiMiR 2D να είναι οι μόνες διαθέσιμες 2D επιλογές.

3. Προηγμένοι αλγόριθμοι προσομοίωσης της καταλληλότητας ενδιαιτήματος (μηχανική εκμάθηση, ασαφής λογική, Μπεϋζιανή ανάλυση), οι οποίοι έχουν αποδειχθεί περισσότερο ακριβείς από τις HSCs, ειδικά για βιοτικά στοιχεία εκτός των ψαριών, δεν εφαρμόζονται επί του παρόντος (πάλι, μόνο το River2D μια επιλογή για την ασαφή λογική).

Συνδυαστικά λογισμικά (2D υδροδυναμικό υπομοντέλο + υπομοντέλο ενδιαιτήματος βασισμένο σε προηγμένους αλγόριθμους πρόβλεψης) εστιασμένα στα μακροασπόνδυλα δεν υπάρχουν. Συνεπώς, οι τρέχουσες εκτιμήσεις οικολογικής παροχής που βασίζονται σε HHM, χρησιμοποιούν ίσως άλλα βιοτικά στοιχεία ως δείκτες οικολογικής παροχής αλλά εφαρμόζουν εργαλεία-λογισμικά προσομοίωσης καταλληλότητας ενδιαιτήματος που έχουν αναπτυχθεί για την ιχθυοπανίδα.

Στο συγκεκριμένο κεφάλαιο περιγράφεται το λογισμικό HABFUZZ. Πρόκειται για ένα εργαλείο που έρχεται να καλύψει το ανωτέρω ερευνητικό κενό εφαρμόζοντας αλγορίθμους ασαφούς λογικής και Μπεϋζιανής ανάλυσης για την πρόβλεψη-προσομοίωση της καταλληλότητας ενδιαιτήματος σε κάθε κόμβο ενός υπολογιστικού πλέγματος που έχει δημιουργηθεί σε προηγούμενη 2D υδροδυναμική προσομοίωση ποταμού. Είναι ένα υπομοντέλο ενδιαιτήματος που αναπτύχθηκε στη γλώσσα προγραμματισμού FORTRAN ώστε να συνδυάζεται εύκολα με το υδροδυναμικό υπομοντέλο TELEMAC 2D (αλλά μπορεί να χρησιμοποιηθεί και με άλλα 2D υδροδυναμικά μοντέλα) για την ανάπτυξη σεναρίων οικολογικής παροχής με τη χρήση αλγόριθμων ασαφούς λογικής. Το HABFUZZ χρησιμοποιεί την 'έξοδο' (αποτέλεσμα) του TELEMAC 2D (προσομοιωμένες τιμές V, D και S σε κάθε κόμβο του υπολογιστικού πλέγματος σε διάφορα σενάρια παροχής) και υπολογίζει την καταλληλότητα ενδιαιτήματος σε κάθε κόμβο (δηλαδή για κάθε συνδυασμό V, D και S) με βάση ένα σύνολο δεδομένων αναφοράς BM που συλλέχθηκαν από ελληνικά ποτάμια. Η 'έξοδος' του HABFUZZ είναι ένα αρχείο txt με τις τιμές καταλληλότητας ενδιαιτήματος για κάθε συνδυασμό μικροενδιαιτήματος.

Το HABFUZZ λειτουργεί σε περιβάλλον γραμμής εντολών. Πριν την εκκίνηση της εφαρμογής, ο χρήστης θα πρέπει να τροφοδοτήσει το λογισμικό με δύο αρχεία txt, (i) ένα αρχείο με τα δεδομένα εκπαίδευσης-εκμάθησης του μοντέλου (training dataset), δηλαδή ένα σύνολο δειγμάτων-παρατηρήσεων μικροενδιαιτήματος γνωστής καταλληλότητας (V, D, S, T και K) και (ii) ένα αρχείο με τα δεδομένα πρόβλεψης-ζητούμενα, δηλαδή ένα σύνολο δειγμάτων άγνωστης K την οποία το HABFUZZ καλείται να προβλέψει βάσει του αρχείου δεδομένων εκμάθησης. Κατά τη διάρκεια της εκτέλεσης του HABFUZZ, το πρόγραμμα ζητάει από τον χρήση να επιλέξει:

1. Τη μέθοδο προσομοίωσης - είτε τη χρήση των κλασικών αλγόριθμων ασαφούς λογικής (FL) είτε τη χρήση Μπεϋζιανής θεωρίας πιθανοτήτων ασαφούς λογικής (FRB)
2. Τον τρόπο σταυρωτής επαλήθευσης-επικύρωσης (cross-validation scheme) - είτε Monte Carlo cross validation είτε ten-fold cross validation
3. Σε περίπτωση επιλογής του FL αλγόριθμου και μόνο, το HABFUZZ ζητά επιπλέον από τον χρήστη να επιλέξει μεταξύ τριών σεναρίων κατάταξης της καταλληλότητας ενδιαιτήματος όταν δύο ίδιο συνδυασμοί V, D, S, T έχουν διαφορετική καταλληλότητα - είτε average scenario, όπου επιλέγεται η μέση καταλληλότητα, είτε optimum scenario όπου επιλέγεται η μέγιστη παρατηρούμενη καταλληλότητα για τον συγκεκριμένο συνδυασμό, είτε worst scenario όπου επιλέγεται η ελάχιστη καταλληλότητα.
4. Επίσης σε περίπτωση επιλογής του FL αλγόριθμου και μόνο, ο χρήστης καλείται να επιλέξει και τη μέθοδο αποσαφήνισης (defuzzification), μία εκ των (i) centroid, (ii) maximum membership, (iii) mean of maximum και (iv) σταθμισμένος μέσος όρος

Μετά από τα παραπάνω, το HABFUZZ υλοποιεί τον επιλεγμένο αλγόριθμο, ενημερώνοντας τον χρήστη για τα βήματα τα οποία υλοποιεί και επίσης ενημερώνοντάς τον όταν η διαδικασία έχει ολοκληρωθεί. Η 'έξοδος' του προγράμματος όπως προαναφέρθηκε είναι ένα αρχείο txt με τις τιμές K για κάθε συνδυασμό V, D, S και T (μικροενδιαίτημα) του αρχείου με τα δεδομένα

πρόβλεψης. Επιπλέον, το πρόγραμμα δημιουργεί και ένα log αρχείο txt με διάφορες παραμέτρους κατά τη διάρκεια της εκτέλεσης. Τέλος, επί της οθόνης γραμμής εντολών εξάγονται διάφοροι δείκτες καταλληλότητας ενδιαιτήματος καθώς και το αποτέλεσμα της σταυρωτής επικύρωσης ως ποσοστό σωστών προβλέψεων επί του συνόλου των μικροενδιαιτημάτων πρόβλεψης στο αρχείο εκμάθησης-εκπαίδευσης.

Κεφάλαιο 4 | Συγκριτική αξιολόγηση αλγόριθμων πρόβλεψης της καταλληλότητας ενδιαιτήματος με στόχο τη χρήση τους για την ανάπτυξη σεναρίων οικολογικής παροχής

Στο κεφάλαιο αυτό περιγράφονται τα αποτελέσματα σύγκρισης διαφόρων αλγόριθμων πρόβλεψης της καταλληλότητας ενδιαιτήματος ΒΜ βάσει ενός συνόλου 380 μικροενδιαιτημάτων -δεδομένων αναφοράς- που συλλέχθηκαν κατά το έτος 2015 σε εννέα θέσεις δειγματοληψίας σε ελληνικά ποτάμια απαλλαγμένα από ρύπανση και ανθρωπογενείς δραστηριότητες (Εύηνος -1-, Μόρνος -1-, Αχελώος -3-, Λάδων -1-, Κράθυς -1-, Παραπείρος -2-). Το ερώτημα στο οποίο η έρευνα αυτή καλείται να δώσει απάντηση είναι το εξής: Μήπως λόγω των δεδομένων ιδιοτήτων του συγκεκριμένου, αλλά και άλλων παρόμοιων υδρο-οικολογικών σετ δεδομένων, δηλαδή (i) πολύπλοκες αλληλεπιδράσεις μεταξύ των ανεξάρτητων μεταβλητών που καθορίζουν το μικροενδιαίτημα (V, D, S, T), (ii) εκτεταμένη διακύμανση των τιμών της εξαρτημένης μεταβλητής (K), απαιτείται η εφαρμογή συγκεκριμένων μεθόδων πρόβλεψης-προσομοίωσης για να αποφευχθεί η εξαγωγή εσφαλμένων αποτελεσμάτων και να ενισχυθεί η ακρίβεια πρόβλεψης των HHMs; Επιπλέον, προτείνονται λύσεις για την εργασία με πολυμεταβλητά υδρο-οικολογικά δεδομένα ώστε αυτά να μπορούν να χρησιμοποιηθούν στην εκτίμηση οικολογικής παροχής με τη χρήση υδροδυναμικών μοντέλων καταλληλότητας ενδιαιτήματος.

4.1. Συλλογή δεδομένων αναφοράς

Δείγματα-μικροενδιαιτήματα που συνδέουν τη βιοκοινότητα των ΒΜ με παραμέτρους ενδιαιτήματος συλλέχθηκαν από εννέα θέσεις δειγματοληψίας σε ποτάμια της κεντρικής και νότιας ηπειρωτικής Ελλάδας χωρίς ρύπανση και με καθόλου ή με ελάχιστες ανθρωπογενείς παρεμβάσεις. Σε κάθε θέση συλλέχθηκαν 20 δείγματα βενθικών μακροασπονδύλων ώστε να καλυφθούν όλα τα διαθέσιμα μικροενδιαιτήματα και στο σημείο του κάθε δείγματος-μικροενδιαιτήματος καταγράφονταν οι τιμές V, D, S και T. Τα δείγματα των ΒΜ (20 δείγματα x 9 θέσεις δειγματοληψίας x 3 εποχές) διατηρήθηκαν σε ξεχωριστά δοχεία και αναλύθηκαν στο επίπεδο της οικογένειας. Συνολικά, λαμβάνοντας υπόψη και τις καιρικές συνθήκες, συλλέχθηκαν 380 δείγματα τα οποία αποτέλεσαν και το σετ δεδομένων της συγκεκριμένης έρευνας.

4.2. Επεξεργασία δεδομένων

Μετά την ανάλυση των δειγμάτων ΒΜ υπολογίστηκαν, πέραν της αφθονίας της κάθε οικογένειας, συγκεκριμένοι δείκτες-μετρικές: (i) αριθμός οικογενειών-taxa, (ii) ποικιλότητα (δείκτης Shannon), (iii) αριθμός των Εφημερόπτερων, Πλεκόπτερων και Τριχόπτερων taxa (EPT taxa). Στη συνέχεια, βάσει των ανωτέρω μετρικών, υπολογίστηκε η καταλληλότητα (K) κάθε δείγματος-μικροενδιαιτήματος σε κλίμακα από 0 (ακατάλληλο) ως 1 (κατάλληλο). Έχοντας ως αφετηρία τελικά το σετ των 380 δεδομένων αναφοράς όπου πλέον συσχετίζονται οι μεταβλητές του ενδιαιτήματος V, D, S και T με την K πραγματοποιήθηκε σύγκριση της ικανότητας πρόβλεψης (ακρίβειας) των παρακάτω αλγόριθμων: (i) Καμπύλες Καταλληλότητας Ενδιαιτή-

ματος (HSC - Bovee, 1986), (ii) Boosted Regression Trees (BRT - Elith et al., 2008), (iii) Random Forests (RF - Breiman, 2001) με χρήση της γλώσσας προγραμματισμού R v3.1.0. (R Core Team, 2014), (iv) Ασαφής Λογική (Fuzzy Logic (FL), μέθοδος των Mamdani-Assilian με χρήση διαφόρων τεχνικών αποσαφήνισης (Zadeh, 1965; Mamdani and Assilian, 1975; Ross, 2010) και (v) Μπεϋζιανή Πιθανολογική Ανάλυση Ασαφούς Λογικής (FRB) σύμφωνα με τους Brookes et al. (2010), με χρήση του λογισμικού HABFUZZ (Theodoropoulos et al., 2016). Για την αξιολόγηση της ακρίβειας πρόβλεψης του κάθε αλγόριθμου χρησιμοποιήθηκε η μέθοδος της δεκάκις επαναλαμβανόμενης σταυρωτής επικύρωσης (Kohavi, 1995). Το αρχικό σύνολο των 380 δειγμάτων χωρίστηκε τυχαία σε δέκα ισομεγέθη υποσύνολα. Εννέα υποσύνολα (342 δείγματα) χρησιμοποιούνταν κάθε φορά ως δεδομένα εκμάθησης-εκπαίδευσης των μοντέλων και ένα υποσύνολο (38 δείγματα) χρησιμοποιούταν για την επαλήθευση-επικύρωση του μοντέλου. Αυτή η διαδικασία επαναλήφθηκε δέκα φορές, χρησιμοποιώντας ένα διαφορετικό υποσύνολο για επικύρωση σε κάθε επανάληψη. Η απόδοση του κάθε μοντέλου (ακρίβεια πρόβλεψης) αξιολογήθηκε τελικά ως το μέσο ποσοστό των σωστά ταξινομημένων δειγμάτων (CCI) κάθε επανάληψης της ανωτέρω διαδικασίας επί (i) πενταβάθμιας και (ii) τριβάθμιας κλίμακας καταλληλότητας, ήτοι επί της ικανότητας του κάθε αλγόριθμου να προβλέψει σωστά μία από τις 1:Κακή, 2:Ελλιπής, 3:Μέτρια, 4:Καλή, 5:Υψηλή (πενταβάθμια) και 1:Χαμηλή, 2:Μέτρια, 3:Αποδεκτή (τριβάθμια).

4.3. Αποτελέσματα και συζήτηση

Από τη σύγκριση των αλγόριθμων προέκυψαν τα παρακάτω: Κανένας αλγόριθμος δεν μπόρεσε να προβλέψει με ικανοποιητική ακρίβεια την καταλληλότητα ενδιαιτήματος επί πενταβάθμιας κλίμακας. Η μέση απόδοση κυμάνθηκε από 29,63% μέχρι 38,66% η οποία θεωρείται πολύ χαμηλή για να δώσει αξιόπιστα αποτελέσματα. Επί τριβάθμιας κλίμακας, η μέση απόδοση κυμάνθηκε από 49,74% μέχρι 67,92%, γεγονός που επιτρέπει τη χρήση των αλγόριθμων επί τριβάθμιας κλίμακας Κ για σχετικά αξιόπιστες προβλέψεις της καταλληλότητας ενδιαιτήματος. Από τους αλγόριθμους που εξετάστηκαν, τη μεγαλύτερη ακρίβεια πρόβλεψης είχε το μοντέλο BRT (67,92%) , ακολουθούμενο από τα RF (61,85%) και HSC (61,38%). Και οι τρεις όμως αλγόριθμοι, λόγω μη ομοιόμορφης αντιπροσώπευσης της χαμηλότερης κλάσης καταλληλότητας στο σετ δεδομένων (κλάση 1:Χαμηλή) δεν μπόρεσαν να προβλέψουν με ικανοποιητική ακρίβεια την καταλληλότητα για τη συγκεκριμένη κλάση (απόδοση <10% και για τους τρεις αλγόριθμους), σε αντίθεση με τον FRB αλγόριθμο ο οποίος εμφάνισε μέση απόδοση 61,2%. Σχετική μετατροπή του αλγόριθμου RF ώστε να βελτιωθεί η ικανότητα πρόβλεψης της χαμηλής Κ κλάσης αύξησε την απόδοση στο 20% αλλά η συνολική απόδοση πρόβλεψης μειώθηκε στο 55%.

Αναφορικά με την ακρίβεια πρόβλεψης της καταλληλότητας ενδιαιτήματος, προηγούμενες έρευνες αναφέρουν ποικίλα αποτελέσματα, κυρίως λόγω και των διαφορετικών μεθοδολογικών προσεγγίσεων που εφαρμόζονται αλλά και λόγω της χρήσης διαφορετικών σετ δεδομένων αναφοράς. Πενταβάθμια κλίμακα πρόβλεψης της καταλληλότητας σπάνια έχει χρησιμοποιηθεί στον παρελθόν. Όπως αναφέρεται εν μέρει από τους Lange et al. (2015) και επιβεβαιώνεται και από τα αποτελέσματα της συγκεκριμένης έρευνας, η εφαρμογή πενταβάθμιας κλίμακας πρόβλεψης της καταλληλότητας (σύμφωνα για παράδειγμα με την ταξινόμηση της WFD) είναι απαγορευτική λόγω της χαμηλής ακρίβειας πρόβλεψης των μοντέλων. Επιπλέον, υπάρχοντα μοντέλα καταλληλότητας ενδιαιτήματος συσχετίζουν την καταλληλότητα απευθείας με την αφθονία συγκεκριμένων taxa (είτε ψαριών είτε ΒΜ) ή βασίζονται σε δεδομένα παρουσίας-απουσίας. Σε αυτό το πλαίσιο, μοντέλα Ασαφούς Λογικής με χρήση της αφθονίας ΒΜ ως καταλληλότητας (van Broekhoven et al., 2006, Mouton et al., 2009) έδειξαν απόδοση μεταξύ 50% και 66%. Μοντέλα Ασαφούς Λογικής με χρήση δεδομένων παρουσίας-απουσίας ψαριών (Muñoz-Mas et al., 2016) υπολόγισαν απόδοση μεταξύ 45% και 48%. Επιπλέον, οι προηγούμενες εφαρμογές μοντέλων RF με χρήση ψαριών (Mouton et al.,

2011; Vezza et al., 2015) επιβεβαιώνουν την αυξημένη ακρίβεια της συγκεκριμένης μεθόδου, υπολογίζοντας απόδοση >70%.

Εν κατακλείδι, τα αποτελέσματα έδειξαν ότι αλγόριθμοι μηχανικής εκμάθησης (RF και BRT) μπορούν να χρησιμοποιηθούν με σχετική ασφάλεια για την πρόβλεψη της καταλληλότητας ενδιαιτήματος ΒΜ επί δεδομένων αναφοράς (σετ εκμάθησης) στα οποία οι κλάσεις καταλληλότητας έχουν ομοιόμορφη αντιπροσώπευση. Σε περιπτώσεις όμως ανομοιομορφίας των δεδομένων αναφοράς, αλγόριθμοι Ασαφούς Λογικής και περισσότερο ο FRB θα πρέπει να προτιμώνται καθώς φαίνεται πως δεν επηρεάζονται και εμφανίζουν σταθερά υψηλή ικανότητα πρόβλεψης.

Κεφάλαιο 5 | Περιπτωσιακή μελέτη 1: Εκτίμηση οικολογικής παροχής με τη χρήση υδροδυναμικών μοντέλων καταλληλότητας ενδιαιτήματος βενθικών μακροασπονδύλων κατάντη του φράγματος του ποταμού Παραπείρου (Αχαΐα, Δυτική Ελλάδα)

Σε παγκόσμιο επίπεδο, είναι γενικώς αποδεκτό ότι τα υδροδυναμικά μοντέλα καταλληλότητας ενδιαιτήματος αποτελούν αξιόπιστα εργαλεία εκτίμησης της οικολογικής παροχής. Στην Ευρώπη για παράδειγμα, πρόσφατα (Κατευθυντήριο Κείμενο -ΚΚ- ΟΠΥ No. 34, 2015) έχει προταθεί μια ιεραρχία τριών κατηγοριών μεθοδολογιών εκτίμησης της οικολογικής παροχής, με τα HHMs να βρίσκονται στο 'επίπεδο 3', θεωρούμενα ως εφαρμόσιμα σε καταστάσεις όπου απαιτείται υψηλός βαθμός βεβαιότητας πρόβλεψης ώστε να παρέχονται στους διαχειριστές των υδάτων κατάλληλες συστάσεις σχετικά με την οικολογική παροχή. Όμως, το χαμηλό ποσοστό (18%) των περιπτωσιακών μελετών που χρησιμοποιούν HHMs στο σχετικό ΚΚ είναι ενδεικτικό του ‘χάσματος’ της θεωρητικής έρευνας και της πρακτικής εφαρμογής των HHMs. Ιδιαίτερα στην Ελλάδα, τα HHMs έχουν ενσωματωθεί πρόσφατα στις εκτιμήσεις οικολογικής παροχής και επί του παρόντος επικεντρώνονται αποκλειστικά στα ψάρια (Muñoz-Mas et al., 2016, Papadaki et al., 2017), ενώ το νομικό πλαίσιο για τις οικολογικές παροχές εξακολουθεί να βασίζεται μόνο σε υδρολογικά κριτήρια (Υπουργείο Περιβάλλοντος, Ενέργειας και Κλιματικής Αλλαγής, 2011). Οι λόγοι για αυτή την περιορισμένη εφαρμογή των HHMs σχετίζονται κυρίως με το κόστος, το χρόνο εφαρμογής, την απαιτούμενη τεχνογνωσία-εμπειρία και τη διαθεσιμότητα υδρο-οικολογικών δεδομένων (Jorgensen and Bendoricchio, 2001, Conallin et al., 2010). Η εκτίμηση της οικολογικής παροχής με τη χρήση HHMs απαιτεί αναπόφευκτα μια δαπανηρή και χρονοβόρα συλλογή υδραυλικών και υδρομετρικών στοιχείων για τη βαθμονόμηση και επικύρωση των σχετικών μοντέλων (Spense and Hickley, 2000) και συνήθως απαιτούνται επιπρόσθετες, προσεκτικά σχεδιασμένες επιτόπιες επισκέψεις για τον υπολογισμό των προτιμήσεων ενδιαιτήματος των υδρόβιων οργανισμών (Heggenes et al., 1990).

Στο κεφάλαιο αυτό περιγράφεται η εφαρμογή ενός δισδιάστατου υδροδυναμικού μοντέλου καταλληλότητας ενδιαιτήματος για την ανάπτυξη σεναρίων οικολογικής παροχής βασισμένων στις προτιμήσεις των ΒΜ στον ποταμό Παραπείρο (Αχαΐα, Δυτική Ελλάδα). Τα ΒΜ χρησιμοποιήθηκαν ως δείκτες και με βάση τα συμπεράσματα του προηγούμενου κεφαλαίου εφαρμόστηκε ο FRB αλγόριθμος για την ακριβή εκτίμηση των προτιμήσεών ενδιαιτήματος. Επιπλέον, παρουσιάζεται ανάλυση του κόστους και του χρόνου που χρειάστηκε για την εφαρμογή της συγκεκριμένης περιπτωσιακής μελέτης. Ο κύριος σκοπός αυτού του κεφαλαίου είναι (i) η επίδειξη της χρήσης των ΒΜ σε υδροδυναμικά μοντέλα καταλληλότητας ενδιαιτήματος (ii) η επισήμανση των χαρακτηριστικών των HHM που τα καθιστούν ιδανικά εργαλεία

για οικοσυστημικής προσέγγισης εκτιμήσεις οικολογικής παροχής, (ii) η συζήτηση επί των μειονεκτημάτων τους και η πρόταση σχετικών, κατάλληλων λύσεων και (iv) η επισήμανση ότι οικοσυστημικής προσέγγισης εκτιμήσεις οικολογικής παροχής με τη χρήση HHMs μπορούν να είναι οικονομικά και χρονικά αποδοτικές και θα πρέπει τελικά να προτιμώνται έναντι άλλων επιλογών όταν αναζητάται ακρίβεια στην τελική εκτίμηση-πρόβλεψη.

5.1. Περιοχή μελέτης

Ο ποταμός Παραπείρος βρίσκεται στη Δυτική Ελλάδα. Είναι παραπόταμος του ποταμού Πείρου, με έκταση λεκάνης απορροής 118 km^2. Ο Παραπείρος πηγάζει στα ορεινά τμήματα της λεκάνης απορροής, στο όρος Ερύμανθος και μετά από απόσταση 25 χιλιομέτρων ενώνεται με τον Πείρο ο οποίος εκβάλλει τελικά στον Πατραϊκό Κόλπο.

5.2. Υδρομετρικά-υδραυλικά δεδομένα, βαθμονόμηση και επαλήθευση του υδροδυναμικού μοντέλου

Σε μία περιοχή μήκους 277 m κατάντη του φράγματος του Παραπείρου συλλέχθηκαν δεδομένα τοπογραφίας υπό τη μορφή γεωγραφικών συντεταγμένων (μήκος, πλάτος, υψόμετρο). Συνολικά συλλέχθηκαν 863 σημεία συντεταγμένων και με τη χρήση του λογισμικού TELEMAC 2D δημιουργήθηκε υπολογιστικό πλέγμα αποτελούμενο από 5170 κόμβους και 9875 τριγωνικά στοιχεία με 1 m ανάλυση. Για τη βαθμονόμηση του υδροδυναμικού μοντέλου συλλέχθηκαν δεδομένα V και D σε 15 τυχαίες θέσεις εντός της περιοχή μελέτης σε δύο διαφορετικές παροχές (0.3 m^3/s και 1 m^3/s) . Η πρώτη παροχή χρησιμοποιήθηκε για τη βαθμονόμηση και η δεύτερη για την επαλήθευση του μοντέλου.

5.3. Καταλληλότητα ενδιαιτήματος και οικολογική παροχή

Για την εκτίμηση των προτιμήσεων ενδιαιτήματος των ΒΜ χρησιμοποιήθηκε το σετ δεδομένων που παρουσιάστηκε στο Κεφ. 4. Η καταλληλότητα του ενδιαιτήματος (K) εκφράστηκε με τη δημιουργία ενός δείκτη καταλληλότητας που περιλάμβανε τις παρακάτω μετρικές ΒΜ: (i) αριθμός taxa, (ii) ποικιλότητα (δείκτης Shannon), (iii) αριθμός Εφημερόπτερων, Πλεκόπτερων και Τριχόπτερων taxa και (iv) αφθονία ΒΜ. Στον συγκεκριμένο δείκτη, η κάθε μετρική μετασχηματίστηκε - κανονικοποιήθηκε σε κλίμακα 0 ως 1, διαιρώντας τη με τη μέγιστη τιμή της συγκεκριμένης μετρικής στην κάθε θέση δειγματοληψίας (σύνολο 9 θέσεις) από τις οποίες συλλέχθηκε το σετ των 380 δεδομένων - μικροενδιαιτημάτων. Με τον τρόπο αυτό ομαλοποιήθηκαν κατά το μέγιστο δυνατό και οι διαφορές στις μετρικές λόγω διαφορετικής τοποθεσίας και εποχής. Το συγκεκριμένο σετ δεδομένων, με την K εκφρασμένη μέσω του παραπάνω δείκτη, χρησιμοποιήθηκε για την εκμάθηση και σταυρωτή επικύρωση FRB αλγόριθμου με χρήση του λογισμικού HABFUZZ.

Η έξοδος (αποτελέσματα) του υδροδυναμικού υπομοντέλου χρησιμοποιήθηκε ως είσοδος στο υπομοντέλο ενδιαιτήματος και τελικά υπολογίστηκε η καταλληλότητα ενδιαιτήματος για τη συνολική περιοχή μελέτης σε διαφορετικά σενάρια παροχών. Για την επιλογή του καταλληλότερου σεναρίου (οικολογικής παροχής) χρησιμοποιήθηκε σχετικός δείκτης ο οποίος έλαβε υπόψη του την καταλληλότητα του κάθε ενδιαιτήματος ανά παροχή, των αριθμό των υγρών κόμβων και τη συνεκτικότητα των κατάλληλων ενδιαιτημάτων.

5.4. Αποτελέσματα και συζήτηση

Τα αποτελέσματα της μελέτης έδειξαν ότι η οικολογική παροχή των 0,2 m^3/s, που έχει προταθεί μέσω υδρολογικών μεθόδων για το φράγμα του Παραπείρου στη σχετική μελέτη περιβαλλοντικών επιπτώσεων δεν μπορεί να παρέχει βέλτιστες συνθήκες για την υποστήριξη μια λειτουργικής κοινότητας ΒΜ. Με βάση τη συγκεκριμένη έρευνα, η καταλληλότητα ενδιαιτήματος ήταν υψηλότερη σε παροχή 2 m^3/s και για τις δύο εναλλακτικές κατάρτισης, ενώ αποδεκτές τιμές (με καταλληλότητα ≥ 0,6) αποτελούν οι 0,8 m^3/s, 0,6 m^3/s, 1 m^3/s και 3 m^3/s. Ενώ όμως οι βέλτιστες συνθήκες για τα ΒΜ επικρατούν σε παροχές 1 m^3/s ή 2 m^3/s, οι

διαχειριστές είναι πιθανό να επιλέξουν να εφαρμόσουν ένα άλλο σενάριο οικολογικής παροχής, αναζητώντας μία ισορροπία μεταξύ της ανθρώπινης κατανάλωσης και της ζήτησης νερού από το υδρόβιο οικοσύστημα. Αυτή η παροχή όμως δεν μπορεί να είναι μικρότερη των 0.6 m^3/s καθώς σύμφωνα με την πενταβάθμια κλίμακα που εφαρμόζεται στην ΟΠΥ 2000/60/ΕΕ, η καταλληλότητα σε μικρότερες παροχές γίνεται μέτρια (μη αποδεκτή).

Όπως αναφέρθηκε προηγουμένως, η εφαρμογή εκτιμήσεων οικολογικής παροχής με χρήση HHMs είναι δυσανάλογα περιορισμένη σε σύγκριση με τις αντίστοιχες υδρολογικές μεθόδους για λόγους που συνδέονται κυρίως με τον χρόνο, το κόστος, την απαιτούμενη τεχνογνωσία και τη διαθεσιμότητα σχετικών υδρο-οικολογικών δεδομένων (Jorgensen and Bendoricchio, 2001; Conallin et al., 2010). Σχετικά με τα ανωτέρω, η συγκεκριμένη έρευνα πραγματοποιήθηκε από μία μικρή ομάδα βιολόγων και υδραυλικών-περιβαλλοντικών μηχανικών.

Σε ότι αφορά τον χρόνο και το κόστος υλοποίησης, το πιο δαπανηρό στάδιο σε τέτοιες εφαρμογές είναι η συλλογή των υδρο-οικολογικών δεδομένων αναφοράς (Theodoropoulos et al., 2018a). Εντούτοις, μόλις συλλεχθεί το σύνολο των δεδομένων αναφοράς, η υδροδυναμική προσομοίωση μπορεί να πραγματοποιηθεί με δύο μόνο επιτόπιες επισκέψεις. Μία για τη συλλογή τοπογραφικών δεδομένων και υδρομετρικών-υδραυλικών δεδομένων για τη βαθμονόμηση του υδροδυναμικού υπομοντέλου και μία επιπλέον επίσκεψη για τη συλλογή μιας δεύτερης σειράς δεδομένων για την επαλήθευση-επικύρωσή του. Αυτή η χρονική περίοδος μπορεί να θεωρηθεί σύντομη, λαμβανομένης υπόψη της πολύτιμης οπτικής απεικόνισης μιας εφαρμογής HHM, η οποία προσφέρει μια επιστημονική βάση συζήτησης μεταξύ επιστημόνων, διαχειριστών και τοπικών φορέων κατά τη διαδικασία λήψης αποφάσεων.

Από την συγκεκριμένη έρευνα φάνηκε ότι η συλλογή ενός αξιόπιστου σετ υδρο-οικολογικών δεδομένων αναφοράς είναι ένα βασικό βήμα για την ανάπτυξη σεναρίων οικολογικής παροχής με χρήση υδροδυναμικών μοντέλων ενδιαιτήματος. Είτε ως καμπύλες καταλληλότητας είτε ως κανόνες ασαφούς λογικής, οι προτιμήσεις ενδιαιτήματος υδρόβιων οργανισμών έχουν αρκετές φορές μελετηθεί αλλά η γενίκευση αυτών των προτιμήσεων και η δυνατότητα μεταφοράς τους σε άλλα ποτάμια παρουσιάζει δυσκολίες (Heggenes, 1990, Holm et al., 2001, Lancaster and Downes, 2010). Πρόσφατα επιχειρήθηκαν γενικευμένες προσεγγίσεις για να ξεπεραστεί αυτός ο περιορισμός (Lamouroux και Jowett, 2005 · Booker, 2016). Βάσει της συγκεκριμένη έρευνας για τα ΒΜ, μια χρήσιμη προσέγγιση για την υπέρβαση αυτού του 'εμποδίου' θα απαιτούσε: (i) συλλογή δειγμάτων αναφοράς από ποτάμια παρόμοιας τυπολογίας, που ουσιαστικά θα έχουν παρόμοιες περιβαλλοντικές και υδραυλικές συνθήκες (θερμοκρασία, ταχύτητες ροής, υποστρώματα), (ii) υπολογισμό της καταλληλότητας ενδιαιτήματος με χρήση μετρικών ΒΜ και όχι με χρήση συγκεκριμένων taxa (Theodoropoulos et al., 2018a), (iii) κανονικοποίηση της καταλληλότητας των οικοτόπων ανά εποχή και τοποθεσία. Αυτό αποτελεί βασικό βήμα για την εξάλειψη (τουλάχιστον εν μέρει) εποχικών και γεωγραφικών διακυμάνσεων.

Κεφάλαιο 6 | Περιπτωσιακή μελέτη 2: Εκτίμηση οικολογικής παροχής με τη χρήση υδροδυναμικών μοντέλων καταλληλότητας ενδιαιτήματος βενθικών μακροασπονδύλων κατάντη του φράγματος Μαραθώνα (ρέμα Οινόης, Αττική, Ελλάδα)

Στο κεφάλαιο αυτό, παρόμοια με το κεφάλαιο 5, περιγράφεται η εφαρμογή ενός δισδιάστατου υδροδυναμικού μοντέλου καταλληλότητας ενδιαιτήματος για την ανάπτυξη σεναρίων οικολογικής παροχής βασισμένων στις προτιμήσεις των ΒΜ στο ρέμα της Οινόης (Αττική, κατάντη του φράγματος Μαραθώνα). Επιπλέον, γίνεται σύγκριση των σεναρίων οικολογικής παροχής, βασισμένων στη χρήση υδροδυναμικών μοντέλων καταλληλότητας ενδιαιτήματος ΒΜ με τα αντίστοιχα σενάρια που προέκυψαν με τη χρήση υδρολογικών μεθόδων για την ίδια περιοχή. Ο απώτερος στόχος αυτού του κεφαλαίου, πέραν της επίδειξης της σχετικής προσομοίωσης καταλληλότητας ενδιαιτήματος, είναι να εξεταστεί εάν η εφαρμογή ΗΗΜ μεθόδων εκτίμησης της οικολογικής παροχής δίνει παρόμοια αποτελέσματα με τις υδρολογικές μεθόδους, ώστε τελικά να διερευνηθεί η πιθανότητα χρήσης των υδρολογικών μεθόδων ως αυτόνομων εργαλείων εκτίμησης της οικολογικής παροχής. Συζητείται επίσης η δυνατότητα συνδυασμού των δύο μεθόδων ώστε να αυξηθεί πιθανώς η εμπιστοσύνη στην πρόβλεψη και επιλογή οικολογικών παροχών.

5.1. Περιοχή μελέτης

Το ρέμα της Οινόης βρίσκεται κάτω από το φράγμα του Μαραθώνα, το οποίο έχει ύψος 54 m και συγκεντρώνει τις απορροές των ρεμάτων Χάραδρου και Βαρνάβα, παρέχοντας πόσιμο νερό σε ένα μεγάλο μέρος του πληθυσμού της Αθήνας και των γύρω περιοχών. Η λεκάνη απορροής έχει έκταση 118 km^2 και τα δύο ρέματα ενώνονται λίγο ανάντη του φράγματος δημιουργώντας το ρέμα της Οινόης το οποίο εκβάλλει στο Αιγαίο Πέλαγος μετά από 10 km διαδρομής.

5.2. Υδρολογικά δεδομένα

Ημερήσια υδρολογικά δεδομένα από τη λειτουργία του φράγματος του Μαραθώνα αποκτήθηκαν για μια περίοδο 11 ετών (2002-2013). Τα δεδομένα αυτά χρησιμοποιήθηκαν για τον υπολογισμό της εισροής νερού από τα ρέματα Χάραδρου και Βαρνάβα. Αναπτύχθηκε και εφαρμόστηκε ένα μοντέλο υδατικού ισοζυγίου. Οι εισροές που ελήφθησαν υπόψη ήταν η τροφοδοσία με νερό του φράγματος από τα ανάντη ρέματα και ο ημερήσιος όγκος βροχόπτωσης και η εκροή ήταν ο όγκος του νερού που αντλούταν για την παροχή πόσιμου νερού στην Αθήνα. Οι υπολογισθείσες ημερήσιες παροχές από τα ρέματα Βαρνάβα και Χάραδρου θεωρήθηκαν ως οι φυσικές ροές των ποταμών από τις οποίες υπολογίστηκαν σενάρια οικολογικής παροχής χρησιμοποιώντας (i) τη μέθοδο Tennant (Tennant, 1976), (ii) τη μέθοδο Lyons (Bounds and Lyons, 1979), (iii) τη μέθοδο της Βασικής Παροχής Διατήρησης (QBM - Alcácer-Santos, 2004). Επιπλέον, με βάση τα ανωτέρω δεδομένα υπολογίστηκαν τρία ακόμη σενάρια οικολογικής παροχής σύμφωνα με τις απαιτήσεις της σχετικής Ελληνικής νομοθεσίας, (a) 30% της μέσης μηνιαίας παροχής για τους μήνες Ιούνιο, Ιούλιο και Αύγουστο, (b) 50% της μέσης μηνιαίας παροχής του μήνα Σεπτέμβριο και (c) 0.03 m^3/s ως την ελάχιστη αποδεκτή παροχή σε κάθε περίπτωση.

5.3. Υδροδυναμική προσομοίωση και προσομοίωση καταλληλότητας ενδιαιτήματος

Σε μία περιοχή μήκους 370 m κατάντη του φράγματος του Μαραθώνα συλλέχθηκαν δεδομένα τοπογραφίας υπό τη μορφή γεωγραφικών συντεταγμένων (μήκος, πλάτος, υψόμετρο). Συνολικά συλλέχθηκαν 459 σημεία συντεταγμένων και με τη χρήση του λογισμικού TELEMAC 2D δημιουργήθηκε υπολογιστικό πλέγμα αποτελούμενο από 3198 κόμβους και 7140 τριγωνι-

κά στοιχεία με 0,9 m χωρική ανάλυση. Για τη βαθμονόμηση του υδροδυναμικού μοντέλου συλλέχθηκαν δεδομένα V και D σε 15 τυχαίες θέσεις εντός της περιοχή μελέτης σε δύο διαφορετικές παροχές (0,03 m^3/s και 0,3 m^3/s) . Η πρώτη παροχή χρησιμοποιήθηκε για τη βαθμονόμηση και η δεύτερη για την επαλήθευση του μοντέλου. Για την προσομοίωση της καταλληλότητας ενδιαιτήματος ΒΜ χρησιμοποιήθηκε η ίδια διαδικασία με την περιγραφείσα στο προηγούμενο κεφάλαιο. Η έξοδος του υδροδυναμικού υπομοντέλου χρησιμοποιήθηκε ως είσοδος στο υπομοντέλο ενδιαιτήματος και τελικά υπολογίστηκε η καταλληλότητα ενδιαιτήματος για τη συνολική περιοχή μελέτης σε 16 διαφορετικά σενάρια παροχών (από 0.01 m^3/s έως 5 m^3/s). Για την επιλογή του καταλληλότερου σεναρίου (οικολογικής παροχής) χρησιμοποιήθηκε σχετικός δείκτης ο οποίος έλαβε υπόψη του την καταλληλότητα του κάθε ενδιαιτήματος ανά παροχή, των αριθμό των υγρών κόμβων και τη συνεκτικότητα των κατάλληλων ενδιαιτημάτων.

5.4. Αποτελέσματα και συζήτηση

Τα αποτελέσματα της έρευνας έδειξαν ότι παροχές από 0,17 m^3/s έως 1,5 m^3/s είναι κατάλληλες για τη διατήρηση της λειτουργικότητας των κοινοτήτων ΒΜ κατάντη του φράγματος του Μαραθώνα. Σε μικρότερες και μεγαλύτερες παροχές, η καταλληλότητα ενδιαιτήματος γίνεται μη αποδεκτή βάσει της ΟΠΥ 2000/60 /ΕΕ. Οι οικολογικές παροχές που υπολογίστηκαν με χρήση υδρολογικών μεθόδων κυμάνθηκαν από 0,0006 m^3/s (μέθοδος της QBR) έως 0,18 m^3/s (μέθοδος Tennant - 30% της μέσης ετήσιας παροχής), ενώ σύμφωνα με την Εθνική νομοθεσία η οικολογική παροχή θα πρέπει να κυμαίνεται μεταξύ 0,03 m^3/s και 0,135 m^3/s.

Βάσει των ανωτέρω, οι οικολογικές παροχές που υπολογίστηκαν με χρήση υδρολογικών μεθόδων ήταν χαμηλότερες από την ελάχιστη οικολογική παροχή που υπολογίστηκε βάσει των ΗΗΜ. Μόνο το σενάριο 30%-QAA της μεθόδου Tennant (0,18 m^3/s) ήταν σε συμφωνία με την οικολογική παροχή βάσει των ΗΗΜ. Αυτό πρακτικά σημαίνει ότι μόνο ένα από τα οκτώ υδρολογικά σενάρια συμφώνησε με την ελάχιστα αποδεκτή οικολογική παροχή (πιθανότητα συμφωνίας 12,5%). Ωστόσο, δεδομένου ότι η τιμή 30%-QAA αναφέρεται στην 'άριστη' κατάσταση του οικοσυστήματος με βάση τις συστάσεις της μεθόδου Tennant, ελλείψει σχετικής οικοσυστημικής μελέτης, οι διαχειριστές πιθανώς θα προτιμούσαν να εφαρμόσουν το σενάριο 20%-QAA ή το σενάριο 10%-QAA που αντιστοιχούν στην 'καλή' και 'αποδεκτή' κατάσταση αντίστοιχα. Ως εκ τούτου, οι υδρολογικές μέθοδοι θα πρέπει να χρησιμοποιούνται με προσοχή όταν δεν υπάρχουν διαθέσιμες ΗΗΜ μέθοδοι. Δεδομένου ότι μια υγιής κοινότητα ΒΜ στο ρέμα της Οινόης εξασφαλίζεται σε Q = 0,5 m^3/s, η απόδοση οικολογικής παροχής βάσει υδρολογικών μεθόδων, πιθανώς (με πιθανότητα 87,5%) να μην είναι η κατάλληλη. Αυτά τα αποτελέσματα είναι σύμφωνα με προηγούμενη βιβλιογραφία που επισημαίνει τον 'κίνδυνο' από τη χρήση των υδρολογικών μεθόδων ως αυτόνομων εργαλείων εκτίμησης της οικολογικής παροχής (Acreman and Dunbar, 2004, Linnansaari et al., 2013, Arthington 2012, Papadaki et al., 2017).

Σχετικά με τον συνδυασμό των υδρολογικών μεθόδων με τις ΗΗΜ μεθόδους εκτίμησης της οικολογικής παροχής, οι Stamou et al. (2018) επισημαίνουν ότι οι συνδυαστικές μέθοδοι θα μπορούσαν να οδηγήσουν σε περισσότερο 'ρεαλιστικές' οικολογικές παροχές βάσει των ιστορικών υδρολογικών συνθηκών της εκάστοτε περιοχής μελέτης και λαμβάνοντας επιπλέον υπόψη τι μπορεί να αποδοθεί στο οικοσύστημα από κοινωνικής πλευράς. Το συμπέρασμα αυτό όμως, δεν θα πρέπει να παρερμηνευθεί ως 'μείωση της οικολογικής παροχής στα κατάντη ώστε μεγιστοποιηθούν πιθανά βραχυπρόθεσμα ανθρώπινα οφέλη στα ανάντη' (Homa et al., 2005, Jager and Smith, 2008). Η οικολογική παροχή δεν θα πρέπει να παρεκκλίνει για πολύ από αυτή που υπολογίστηκε με βάση τις ΗΗΜ μεθόδους ώστε να εξασφαλιστεί η μακροπρόθεσμη λειτουργικότητα των κατάντη οικοσυστημάτων.

References

1. Acreman M., 2016. Environmental flows - basics for novices. Water 3, 622-628.
2. Acreman M.C., Ferguson J.D., 2010. Environmental flows and European Water Framework Directive. Freshwater Biology 55, 32–48.
3. Acreman M.C., Aldrick J., Binnie C., Black A., Cowx I., Dawson H., Dunbar M., Extence C., Hannaford J., Harby A., Holmes N., Jarritt N., Old G., Peirson G., Webb J., Wood P., 2009. Environmental flows from dams: the water framework directive. Proceedings of the Institution of Civil Engineers - Engineering Sustainability 162, 13-22.
4. Acreman M.C., Dunbar M.J., 2004. Defining environmental river flow requirements: a review. Hydrology and Earth System Sciences 8, 861–876.
5. Ahmadi-Nedushan B., St-Hilaire A., Bérubé M., Robichaud E., Thiémonge N., Bobée B., 2006. A review on statistical methods for the evaluation of the aquatic habitat suitability for instream flow assessment. River Research and Applications 22, 503-523.
6. Ali A, Shamsuddin S.M., Ralescu A.L., 2015. Classification with class imbalance problem: a review. International Journal of Advances in Soft Computing and its Applications 7, 176-204.
7. Allan J.D., Castillo M.M., 2007. Stream Ecology - Structure and Function of Running Waters. Springer, Dordrecht.
8. Allan J.D., 1995. Stream ecology: structure and function of running waters. Chapman and Hall, London, UK.
9. Anderson J.D., 2009. Governing equations of fluid dynamics. In Wendt J. (Ed.): Computational fluid dynamics - an introduction. Springer-Verlag, Berlin Heidelberg.
10. AQEM consortium, 2002. Manual for the application of the AQEM method: A comprehensive method to assess European streams using macroinvertebrates, developed for the purpose of the Water Framework Directive. Version 1.0.
11. Argerich A., Puig M.A., Pupilli E., 2004. Effect of floods of different magnitude on the macroinvertebrate communities of Matarranya stream (Ebro river basin, NE Spain). Limnetica 23, 283-294.
12. Armanini D.G., Idigoras-Chaumel A., Monk W.A., Marty J., Smokorowski K., Power M., Baird D.J., 2014. Benthic macroinvertebrate flow sensitivity as a tool to assess effects of hydropower related ramping activities in streams in Ontario (Canada). Ecological Indicators 46, 466-476.
13. Arthington A.H., 2012. Environmental flows: saving rivers in the third millennium. Freshwater Ecology Series, University of California Press.
14. Arthington A.H., 1998. Comparative evaluation of environmental flow assessment techniques: Review of holistic methodologies. LWRRDC Occasional Paper 26/98. Land and Water Resources Research and Development Corporation, Canberra, Australia.
15. Barbour M.T., Gerritsen J., Snyder B.D., Stribling J.B., 1999. Rapid bioassessment protocols for use in streams and wadeable rivers periphyton benthic macroinvertebrate and fish. 2nd edition. United States Environmental Protection Agency Press, Washington DC, USA.
16. Belmar O., Bruno D., Martinez-Capel F., Barquin J., Velasco J., 2013. Effects of flow regime alteration on fluvial habitats and riparian quality in a semiarid Mediterranean basin. Ecological Indicators 13, 52-64.
17. Benjankar R., Tonina D., McKean J., 2014. One-dimensional and two-dimensional hydrodynamic modeling derived flow properties: impacts on aquatic habitat quality predictions. Earth Surface Processes and Landforms 40, 340-356.
18. Biggs B.J.F., Hickey C.W., 1994. Periphyton responses to a hydraulic gradient in a regulated river in New Zealand. Freshwater Biology 32, 49-59.
19. Booker D.J., Dunbar M.J., Ibbotson A.T., 2004. Predicting juvenile salmonid drift-feeding habitat quality using a three dimensional hydraulic-bioenergetic model. Ecological Modelling 177, 157-177.

20. Booker D.J., 2016. Generalized models of riverine fish habitat. Journal of Ecohydraulics 1, 31-49.
21. Borchardt D., 1993. Effects of flow refugia and drift loss of benthic macroinvertebrates: implications for habitat restoration in lowland streams. Freshwater Biology 29, 221-227.
22. Bounds R., Lyons B., 1979. Existing Reservoir and Stream Management: Statewide Minimum Streamflow Recommendations. Texas Parks and Wildlife Department, Austin, Texas.
23. Bovee K.D., 1986. Development and evaluation of habitat suitability criteria for use in the instream flow incremental methodology. Instream Flow Information Paper #21 FWS/OBS-86/7. USDI Fish and Wildlife Service, Washington DC, USA.
24. Bovee K.D., 1982. A guide to stream habitat analysis using the instream flow incremental methodology. Instream Flow Information Paper #12, USDI Fish and Wildlife Services, Office of Biology Services, Washington DC, USA.
25. Bovee K.D., Milhous R., 1978. Hydraulic simulation in instream flow studies: Theory and techniques. Instream Flow Information Paper 5, Cooperative Instream Flow Service Group, Fort Collins, USA.
26. Bradley B.A., Olsson A.D., Wang O., Dickson B.G., Pelech L., Sesnie S.E., Zachmann L.J., 2012. Species detection vs. habitat suitability: Are we biasing habitat suitability models with remotely sensed data? Ecological Modelling 244, 57-64.
27. Breiman L., 2001. Random Forests. Machine Learning 45, 5-32.
28. Breiman L., Friedman J.H., Olshen R.A., Stone C.J., 1984. Classification and regression trees. Pacific Grove. Wadsworth.
29. Brisbane Declaration, 2007. The Brisbane Declaration: environmental flows are essential for freshwater ecosystem health and human well-being. 10th International River Symposium, 3-6 September 2007, Brisbane, Australia.
30. Brittain J.E., Eikeland T.J., 1988. Invertebrate drift - a review. Hydrobiologia 166, 77-93.
31. Brookes C.J., Kumar V., Lane S.N., 2010. A comparison of Fuzzy, Bayesian and Weighted Average formulations of an in-stream habitat suitability model. Proceedings of the International Congress on Environmental Modelling and Software, Ottawa, Canada.
32. Broomhead D.S., Lowe D., 1988. Multivariate functional interpolation and adaptive network. Complex Systems 2, 321-355.
33. Buffagni A., Erba S., Cazzola M., Murray-Bligh J., Hanja S., Genoni P., 2006. The STAR common metrics approach to the WFD intercalibration process: Full application for small, lowland rivers in three European countries. Hydrobiologia 566, 379-399.
34. Bunn S.E., Arthington A.H., 2002. Basic principles and ecological consequences of altered flow regimes for aquatic biodiversity. Environmental Management 30, 492-507.
35. Caiola N., Ibanez C., Verdu J., Munne A., 2014. Effects of flow regulation on the establishment of alien fish species: A community structure approach to biological validation of environmental flows. Ecological Indicators 45, 598-604.
36. Caissie D., El-Jabi N., 2003. Instream flow assessment: From holistic approaches to habitat modelling. Canadian Water Resources Journal 28, 173-183.
37. Campaioli S., Ghetti P.F., Minelli A., 1994. Manuale per il riconoscimento dei macroinvertebrati delle acque dolci italiane. Provincia Autonoma di Trento, Italy.
38. Chen A, Weisbrod N., 2016. Assessment of anthropogenic impact on the environmental flows of semi-arid watersheds: the case study of the lower Jordan River. In Borchardt D., Bogardi J., Ibisch R. (Eds.): Integrated water resources management: concept, research and implementation. Springer, Berlin.
39. Chessman B.C., 2015. Relationships between lotic macroinvertebrate traits and responses to extreme drought. Freshwater Biology 60, 50-63.
40. Chow V.T., 1959. Open Channel Hydraulics. McGraw-Hill, New York, USA.

41. Conallin J., Boegh E., Jensen J.K., 2010. Instream physical habitat modelling types: an analysis as stream hydromorphological modelling tools for EU water resource managers. International Journal of River Basin Management 8, 93-107.
42. Crosskey R.W., 1990. The Natural History of Blackflies. John Wiley, New York, USA.
43. Dakou E., D' heygere T., Dedecker A.P., Goethals P.L.M., Lazaridou-Dimitriadou M., De Pauw N., 2007. Decision tree models for prediction of macroinvertebrate taxa in the river Axios (Northern Greece). Aquatic Ecology 41, 399-411.
44. Davis R., Hirji R., 2003. Environmental Flows: Case Studies. Water Resources and Environment. Technical Note C2. World Bank. Washington DC, USA.
45. DHI, 2017. MIKE 11 - A modelling system for rivers and channels. DHI.
46. Digga A., 2012. Review of the Environmental Impact Assessment for the construction of the Peiros-Parapeiros River Dam in the Prefecture of Achaia and assessment of the application of the relevant environmental requirements. M.Sc. Thesis. University of Patras, Department of Biology, Patras, Greece (in Greek).
47. Dobson M., Hildrew A.G., 1992. A test of resource limitation among shredding detritivores in low order streams in southern England. Journal of Animal Ecology 61, 69-78.
48. Dunbar M.J., Alfredsen K., Harby A., 2012. Hydraulic-habitat modelling for setting environmental river flow needs for salmonids. Fisheries Management and Ecology 19, 500-517.
49. Dyson M., Bergkamp M., Scanlon J., 2003. Flow: The Essentials of Environmental Flows. IUCN, Gland, Switzerland and Cambridge, UK.
50. Dore J., Robinson J., Smith M. 2010. Negotiate - Reaching agreements over water. IUCN, Gland, Switzerland.
51. Effenberger M., Engel J., Diehl S., Matthaei C.D., 2008. Disturbance history influences the distribution of stream invertebrates by altering microhabitat parameters: a field experiment. Freshwater Biology 53, 996-1011.
52. Efstratiadis A., Tegos A., Varveris A., Koutsoyiannis D., 2014. Assessment of environmental flows under limited data availability: case study of the Acheloos River, Greece. Hydrological Sciences Journal 59, 731-750.
53. Ehrlinger J., 2016. Visually Exploring Random Forests. R package version 2.0.1.
54. Elith J., Leathwick J.R., Hastie T., 2008. A working guide to boosted regression trees. Journal of Animal Ecology 74, 802-813.
55. Elton C., 1927. Animal Ecology. Sidgwick & Jackson, London, UK.
56. Englund G., Malmqvist B., 1996. Effects of flow regulation, habitat area and isolation on the macroinvertebrate fauna of rapids in North Swedish Rivers. Regulated Rivers: Research and Management 12, 433-445.
57. European Commission, 2007. Directive 2007/60/EC of the European Parliament and of the Council of 23 October 2007 on the assessment and management of flood risks. Official Journal of the European Union L288, 27-34.
58. European Union Council, 2000. Directive 2000/60/EC of the European Parliament and of the Council of 23 October 2000 establishing a framework for Community action in the field of water policy. Official Journal of the European Communities 43(L327), 1-73.
59. Everaert G., Neve J.D., Boets P., Dominguez-Granda L., Mereta S.T., Ambelu A., Hoang T.H., Goethals P.L.M., Thas O., 2014. Comparison of the abiotic preferences of macroinvertebrates in tropical river basins. PLoS One 9(10), e108898.
60. Frutiger A., 1988. Walking on suckers: New insights into the locomotory behavior of larval net-winged midges (Diptera: Blephariceridae). Journal of the North American Benthological Society 17, 104-120.
61. Fukuda S., De Baets B., Waegeman W., Verwaeren J., Mouton A.M., 2013. Habitat prediction and knowledge extraction for spawning European grayling *(Thymallus*

thymallus L.) using a broad range of species distribution models. Environmental Modelling and Software 47, 1-6.
62. Fuladipanah M., Jorabloo M., 2015. Hydrological method to evaluate environmental flow (case study: Gharasou River, Ardabil). International Journal of Environmental and Ecological Engineering 9, 62-65.
63. Fuller R.L., Griego C., Muehlbauer J.D., Dennison J., Doyle M.W., 2010. Response of stream macroinvertebrates in flow refugia and high-scour areas to a series of floods: a reciprocal replacement study. Journal of the North American Benthological Society 29, 750-760.
64. Gabriels W., Lock K., De Pauw N., Goethals P.L.M., 2010. Multimetric Macroinvertebrate Index Flanders (MMIF) for biological assessment of rivers and lakes in Flanders (Belgium). Limnologica 40, 199-207.
65. Galland J.C., Gontal N., Hervouet J.M., 1991. TELEMAC: A new numerical model for solving shallow water equations. Advances in Water Resources 14, 138-148.
66. George D., Mallery P., 2010. SPSS for Windows Step by Step: A Simple Guide and Reference 17.0 Update. 10th Edition. Pearson, Boston, USA.
67. Georgian T., Thorp J.H., 1992. Effects of microhabitat selection on feeding rates of net-spinning caddisfly larvae. Ecology 73, 229-240.
68. Gibbins C.N., Dilks C.F., Malcolm R., Soulsby C., Juggins S., 2001. Invertebrate communities and hydrological variation in Cairngorm mountain streams. Hydrobiologia 462, 205-219.
69. Giller P.S., Malmqvist B., 1998. The biology of streams and rivers. Oxford University Press, New York, USA.
70. Gjerlov C., Hildrew A.G., Jones J.I., 2003. Mobility of stream invertebrates in relation to disturbance and refugia: a test of habitat templet theory. Journal of the North American Benthological Society 22, 207-223.
71. Glozier N.E., Culp J.M., Scrimgeour G.J., 1997. Transferability of habitat suitability curves for a benthic Minnow, Rhinichthys cataractae. Journal of Freshwater Ecology 12, 379-393.
72. Gopal B., 2013. Methodologies for the assessment of environmental flows. In Gopal B. (Ed.): Environmental flows: An introduction for water resources managers. National Institute of Ecology, New Delhi, India.
73. Gore J.A., Layzer J.B., Mead J., 2001. Macroinvertebrate instream flow studies after 20 years: a role in stream management and restoration. Regulated Rivers: Research and Management 17, 527-542.
74. Gore J.A., 1989. Models for predicting benthic macroinvertebrate habitat suitability under regulated flows. In Gore J.A., Petts G.E. (Eds.): Alternatives in regulated river management. CRC Press Inc., Boca Rato, Florida, USA.
75. Greenberg L., Svendsen P., Harby A., 1996. Availability of microhabitats and their use by brown trout (*Salmo trutta*) and grayling (*Thymallus thymallus*) in the river Vojman, Sweden. Regulated Rivers: Research and Management 12, 287–303
76. Grinnell J., Storer T.I., 1924. Animal life in the Yosemite - An account of the mammals, birds, reptiles and amphibians in a cross-section of the Sierra Nevada. University of California Press, Berkeley, California, USA.
77. Haapala A., Muotka T., Laasonen P., 2003. Distribution of benthic macroinvertebrates and leaf litter in relation to streambed retentivity: implications for headwater stream restoration. Boreal Environment Research 8, 19-30.
78. Harlow F.H., 2004. Fluid dynamics in Group T-3 Los Alamos National Laboratory (LA-UR-03-3852). Journal of Computational Physics 195, 414-433.

79. Hart D.D., Finelli C.M., 1999. Physical-biological coupling in streams: the pervasive effects of flow on benthic organisms. Annual Review of Ecology, Evolution and Systematics 30, 363-395.
80. Hartmann E.A., Mihuc T.B., 2008. Composition and abundance of stream macroinvertebrates as a determinant of water quality up and down stream of the Imperial Dam, Saranac River, New York. Scientia Discipulorum 3, 21-27.
81. Hastie T.J., Tibshirani R.J., 1990. Generalized Additive Models. Chapman & Hall, London, UK.
82. Heggenes J., Brabrand A., Saltveit S., 1990. Comparison of three methods for studies of stream habitat use by young brown trout and Atlantic salmon. Transactions of the American Fisheries Society 119, 101-111.
83. Heggenes J., Saltveit S.J., 1990. Seasonal and spatial microhabitat selection and segregation in young Atlantic salmon, *Salmo salar* L., and brown trout, *Salmo trutta* L., in a Norwegian river. Journal of Fish Biology 36, 707–720.
84. Herbst D.B., Cooper S.D., 2010. Before and after the deluge: rain-on-snow flooding effects on aquatic invertebrate communities of small streams in the Sierra Nevada, California. Journal of the North American Benthological Society 29, 1354-1366.
85. Hervouet J.M., 2007. Hydrodynamics of free surface flows: Modelling with the finite element method. John Wiley & Sons.
86. Hijmans R.J., Phillips S., Leathwick J., Elith J., 2016. Species Distribution Modeling. Documentation for package 'dismo' version 1.0-15. https://cran.r-project.org/web/packages/dismo/dismo.pdf [last accessed 30 Aug 2018].
87. Hirzel A.H., Le Lay G., 2008. Habitat suitability modelling and niche theory. Journal of Applied Ecology 45, 1372-1381.
88. Hladyz S., Nielsen D.L., Suter P.J., Krull E.S., 2012. Temporal variations in organic carbon utilization by consumers in a lowland river. River Research and Applications 28, 513-528.
89. Holm C.F.H., Armstrong J.D., Gilvear D.J., 2001. Investigating a major assumption of predictive instream habitat models: is water velocity preference of juvenile Atlantic salmon independent of discharge? Journal of Fish Biology 59, 1653-1666.
90. Holmquist JG, Schmidt-Gengenbach J, Roche JW. 2015. Stream macroinvertebrates and habitat below and above two wilderness fords used by mules, horses, and hikers in Yosemite National Park. Western North American Naturalist 75, 311-324.
91. Homa E.S., Vogel R.M., Smith M.P., Apse C.D., Huber-Lee A., Seiber J., 2005. An Optimization Approach for Balancing Human and Ecological Flow Needs. World Water and Environmental Resources Congress. ASCE, Anchorage, Alaska.
92. Horta F., Santos H., Tavares L., Antunes M., Pinheiro P., Callisto M., 2009. Assessment of benthic macroinvertebrate habitat suitability in a tropical watershed. http://labs.icb.ufmg.br/benthos/index_arquivos/pdfs_pagina/fe2009.pdf [last accessed 30 Aug 2018].
93. Hutchinson G.E., 1957. Concluding remarks. Cold Spring Harbor Symposia on Quantitative Biology 22, 415-427.
94. Ishwaran H., Kogalur U.B., 2017. Random Forests for Survival, Regression and Classification (RF-SRC), R package version 2.4.2.
95. Jacobsen D., Encalada A., 1998. The macroinvertebrate fauna of Ecuadorian highland streams and the influence of wet and dry seasons. Archiv fur Hydrobiologie 142, 53-70.
96. Jager H.I., Smith B.T., 2008. Sustainable reservoir operation: Can we generate hydropower and preserve ecosystem values? River Research and Applications 24, 340-352.
97. Johnson R.H., 1910. Determinate evolution in the color-pattern of the lady-beetles. Carnegie Institution of Washington, Washington DC, USA.

98. Jorde K., Schneider M., Peter A., Zoellner F., 2001. Fuzzy based models for the evaluation of fish habitat quality and instream flow assessment. Proceedings of the 3rd International Symposium on Environmental Hydraulics. 5-8 December, Tempe, Arizona, USA.
99. Jorgensen S.E., Bendoricchio G., 2001. Fundamentals of ecological modelling. 3rd edition. Cambridge University Press, Oxford, UK.
100. Jowett I.G., Hayes J.W., Duncan M.J., 2008. A guide to instream habitat survey methods and analysis. Report No. 54. NIWA Science and Technology Series.
101. Jowett I.G., Richardson J., Biggs B.J.F., Hickey C.W., Quinn J.M., 1991. Microhabitat preferences of benthic invertebrates and the development of generalized *Deleatidium spp.* habitat suitability curves, applied to four New Zealand Rivers. New Zealand Journal of Marine and Freshwater Research 25, 187-199.
102. Jun Y.C., Won D.H., Lee S.H., Kong D.S., Hwang S.J., 2012. A Multimetric Benthic Macroinvertebrate Index for the Assessment of Stream Biotic Integrity in Korea. International Journal of Environmental Research and Public Health 9, 3599-3628.
103. Kappes H., Sundermann A., Haase P., 2011. Distant land use affects terrestrial and aquatic habitats of high naturalness. Biodiversity and Conservation 20, 2297-2309.
104. Karaouzas I., Skoulikidis N., Giannakou U., Albanis T.A., 2011. Spatial and temporal effects of olive mill wastewaters to stream macroinvertebrates and aquatic ecosystems status. Water Research 45, 6334-6346.
105. Kearny M., 2006. Habitat, environment and niche: what are we modelling? Oikos 115, 186-191.
106. Kelly D.J., Hayes J.W., Allen C., West D., Hudson H., 2015. Evaluating habitat suitability curves for predicting variation in macroinvertebrate biomass with weighted usable area in braided rivers in New Zealand. New Zealand Journal of Marine and Freshwater Research 49, 398-418.
107. King J.M., Tharme R.E., De Villiers M.S., 2008. Environmental flow assessments for rivers: Manual for the Building Block Methodology. WRC Report No. TT 354/08. Cape Town, South Africa.
108. Kohavi R., 1995. A study of cross-validation and bootstrap for accuracy estimation and model selection. Proceedings of the 14th International Joint Conference on Artificial Intelligence 1137-1143.
109. Komínková D., Caletková J., Vitvar T., 2017. Analysis of environmental flow requirements for macroinvertebrates in a creek affected by urban drainage (Prague metropolitan area, Czech Republic). Urban Ecosystems 20, 785-797.
110. Koutrakis E.T., Triantafillidis, S., Sapounidis, A.S., Vezza, P., Kamidis, N., Sylaios, G., Comoglio, C., 2018. Evaluation of ecological flows in highly regulated rivers using the mesohabitat approach: A case study on the Nestos River, N. Greece. Ecohydrology and Hydrobiology (in press). DOI: 10.1016/j.ecohyd.2018.01.002.
111. Lake P.S., 2011. Drought and Aquatic Ecosystems. Effects and Responses. Wiley-Blackwell, Chichester, UK.
112. Lake P.S., 2000. Disturbance, patchiness, and diversity in streams. Journal of the North American Benthological Society 19, 573-592.
113. Lamouroux N., Jowett I.G., 2005. Generalized instream habitat models. Canadian Journal of Fisheries and Aquatic Sciences 62, 7-14.
114. Lamouroux N., Mérigoux S., Capra H., Dolédec S., Jowett I.G., Statzner B., 2010. The generality of abundance-environment relationships in microhabitats: a comment on Lancaster and Downes (2009). River Research and Applications 26, 915-920.
115. Lamouroux N., Mérigoux S., Dolédec S., Snelder T.H., 2013. Transferability of hydraulic preference models for aquatic macroinvertebrates. River Research and Applications 29, 933-937.

116. Lancaster J., Downes B.J., 2010. Linking the hydraulic world of individual organisms to ecological processes: Putting ecology into ecohydraulics. River Research and Applications 26, 385-403.
117. Lancaster J., Hildrew A.G., 1993. Flow refugia and the microdistribution of lotic macroinvertebrates. Journal of the North American Benthological Society 12, 385-393.
118. Lange C., Schneider M., Mutz M., Haustein M., Halle M., Seidel M., Sieker H., Wolter C., Hinkelmann R., 2015. Model-based design for restoration of a small urban river. Journal of Hydro-environment Research 9, 226-236.
119. Lazaridou-Dimitriadou M., 2002. Seasonal variation of the water quality of rivers and streams of eastern Mediterranean. Web Ecology 3, 20-32.
120. Leathwick J.R., Elith J., Francis M.P., Hastie T., Taylor P., 2006. Variation in demersal fish species richness in the oceans surrounding New Zealand: an analysis using boosted regression trees. Marine Ecology Progress Series 321, 267-281.
121. Leclerc M., Boudreault A., Bechara T.A., Corfa G., 1995. Two-dimensional hydrodynamic modeling: A neglected tool in the instream flow incremental methodology. Transactions of the American Fisheries Society 124, 645-662.
122. Leclere J., Oberdorff T., Belliard J., Leprieur F., 2011. A comparison of modeling techniques to predict juvenile 0+ fish species occurrences in a large river system. Ecological Informatics 6, 276-285.
123. Lee J.H., Kil J.T., Jeong S., 2010. Evaluation of physical fish habitat quality enhancement designs in urban streams using a 2D hydrodynamic model. Ecological Engineering 36, 1251-1259.
124. Leigh C., Bush A., Harrison E.T., Ho S.S., Luke L., Rolls R.J., Ledger M.E., 2015. Ecological effects of extreme climatic events on riverine ecosystems: insights from Australia. Freshwater Biology 60, 2620-2638.
125. Leitner P., Hauer C., Graf W., 2017. Habitat use and tolerance levels of macroinvertebrates concerning hydraulic stress in hydropeaking rivers - A case study at the Ziller River in Austria. Science of the Total Environment 575, 112-118.
126. Leps J., Smilauer P., 2003. Multivariate analysis of ecological data using CANOCO. Cambridge University Press, New York, USA.
127. Levene H., 1960. Robust testes for equality of variances. In Olkin I. (Ed.): Contributions to Probability and Statistics. Stanford University Press, Palo Alto, California, USA.
128. Li F., Cai Q., Fu X., Liu J., 2009. Construction of habitat suitability models (HSMs) for benthic macroinvertebrate and their applications to instream environmental flows: A case study in Xiangxi River of Three Gorges Reservoir region, China. Progress in Natural Science 19, 359-367.
129. Liaw A., Wiener M., 2002. Classification and regression by random forest. R News. 2/3, 18–22.
130. Lin Y., Lin W., Wu W., 2015. Uncertainty in various habitat suitability models and its impact on habitat suitability estimates for fish. Water 7, 4088-4107.
131. Linnansaari T., Monk W.A., Baird D.J., Curry R.A., 2013. Review of approaches and methods to assess environmental flows across Canada and internationally (Research Document 2012/039). DFO Canadian Science Advisory Secretariat.
132. Liu G.R., Quek S.S., 2014. The Finite Element Method: A Practical Course. 2nd edition. Butterworth-Heinemann, Oxford, UK.
133. Liu K.F.R., Yeh K., Chen C.W., Liang H.H., Shen W.S., 2013. Using Bayesian belief networks and fuzzy logic to evaluate aquatic ecological risk. International Journal of Environmental Science and Development 4, 419-424.
134. Loucks D.P., 2000. Sustainable Water Resources Management. Water International 25, 3-10.

135. MacCormack R.W., 1969. The effect of viscosity in hypervelocity impact cratering. AIAA (American Institute of Aeronautics and Astronautics) Paper 69-354.
136. Maddock I., 1999. The importance of physical habitat assessment for evaluating river health. Freshwater Biology 41, 373-391.
137. Maki-Petäys A., Muotka T., Huusko A., Tikkanen P., Kreivi P., 1997. Seasonal changes in habitat use and preference by juvenile brown trout, Salmo trutta, in a northern boreal river. Canadian Journal of Fisheries and Aquatic Sciences 54, 520-530.
138. Mamdani E.H., Assilian S., 1975. An experiment in linguistic synthesis with a fuzzy logic Controller. International Journal of Man-Machine Studies 7, 1-13.
139. McCullagh P., Nelder J.A., 1989. Generalized Linear Models. 2nd edition. Chapman & Hall, London, UK.
140. Mechleri B.D., 2008. Hydrological simulations in river basins with limited data availability. M.Sc. Thesis. University of Patras, School of Civil Engineering, Patras, Greece (in Greek).
141. Melo A.S., Niyogi D.K., Matthaei C.D., Townsend C.R., 2003. Resistance, resilience, and patchiness of invertebrate assemblages in native tussock and pasture streams in New Zealand after a hydrological disturbance. Canadian Journal of Fisheries and Aquatic Sciences 60, 731–739.
142. Mérigoux S., Dolédec S., 2004. Hydraulic requirements of stream communities: a case study on invertebrates. Freshwater Biology 49, 600-613.
143. Mesa L.M., 2010. Effect of spates and land use on macroinvertebrate community in Neotropical Andean streams. Hydrobiologia 641, 85-95.
144. Milhous R.T., Updike M.A., Schneider D.M., 1989. Physical Habitat Simulation System Reference Manual-version II. U.S. Fish and Wildlife Service Biological Report 89 (16), Washington DC, USA.
145. Milhous R.T., Waddle J.T., 2012. Physical Habitat Simulation (PHABSIM) Software for Windows (v.1.5.1). USGS Fort Collins Science Center. Fort Collins, USA.
146. Ministry of Environment, Energy and Climate Change, 2011. Report 196978/2011. FEK518/B/5/04/2011.
147. Monk W.A., Wood P.J., Hannah D.M., Wilson D.A., Extence C.A., Chadd R.P., 2006. Flow variability and macroinvertebrate community response within riverine systems. River Research and Applications 22, 595-615.
148. Moyle P.B., Williams J.G., Kiernan J.D., 2011. Improving environmental flow methods used in California. Federal Energy Regulatory Commission Relicensing. California Energy Commission, PIER. CEC-500-2011-037, California, USA.
149. Mouton A.M., Alcaraz-Hernández J.D., De Baets B., Goethals P.L.M., Martínez-Capel F., 2011. Data-driven fuzzy habitat suitability models for brown trout in Spanish Mediterranean rivers. Environmental Modelling and Software. 26, 615-622.
150. Mouton A.M., De Baets B., Goethals P.L.M., 2009. Knowledge-based versus data-driven fuzzy habitat suitability models for river management. Environmental Modelling and Software 24, 982-993.
151. Mundahl N.D., Hunt A.M., 2011. Recovery of stream invertebrates after catastrophic flooding in southeastern Minnesota, USA. Journal of Freshwater Ecology 26, 445-457.
152. Muñoz-Mas R., Papadaki Ch., Martínez-Capel F., Zogaris S., Ntoanidis L., Dimitriou E., 2016. Generalized additive and fuzzy models in environmental flow assessment: A comparison employing the West Balkan trout (*Salmo farioides*; Karaman, 1938). Ecological Engineering 91, 365-377.
153. Muñoz-Mas R., Martínez-Capel F., Schneider M., Mouton A.N., 2012. Assessment of brown trout habitat suitability in the Jucar River Basin (SPAIN): Comparison of data-driven approaches with fuzzy-logic models and univariate suitability curves. Science of the Total Environment 440, 123-131.

154. NRCS (Natural Resources Conservation Service), 2012. Chapter 14 - Stage Discharge Relations. Part 630 Hydrology, National Engineering Handbook. Natural Resources Conservation Service, Washington DC, USA.
155. Negishi, N.J., Richardson, J.S., 2006. An experimental test of the effects of floods resources and hydraulic refuge on patch colonization by stream macroinvertebrates during spates. Journal of Animal Ecology 75, 118–129.
156. Nikghalb S., Shokoohi A., Singh V.P., Yu R., 2016. Ecological regime versus minimum environmental flow: comparison of results for a river in a semi Mediterranean region. Water Resources Management 30, 4969-4984.
157. Nolan K.M., Shields R.R., 2000. Measurement of stream discharge by wading. US Geological Survey. Water Resources Investigation Report 00-4036 (CD-ROM).
158. Nykanen M., Huusko A., Maki-Petays A., 2001. Seasonal changes in the habitat use and movements of adult European grayling in a large subarctic river. Journal of Fish Biology 58, 506-519.
159. Olden J.D., Lawler J.J., Poff N.L., 2008. Machine learning methods without tears: a primer for ecologists. Quarterly Review of Biology 83, 171–193.
160. Orth D.J., 1987. Ecological considerations in the development and application of instream flow habitat models. Regulated Rivers: Research and Management 1, 171-181.
161. OWRB (Oklahoma Water Resources Boards), 2011. Instream Flow Issues & Recommendations. Oklahoma Comprehensive Water Plan Supplemental Report, Oklahoma, USA.
162. Papadaki C., Soulis K., Ntoanidis L., Zogaris S., Dercas N., Dimitriou E., 2017. Comparative assessment of environmental flow estimation methods in a Mediterranean mountain river. Environmental Management 60, 280-292.
163. Papadaki C., Soulis K., Muñoz-Mas R., Martinez-Capel F., Zogaris S., Ntoanidis L., Dimitriou E., 2016. Potential impacts of climate change on flow regime and fish habitat in mountain rivers of the south-western Balkans. Science of the Total Environment 540, 418-428.
164. Pastuchova Z., Greskova A., Lehotsky M., 2010. Spatial distribution pattern of macroinvertebrates in relation to morphohydraulic habitat structure: Perspectives for ecological stream assessment. Polish Journal of Ecology 58, 347-360.
165. Patsia A., Lazaridou, M., 2011. Water quality through the Directive 2000/60 E.C.: Guide for benthic invertebrates of running waters of Greece. ION, Athens, Greece.
166. Pearl J., 1988. Probabilistic reasoning in intelligent systems: Networks of plausible inference. Morgan Kaufmann, California, USA.
167. Peters J., De Baets B., Verhoest N.E.C., Samson R., Degroeve S., De Becker P., Huybrechts W., 2007. Random forests as a tool for ecohydrological distribution modelling. Ecological Modeling 207, 304-318.
168. Pilière A., Schipper A.M., Breure A.M., Posthuma L., De Zwart D., Dyer S.D., Huijbregts M.A.J., 2014. Comparing responses of freshwater fish and invertebrate community integrity along multiple environmental gradients. Ecological Indicators 43, 215–226.
169. Pitt J., Kendy E., 2017. Shaping the 2014 Colorado River Delta pulse flow: rapid environmental flow design for ecological outcomes and scientific learning. Ecological Engineering 106, 704-714.
170. Poff N.L., Richter B., Arthington A.H., Bunn S.E., Naiman R.J., Kendy E., Acreman M., Apse C., Bledsoe B.P., Freeman M., Henriksen J., Jacobson R.B., Kennen J., Merritt D.M., O'Keeffe J., Olden J.D., Rogers K., Tharme R.E., Warner A., 2010. The Ecological Limits of Hydrologic Alteration (ELOHA): a new framework for developing regional environmental flow standards. Freshwater Biology 155, 147-170.

171. Poff N.L., Zimmerman J.K.H., 2010. Ecological responses to altered flow regimes: a literature review to inform the science and management of environmental flows. Freshwater Biology 55, 194-205.
172. Pritchard P.J., 2011. Fox and McDonald's introduction to fluid mechanics. John Wiley & Sons, USA.
173. Quinn G.P., Keough M.J., 2002. Experimental design and data analysis for biologists. Cambridge University Press, New York, USA.
174. R Core Team 2014. R: A language and environment for statistical computing. R Foundation for Statistical Computing. Vienna. Austria. http://www.R-project.org/ [last accessed 30 Aug 2018].
175. Recknagel F., 2001. Applications of machine learning to ecological modelling. Ecological Modeling 146, 303-310.
176. Rempel L.L., Richardson J.S., Healey M.C., 1999. Flow refugia for benthic macroinvertebrates during flooding of a large river. Journal of the North American Benthological Society 18, 34-48.
177. Richter B.D., Baumgartner J.V., Powell J., Braun D.P., 1996. A method for assessing hydrologic alteration within ecosystems. Conservation Biology 10, 1163-1174.
178. Rivaes R., Boavida I., Santos J.M., Pinheiro A.N., Ferreira T., 2017. Importance of considering riparian vegetation requirements for the long-term efficiency of environmental flows. Hydrology and Earth System Sciences 21, 5763-5780.
179. Ronan T., Qi Z., Naegle K.M., 2016. Avoiding common pitfalls when clustering biological data. Science Signaling 9(432), re6.
180. Rosenberg D.M., Resh V.H., 1993. Freshwater biomonitoring and benthic macroinvertebrates. Chapman & Hall, New York, USA.
181. Ross T.J., 2010. Fuzzy logic with engineering applications. 3rd edition. John Wiley & Sons, UK.
182. Rosser Z.C., Pearson R.G., 1995. Responses of rock fauna to physical disturbance in two Australian tropical rainforest streams. Journal of the North American Benthological Society 14, 183-196.
183. Rydgren K., Økland R.H., Økland T., 2003. Species response curves along environmental gradients: a case study from SE Norwegian swamp forests. Journal of Vegetation Science 14, 869–880.
184. Schneider M., Noack M., Gebler T., Kopecki I., 2010. Handbook for the Habitat Simulation Model CASiMiR, Module CASiMiR, Base Version. http://www.casimir-software.de/ENG/download_eng.html [last accessed 30 Aug 2018].
185. Schneider M., Jorde K., Zöllner F., Kerle F., 2001. Development of a user-friendly software for ecological investigations on river systems, integration of a fuzzy rule-based approach. Proceedings of the 15th International Symposium, Informatics for Environmental Protection, ETH Zurich, Switzerland.
186. Shearer K.A., Hayes J.W., Jowett I.G., Olsen D.A., 2015. Habitat suitability curves for benthic macroinvertebrates from a small New Zealand river. New Zealand Journal of Marine and Freshwater Research 49, 178-191.
187. Shokoohi A., Amini M., 2014. Introducing a new method to determine rivers' ecological water requirement in comparison with hydrological and hydraulic methods. International Journal of Environmental Science Technology 11, 747-756.
188. Skoulikidis N.Th., Vardakas L., Karazouzas I., Economou A.N., Dimitriou E., Zogaris S., 2011. Assessing water stress in Mediterranean lotic systems: Insights from an artificially intermittent river in Greece. Aquatic Sciences 73, 581-597.
189. Solans M.A., Jalón D., 2016. Basic tools for setting environmental flows at the regional scale: application of the ELOHA framework in a Mediterranean river basin. Ecohydrology 9, 1517-1538.

190. Spense R., Hickley P., 2000. The use of PHABSIM in the management of water resources and fisheries in England and Wales. Ecological Engineering 16, 153-158.
191. Stamou A., Polydera A., Papadonikolaki G., Martínez-Capel F., Muñoz-Mas R., Papadaki Ch., Zogaris S., Bui M.D., Rutschmann P., Dimitriou E., 2018. Determination of environmental flows in rivers using an integrated hydrological-hydrodynamic-habitat modelling approach. Journal of Environmental Management 209, 273-285
192. Stamou A.I., Rutschmann P., 2011. Teaching simple water quality models. Education for Chemical Engineers 6, 132-141.
193. Steffler P., Blackburn J., 2002. River 2D: Two-Dimensional Depth Averaged Model of River Hydrodynamics and Fish Habitat. Introduction to Depth Averaged Modelling and User's Manual. University of Alberta, Canada.
194. Stephenson J.M., Morin A., 2009. Covariation of stream community structure and biomass of algae, invertebrates and fish with forest cover at multiple spatial scales. Freshwater Biology 54, 2139-2154.
195. Studdert E.W., Johnson J.H., 2015. Seasonal variation in habitat use of juvenile steelhead in a tributary of Lake Ontario. Northeastern Naturalist 22, 717-729.
196. Suarez M.L., Sanchez-Montoya M.M., Gomez R., Arce M.I., Del Campo R., Vidal-Abarca M.R., 2017. Functional response of aquatic invertebrate communities along two natural stress gradients (water salinity and flow intermittence) in Mediterranean streams. Aquatic Sciences 79, 1-12.
197. Sundermann A., Gerhardt M., Kappes H., Haase P., 2013. Stressor prioritization in riverine ecosystems: Which environmental factors shape benthic invertebrate assemblage metrics? Ecological Indicators 27, 83-96.
198. Sun Y., Kamel M.S., Wong A.K.C., Wang Y., 2007. Cost-sensitive boosting for classification of imbalanced data. Pattern Recognition 40, 3358-3378.
199. Sun Y., Wong A.K.C., Kamel M.S., 2009. Classification of imbalanced data: a review. International Journal of Pattern Recognition and Artificial Intelligence 23, 687-719.
200. Tachet H., Richoux P., Bournaud M., Usseglio-Polatera P., 2010. Invertebres d'eau douche: systematique, biologie, ecologie. CNRS, Paris, France.
201. Tare V., Gurjar S.K., Mohanta H., Kapoor V., Modi A., Mathur R.P., Sinha, R. (2017). Eco-geomorphological approach for environmental flows assessment in monsoon-driven highland rivers: A case study of upper Ganga, India. Journal of Hydrology: Regional Studies 13, 110-121.
202. Tennant D.L., 1976. Instream flow regimens for fish, wildlife, recreation and related environmental resources. Fisheries 1, 6-10.
203. Tharme R.E., 2003. A global perspective on environmental flow assessment: Emerging trends in the development and application of environmental flow methodologies for rivers. River Research and Applications 19, 397-441.
204. Theodoropoulos C., Vourka A., Skoulikidis N., Rutschmann P., Stamou A., 2018a. Evaluating the performance of habitat models for predicting the environmental flow requirements of benthic macroinvertebrates. Journal of Ecohydraulics (in press). DOI: 10.1080/24705357.2018.1440360.
205. Theodoropoulos C., Skoulikidis N., Rutschmann P., Stamou A., 2018b. Ecosystem-based environmental flow assessment in a Greek regulated river with the use of 2D hydrodynamic habitat modelling. River Research and Applications 34, 538-547.
206. Theodoropoulos C., Vourka A., Stamou A., Rutschmann P., Skoulikidis N., 2017. Response of freshwater macroinvertebrates to rainfall-induced high flows: A hydroecological approach. Ecological Indicators 73, 432-442.
207. Theodoropoulos C., Skoulikidis N., Stamou A., 2016. Habfuzz: A tool to calculate the instream hydraulic habitat suitability using fuzzy logic and fuzzy Bayesian inference. Journal of Open Source Software 1(6), 82. DOI:10.21105/joss.00082.

208. Theodoropoulos C., Papadonikolaki G., Stamou A., Bui M.D., Rutschmann P., Skoulikidis N., 2015a. A methodology for the determination of environmental flow releases from dams based on hydrodynamic habitat modelling and benthic macroinvertebrates. Proceedings of the 14th International Conference on Environmental Science & Technology. 3-5 Sep 2015. Rhodes, Greece.
209. Theodoropoulos C., Aspridis D., Iliopoulou-Georgudaki J., 2015b. The influence of land use on freshwater macroinvertebrates in a regulated and temporary Mediterranean river network. Hydrobiologia 751, 201-213.
210. Theodoropoulos C., Iliopoulou-Georgudaki J., 2010. Response of biota to land use changes and water quality degradation in two-medium sized river basins in southwestern Greece. Ecological Indicators 10, 1231-1238.
211. Tirelli T., Pessani D., 2009. Use of decision tree and artificial neural network approaches to model presence/absence of *Telestes muticellus* in Piedmont (North-Western Italy). River Research Applications 25, 1001-1012.
212. Tonina D., Jorde K., 2013. Hydraulic modeling approaches for ecohydraulics studies: 3D, 2D, 1D and non-numerical modeling. In Maddock I., Harby A., Kemp P., Wood P. (Eds): Ecohydraulics: An Integrated Approach. John Wiley & Sons, Chichester, UK.
213. USACE, 2016. HEC-RAS river analysis system. User's manual, version 5.0. U.S. Army Corps of Engineers, Institute of Water Resources, Davis, US.
214. Van Broekhoven E., Adriaenssens V., De Baets B., Verdonschot P.F.M., 2006. Fuzzy rule-based macroinvertebrate habitat suitability models for running waters. Ecological Modeling 198, 71-84.
215. Van de Bund W., Cardoso A.C., Heiskanen A.S., Noges P., 2004. Overview of common intercalibration types and guidelines for the selection of intercalibration sites. Ecostat WG 2.A, Version 5.1.
216. Vezza P., Muñoz-Mas R., Martínez-Capel F., Mouton A., 2015. Random forests to evaluate biotic interactions in fish distribution models. Environmental Modelling and Software 67, 173-183.
217. Vismara R., Azzellino A., Bosi R., Crosa A., Gentili G., 2001. Habitat suitability curves for brown trout (*Salmo trutta fario* L.) in the river Adda, Northern Italy: Comparing univariate and multivariate approaches. Regulated Rivers: Research and Management 17, 37-50.
218. Waddle T.J., 2001. PHABSIM for Windows User's Manual and Exercises. U.S. Geological Survey Open-File Report 2001-340.
219. Waddle T.J., Holmquist J.G., 2013. Macroinvertebrate response to flow changes in a subalpine stream: Predictions from two-dimensional hydrodynamic models. River Research and Applications 29, 366-379.
220. Wageningen Software Labs, 2004. Manual for AQEM European Stream Assessment Program version 2.3. http://www.fliessgewaesserbewertung.de/downloads/aqem_assessment_software_manual_english_2_3.pdf [last accessed 30 Aug 2018].
221. Waite I.R., Kennen J.G., May J.T., Brown L.R., Cuffney T.F., Jones K.A., Orlando J.L., 2014. Stream Macroinvertebrate Response Models for Bioassessment Metrics: Addressing the Issue of Spatial Scale. PLoS ONE 9(3), e90944. DOI:10.1371/journal.pone.0090944.
222. Wallace J.B., Merritt R.W., 1980. Filter-feeding ecology of aquatic insects. Annual Review of Entomology 25, 103-132.
223. WFD CIS Guidance Document No. 10. Rivers and Lakes - Typology, Reference Conditions and Classification Systems. Directorate General Environment of the European Commission, Brussels, ISBN No. 92-894-5614-0, ISSN No. 1725-1087.
224. WFD CIS Guidance Document No. 31, 2015. Ecological flows in the implementation of the Water Framework Directive. Directorate General Environment of the European Commission, Brussels, ISBN No. 978-92-79-45758-6, ISSN No. 1725-1087.

225. Wickham H, Winston C., 2016. ggplot2: An Implementation of the Grammar of Graphics. https://CRAN.R-project.org/package=ggplot2 [last accessed 30 Aug 2018].
226. Ye Z., Shen Y., Chen Y., 2012. Multiple methods for calculating minimum ecological flux of the desiccated Lower Tarim River, Western China. Ecohydrology 6, 1040-1047.
227. Yi Y., Cheng X., Yang Z., Wieprecht S., Zhang S., Wu Y., 2017. Evaluating the ecological influence of hydraulic projects: A review of aquatic habitat suitability models. Renewable and Sustainable Energy Reviews 68, 748-762.
228. Zadeh L.A., 1965. Fuzzy sets. Information and Control 8, 338–353.
229. Zhang Q., Xiao M.Z., Liu C.L., Singh V.P., 2014. Reservoir-induced hydrological alterations and environmental flow variation in the East River, the Pearl River basin, China. Stochastic Environmental Research and Risk Assessment 28, 2119-2131.

Appendix

Table A1

Characteristics of the 142 sampled microhabitats (MHs) used in the analysis of chapter 2. 1-80, pre-impact MHs; 81-142, post-impact MHs

Sample	1	2	3	4	5	6	7	8	9	10	11	12	13	14	15	16	17	18	19	20
S	LG	LS	BO	SS	BO	LS	LG	SS	FG	SAND	LG	BO	LS	LS	SS	LS	LS	SS	BO	LG
D (m)	0.14	0.18	0.16	0.2	0.18	0.24	0.18	0.17	0.27	0.2	0.37	0.24	0.37	0.27	0.09	0.36	0.28	0.24	0.18	0.13
V (m/s)	0.42	0.6	0.14	0.24	0.16	0.06	0.24	0.23	0.01	0	0.09	0.05	0.37	0.13	0.13	0.06	0.03	0.62	0.34	0.29
Sample	21	22	23	24	25	26	27	28	29	30	31	32	33	34	35	36	37	38	39	40
S	BO	SS	LS	LG	SS	BO	LS	BO	LS	LG	SS	LS	BO	LS	BO	SS	LG	LS	SS	LG
D (m)	0.09	0.12	0.07	0.04	0.21	0.24	0.18	0.18	0.24	0.15	0.24	0.09	0.14	0.07	0.22	0.17	0.11	0.2	0.07	0.14
V (m/s)	0	0.13	0.03	0.33	0.05	0	0	0	0.09	0	0.09	0.75	0.05	0.19	0.01	0.15	0.21	0	0.27	0.08
Sample	41	42	43	44	45	46	47	48	49	50	51	52	53	54	55	56	57	58	59	60
S	LS	BO	SS	LS	SAND	BO	LS	LS	BO	LS	LS	LS	SS	BO	BO	LS	SS	BO	LG	LG
D (m)	0.44	0.24	0.54	0.64	0.37	0.66	0.8	0.18	0.23	0.18	0.24	0.26	0.29	0.62	0.42	0.38	0.04	0.06	0.12	0.17
V (m/s)	0.15	0	0.11	0.06	0	0.03	0.15	0.32	0.25	0.51	0.12	0.46	0.07	0.13	0.02	0.2	0.34	0.49	0.41	0.27
Sample	61	62	63	64	65	66	67	68	69	70	71	72	73	74	75	76	77	78	79	80
S	LS	SS	LG	BO	SS	MG	MG	SS	BO	SS	LG	LS	BO	LS	LS	BO	LS	MG	SS	BO
D (m)	0.21	0.26	0.34	0.18	0.44	0.21	0.11	0.21	0.25	0.48	0.16	0.16	0.14	0.21	0.53	0.18	0.32	0.14	0.1	0.31
V (m/s)	0.38	0.08	0.27	0	0.67	0.54	0	0.15	0.05	0.47	0.48	0.58	0.46	0.62	0.1	0.08	0.6	0.41	0.38	0.05
Sample	81	82	83	84	85	86	87	88	89	90	91	92	93	94	95	96	97	98	99	100
S	LS	SS	LG	SS	LS	LG	LS	LS	LG	SS	LS	BO	LS	SS	LS	BO	SS	SS	LG	LG
D (m)	0.53	0.43	0.4	0.38	0.45	0.36	0.42	0.35	0.48	0.33	0.09	0.18	0.34	0.25	0.26	0.29	0.09	0.2	0.15	0.21
V (m/s)	0.48	0.51	0.47	0.55	0.46	0.74	0.68	0.33	0.28	0.07	0.26	0.3	0.2	0.27	0.19	0.35	0.59	0.27	0.01	0.08
101	102	103	104	105	106	107	108	109	110	111	112	113	114	115	116	117	118	119	120	121
BO	LS	BO	SS	LG	LG	SS	BO	SS	SS	BO	SS	LS	LS	LS	SS	SS	LS	LS	LS	SS
0.14	0.27	0.14	0.4	0.41	0.37	0.44	0.2	0.5	0.39	0.24	0.21	0.53	0.16	0.2	0.33	0.17	0.35	0.22	0.08	0.25
0.72	0.85	0	0.45	0.42	0.28	0.32	0	0.88	0.64	0	0.34	0.14	0.48	0.21	0.82	0.51	0.49	0.4	1.17	1.28
122	123	124	125	126	127	128	129	130	131	132	133	134	135	136	137	138	139	140	141	142
SS	SS	BO	LS	LS	BO	SS	SS	LS	LS	FG	LS	SS	LS	LS	SS	BO	BO	LS	SS	LS
0.11	0.44	0.26	0.43	0.14	0.34	0.14	0.36	0.39	0.4	0.07	0.4	0.43	0.37	0.16	0.26	0.34	0.25	0.27	0.17	0.23
0.66	0.75	0.23	1.65	0.2	0.03	0.13	0.32	0.7	0.73	0	0.27	0.92	0.27	0.49	0.43	0.08	0.13	0.33	0.18	0.39

Table A2

T-test results for the macroinvertebrate metrics before and after the high flow event (chapter 2).

Metrics	df	Sig. (2-tailed)
N Taxa	98.269	<0.000001
EPT Taxa	85.173	<0.000001
Shannon's Diversity Index	69.699	<0.000001
% Grazers and scrapers	65.882	0.000026
% Miners	137.798	<0.000001
% Shredders	140	0.001000
% Gatherers/Collectors	66.571	<0.000001
% Active filter feeders	135.528	<0.000001
% Passive filter feeders	107.845	0.044000
% Predators	76.562	0.049960
% Parasites	126.689	<0.000001

Table A3

Independent sample t-test results of chapter 2 for the macroinvertebrate metrics per substrate. Metrics with statistically significant differences ($p<0.05$) between the pre- and post-impact samples are indicated in bold.

Metrics	Boulders		Large stones		Large gravel	
	df	Sig. (2-tailed)	df	Sig. (2-tailed)	df	Sig. (2-tailed)
Abundance	27.5	**0.000017**	37.3	**<0.000001**	15.5	**0.000031**
No. of taxa	28	**0.001000**	35.3	**0.000013**	17	**0.000214**
EPT taxa	28	**0.004900**	30.9	**0.000800**	7.8	**0.009000**
Shannon's Diversity Index	10.1	0.180000	25.9	**0.001900**	6.2	**0.041000**
% Grazers/ scrapers	9.6	0.086000	24.3	**0.041000**	6.4	0.592000
% Miners	27.6	**0.000074**	41.8	**0.000070**	17	0.346000
% Shredders	28	0.844000	46	**0.042000**	17	0.173000
% Gatherers/ collectors	9.4	**0.004000**	23.9	**0.005000**	17	0.364000
% Active filter feeders	28	**0.000222**	40	**0.000060**	17	0.196000
% Passive filter feeders	28	**0.056000**	46	0.107000	13.2	0.483000
% Predators	10.5	0.530000	28.6	0.134000	6.9	0.432000
% Parasites	27.7	**0.000071**	32.3	**0.000010**	17	0.357000

Table A4

Characteristics of the simplified BRT models developed in chapter 2.

Metrics	Bag fraction	Learning rate	No of trees	No of variables	McFadden's pseudo – R^2*
Abundance	0.5	0.002	1550	4	0.68
N Taxa	0.5	0.002	2300	5	0.57
EPT taxa	0.5	0.002	3800	5	0.61
Shannon's Diversity Index	0.5	0.002	2650	4	0.66

* pseudo-R^2 = 1 - (residual deviance/total deviance)

Table A5. Detailed characteristics of the 380 microhabitats sampled over three seasons during 2015 in nine reference sites in Greece. EPT: Ephemeroptera, Plecoptera, Trichoptera; SW: Shannon-Wiener diversity index. For substrate classes abbreviations see chapter 3.

Sample No.	Site No.	Site name	Sample code	Sampling date	No. taxa	No. EPT taxa	SW diversity	Abundance	Water temperature (°C)	Substrate (Abbr.)	Substrate (No.)	Depth (m)	Average flow velocity (m/s)	Suitability (κ)
1	1	Fouskari	FouSp1	09-05-15	14	7	2.29	48	18.4	SS	0.04	0.32	0.59	0.806
2	1	Fouskari	FouSp2	09-05-15	9	6	1.684	46	18.3	BO	0.07	0.26	0.03	0.590
3	1	Fouskari	FouSp3	09-05-15	8	3	1.802	21	19.1	SS	0.04	0.57	0.25	0.496
4	1	Fouskari	FouSp4	09-05-15	13	8	1.928	101	19.3	BO	0.07	0.1	0.55	0.809
5	1	Fouskari	FouSp5	09-05-15	8	5	1.874	20	18.3	SS	0.04	0.15	0.18	0.544
6	1	Fouskari	FouSp6	09-05-15	6	3	1.586	13	18.8	BO	0.07	0.38	1.07	0.414
7	1	Fouskari	FouSp7	09-05-15	11	4	1.341	95	19.1	LS	0.05	0.17	0	0.602
8	1	Fouskari	FouSp8	09-05-15	15	9	2.379	49	19.1	SS	0.04	0.17	0.3	0.881
9	1	Fouskari	FouSp9	09-05-15	16	10	2.267	62	19.3	BO	0.07	0.23	0.37	0.924
10	1	Fouskari	FouSp10	09-05-15	11	5	2.085	26	19.2	LG	0.03	0.22	0.04	0.647
11	1	Fouskari	FouSp11	09-05-15	12	7	2.054	65	18.1	LG	0.03	0.08	0.54	0.746
12	1	Fouskari	FouSp12	09-05-15	8	5	1.682	21	19	BO	0.07	0.39	0.15	0.521
13	1	Fouskari	FouSp13	09-05-15	13	7	1.923	88	18.8	LG	0.03	0.08	0.16	0.776
14	1	Fouskari	FouSp14	09-05-15	5	0	1.378	13	18.3	MG	0.026	0.16	0.02	0.304
15	1	Fouskari	FouSp15	09-05-15	12	5	2.13	47	18.2	SS	0.04	0.4	0.6	0.697
16	1	Fouskari	FouSp16	09-05-15	12	7	2.067	62	20.3	LG	0.03	0.17	0.66	0.744
17	1	Fouskari	FouSp17	09-05-15	17	9	2.292	98	19.6	SS	0.04	0.21	0.32	0.966
18	1	Fouskari	FouSp18	09-05-15	8	4	1.803	20	20.7	LG	0.03	0.27	0.41	0.515
19	1	Fouskari	FouSp19	09-05-15	8	5	1.53	26	19.3	SS	0.04	0.33	0.48	0.507
20	1	Fouskari	FouSp20	09-05-15	6	3	1.498	10	20	LG	0.03	0.08	0.16	0.400
21	3	Ag. Dimitrios	AgDSp1	16-05-15	11	7	1.881	66	14	LS	0.05	0.07	0.08	0.632
22	3	Ag. Dimitrios	AgDSp2	16-05-15	11	6	1.433	241	14	BO	0.07	0.13	0.15	0.590
23	3	Ag. Dimitrios	AgDSp3	16-05-15	13	8	1.704	166	14	SS	0.04	0.2	0.51	0.690
24	3	Ag. Dimitrios	AgDSp4	16-05-15	9	6	1.512	104	13.9	LS	0.05	0.24	0.18	0.529
25	3	Ag. Dimitrios	AgDSp5	16-05-15	9	5	1.512	29	14	LG	0.03	0.1	0.34	0.495
26	3	Ag. Dimitrios	AgDSp6	16-05-15	7	5	1.489	85	14	BO	0.07	0.25	0	0.462

27	3	Ag. Dimitrios	AgDSp7	16-05-15	15	9	2.182	101	14.1	LG	0.03	0.11	0.09	0.801
28	3	Ag. Dimitrios	AgDSp8	16-05-15	10	6	1.539	71	14.2	SS	0.04	0.21	0.88	0.547
29	3	Ag. Dimitrios	AgDSp9	16-05-15	5	4	1.16	16	14.3	FG	0.024	0.22	0.07	0.341
30	3	Ag. Dimitrios	AgDSp10	16-05-15	10	6	1.837	108	14.3	LS	0.05	0.26	0.22	0.596
31	3	Ag. Dimitrios	AgDSp11	16-05-15	9	6	1.663	113	14.4	LG	0.03	0.15	0.85	0.552
32	3	Ag. Dimitrios	AgDSp12	16-05-15	19	11	1.918	458	14.6	BO	0.07	0.12	0	0.964
33	3	Ag. Dimitrios	AgDSp13	16-05-15	19	8	1.927	211	14.6	LG	0.03	0.17	0.23	0.856
34	3	Ag. Dimitrios	AgDSp14	16-05-15	12	7	1.657	131	14.7	LS	0.05	0.26	0.65	0.636
35	3	Ag. Dimitrios	AgDSp15	16-05-15	10	7	1.29	75	14.8	BO	0.07	0.28	0.27	0.532
36	3	Ag. Dimitrios	AgDSp16	16-05-15	7	4	1.29	65	14.9	FG	0.024	0.42	0.48	0.412
37	3	Ag. Dimitrios	AgDSp17	16-05-15	12	8	1.903	138	15.3	SS	0.04	0.18	0.74	0.690
38	3	Ag. Dimitrios	AgDSp18	16-05-15	14	7	1.662	140	15.4	SS	0.04	0.23	0.82	0.681
39	3	Ag. Dimitrios	AgDSp19	16-05-15	14	10	1.858	174	15.3	BO	0.07	0.25	1.08	0.770
40	3	Ag. Dimitrios	AgDSp20	16-05-15	11	8	1.452	167	15.3	SS	0.04	0.37	0.65	0.613
41	4	Parapeiros_W	ParWSp1	17-05-15	10	6	1.811	44	17.9	SS	0.04	0.15	0.69	0.733
42	4	Parapeiros_W	ParWSp2	17-05-15	6	4	1.577	22	17.6	LS	0.05	0.16	0.66	0.512
43	4	Parapeiros_W	ParWSp3	17-05-15	12	7	1.934	118	17.8	BO	0.07	0.18	0.47	0.898
44	4	Parapeiros_W	ParWSp4	17-05-15	7	3	1.778	13	17.8	LS	0.05	0.26	0.16	0.531
45	4	Parapeiros_W	ParWSp5	17-05-15	12	6	1.62	88	18	BO	0.07	0.18	0.3	0.803
46	4	Parapeiros_W	ParWSp6	17-05-15	9	6	1.964	25	18.1	SS	0.04	0.26	0.19	0.709
47	4	Parapeiros_W	ParWSp7	17-05-15	9	5	1.747	33	18.3	BO	0.07	0.2	0.05	0.658
48	4	Parapeiros_W	ParWSp8	17-05-15	5	4	1.352	12	18.7	LG	0.03	0.11	0.13	0.446
49	4	Parapeiros_W	ParWSp9	17-05-15	8	5	1.858	16	18.6	LS	0.05	0.25	0.42	0.630
50	4	Parapeiros_W	ParWSp10	17-05-15	10	6	1.818	68	19	BO	0.07	0.22	0.01	0.755
51	4	Parapeiros_W	ParWSp11	17-05-15	5	2	1.55	7	19	LS	0.05	0.28	0.6	0.410
52	4	Parapeiros_W	ParWSp12	17-05-15	9	5	1.85	24	19.7	LG	0.03	0.19	0.16	0.664
53	4	Parapeiros_W	ParWSp13	17-05-15	5	4	1.433	14	19.4	LS	0.05	0.34	0.36	0.458
54	4	Parapeiros_W	ParWSp14	17-05-15	11	6	2.274	16	19.4	LS	0.05	0.26	0.68	0.799
55	4	Parapeiros_W	ParWSp15	17-05-15	9	6	2.083	21	19.7	LG	0.03	0.17	0.83	0.721
56	4	Parapeiros_W	ParWSp16	17-05-15	14	7	2.03	97	19.7	BO	0.07	0.23	0.44	0.950
57	4	Parapeiros_W	ParWSp17	17-05-15	6	4	1.609	10	19.9	LG	0.03	0.28	0.35	0.506
58	4	Parapeiros_W	ParWSp18	17-05-15	8	5	1.961	22	20	BO	0.07	0.26	0.45	0.649

59	4	Parapeiros_W	ParWSp19	17-05-15	7	4	1.838	22	20.3	LS	0.05	0.19	0.22	0.575
60	4	Parapeiros_W	ParWSp20	17-05-15	9	5	1.716	45	20.6	SS	0.04	0.17	0	0.665
61	5	Evinos_Up	EviSp1	11-05-15	5	4	1.128	14	13.6	SS	0.04	0.2	0.09	0.567
62	5	Evinos_Up	EviSp2	11-05-15	4	3	1.154	7	12.6	BO	0.07	0.36	0.81	0.484
63	5	Evinos_Up	EviSp3	11-05-15	2	1	0.693	2	12.5	LS	0.05	0.53	1.44	0.245
64	5	Evinos_Up	EviSp4	11-05-15	7	4	1.687	20	11.6	LG	0.03	0.08	0.25	0.768
65	5	Evinos_Up	EviSp5	11-05-15	2	2	0.679	12	11.8	LS	0.05	0.27	1.58	0.292
66	5	Evinos_Up	EviSp6	11-05-15	8	7	1.447	40	11.6	LS	0.05	0.13	0.64	0.898
67	5	Evinos_Up	EviSp7	11-05-15	4	3	1.332	5	11.5	BO	0.07	0.34	0.77	0.511
68	5	Evinos_Up	EviSp8	11-05-15	1	1	0	1	11.6	SS	0.04	0.16	0.00	0.075
69	5	Evinos_Up	EviSp9	11-05-15	5	4	1.263	15	11.7	LS	0.05	0.24	0.13	0.593
70	5	Evinos_Up	EviSp10	11-05-15	2	1	0.451	6	11.8	SS	0.04	0.33	0.80	0.210
71	5	Evinos_Up	EviSp11	11-05-15	3	2	1.04	4	13.9	LS	0.05	0.39	0.59	0.384
72	5	Evinos_Up	EviSp12	11-05-15	3	2	1.04	4	13	MG	0.026	0.13	0.01	0.384
73	5	Evinos_Up	EviSp13	11-05-15	2	2	0.637	3	13	BO	0.07	0.51	0.95	0.266
74	5	Evinos_Up	EviSp14	11-05-15	5	2	1.367	11	12.3	LG	0.03	0.36	0.54	0.546
75	5	Evinos_Up	EviSp15	11-05-15	5	3	1.465	9	12.1	LS	0.05	0.25	0.53	0.588
76	5	Evinos_Up	EviSp16	11-05-15	2	1	0.637	3	12.5	FG	0.024	0.24	0.01	0.237
77	5	Evinos_Up	EviSp17	11-05-15	3	2	1.036	11	12.3	BO	0.07	0.31	0.78	0.398
78	5	Evinos_Up	EviSp18	11-05-15	8	4	1.381	40	12.1	BO	0.07	0.28	0.06	0.801
79	5	Evinos_Up	EviSp19	11-05-15	9	7	1.4	47	12	LG	0.03	0.13	0.56	0.949
80	5	Evinos_Up	EviSp20	11-05-15	2	2	0.693	2	11.9	LS	0.05	0.19	0.00	0.274
81	6	Mornos_Up	MorSp1	10-05-15	7	5	1.946	7	15.3	SS	0.04	0.18	0.23	0.809
82	6	Mornos_Up	MorSp2	10-05-15	4	2	1.332	5	14.8	BO	0.07	0.28	0.1	0.474
83	6	Mornos_Up	MorSp3	10-05-15	1	1	0	1	14.6	BO	0.07	0.35	0.1	0.082
84	6	Mornos_Up	MorSp4	10-05-15	4	4	1.33	6	14.5	LG	0.03	0.38	0.33	0.534
85	6	Mornos_Up	MorSp5	10-05-15	1	1	0	2	14.8	LG	0.03	0.19	0	0.085
86	6	Mornos_Up	MorSp6	10-05-15	8	7	1.979	12	14.6	LS	0.05	0.32	0.5	0.936
87	6	Mornos_Up	MorSp7	10-05-15	5	3	1.55	7	14.8	LS	0.05	0.21	0.04	0.592
88	6	Mornos_Up	MorSp8	10-05-15	2	1	0.693	2	14.8	FG	0.024	0.03	0	0.240
89	6	Mornos_Up	MorSp9	10-05-15	7	3	1.636	14	14.8	LG	0.03	0.19	0.6	0.726
90	6	Mornos_Up	MorSp10	10-05-15	3	2	1.04	4	15.2	BO	0.07	0.15	0.1	0.377

91	6	Mornos_Up	MorSp11	10-05-15	2	1	0.5	10	14.9	SS	0.04	0.52	0.1	0.235
92	6	Mornos_Up	MorSp12	10-05-15	3	1	0.9	8	15.2	SAND	0.022	0.049	0.1	0.339
93	6	Mornos_Up	MorSp13	10-05-15	5	4	1.609	5	14.9	LS	0.05	0.58	0.41	0.623
94	6	Mornos_Up	MorSp14	10-05-15	6	2	1.27	33	15	SAND	0.022	0.08	0.04	0.650
95	6	Mornos_Up	MorSp15	10-05-15	3	2	1.04	4	15	BO	0.07	0.37	0.2	0.377
96	6	Mornos_Up	MorSp16	10-05-15	3	2	1.099	3	15	MG	0.026	0.14	0.01	0.383
97	6	Mornos_Up	MorSp17	10-05-15	3	2	1.04	4	14.9	LS	0.05	0.45	0.33	0.377
98	6	Mornos_Up	MorSp18	10-05-15	7	5	1.834	10	15	SS	0.04	0.18	0.56	0.801
99	6	Mornos_Up	MorSp19	10-05-15	8	5	1.951	13	14.9	LS	0.05	0.19	0.6	0.878
100	6	Mornos_Up	MorSp20	10-05-15	6	4	1.609	10	14.8	LG	0.03	0.14	0.24	0.688
101	7	Per06.1	Per06Sp1	12-05-15	8	6	1.87	37	10.3	LG	0.03	0.12	0.16	0.654
102	7	Per06.1	Per06Sp2	12-05-15	8	5	1.616	45	10.2	LS	0.05	0.37	0.39	0.596
103	7	Per06.1	Per06Sp3	12-05-15	10	7	1.947	30	10.1	BO	0.07	0.18	0.1	0.737
104	7	Per06.1	Per06Sp4	12-05-15	12	8	1.646	109	10.3	SS	0.04	0.19	0.7	0.807
105	7	Per06.1	Per06Sp5	12-05-15	13	9	1.717	116	10.3	LS	0.05	0.29	0.71	0.870
106	7	Per06.1	Per06Sp6	12-05-15	7	5	1.412	56	10	LS	0.05	0.23	0.71	0.544
107	7	Per06.1	Per06Sp7	12-05-15	7	5	1.666	86	10.6	LG	0.03	0.38	0.04	0.598
108	7	Per06.1	Per06Sp8	12-05-15	8	5	1.67	68	10.7	LS	0.05	0.36	0.39	0.616
109	7	Per06.1	Per06Sp9	12-05-15	12	7	1.909	82	10.5	SS	0.04	0.14	0.24	0.811
110	7	Per06.1	Per06Sp10	12-05-15	7	5	1.741	28	10.2	BO	0.07	0.26	0.32	0.580
111	7	Per06.1	Per06Sp11	12-05-15	14	7	1.663	170	11.2	BO	0.07	0.21	0.26	0.871
112	7	Per06.1	Per06Sp12	12-05-15	14	9	1.662	142	10.9	BO	0.07	0.27	1.11	0.902
113	7	Per06.1	Per06Sp13	12-05-15	5	2	0.908	47	10.7	LS	0.05	0.54	0.48	0.342
114	7	Per06.1	Per06Sp14	12-05-15	15	8	1.773	158	10.1	SS	0.04	0.23	0.4	0.931
115	7	Per06.1	Per06Sp15	12-05-15	13	9	1.159	181	10.7	BO	0.07	0.27	0.08	0.817
116	7	Per06.1	Per06Sp16	12-05-15	13	5	1.595	106	11.3	LS	0.05	0.23	1.01	0.757
117	7	Per06.1	Per06Sp17	12-05-15	10	7	1.565	92	10.8	LS	0.05	0.12	0.57	0.710
118	7	Per06.1	Per06Sp18	12-05-15	15	9	1.445	197	10.7	LS	0.05	0.26	0.38	0.923
119	7	Per06.1	Per06Sp19	12-05-15	11	9	1.606	119	10.3	MC	0.02	0.12	0.25	0.801
120	7	Per06.1	Per06Sp20	12-05-15	7	5	1.249	94	10.7	SS	0.04	0.24	0.63	0.538
121	8	SidePer10	SidePSp1	12-05-15	4	1	0.928	46	12.4	BO	0.07	0.61	0.69	0.392
122	8	SidePer10	SidePSp2	12-05-15	6	3	0.945	60	12.2	LG	0.03	0.76	0.495	0.560

123	8	SidePer10	SidePSp3	12-05-15	2	2	0.693	10	12.2	LG	0.03	0.87	0.485	0.295
124	8	SidePer10	SidePSp4	12-05-15	2	1	0.53	9	12.2	MG	0.026	0.48	0.09	0.224
125	8	SidePer10	SidePSp5	12-05-15	4	2	1.095	27	12.2	BO	0.07	0.68	0.42	0.457
126	8	SidePer10	SidePSp6	12-05-15	2	1	0.693	4	12.3	LS	0.05	0.42	1.42	0.253
127	8	SidePer10	SidePSp7	12-05-15	7	3	0.818	166	12.2	LS	0.05	0.28	0.94	0.614
128	8	SidePer10	SidePSp8	12-05-15	5	3	0.765	72	12.2	LS	0.05	0.22	1.01	0.491
129	8	SidePer10	SidePSp9	12-05-15	10	4	1.584	47	12.1	MG	0.026	0.22	0.3	0.877
130	8	SidePer10	SidePSp10	12-05-15	5	2	0.947	77	12.1	LS	0.05	0.08	0.62	0.487
131	8	SidePer10	SidePSp11	12-05-15	7	5	1.29	89	12	LS	0.05	0.19	0.2	0.756
132	8	SidePer10	SidePSp12	12-05-15	7	5	1.347	90	12.2	LS	0.05	0.21	0.86	0.767
133	8	SidePer10	SidePSp13	12-05-15	6	4	0.976	122	12.3	BO	0.07	0.26	0.19	0.628
134	8	SidePer10	SidePSp14	12-05-15	5	3	0.632	280	12.2	LS	0.05	0.23	0.85	0.540
135	8	SidePer10	SidePSp15	12-05-15	2	1	0.251	29	12.2	SAND	0.022	0.07	0	0.178
136	8	SidePer10	SidePSp16	12-05-15	4	3	0.861	59	12.1	LS	0.05	0.47	0.75	0.464
137	8	SidePer10	SidePSp17	12-05-15	9	4	0.873	209	12.1	SS	0.04	0.13	0.52	0.760
138	8	SidePer10	SidePSp18	12-05-15	4	3	0.922	84	12.2	BO	0.07	0.18	0	0.485
139	8	SidePer10	SidePSp19	12-05-15	5	3	1.144	77	12.2	SS	0.04	0.04	0.6	0.564
140	8	SidePer10	SidePSp20	12-05-15	7	3	1.38	28	12.3	BO	0.07	0.21	0.08	0.671
141	9	Spilia	SpilSp1	13-05-15	6	5	1.393	76	10.7	LS	0.05	0.21	0.81	0.751
142	9	Spilia	SpilSp2	13-05-15	7	4	1.541	39	10.7	SS	0.04	0.26	0.52	0.756
143	9	Spilia	SpilSp3	13-05-15	5	3	1.371	20	10.6	LG	0.03	0.34	0.49	0.586
144	9	Spilia	SpilSp4	13-05-15	6	5	1.335	62	10.8	BO	0.07	0.18	0	0.728
145	9	Spilia	SpilSp5	13-05-15	4	2	1.332	5	10.9	SS	0.04	0.44	1.08	0.488
146	9	Spilia	SpilSp6	13-05-15	5	3	0.913	69	10.8	MG	0.026	0.21	0.82	0.548
147	9	Spilia	SpilSp7	13-05-15	9	5	1.228	40	10.5	MG	0.026	0.11	0	0.823
148	9	Spilia	SpilSp8	13-05-15	8	5	1.44	74	11.1	SS	0.04	0.21	0.49	0.847
149	9	Spilia	SpilSp9	13-05-15	8	4	1.666	58	11.2	BO	0.07	0.25	0.64	0.839
150	9	Spilia	SpilSp10	13-05-15	3	2	0.986	23	11.3	SS	0.04	0.48	0.79	0.397
151	9	Spilia	SpilSp11	13-05-15	7	4	1.514	86	11.3	LG	0.03	0.16	0.48	0.793
152	9	Spilia	SpilSp12	13-05-15	9	6	1.446	112	11.5	LS	0.05	0.16	0.58	0.959
153	9	Spilia	SpilSp13	13-05-15	8	6	1.367	101	11.3	BO	0.07	0.14	0.46	0.891
154	9	Spilia	SpilSp14	13-05-15	6	4	1.518	36	11.3	LS	0.05	0.21	1.38	0.704

155	9	Spilia	SpilSp15	13-05-15	4	2	1.094	19	11.2	LS	0.05	0.53	0.45	0.458
156	9	Spilia	SpilSp16	13-05-15	8	6	1.441	48	11.3	BO	0.07	0.18	1.13	0.857
157	9	Spilia	SpilSp17	13-05-15	6	3	1.358	29	11.3	LS	0.05	0.32	1.22	0.636
158	9	Spilia	SpilSp18	13-05-15	4	3	1.186	25	11.5	MG	0.026	0.14	0.41	0.513
159	9	Spilia	SpilSp19	13-05-15	9	5	1.673	43	11.2	SS	0.04	0.1	0.38	0.905
160	9	Spilia	SpilSp20	13-05-15	6	4	0.904	58	11.1	BO	0.07	0.31	0.19	0.614
161	1	Fouskari	FouSu1	24-08-15	3	2	1.04	4	23.5	LG	0.03	0.3	0.36	0.324
162	1	Fouskari	FouSu2	24-08-15	8	4	1.895	22	22.7	LS	0.05	0.28	0.26	0.691
163	1	Fouskari	FouSu3	24-08-15	11	5	1.762	44	21.8	LS	0.05	0.27	0.21	0.809
164	1	Fouskari	FouSu4	24-08-15	3	2	1.04	4	21.7	LG	0.03	0.18	0.3	0.324
165	1	Fouskari	FouSu5	24-08-15	6	4	1.473	16	21.5	SS	0.04	0.61	0.46	0.555
166	1	Fouskari	FouSu6	24-08-15	4	2	1.277	7	21.5	SS	0.04	0.27	0.06	0.396
167	1	Fouskari	FouSu7	24-08-15	4	3	1.162	11	21.5	BO	0.07	0.37	0.3	0.408
168	1	Fouskari	FouSu8	24-08-15	2	1	0.693	2	21.6	SS	0.04	0.76	0	0.206
169	1	Fouskari	FouSu9	24-08-15	3	1	0.578	17	23	LG	0.03	0.34	0.88	0.228
170	1	Fouskari	FouSu10	24-08-15	2	2	0.287	12	22.3	BO	0.07	0.24	0.08	0.175
171	1	Fouskari	FouSu11	24-08-15	4	3	0.873	26	22.1	SS	0.04	0.19	0.75	0.369
172	1	Fouskari	FouSu12	24-08-15	6	4	1.447	17	22.8	SS	0.04	0.14	0.08	0.551
173	1	Fouskari	FouSu13	24-08-15	5	2	1.295	11	22.4	LS	0.05	0.14	0.6	0.434
174	1	Fouskari	FouSu14	24-08-15	9	6	1.697	63	23.1	SS	0.04	0.07	0.58	0.769
175	1	Fouskari	FouSu15	24-08-15	7	5	1.748	14	22.1	BO	0.07	0.22	0.07	0.659
176	1	Fouskari	FouSu16	24-08-15	12	6	1.754	57	22.4	SS	0.04	0.15	0.55	0.876
177	1	Fouskari	FouSu17	24-08-15	10	7	1.54	53	21.4	LG	0.03	0.16	0.19	0.802
178	1	Fouskari	FouSu18	24-08-15	12	6	1.718	215	21.7	BO	0.07	0.2	0.66	0.943
179	1	Fouskari	FouSu19	24-08-15	8	3	1.813	29	21.5	LG	0.03	0.09	0.12	0.653
180	1	Fouskari	FouSu20	24-08-15	8	3	1.235	82	20.9	LS	0.05	0.14	0.34	0.586
181	2	Krathis_Up	KrSu1	25-08-15	10	4	0.722	127	11.7	MG	0.026	0.26	0.29	0.582
182	2	Krathis_Up	KrSu2	25-08-15	4	2	0.325	82	11.9	LG	0.03	0.39	0.15	0.260
183	2	Krathis_Up	KrSu3	25-08-15	3	1	0.684	9	11.6	BO	0.07	0.21	0	0.238
184	2	Krathis_Up	KrSu4	25-08-15	10	3	1.795	28	12	LG	0.03	0.31	0.1	0.702
185	2	Krathis_Up	KrSu5	25-08-15	7	3	1.481	38	12.3	SAND	0.022	0.32	0.01	0.560
186	2	Krathis_Up	KrSu6	25-08-15	12	4	0.628	175	11.7	LS	0.05	0.13	0.43	0.643

187	2	Krathis_Up	KrSu7	25-08-15	9	3	0.341	322	12.2	LS	0.05	0.24	0.84	0.520
188	2	Krathis_Up	KrSu8	25-08-15	5	2	0.318	144	12	LS	0.05	0.2	0.77	0.309
189	2	Krathis_Up	KrSu9	25-08-15	9	4	1.669	52	12	SILT	0.02	0.24	0	0.686
190	2	Krathis_Up	KrSu10	25-08-15	13	7	0.778	207	12.4	BO	0.07	0.28	0.16	0.794
191	2	Krathis_Up	KrSu11	25-08-15	7	5	0.364	147	12	BO	0.07	0.22	0.19	0.465
192	2	Krathis_Up	KrSu12	25-08-15	10	5	0.703	136	11.7	SS	0.04	0.19	0.23	0.610
193	2	Krathis_Up	KrSu13	25-08-15	6	2	0.537	151	11.7	LS	0.05	0.22	0.1	0.378
194	2	Krathis_Up	KrSu14	25-08-15	4	3	0.535	161	12.1	LS	0.05	0.34	0.3	0.348
195	2	Krathis_Up	KrSu15	25-08-15	6	3	0.888	46	12.1	BO	0.07	0.05	0.13	0.433
196	2	Krathis_Up	KrSu16	25-08-15	11	4	1.305	104	11.9	SS	0.04	0.14	0.46	0.703
197	2	Krathis_Up	KrSu17	25-08-15	6	2	0.431	115	11.9	LG	0.03	0.16	0.14	0.350
198	2	Krathis_Up	KrSu18	25-08-15	12	5	1.614	78	11.9	LS	0.05	0.07	0.61	0.806
199	2	Krathis_Up	KrSu19	25-08-15	13	6	1.525	98	12.2	BO	0.07	0.16	0.22	0.857
200	2	Krathis_Up	KrSu20	25-08-15	5	3	0.169	174	12.2	BO	0.07	0.24	0.11	0.322
201	3	Ag. Dimitrios	AgDSu1	25-08-15	15	6	1.87	194	24	SS	0.04	0.13	1.03	0.838
202	3	Ag. Dimitrios	AgDSu2	25-08-15	9	5	1.401	110	23.9	MG	0.026	0.07	0.19	0.582
203	3	Ag. Dimitrios	AgDSu3	25-08-15	14	6	1.904	115	23.8	LS	0.05	0.1	0.07	0.803
204	3	Ag. Dimitrios	AgDSu4	25-08-15	15	7	1.722	481	23.6	LG	0.03	0.12	0.1	0.905
205	3	Ag. Dimitrios	AgDSu5	25-08-15	17	7	1.913	216	23.5	LS	0.05	0.09	0	0.925
206	3	Ag. Dimitrios	AgDSu6	25-08-15	15	5	2.052	151	23.3	LG	0.03	0.16	0.4	0.827
207	3	Ag. Dimitrios	AgDSu7	25-08-15	12	5	1.463	72	23.3	LS	0.05	0.08	0	0.654
208	3	Ag. Dimitrios	AgDSu8	25-08-15	13	4	1.72	189	23.5	MG	0.026	0.13	0.12	0.711
209	3	Ag. Dimitrios	AgDSu9	25-08-15	10	5	1.932	36	23.5	BO	0.07	0.17	0	0.668
210	3	Ag. Dimitrios	AgDSu10	25-08-15	17	5	1.997	211	23.4	LG	0.03	0.07	0.23	0.879
211	3	Ag. Dimitrios	AgDSu11	25-08-15	14	6	1.579	109	23.3	LG	0.03	0.06	0.27	0.754
212	3	Ag. Dimitrios	AgDSu12	25-08-15	16	7	1.709	163	23.2	LG	0.03	0.16	0.16	0.860
213	3	Ag. Dimitrios	AgDSu13	25-08-15	10	4	1.732	58	23.2	BO	0.07	0.31	0	0.615
214	3	Ag. Dimitrios	AgDSu14	25-08-15	13	5	1.861	158	23.2	SS	0.04	0.14	0.51	0.754
215	3	Ag. Dimitrios	AgDSu15	25-08-15	15	6	1.627	196	23.2	LS	0.05	0.14	0.09	0.803
216	3	Ag. Dimitrios	AgDSu16	25-08-15	12	5	1.921	120	22.9	LS	0.05	0.2	0.59	0.731
217	3	Ag. Dimitrios	AgDSu17	25-08-15	14	6	1.699	206	23	SS	0.04	0.09	0.46	0.792
218	3	Ag. Dimitrios	AgDSu18	25-08-15	8	5	1.274	39	23.9	BO	0.07	0.19	0	0.525

219	3	Ag. Dimitrios	AgDSu19	25-08-15	12	4	1.863	104	23.7	LG	0.03	0.11	0.23	0.691
220	3	Ag. Dimitrios	AgDSu20	25-08-15	12	6	1.579	53	23.4	LG	0.03	0.08	0.09	0.696
221	4	Parapeiros_W	ParWSu1	26-08-15	12	5	1.877	55	21.2	LS	0.05	0.22	0.09	0.847
222	4	Parapeiros_W	ParWSu2	26-08-15	4	0	1.149	9	21.1	SS	0.04	0.18	0	0.286
223	4	Parapeiros_W	ParWSu3	26-08-15	10	4	1.447	62	21.2	SS	0.04	0.21	0.27	0.695
224	4	Parapeiros_W	ParWSu4	26-08-15	6	2	1.257	32	21.1	BO	0.07	0.16	0.07	0.455
225	4	Parapeiros_W	ParWSu5	26-08-15	11	2	1.581	40	21.4	LS	0.05	0.21	0.22	0.644
226	4	Parapeiros_W	ParWSu6	26-08-15	9	4	1.528	56	21.4	SS	0.04	0.14	0.04	0.676
227	4	Parapeiros_W	ParWSu7	26-08-15	9	4	1.851	82	21.3	BO	0.07	0.2	0.1	0.746
228	4	Parapeiros_W	ParWSu8	26-08-15	10	4	1.725	54	21.6	LS	0.05	0.16	0.28	0.730
229	4	Parapeiros_W	ParWSu9	26-08-15	11	5	1.897	78	21.6	SS	0.04	0.13	0.32	0.843
230	4	Parapeiros_W	ParWSu10	26-08-15	8	3	1.762	19	21.5	BO	0.07	0.13	0	0.613
231	4	Parapeiros_W	ParWSu11	26-08-15	8	3	1.4	50	21.9	LS	0.05	0.16	0.1	0.585
232	4	Parapeiros_W	ParWSu12	26-08-15	8	3	1.532	43	21.9	LS	0.05	0.15	0.23	0.599
233	4	Parapeiros_W	ParWSu13	26-08-15	6	3	1.552	15	22	LS	0.05	0.12	0	0.525
234	4	Parapeiros_W	ParWSu14	26-08-15	5	2	1.414	25	21.8	SS	0.04	0.23	0.18	0.446
235	4	Parapeiros_W	ParWSu15	26-08-15	9	4	1.743	40	21.8	BO	0.07	0.18	0	0.694
236	4	Parapeiros_W	ParWSu16	26-08-15	12	5	2.005	43	21.7	LS	0.05	0.16	0.06	0.856
237	4	Parapeiros_W	ParWSu17	26-08-15	9	3	1.699	30	21.9	LS	0.05	0.12	0.25	0.639
238	4	Parapeiros_W	ParWSu18	26-08-15	15	5	1.91	119	21.9	LS	0.05	0.12	0.16	0.986
239	4	Parapeiros_W	ParWSu19	26-08-15	10	5	2.002	62	22	LS	0.05	0.19	0.49	0.818
240	4	Parapeiros_W	ParWSu20	26-08-15	15	5	1.742	118	22.1	SS	0.04	0.08	0.43	0.960
241	5	Evinos_Up	EviSu1	27-08-15	6	4	1.267	51	17.9	LG	0.03	0.14	0.33	0.540
242	5	Evinos_Up	EviSu2	27-08-15	8	5	1.754	38	17.9	LS	0.05	0.14	0.15	0.693
243	5	Evinos_Up	EviSu3	27-08-15	5	3	1.468	24	17.9	LS	0.05	0.17	0	0.483
244	5	Evinos_Up	EviSu4	27-08-15	7	4	1.609	32	18.4	SS	0.04	0.19	0.47	0.605
245	5	Evinos_Up	EviSu5	27-08-15	12	6	2.111	74	18.4	LS	0.05	0.14	0.21	0.938
246	5	Evinos_Up	EviSu6	27-08-15	8	5	1.703	42	18.4	LG	0.03	0.13	0.1	0.689
247	5	Evinos_Up	EviSu7	27-08-15	5	4	1.295	14	18.5	LS	0.05	0.34	0.12	0.478
248	5	Evinos_Up	EviSu8	27-08-15	10	5	1.771	53	18.5	BO	0.07	0.28	0.02	0.776
249	5	Evinos_Up	EviSu9	27-08-15	7	5	1.002	81	18.7	LG	0.03	0.17	0.27	0.592
250	5	Evinos_Up	EviSu10	27-08-15	8	4	1.749	27	18.7	SS	0.04	0.15	0.65	0.654

251	5	Evinos_Up	EviSu11	27-08-15	7	4	1.225	84	18.7	MG	0.026	0.15	0.07	0.597
252	5	Evinos_Up	EviSu12	27-08-15	6	4	1.58	26	18.8	LS	0.05	0.33	0.39	0.562
253	5	Evinos_Up	EviSu13	27-08-15	8	5	1.61	53	18.4	LG	0.03	0.08	0.2	0.686
254	5	Evinos_Up	EviSu14	27-08-15	9	6	1.775	72	18.4	BO	0.07	0.25	0.61	0.789
255	5	Evinos_Up	EviSu15	27-08-15	7	5	1.693	60	18.5	LS	0.05	0.09	0.37	0.671
256	5	Evinos_Up	EviSu16	27-08-15	10	7	1.811	47	18.7	SS	0.04	0.19	0.28	0.833
257	5	Evinos_Up	EviSu17	27-08-15	10	6	1.837	111	18.9	LS	0.05	0.2	0.32	0.866
258	5	Evinos_Up	EviSu18	27-08-15	10	6	1.968	52	18.9	SS	0.04	0.15	0.28	0.831
259	5	Evinos_Up	EviSu19	27-08-15	9	6	1.605	56	18.9	BO	0.07	0.08	0.09	0.750
260	5	Evinos_Up	EviSu20	27-08-15	9	5	1.881	79	18.9	SS	0.04	0.34	0.93	0.781
261	6	Mornos_Up	MorSu1	26-08-15	15	7	1.998	155	23.8	LG	0.03	0.14	0.49	0.934
262	6	Mornos_Up	MorSu2	26-08-15	11	7	1.971	159	23.8	LS	0.05	0.18	0.71	0.827
263	6	Mornos_Up	MorSu3	26-08-15	12	8	2.103	94	23.7	BO	0.07	0.16	0.38	0.855
264	6	Mornos_Up	MorSu4	26-08-15	11	7	2.199	57	23.6	SS	0.04	0.2	0.24	0.793
265	6	Mornos_Up	MorSu5	26-08-15	9	5	2.062	18	23.6	BO	0.07	0.18	0.09	0.647
266	6	Mornos_Up	MorSu6	26-08-15	9	7	1.924	37	23.6	LS	0.05	0.24	0.32	0.691
267	6	Mornos_Up	MorSu7	26-08-15	11	6	1.953	56	23.7	LG	0.03	0.18	0.24	0.735
268	6	Mornos_Up	MorSu8	26-08-15	8	7	1.802	54	24.4	SS	0.04	0.17	0.24	0.659
269	6	Mornos_Up	MorSu9	26-08-15	5	3	1.557	10	24.2	FG	0.024	0.27	0.1	0.419
270	6	Mornos_Up	MorSu10	26-08-15	8	3	1.049	28	24.2	SAND	0.022	0.2	0	0.443
271	6	Mornos_Up	MorSu11	26-08-15	9	4	2.05	29	24	LG	0.03	0.37	0.13	0.627
272	6	Mornos_Up	MorSu12	26-08-15	8	6	1.848	21	24	BO	0.07	0.24	0.05	0.619
273	6	Mornos_Up	MorSu13	26-08-15	10	7	1.839	42	24	LS	0.05	0.37	0.55	0.709
274	6	Mornos_Up	MorSu14	26-08-15	8	5	1.908	18	24	LS	0.05	0.27	0.14	0.600
275	6	Mornos_Up	MorSu15	26-08-15	6	4	1.667	8	24.1	SS	0.04	0.09	0.13	0.484
276	6	Mornos_Up	MorSu16	26-08-15	7	5	1.748	10	24.1	LS	0.05	0.36	0.16	0.547
277	6	Mornos_Up	MorSu17	26-08-15	13	6	2.288	66	24.1	LS	0.05	0.28	0.31	0.838
278	6	Mornos_Up	MorSu18	26-08-15	12	8	1.857	42	24.5	SS	0.04	0.24	0.85	0.790
279	6	Mornos_Up	MorSu19	26-08-15	13	7	1.735	100	24.4	BO	0.07	0.18	0.42	0.812
280	6	Mornos_Up	MorSu20	26-08-15	7	5	1.618	28	24.4	LG	0.03	0.13	0.29	0.541
281	7	Per06.1	Per06Su1	28-08-15	10	6	1.513	107	12.9	BO	0.07	0.09	0	0.521
282	7	Per06.1	Per06Su2	28-08-15	12	5	2.043	123	12.9	SS	0.04	0.12	0.13	0.612

283	7	Per06.1	Per06Su3	28-08-15	11	7	1.86	72	12.9	LS	0.05	0.07	0.03	0.592
284	7	Per06.1	Per06Su4	28-08-15	20	10	2.233	183	12.9	LG	0.03	0.04	0.33	0.897
285	7	Per06.1	Per06Su5	28-08-15	9	6	1.888	45	13.1	SS	0.04	0.21	0.08	0.532
286	7	Per06.1	Per06Su6	28-08-15	14	7	2.378	32	13.1	BO	0.07	0.24	0.18	0.703
287	7	Per06.1	Per06Su7	28-08-15	10	4	1.815	62	13.1	LS	0.05	0.18	0.06	0.510
288	7	Per06.1	Per06Su8	28-08-15	14	8	1.694	60	13.1	BO	0.07	0.18	0	0.643
289	7	Per06.1	Per06Su9	28-08-15	16	6	1.909	137	13.1	LS	0.05	0.24	0.2	0.694
290	7	Per06.1	Per06Su10	28-08-15	10	5	1.881	40	13.1	LG	0.03	0.15	0	0.530
291	7	Per06.1	Per06Su11	28-08-15	17	7	1.543	111	13.2	SS	0.04	0.24	0.16	0.678
292	7	Per06.1	Per06Su12	28-08-15	12	7	1.865	141	13.2	LS	0.05	0.09	0.75	0.632
293	7	Per06.1	Per06Su13	28-08-15	15	8	2.014	349	13.2	BO	0.07	0.14	0.14	0.785
294	7	Per06.1	Per06Su14	28-08-15	21	11	2.025	283	13.3	LS	0.05	0.07	0.19	0.937
295	7	Per06.1	Per06Su15	28-08-15	15	7	1.027	154	13.6	BO	0.07	0.22	0.24	0.587
296	7	Per06.1	Per06Su16	28-08-15	12	5	2.02	103	13.6	SS	0.04	0.17	0.17	0.604
297	7	Per06.1	Per06Su17	28-08-15	14	9	2.084	211	13.6	LG	0.03	0.11	0.21	0.754
298	7	Per06.1	Per06Su18	28-08-15	13	7	1.301	157	13.6	LS	0.05	0.2	0	0.584
299	7	Per06.1	Per06Su19	28-08-15	13	6	2.056	109	14.1	SS	0.04	0.07	0.27	0.647
300	7	Per06.1	Per06Su20	28-08-15	14	6	1.797	147	14.1	LG	0.03	0.14	0.14	0.645
301	8	SidePer10	SidePSu1	28-08-15	9	6	1.06	89	18.9	LS	0.05	0.44	0.2	0.545
302	8	SidePer10	SidePSu2	28-08-15	15	9	1.642	101	18.9	BO	0.07	0.24	0.08	0.850
303	8	SidePer10	SidePSu3	28-08-15	14	8	1.658	66	18.8	SS	0.04	0.54	0.19	0.791
304	8	SidePer10	SidePSu4	28-08-15	7	3	0.682	74	18.8	LS	0.05	0.64	0.19	0.369
305	8	SidePer10	SidePSu5	28-08-15	7	3	0.44	250	18.9	SAND	0.022	0.37	0	0.405
306	8	SidePer10	SidePSu6	28-08-15	9	5	1.258	37	18.9	BO	0.07	0.66	0.11	0.531
307	8	SidePer10	SidePSu7	28-08-15	6	4	1.523	15	18.9	LS	0.05	0.8	0.16	0.463
308	8	SidePer10	SidePSu8	28-08-15	14	7	1.88	125	18.9	LS	0.05	0.18	0.32	0.824
309	8	SidePer10	SidePSu9	28-08-15	16	7	2.072	139	18.9	BO	0.07	0.23	0.57	0.907
310	8	SidePer10	SidePSu10	28-08-15	11	8	1.778	55	18.9	LS	0.05	0.18	0.51	0.729
311	8	SidePer10	SidePSu11	28-08-15	4	3	1.007	21	18.5	LS	0.05	0.24	0.13	0.319
312	8	SidePer10	SidePSu12	28-08-15	13	6	1.996	91	18.5	LS	0.05	0.26	0.28	0.780
313	8	SidePer10	SidePSu13	28-08-15	7	4	1.371	30	18.4	SS	0.04	0.29	0.63	0.472
314	8	SidePer10	SidePSu14	28-08-15	7	6	1.834	10	17.9	BO	0.07	0.62	0.82	0.574

315	8	SidePer10	SidePSu15	28-08-15	2	1	0.562	4	17.9	BO	0.07	0.42	0.11	0.154
316	8	SidePer10	SidePSu16	28-08-15	15	8	1.943	172	17.9	LS	0.05	0.38	0.09	0.899
317	8	SidePer10	SidePSu17	28-08-15	9	7	1.952	27	17.9	SS	0.04	0.04	0.34	0.670
318	8	SidePer10	SidePSu18	28-08-15	13	7	2.086	100	17.9	BO	0.07	0.06	0.49	0.819
319	8	SidePer10	SidePSu19	28-08-15	15	9	2.099	225	17.9	LG	0.03	0.12	0.41	0.965
320	8	SidePer10	SidePSu20	28-08-15	11	6	1.646	80	17.9	LG	0.03	0.17	0.27	0.676
321	1	Fouskari	FouAu1	20-10-15	11	5	1.307	79	16.9	BO	0.07	0.1	0.47	0.821
322	1	Fouskari	FouAu2	20-10-15	10	5	1.601	110	16.9	SS	0.04	0.14	0.44	0.864
323	1	Fouskari	FouAu3	20-10-15	10	4	1.391	87	16.9	LG	0.03	0.12	0.47	0.775
324	1	Fouskari	FouAu4	20-10-15	5	2	1.398	25	16.9	SS	0.04	0.32	0.45	0.487
325	1	Fouskari	FouAu5	20-10-15	7	3	1.745	26	16.9	LG	0.03	0.3	0.19	0.645
326	1	Fouskari	FouAu6	20-10-15	6	2	1.394	23	16.9	BO	0.07	0.27	0.43	0.518
327	1	Fouskari	FouAu7	20-10-15	12	6	1.768	89	16.9	LG	0.03	0.14	0.16	0.973
328	1	Fouskari	FouAu8	20-10-15	6	3	0.916	33	16.9	FG	0.024	0.17	0.25	0.481
329	1	Fouskari	FouAu9	20-10-15	8	2	1.381	60	16.9	LS	0.05	0.57	0.33	0.616
330	1	Fouskari	FouAu10	20-10-15	6	1	1.247	36	16.9	SS	0.04	0.29	0	0.472
331	1	Fouskari	FouAu11	20-10-15	9	4	1.394	65	17	LS	0.05	0.24	0.78	0.722
332	1	Fouskari	FouAu12	20-10-15	8	4	1.067	52	17	BO	0.07	0.34	0.36	0.623
333	1	Fouskari	FouAu13	20-10-15	9	5	1.6	49	17	SS	0.04	0.16	0.32	0.775
334	1	Fouskari	FouAu14	20-10-15	5	2	0.681	52	17.1	SS	0.04	0.13	0.02	0.393
335	1	Fouskari	FouAu15	20-10-15	8	4	1.432	49	17.1	LS	0.05	0.22	0.43	0.681
336	1	Fouskari	FouAu16	20-10-15	12	6	1.748	105	17.1	BO	0.07	0.22	0.04	0.984
337	1	Fouskari	FouAu17	20-10-15	11	6	1.285	62	17.1	SS	0.04	0.09	0.32	0.835
338	1	Fouskari	FouAu18	20-10-15	8	4	1.544	51	17.1	LG	0.03	0.13	0.05	0.701
339	1	Fouskari	FouAu19	20-10-15	10	6	1.818	30	17.1	LS	0.05	0.23	0.75	0.861
340	1	Fouskari	FouAu20	20-10-15	7	3	1.051	54	17.1	SS	0.04	0.09	0.15	0.556
341	2	Krathis_Up	KrAu1	21-10-15	9	4	1.711	24	11.1	LG	0.03	0.05	0.25	0.616
342	2	Krathis_Up	KrAu2	21-10-15	11	5	1.463	67	11.1	LG	0.03	0.12	0.4	0.707
343	2	Krathis_Up	KrAu3	21-10-15	8	4	1.255	46	11.1	SAND	0.022	0.22	0	0.548
344	2	Krathis_Up	KrAu4	21-10-15	7	4	1.465	43	11.1	MG	0.026	0.13	0.2	0.548
345	2	Krathis_Up	KrAu5	21-10-15	9	4	2.059	19	11.1	SS	0.04	0.16	0.5	0.659
346	2	Krathis_Up	KrAu6	21-10-15	4	3	0.574	27	11.1	BO	0.07	0.22	0.88	0.299

347	2	Krathis_Up	KrAu7	21-10-15	3	3	0.831	16	11.1	LS	0.05	0.26	1.08	0.297
348	2	Krathis_Up	KrAu8	21-10-15	15	7	2.16	56	11.1	SS	0.04	0.12	0.22	0.957
349	2	Krathis_Up	KrAu9	21-10-15	11	5	1.398	79	11.1	LS	0.05	0.14	0.14	0.710
350	2	Krathis_Up	KrAu10	21-10-15	6	3	0.602	51	11.1	BO	0.07	0.3	0.27	0.381
351	2	Krathis_Up	KrAu11	21-10-15	9	5	1.542	23	11.1	LS	0.05	0.2	0.13	0.620
352	2	Krathis_Up	KrAu12	21-10-15	7	4	0.746	55	11.1	SS	0.04	0.24	0.53	0.460
353	2	Krathis_Up	KrAu13	21-10-15	10	4	2.011	20	11.1	LG	0.03	0.1	0.35	0.680
354	2	Krathis_Up	KrAu14	21-10-15	4	2	1.143	16	11.1	LS	0.05	0.06	0.39	0.339
355	2	Krathis_Up	KrAu15	21-10-15	13	7	1.82	62	11.1	LG	0.03	0.1	0.27	0.862
356	2	Krathis_Up	KrAu16	21-10-15	8	5	1.245	61	11.1	LS	0.05	0.21	0.36	0.591
357	2	Krathis_Up	KrAu17	21-10-15	12	6	1.52	99	11.1	SS	0.04	0.14	0.65	0.803
358	2	Krathis_Up	KrAu18	21-10-15	12	6	1.848	71	11.1	SS	0.04	0.16	0.41	0.820
359	2	Krathis_Up	KrAu19	21-10-15	12	5	1.877	35	11.1	MG	0.026	0.16	0.08	0.759
360	2	Krathis_Up	KrAu20	21-10-15	5	1	0.813	23	11.1	SS	0.04	0.23	0.15	0.298
361	3	Ag. Dimitrios	AgDAu1	21-10-15	10	4	1.812	31	16.9	SS	0.04	0.05	0.31	0.686
362	3	Ag. Dimitrios	AgDAu2	21-10-15	15	5	2.023	97	16.9	LG	0.03	0.09	0.28	0.919
363	3	Ag. Dimitrios	AgDAu3	21-10-15	9	3	1.624	89	16.8	LS	0.05	0.13	0.28	0.629
364	3	Ag. Dimitrios	AgDAu4	21-10-15	11	5	1.773	65	16.9	SS	0.04	0.15	0.35	0.758
365	3	Ag. Dimitrios	AgDAu5	21-10-15	6	4	1.366	33	16.8	SS	0.04	0.04	0.34	0.514
366	3	Ag. Dimitrios	AgDAu6	21-10-15	4	2	1.242	6	16.8	BO	0.07	0.06	0	0.361
367	3	Ag. Dimitrios	AgDAu7	21-10-15	9	4	1.595	35	16.9	FG	0.024	0.13	0.03	0.629
368	3	Ag. Dimitrios	AgDAu8	21-10-15	9	4	1.172	86	16.8	LG	0.03	0.16	0.38	0.594
369	3	Ag. Dimitrios	AgDAu9	21-10-15	10	3	1.331	79	16.8	LG	0.03	0.09	0.28	0.607
370	3	Ag. Dimitrios	AgDAu10	21-10-15	11	6	1.2	165	16.8	LG	0.03	0.08	0.36	0.761
371	3	Ag. Dimitrios	AgDAu11	21-10-15	10	4	1.833	23	16.8	SS	0.04	0.2	0.52	0.684
372	3	Ag. Dimitrios	AgDAu12	21-10-15	3	1	0.566	12	16.8	FG	0.024	0.14	0.05	0.204
373	3	Ag. Dimitrios	AgDAu13	21-10-15	7	3	0.704	45	16.8	SS	0.04	0.14	0.21	0.416
374	3	Ag. Dimitrios	AgDAu14	21-10-15	9	5	1.498	87	16.8	BO	0.07	0.14	0.07	0.676
375	3	Ag. Dimitrios	AgDAu15	21-10-15	10	6	1.497	59	16.8	BO	0.07	0.12	0	0.721
376	3	Ag. Dimitrios	AgDAu16	21-10-15	4	3	1.137	15	16.8	LS	0.05	0.33	0.33	0.383
377	3	Ag. Dimitrios	AgDAu17	21-10-15	6	4	0.9	26	16.8	LS	0.05	0.1	0.1	0.441
378	3	Ag. Dimitrios	AgDAu18	21-10-15	3	2	1.04	4	16.8	MG	0.026	0.24	0.1	0.303

379	3	Ag. Dimitrios	AgDAu19	21-10-15	13	6	1.811	184	16.2	SS	0.04	0.5	0.27	0.915
380	3	Ag. Dimitrios	AgDAu20	21-10-15	5	2	0.847	26	16.8	LS	0.05	0.3	0.12	0.340